

T 77-13239 C.1

Contract No. NAS9-12761  
DRL No. MSC-08056  
Line Item No. 4  
DRD No. MA-129T

NASA CR-

151471

GRUMMAN

Development and Design Applications  
of a  
Closed Pore External Insulation  
Thermal Protection System

Final Report  
30 November 1972

LIBRARY COPY

AUG 2 1977

JOHNSON SPACE CENTER  
HOUSTON, TEXAS

N77-83275

Unclas  
00/34 41738

(NASA-CR-154923) DEVELOPMENT AND DESIGN  
APPLICATIONS OF A CLOSED PORE EXTERNAL  
INSULATION THERMAL PROTECTION SYSTEM Final  
Report (Grumman Aerospace Corp.) 214 p

Grumman Aerospace Corporation  
Bethpage, New York 11714

Development and Design Applications  
of a  
Closed Pore External Insulation  
Thermal Protection System

by

A. Varisco, A. Tobin and H. G. Harris  
Grumman Aerospace Corporation  
Bethpage, New York 11714

Final Report No. 72-43NAS  
30 November 1972

Approved by

W. Ludwig  
Shuttle Research and  
Technology Manager

Approved by

Charles A. Tagliavini  
Study Manager

Approved by

Angelo Varisco  
Project Engineer

Contract No. NAS9-12781  
DRL No. MSC-06856  
Line Item No. 4  
DRD No. MA-129T

Prepared for  
NASA Manned Spacecraft Center  
Houston, Texas 77058

Development: FOREWORD

This final report was prepared by Grumman Aerospace Corporation for NASA-MSC, under Contract NAS 9-12781, Development of Closed Pore Insulation Thermal Protection Systems for Shuttle. It covers the period 1 June 1972 to 30 November 1972, which is the extent of the six month contract. This work was performed for the National Aeronautics and Space Administration, Manned Spacecraft Center, under the direction of the Thermal Technology Branch of the Structures and Mechanics Division with Mr. D.J. Tillian as the Contracting Officer's Representative. Mr. A. Varisco is the Program Project Engineer and Dr. A. Tobin is the Assistant Project Engineer for the Grumman Aerospace Corporation.

The authors wish to acknowledge the following Grumman personnel's contribution to the successful completion of the program: A. Flescher, G. Baumann, R. H. Anderson, E. Leszak (Materials and Processes); A. Zier, F. Halfen, C. De Angelis, F. O. Curasi (Design); Dr. H. G. Harris, L. Rose (Structural Mechanics); P. Coschignano, V. Biagiotti (Structural Analysis); R. H. Truran, C. Dunkerley (Test).

DISTRIBUTION LIST

NASA Manned Spacecraft Center  
Attn: Paul W. Liebhardt/BC42  
Space Shuttle Procurement Section  
Houston, TX 77058

(one copy)

NASA Manned Spacecraft Center  
Attn: Charles M. Grant/JN2  
Documentation Management Office  
Houston, TX 77058

(Three copies)

NASA Manned Spacecraft Center  
Attn: John Wheeler/JM7  
Technology Utilization Office  
Houston, TX 77058

(One copy)

NASA Manned Spacecraft Center  
Attn: Don Tillian/ES3  
Structures and Mechanics Division  
Houston, TX 77058

(forty-five copies)

## TABLE OF CONTENTS

	Page
Foreword.....	i
Distribution List.....	ii
Table of Contents.....	iii
List of Tables.....	vi
List of Figures.....	vii
List of Appendices.....	xi
List of References.....	xii
 <u>SECTION 1</u>	
Introduction and Summary	
1.1 - Introduction.....	1
1.2 - Summary.....	2
 <u>SECTION 2</u>	
Program Plan	3
 <u>SECTION 3</u>	
Shuttle TPS Requirements	
3.1 - Environmental Conditions.....	6
3.2 - Structural Design Requirements.....	6
3.3 - Thermal Design Requirements.....	7
 <u>SECTION 4</u>	
Material Characterization.....	23
4.1 - Material Description.....	23
4.2 - Material Property Data.....	55
4.2.1 General.....	55
4.2.2 Flextural Strength.....	55
4.2.3 Tensile Strength.....	62
4.2.4 Compressive Strength.....	62
4.2.5 Uniaxial Tensile Strength.....	67
4.2.6 Bond Strength.....	67
4.2.7 Shear Strength.....	73
4.2.8 Creep Properties.....	73
4.3 - Environmental Testing of CPI Subelements.....	78
4.3.1 CPI Tiles.....	78
4.3.2 CPI Composites.....	82
4.3.3 Salt Spray Tests.....	86
4.4 - NDE Inspection of CPI Materials.....	89

## TABLE OF CONTENTS (Continued)

	Page
<u>SECTION 5</u>	
TPS Concept Development	
5.1 - CPI Material Design Characteristics.....	92
5.2 - Conceptual Design Studies.....	92
5.2.1 General.....	92
5.2.2 Bonded Concepts.....	93
5.2.2.1 CPI Surface Tile.....	94
5.2.2.2 Primary Insulations.....	94
5.2.2.3 Moisture Barrier.....	96
5.2.2.4 Edge Seal Development.....	97
5.2.3 Mechanically Fastened Concepts.....	100
5.2.3.1 CPI/Web-Standoff Concept.....	101
5.2.3.2 CPI/Square Plug Concept.....	103
5.2.3.3 CPI/Post-Snap Washer Concept.....	106
5.2.3.4 CPI/Sandwich Concept.....	108
5.2.3.5 CPI/Post-Sliding Bushing Concept.....	110
(a) - Hexagonal Tile.....	111
(b) - Rectangular Tile.....	113
(c) - Square Tile.....	113
(d) - Alternate Retention Designs.....	116
5.2.3.6 Boundary Layer Gas Seal Concepts.....	118
5.3 - Concept Selection.....	120
5.3.1 General.....	120
5.3.2 Direct Bonded Concept.....	120
5.3.2.1 Design-Drawing, Description.....	120
(a) - Area 1 Kaowool.....	120
(b) - Area 2 Mullite/Kaowool.....	120
5.3.2.2 Structural Analysis.....	126
5.3.2.3 Thermal Analysis.....	126
5.3.2.4 Concept Weight.....	129
5.3.3 Mechanically Fastened - Sliding Bushing Concept.....	129
5.3.3.1 Design - Drawings, Description.....	129
5.3.3.2 Structural Analysis.....	131
5.3.3.3 Thermal Analysis.....	133
5.3.3.4 Concept Weight.....	133
5.3.4 Mechanically Fastened - CPI/Post Snap Washer Concept.....	136

TABLE OF CONTENTS (Continued)

	Page
5.3.4.1 Design - Drawings, Description.....	136
5.3.4.2 Structural Analysis.....	136
5.3.4.3 Thermal Analysis.....	136
5.3.4.4 Concept Weight.....	139
 <u>SECTION 6</u>	
Design Details - Development Evaluation	
6.1 - CPI/Bond Joint Development.....	140
6.1.1 CPI/Mullite Bond Joint Development.....	140
6.1.2 CPI/Kaowool Bond Joint Development.....	140
6.1.3 CPI/CPI Bond Joint Development.....	141
6.2 - CPI/Mechanically Attached - Element Test.....	145
6.2.1 CPI/Post Support Concept With Snap Washers Panel Test..	145
6.2.2 CPI/Sliding Bushing Concept Panel Test.....	145
 <u>SECTION 7</u>	
Conclusions and Recommendations	
7.1 - Conclusions.....	149
7.1.1 Material Development.....	149
7.1.2 Inspection.....	149
7.1.3 Concept Development.....	150
7.2 - Recommendations.....	150

# LIST OF TABLES

Table No.	Title	Page No.
3-1	Summary of Design Requirements.....	8
4-1	Requirements of External Insulation Material....	24
4-2	Chemical Analysis of Cenospheres.....	26
4-3	Typical CPI Data Sheet.....	26
4-4	Physical Properties of CPI.....	33
4-5	Thermal and Chemical Properties of CPI.....	35
4-6	Characteristics of Low Density Fibrous Insulation	45
4-7	Physical Properties of Kaowool Fibers.....	45
4-8	Properties of Kaowool Ceramic Fiber Block.....	47
4-9	Thermal Stability of Kaowool Ceramic Fiber Block	48
4-10	Chemistry of High Purity Kaowool Fibers.....	50
4-11	Properties of Rigidized Mullite Fibers.....	50
4-12	B and W Experimental Mullite Fiber.....	51
4-13	Properties of Fiberfrax H.....	53
4-14	Physical and Chemical Properties of Kaowool Cement.....	53
4-15	Physical and Chemical Properties of Kaowool Rigidizer.....	54
4-16	Summary of Average Mechanical Properties of CPI-4 and CPI-8 Material.....	56
4-17	Summary of Thermal Cycling Test Results on Individual CPI Tiles (Unrestrained).....	80
4-18	Summary of Thermal Cycling Results on CPI/ Rigidized Fiber Composites (CPI Thickness = 0.25").....	83
4-19	Summary of Thermal Cycling Results on CPI/CPI Bonding Experiments (Torus Assembly).....	87



# LIST OF FIGURES

<u>NO.</u>	<u>TITLE</u>	<u>PAGE</u>
2-1	Work Breakdown Structure.....	4
2-2	Program Organization.....	5
3-1	NASA Orbiter Bottom Surface Plan Form Showing the TPS Design Areas.....	9
3-2	Local Heating Rate and Stagnation Temperature History For Orbiter During Launch.....	10
3-3	Local Heating Rates and Stagnation Temperature Histories for Orbiter During Reentry.....	11
3-4	Orbiter Launch Trajectory.....	12
3-5	Orbiter Entry Trajectory.....	13
3-6	Local and Free-Stream Static Pressure Histories on Orbiter Fuselage Centerline During Launch.....	14
3-7	Local and Free-Stream Static Pressure Histories on Orbiter Centerline During Entry.....	15
3-8	Limit Differential Panel Pressure for Ascent.....	16
3-9	Limit Differential Panel Pressure for Entry.....	16
3-10	Ascent and Entry Dynamic Pressures.....	17
3-11	Ascent and Entry Internal Loads for Orbiter Area 1 20 in. Panel Length.....	18
3-12	Ascent and Entry Internal Loads for Orbiter Area 2 24 in. Panel Length.....	19
3-13	Overall SPL vs. Time-Typical Orbiter Mission.....	20
3-14	Sound Pressure Levels - Liftoff.....	21
3-15	Sound Pressure Levels - Air Breathing Engines; Maximum Static Thrust.....	21
3-16	One-Third Octave Band Fluctuating Pressure Levels - Ascent ( $M = 1.4$ , $Q = 600$ psf).....	22
3-17	One-Third Octave Band Fluctuating Pressure Levels - Entry ( $M = 4$ , $Q = 100$ psf).....	22

# LIST OF FIGURES (Continued)

<u>NO.</u>	<u>TITLE</u>	<u>PAGE</u>
4-1	CPI Process Development.....	28
4-2	Photomicrograph of Cenospheres.....	29
4-3	Scanning Electron Microscope Photographs of Sintered Cenosphere Bodies Fired at 1650K for One Hour.....	31
4-4	Thermal Expansion of CPI Materials vs T(K).....	36
4-5	Typical Differential Thermal Analysis Traces of Scaled Up CPI-4 and CPI-8 Tiles.....	37
4-6	Heat Capacity Versus Temperature of Scaled-Up CPI-8 Tiles and Mullite.....	39
4-7	Total Normal Emittance ( $E_{TN}$ ) For CPI-4 and CPI-8 (Coated and Uncoated) and CPI-0 Versus Temperature (K).....	40
4-8	Thermal Conductivity of CPI-4 and CPI-8 versus T(K).....	42
4-9	Thermal Conductivity of Microquartz, Fiberfrax-H and Refrasil Blankets in 1 Atm. Air.....	44
4-10	Thermal Conductivity (W/m-k) of Candidate TPS Insulation Materials vs. T(K).....	44
4-11	Single Load Point Flexural Testing.....	53
4-12	Modulus of Rupture (Flexural Strength) vs. Temperature....	59
4-13	Young's Modulus versus Temperature of CPI Materials.....	60
4-14	Two Load Point Flexural Testing.....	61
4-15	Split Cylinder Test as a Measure of Tensile Strength.....	63
4-16	Split Cylinder Tension Strength Versus Temperature for 2 CPI Compositions .....	64
4-17	Unconfined Compressive Strength Testing.....	65
4-18	Compressive Strength vs. Temperature of CPI.....	66
4-19	Compressive Strength vs. Temperature of CPI-8 for Cycled and Uncycled Material.....	68
4-20	Uniform Axial Tensile Specimen.....	69
4-21	Uniaxial Tension Test of CPI Material.....	70
4-22	Bond Strength Specimen.....	71

# LIST OF FIGURES (Continued)

<u>NO.</u>	<u>TITLE</u>	<u>PAGE</u>
4-23	Bond Testing of the CPI Material.....	72
4-24	Johnson Shear Test.....	74
4-25	Typical Test Specimens from Johnson Shear Test.....	75
4-26	Creep Tests of CPI Beams.....	76
4-27	Flexural Creep Strain vs. Time for CPI-4 and CPI-8 at Two Different Temperatures.....	77
4-28	Temperature vs. Time Variation of Areas 1, 2 and 2P.....	79
4-29	X-Ray Pictures of CPI Tiles.....	90
4-30	X-Ray Picture of CPI Tile with Internal Crack.....	91
5-1	CPI/Bonded Concept.....	95
5-2	CPI/Bonded Area 1 Test Component Prior to Assembly.....	98
5-3	CPI/Bonded Concept Edge Seal Designs.....	99
5-4	CPI/Web Support Concept.....	102
5-5	CPI/Web Standoff Test Component.....	104
5-6	CPI/Post Square Plug Concept.....	105
5-7	CPI/Post Strap Washer Concept.....	107
5-8	CPI/Sandwich Concept.....	109
5-9	CPI/Post-Sliding Bushing Concept Hexagonal Tile Design.....	112
5-10	CPI/Post Sliding Bushing Concept, Rectangular Tile Design..	114
5-11	CPI/Post-Sliding Bushing Concept Square Tile Design.....	115
5-12	CPI/Post-Sliding Bushing Retention Concepts.....	117
5-13	Boundary Layer Gas Seal Concepts for Mechanically Fastened Panels.....	119
5-14	Direct Bond Test Article, Area 1 .....	121
5-15	Photo of CPI/Bonded Area 1 Test Component.....	123
5-16	Direct Bond Test Article, Area 2.....	124
5-17	Photo of CPI/Bonded Area 2P Test Component.....	125

LIST OF FIGURES (Continued)

<u>NO.</u>	<u>TITLE</u>	<u>PAGE</u>
5-18	Critical Temperature Distributions for Area 1 Heating of CPI/Bonded Concept.....	127
5-19	Critical Temperature Distributions for Area 2 Perturbed Direct Bond Scheme Kaowool Peak Temperature 1700°F.....	128
5-20	CPI/Post Sliding Bushing Test Component.....	130
5-21	CPI/Post-Sliding Bushing Test Component (6.5 x 6.5 in. Tile Size).....	132
5-22	Critical Temperature Distributions for Area 1 Heating-Sliding Bushing Concept.....	134
5-23	CPI/Post-Snap Washer Test Component.....	137
5-24	CPI/Post Snap Washer Test Component (4 x 4 in. Tile Size)..	138
6-1	CPI/Kaowool Bonded Tiles After Thermal Cycling.....	142
6-2	CPI/Bond Test Specimens.....	144
6-3	CPI/Post With Snap Washers After First Thermal Cycle.....	146
6-4	Cracks Appearing in Snap-Washer Concept After 58 Thermal Cycles.....	147
6-5	CPI/Sliding Bushing Concept After 29 Thermal Cycles.....	148

# LIST OF APPENDICES

	Page
APPENDIX A MATERIAL STRENGTH DATA .....	152
APPENDIX B RADIANT LAMP RE-ENTRY THERMAL SCREENING TESTS .....	165
APPENDIX C STRESS ANALYSIS OF BONDED CPI DESIGN.....	170
APPENDIX D THERMAL STRESS ANALYSIS OF CPI/MULLITE BONDED CONCEPT FOR AREA 2P HEATING.....	173
APPENDIX E STRESS ANALYSIS OF CPI-4 FOUR SUPPORT CONCEPT - SLIDING BUSHING.....	178
APPENDIX F STRESS ANALYSIS OF CPI-4 FOUR SUPPORT CONCEPT - SNAP WASHER.....	184

## LIST OF REFERENCES

- (1) Tobin, A., Russak, M., Feldman, C., and Reichman, J. "Development of a Closed Pore Insulation Material", NASA Langley Contract NAS1-10718 (in preparation)
- (2) Tobin, A., Russak, M., Feldman, C. and Varisco, A., "Development and Characterization of CPI Surface Insulation," Paper presented at NASA Symposium on "Reusable Surface Insulation for the Space Shuttle, Ames Research Center, Moffett Field, California (1972).
- (3) Tobin, A., et al, "Development of Closed Pore Insulation for Space Shuttle", Paper presented at "NASA Symposium for Reusable Surface Insulation for Space Shuttle", University of Washington, Seattle (1971)
- (4) Varisco, A., and Harris, H. G., "Closed Pore Insulation Thermal Protection System Design Concept Development", Paper presented at "NASA Symposium for Reusable Surface Insulation for Space Shuttle", Ames Research Center, Moffett Field, California (1972)
- (5) Russak, M. and Feldman, C., "Further Characterization of CPI", NASA Langley Contract Extension NAS1-10713 (in preparation)
- (6) Lehman, J., et al, "Reusable Surface Insulation (RSI) Thermal Protection Development for Shuttle", NASA Contract NAS9-12082 (1972)

SECTION 1  
INTRODUCTION & SUMMARY

1.1 Introduction

The thermal protection system for the space shuttle must protect the primary vehicle structure and other vehicle subsystems from the varied space shuttle mission environments. A major constraint on the use of existing materials is the requirement of 100 entries or reuses for the space shuttle thermal protection system. Recent contract activities have indicated that nonmetallic surface insulation materials show promise of being lightweight potentially reusable thermal protection systems. However, these systems require complex brittle coatings to provide a water repellent surface, as these materials readily absorb moisture and have relatively low strength, which complicates their attachment to the primary structure.

A project was initiated at Grumman to develop an insulating material that would not require any coating and would have sufficient strength to be mechanically fastened to the vehicle primary structure. This work led to the development of a unique closed-pore ceramic foam insulation (CPI) which is produced from low cost fly ash cenospheres. This material's outstanding characteristics include its rigidity, machinability and water repellency. It is easily handled and provides a high emittance surface, without the use of coatings. Since it permits the use of mechanical attachments, there is no need for bonding with its inherent difficulty of inspection and carrier panels, thus reducing costs and weight.

This report describes Grumman's work under a NASA-MSC funded program. The program's objectives were to assess the feasibility of utilizing the closed pore insulation material for the shuttle thermal protection system. The program covered three basic tasks:

- Characterization of the CPI material and definition of possible failure modes of the material system
- Development of promising CPI TPS concepts including integration to the vehicle and in-depth structural and thermal analysis
- Fabrication and test program to evaluate thermal and mechanical performance, thermal shock and reuse characteristics, and design details such as joints and seals

## 1.2 Summary

The CPI material was fully characterized in the program. Mechanical property data were developed for flexure, tension, compression, shear, bond and creep. Physical property data were developed for water absorption, thermal expansion, emittance, specific heat, and thermal conductivity.

In the concept development task, two basic approaches emerged for development: directly bonded concepts and mechanically fastened concepts.

The bonded concepts were studied first because of their inherent lightness and simplicity. Two designs were developed, both very similar, but tailored to each of the Area 1 and Area 2P requirements.

In contrast to the bonded concepts, the mechanically fastened concepts take maximum advantage of the CPI material and its ability to carry pressure loads. These concepts were emphasized in the program by NASA direction. Of the many concepts studied, two were selected for fabrication and testing.



SECTION 2  
PROGRAM PLAN

The program plan for this study, shown in Figure 2-1, consists of eight tasks. The program was constructed to assess the feasibility of utilizing the CPI material for the shuttle thermal protection system.

The program's scope was substantially reduced by NASA directive. Task 3.6 TPS Panel Design Development Tests; Task 3.7.2, Prototype TPS Panels Deliverable; and Task 3.8, Manufacturing Plan, were deleted from the program. In an effort to demonstrate the feasibility of CPI TPS Concepts, Task 3.5, Design Details-Development/Evaluation, was expanded to include some complete TPS component testing.

The organization chart for this program is shown in Figure 2-2.





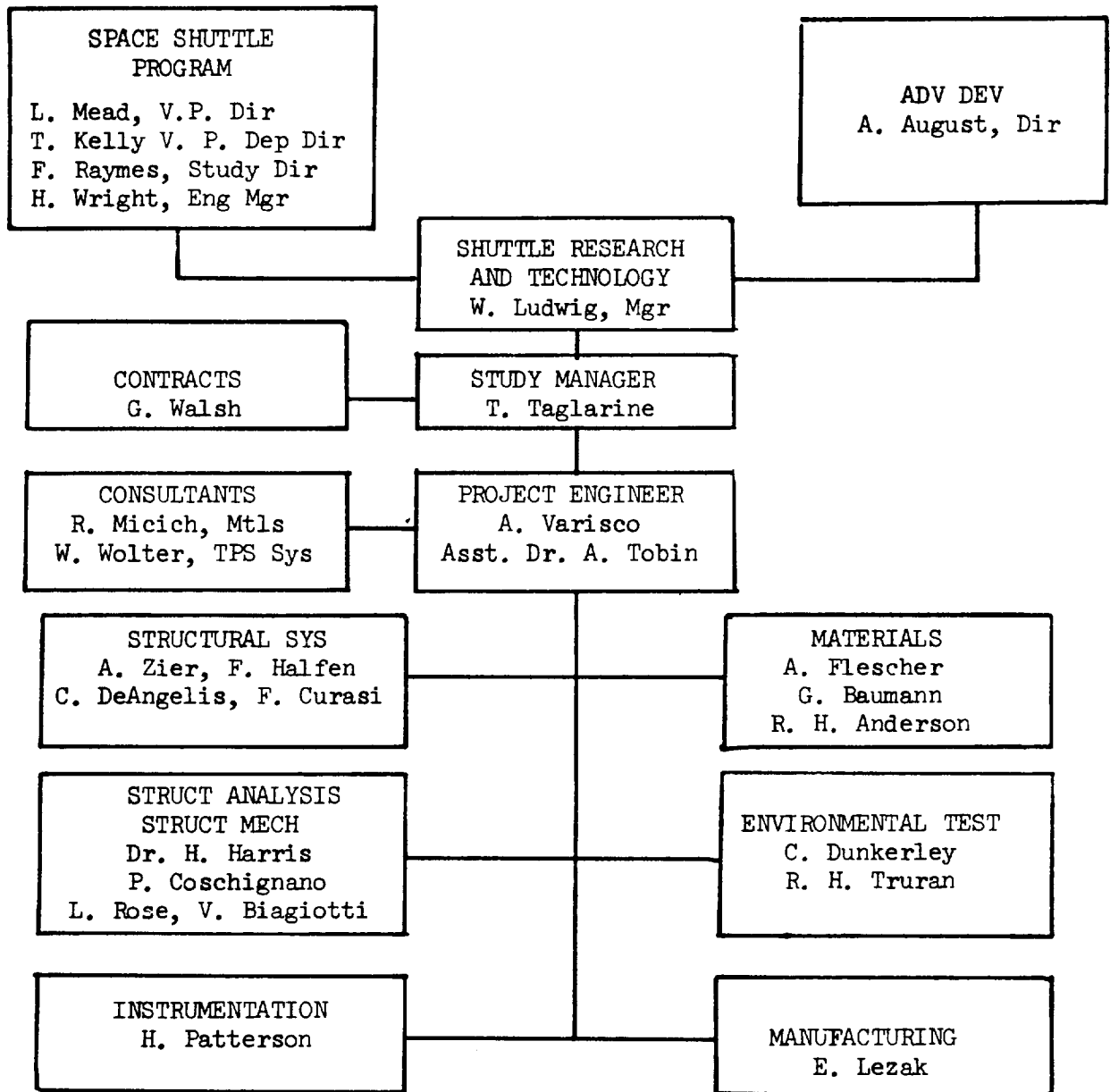


Figure 2-2 Program Organization

## SECTION 3

### SHUTTLE TPS REQUIREMENTS

The primary requirements of the thermal protection system (TPS) are to protect the vehicle primary structure from the thermal environment and to provide an acceptable aerodynamic surface. The system must be lightweight, easily refurbishable, structurally reliable, reusable and have low operating risk and cost. These requirements will be used to formulate design criteria which will serve as the basis for the design of a CPI heat shield. These requirements were based on:

3.1 Environmental Conditions. Specified in Appendix A of the SOW and shown in Figures 3-1 through 3-17.

3.2 Structural Design Requirements. The design factor of safety was taken as 1.5. Thermally induced loads were then multiplied by this factor and margins computed at design temperatures. The combined loading was treated as follows:

- Ultimate Combined Loads. The mechanical external and internal loads and the thermally induced loads were combined in a rational manner according to the equation given below to determine the design loads. Any other loads included in the structure, e.g. during manufacturing, were also combined in a rational manner. In no case was the ratio of the allowable load to the combined limit loads less than 1.35.

$$K_1 P_{\text{external}} + K_2 P_{\text{thermal}} \leq 1.35 (\Sigma P)$$

$$K_1, K_2 \begin{cases} = 1.5 \text{ when additive to } (\Sigma P) \\ = 1.0 \text{ when relieving to } (\Sigma P) \end{cases}$$

$P_{\text{external}}$  = mechanical externally applied limit loads  
(e.g. pressures, internal loads)

$P_{\text{thermal}}$  = thermally induced limit loads

$\Sigma P$  = algebraic sum of  $P_{\text{external}}$ ,  $P_{\text{thermal}}$

- Panel Flutter. External surfaces were free of panel flutter at all dynamic pressure up to 1.5 times the local dynamic pressure

expected to be encountered at any Mach number in flight. The dynamic-pressure margin was determined separately at constant density and at constant Mach number.

3.3 Thermal Design Requirements. Design factors of safety were not applied to the heating rates. The heating rate for Area 2 was perturbed to accommodate a temperature overshoot capability of 2300°F.

Table 3-1 SUMMARY DESIGN REQUIREMENTS

CONCEPT APPLICA- TION	MAX TEMP. OF		MAX PRESSURE PSI. LIMIT		MAX INTERNAL LOAD, LB PER INCH LIMIT		MAX. DYNAMIC PRESSURE, PSF.	MAX OVERALL SOUND PRES- SURE LEVEL dB
	SURFACE	BONDLINE	ASCENT	ENTRY	ASCENT	ENTRY		
Area 1	1400	350	+2.0 -3.0	+0.1* -0.1*	+2800 -4000	+500* -200*	700	161
Area 2P	2300	350	+4.0 -3.0	+0.1* -0.1*	+2800 -2000	+200* -100*	700	161

\* At Peak Temperature

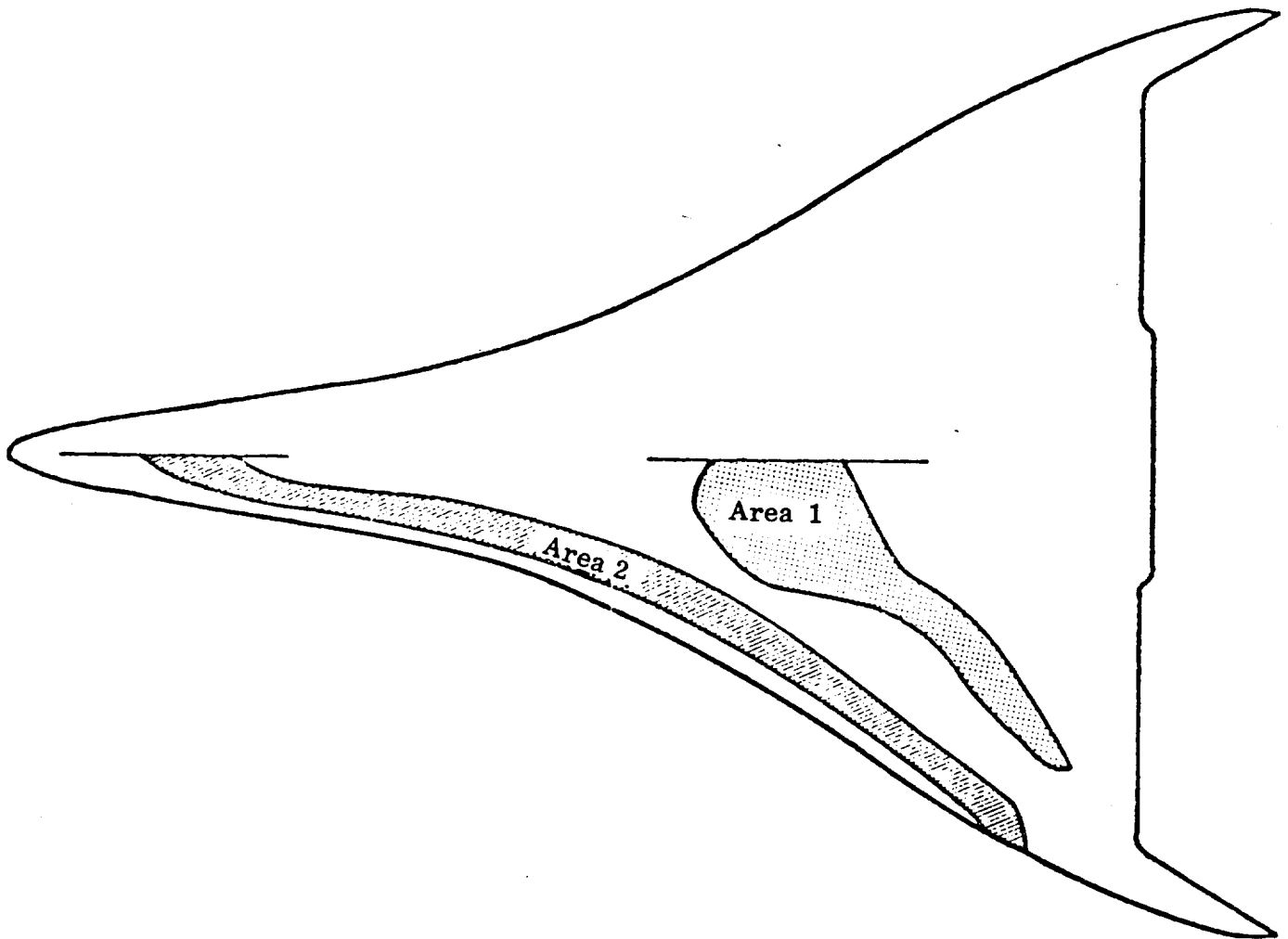


Fig. 3-1 NASA Orbiter Bottom Surface Plan Form Showing the TPS Design Areas



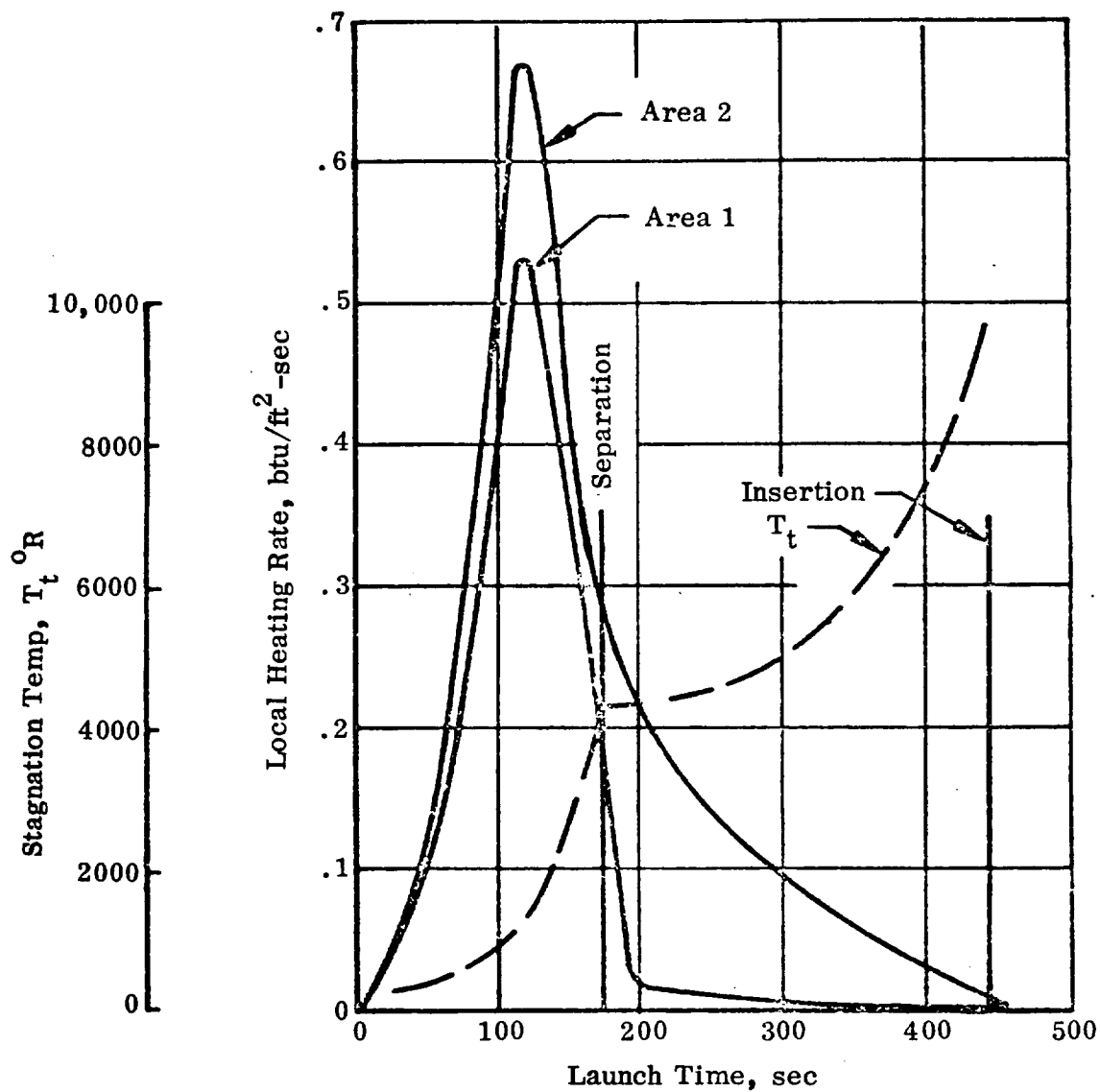


Fig. 3-2 Local Heating Rate and Stagnation Temperature History for Orbiter During Launch

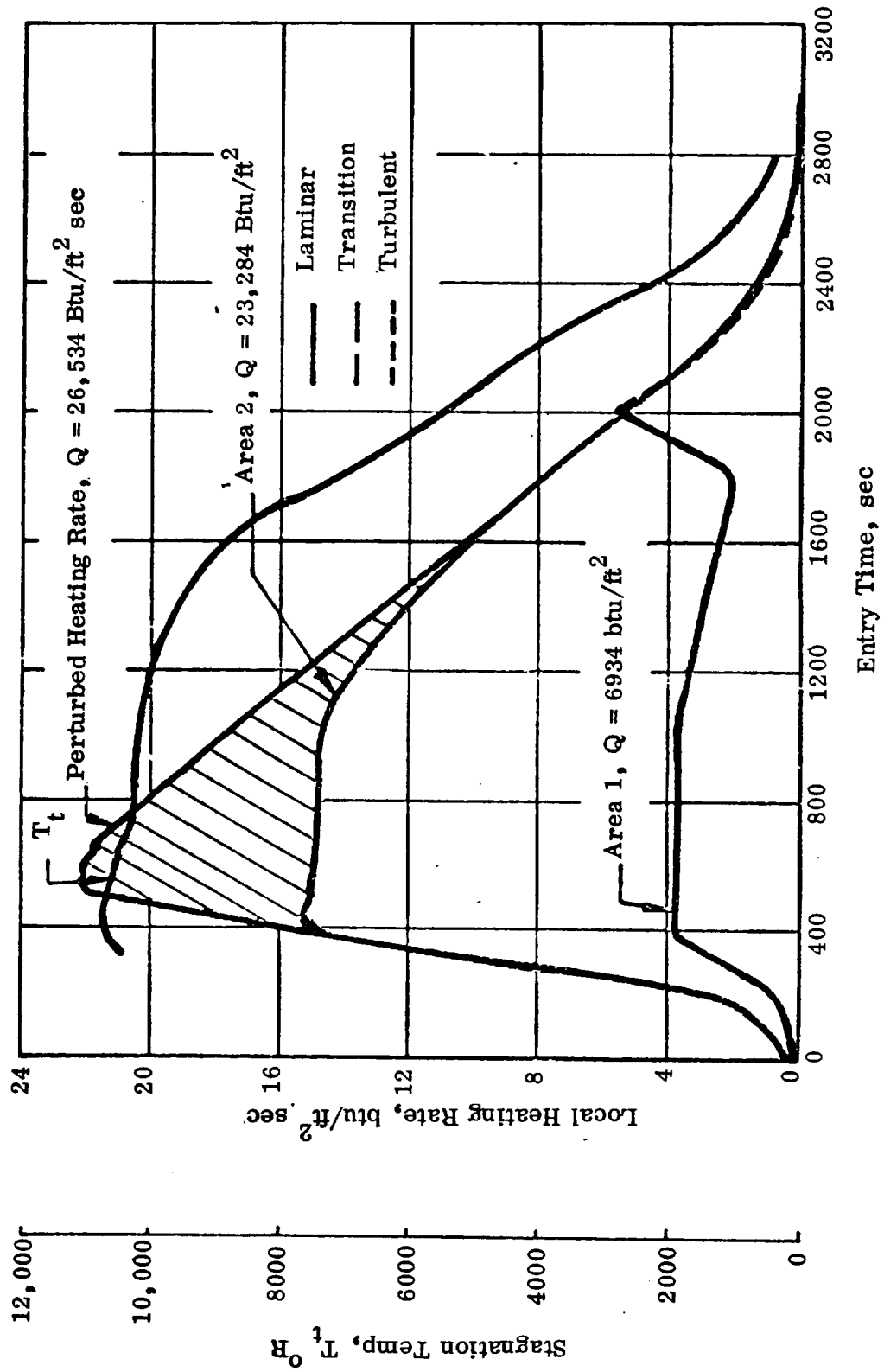


Fig. 3-3 Local Heating Rates and Stagnation Temperatures Histories for Orbiter During Reentry

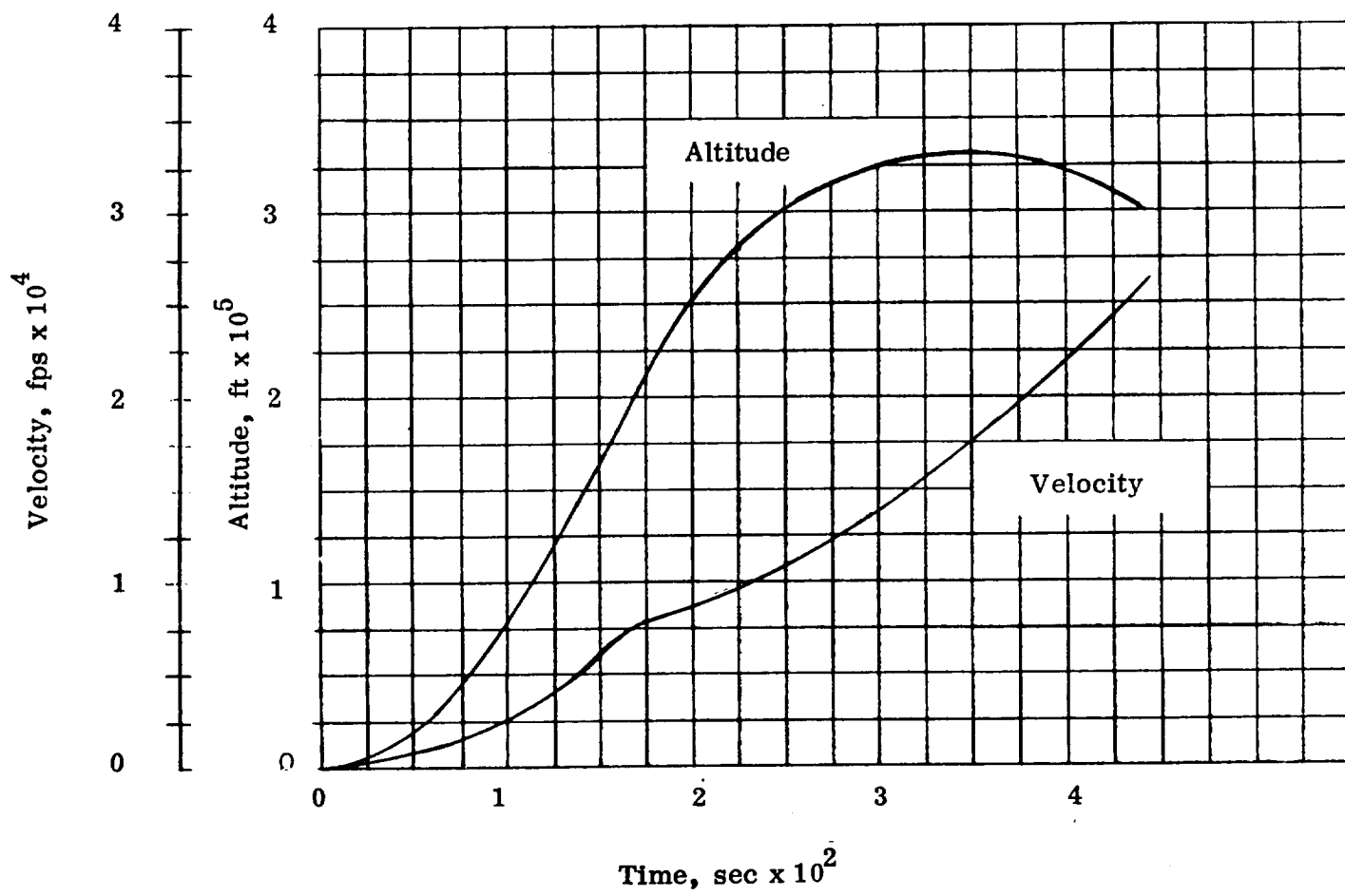


Fig. 3-4 Orbiter Launch Trajectory

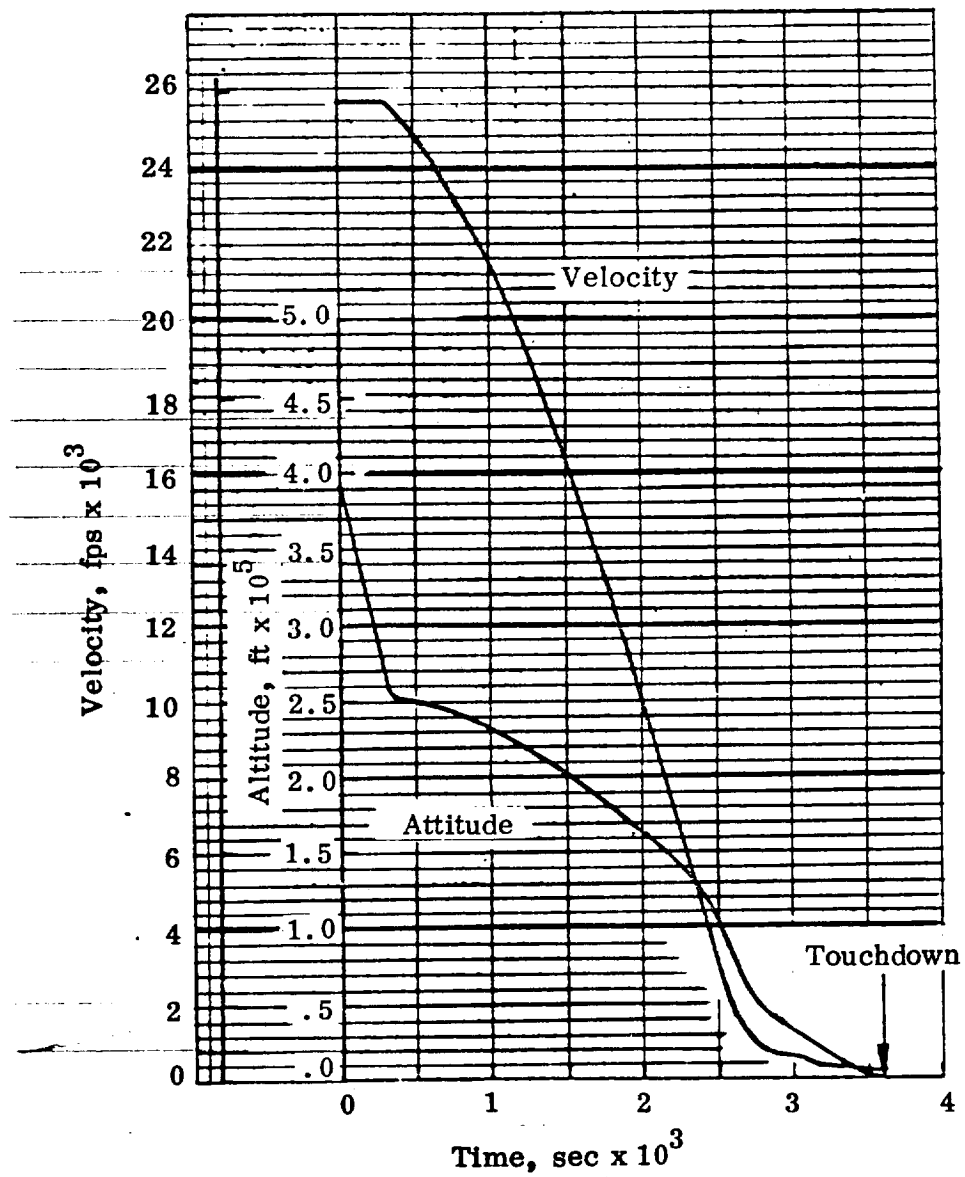


Fig. 3-5 Orbiter Entry Trajectory

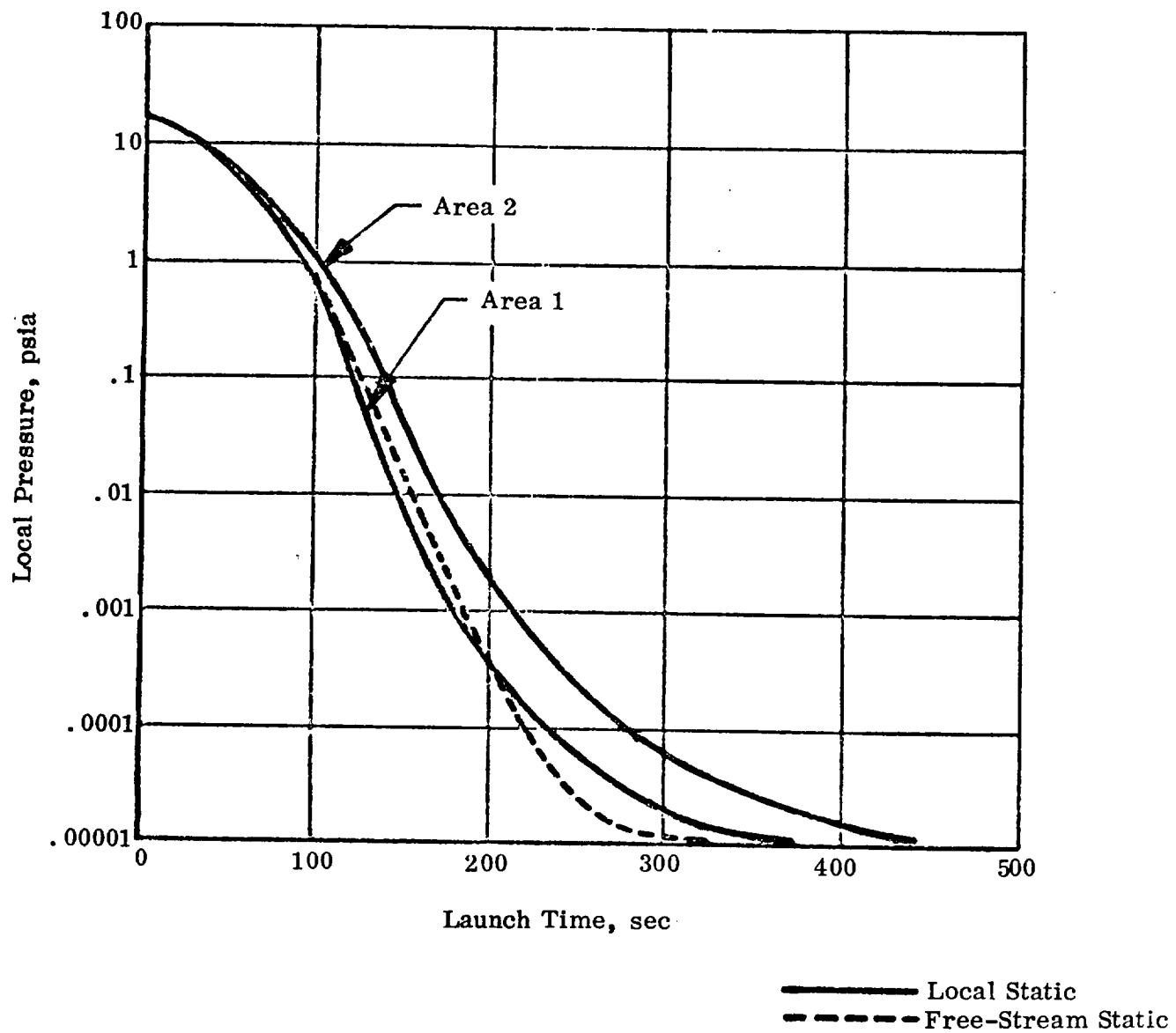


Fig. 3-6 Local and Free-Stream Static Pressure Histories on Orbiter Fuselage Centerline During Launch

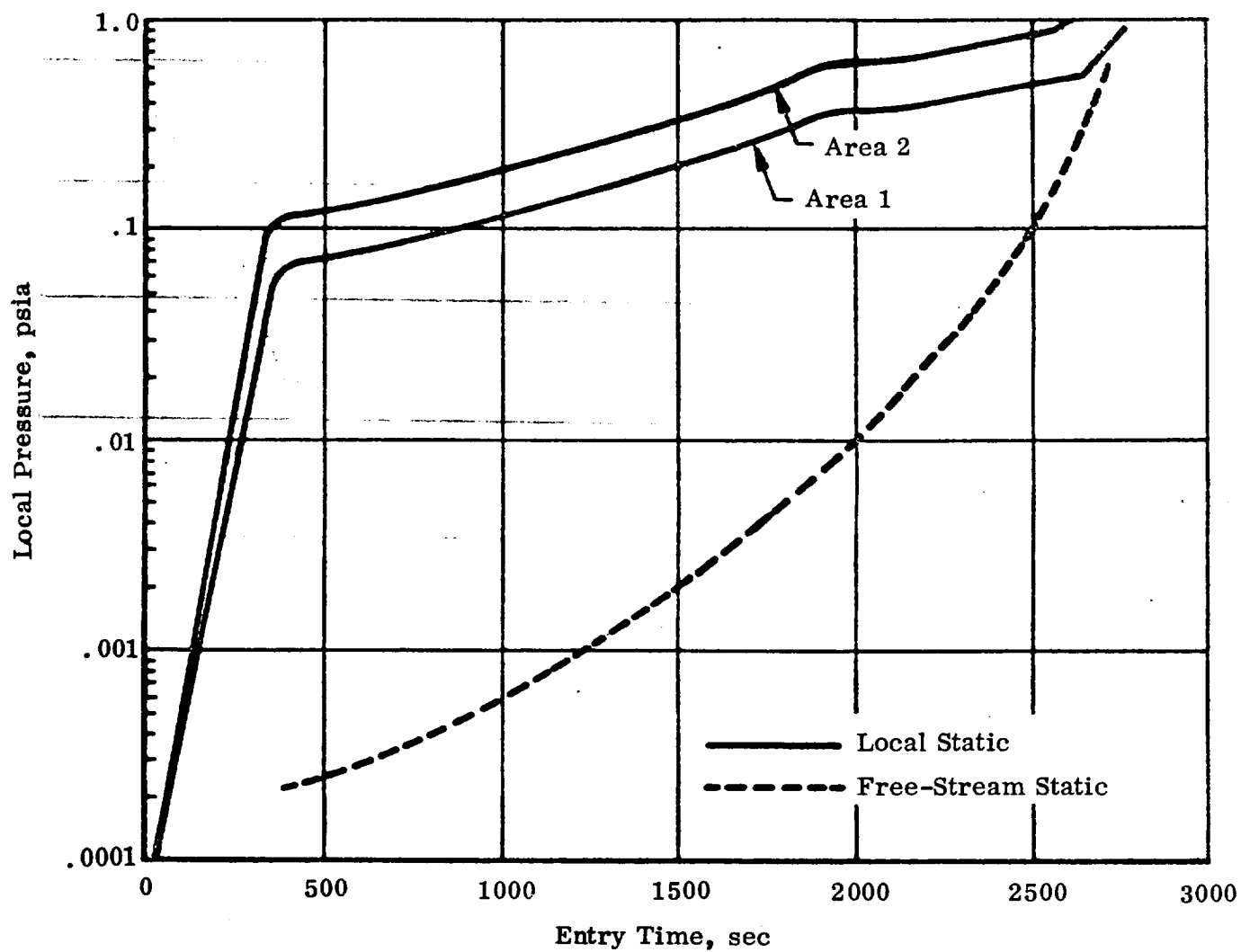


Fig. 3-7 Local and Free-Stream Static Pressure Histories on Orbiter Centerline During Entry

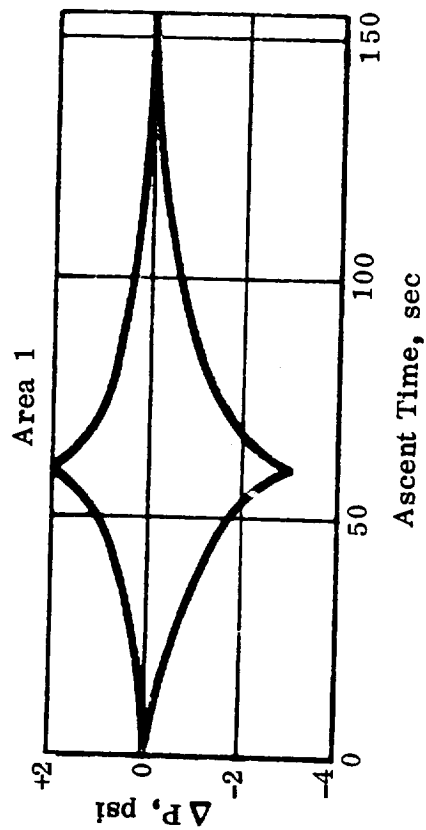
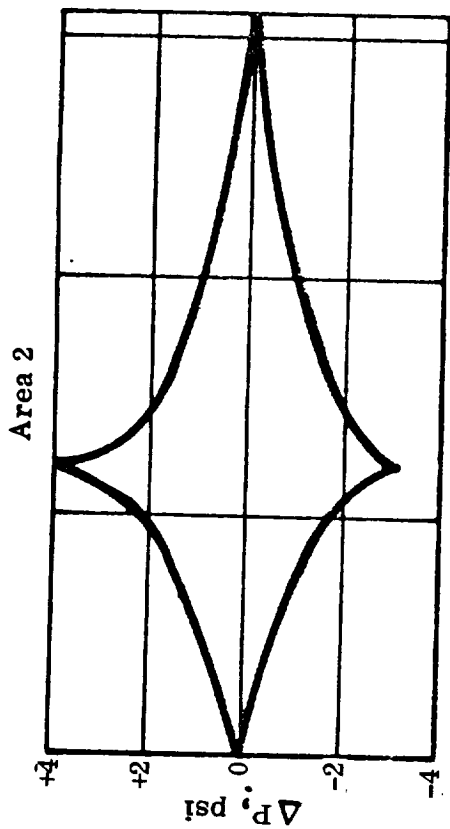


Fig. 3-8 Limit Differential Panel Pressure for Ascent

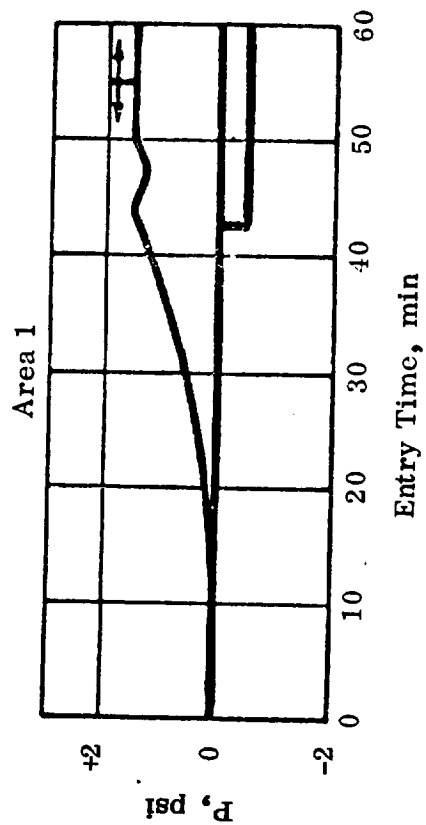
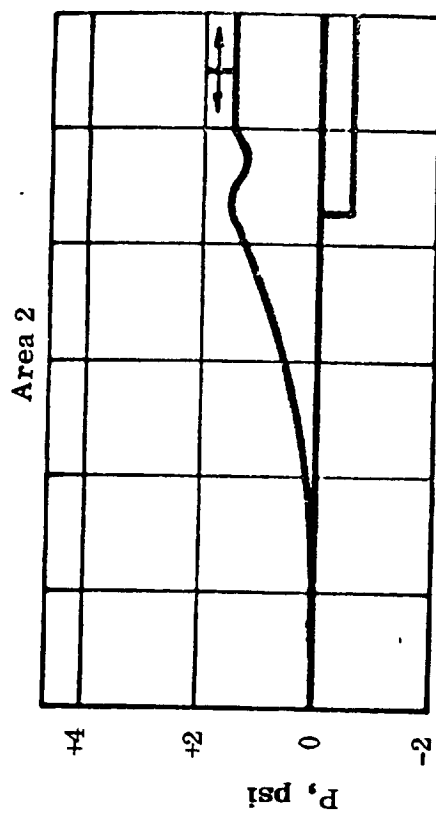


Fig. 3-9 Limit Differential Panel Pressure for Entry

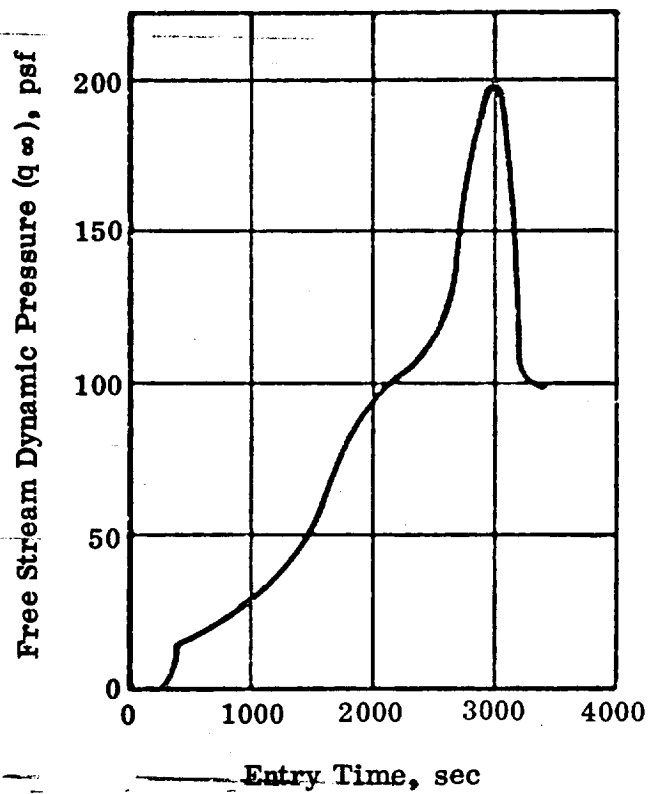
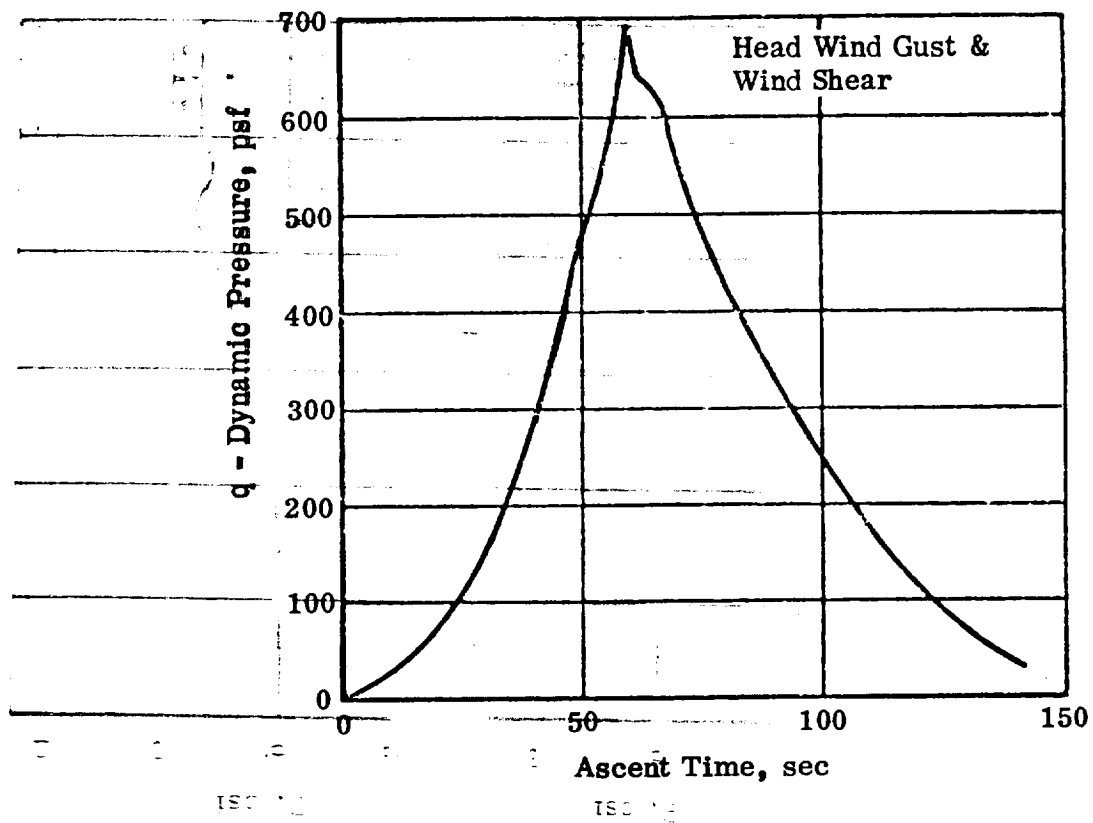


Fig. 3-10 Ascent and Entry Dynamic Pressures



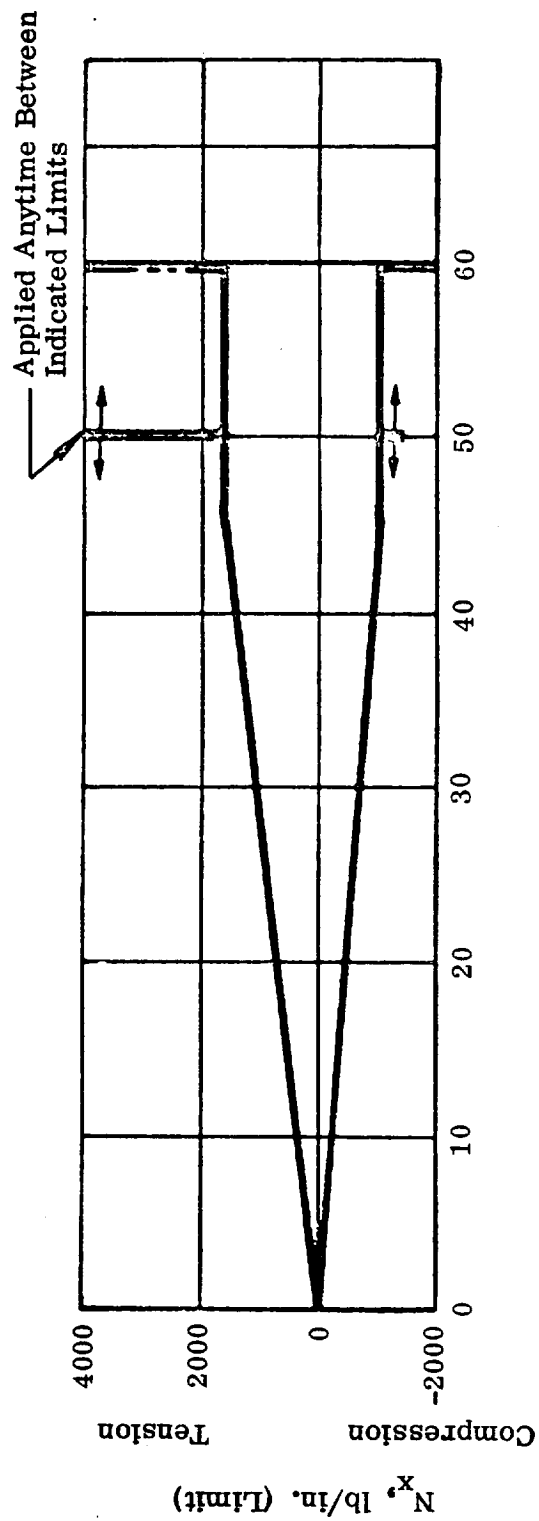
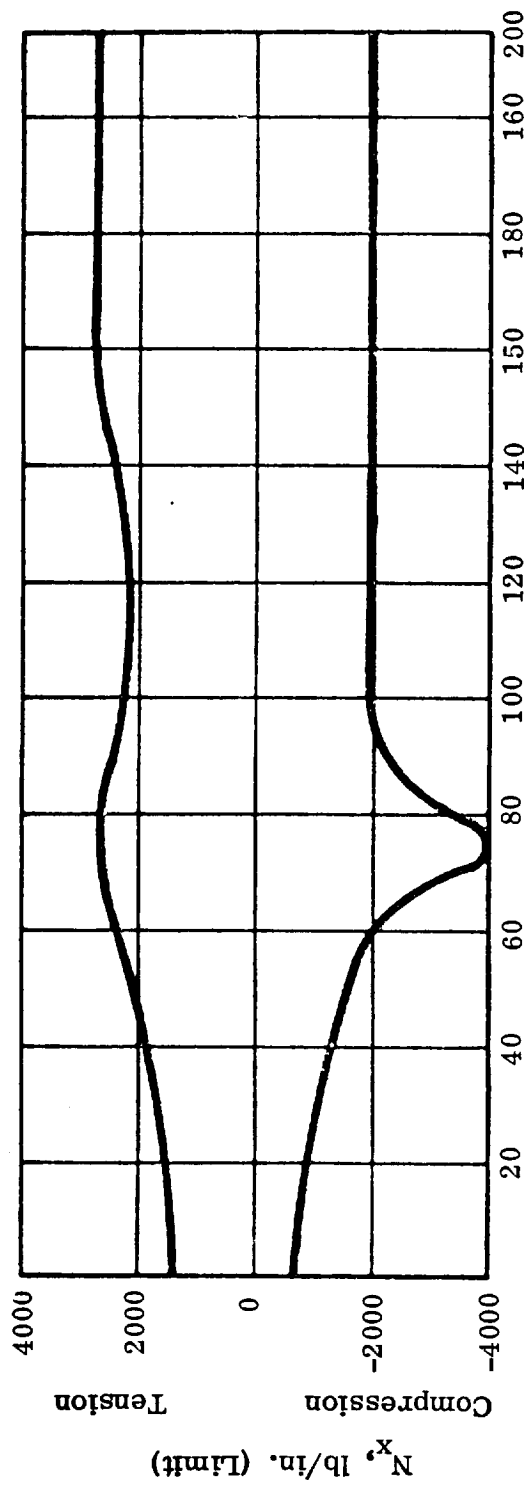


Fig. 3-11 Ascent and Entry Internal Loads for Orbiter Area 1  
20-in. Panel Length

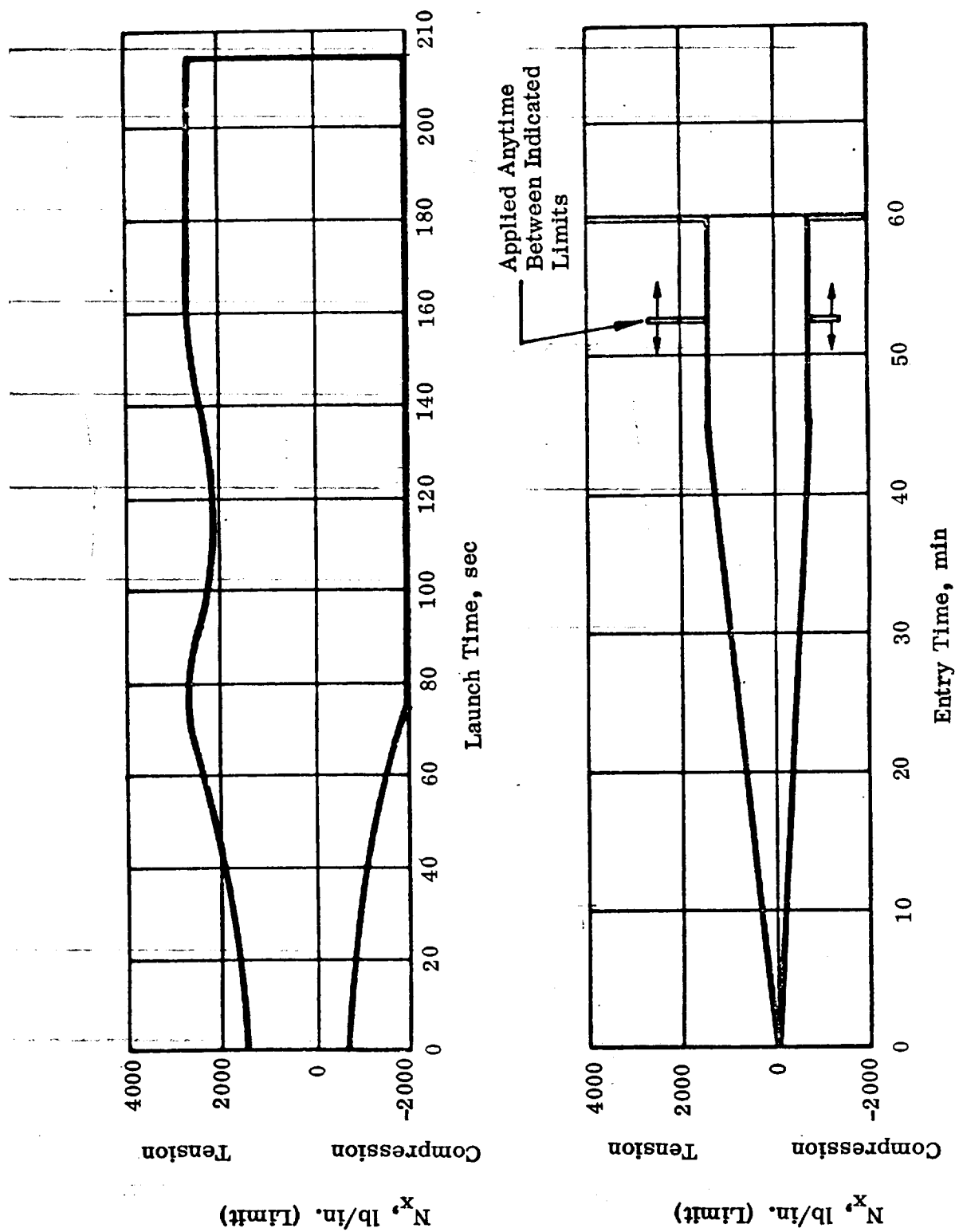


Fig. 3-12 Ascent and Entry Internal Loads for Orbiter Area 2  
24-in. Panel Length

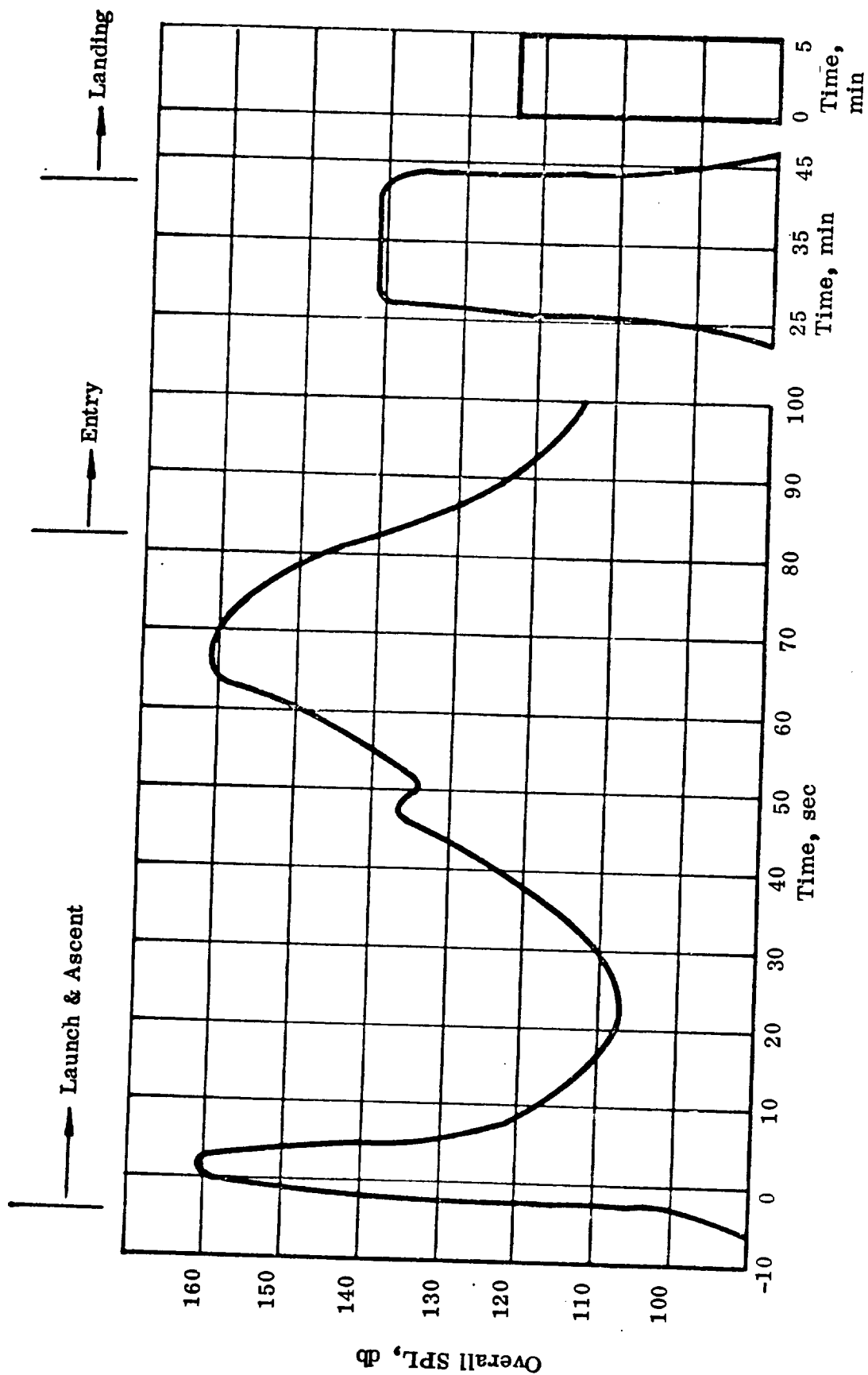


Fig. 3-13 Overall SPL vs Time-Typical Orbiter Mission

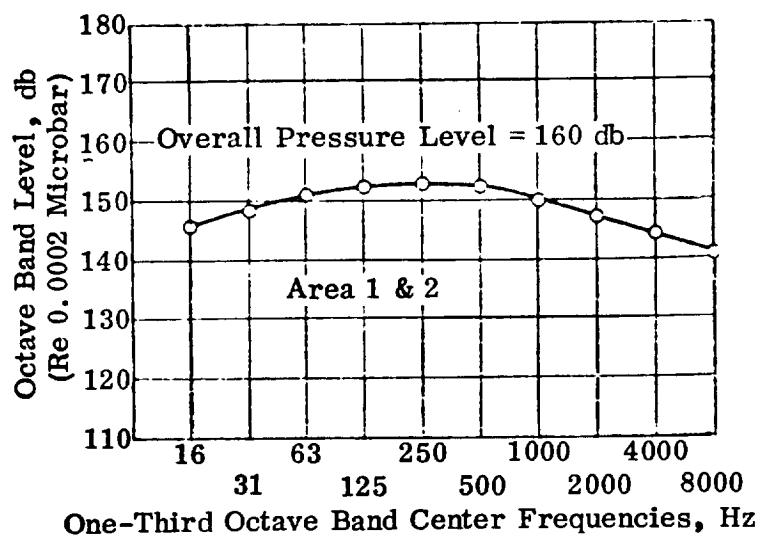


Fig. 3-14 Sound Pressure Levels-Liftoff

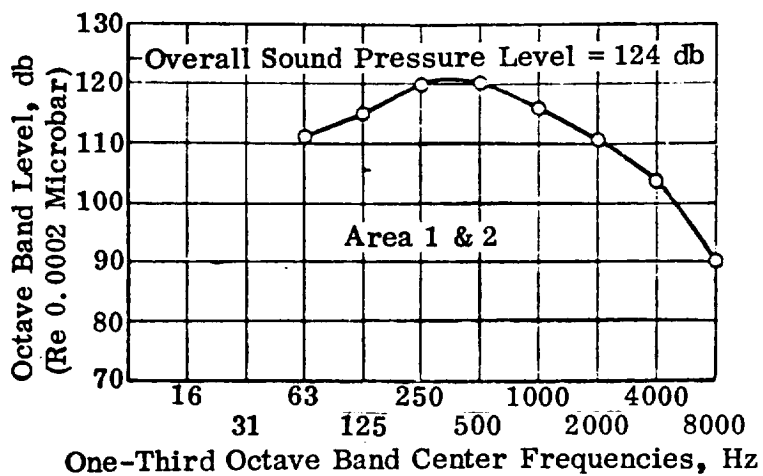


Fig. 3-15 Sound Pressure Levels-Air Breathing Engines; Maximum Static Thrust

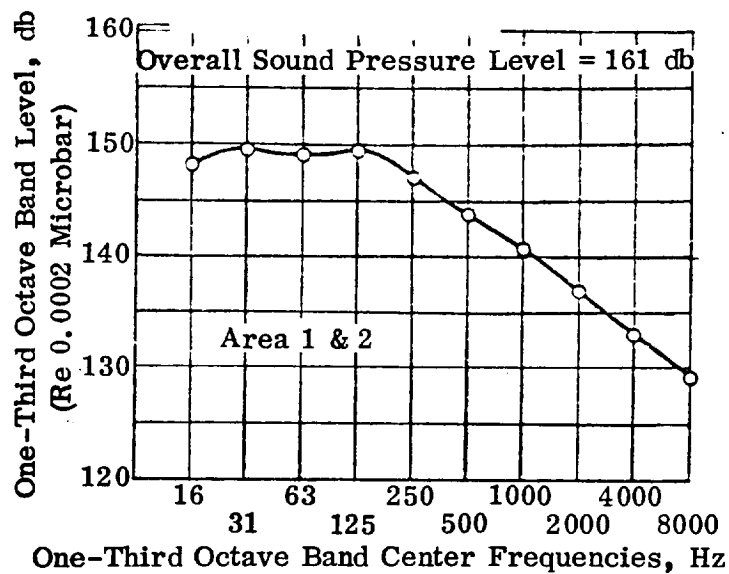


Fig. 3-16 One-Third Octave Band Fluctuating Pressure Levels-Ascent ( $M = 1.4$ ,  $Q = 600$  psf)

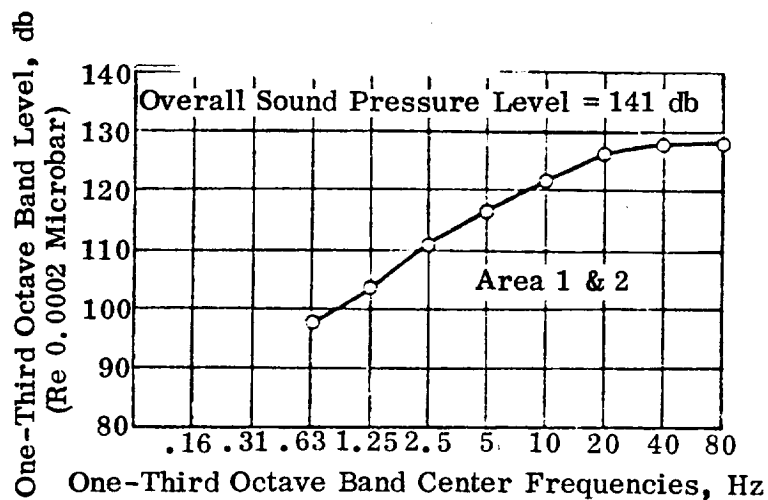


Fig. 3-17 One-Third Octave Band Fluctuating Pressure Levels-Entry ( $M = 4$ ,  $Q = 100$  psf)

#### 4.0 Material Characterization

##### 4.1 Material Description

Closed Pore Insulation (CPI) refers to a class of unique, glass-ceramic materials which were created to allow design approaches to the thermal protection system (TPS), that could eliminate three major design constraints: (1) complex brittle coatings, (2) low strength rigidized fibrous insulations and (3) elastomeric adhesives and strain isolator foam pads which may embrittle during extended cold soak in space operations. These constraints derive from shortcomings in conventional RSI materials.

Table 4-1 gives the requirements of a TPS material for the Space Shuttle mission. After a careful analysis of these requirements and the identification of problem areas associated with RSI-type heat shields, it was decided that a porous foam with a non-interconnecting network of cells would offer the best means for overcoming the above-mentioned problems. Such a material must (1) have an acceptable density range for Shuttle application, (2) have a high emittance built into the material, (3) provide moisture and water resistance by virtue of its non-interconnected cell network, (4) have superior mechanical properties due to the rigid continuous network of cell walls.

A Grumman IRAD Program, designed to meet the above objectives, led to the discovery of the unique ability of fly ash cenospheres to produce high temperature closed cell foams. (Ref. 1)

##### 4.1.1 General Description of Cenospheres

Cenospheres are a pollution by-product of coal burning power plants. When the pulverized coal ash emanating from the exhaust stacks of these furnaces is allowed to settle in collection lagoons, a small constituent of the ash (0.1 to 4.0 wt. %) floats on the surface. This floating fraction of the fly ash (cenospheres) consists of hollow microspheres of an aluminosilicate glass with diameters in the range of 20-200 micrometers. The thickness of the nonporous shells ranges from 2-10 micrometers. The tap density of the cenospheres varies between 250-400 kg/m<sup>3</sup>, depending on the source. The evolution of carbon dioxide and nitrogen gases inside the aluminosilicate particles during their stay in the stack (several milliseconds

Table 4-1 REQUIREMENTS OF EXTERNAL INSULATION MATERIAL

- Low Density
- Low Thermal Conductivity
- Multiple Re-use Under Shuttle Launch & Re-entry Cycling
- Thermal, Chemical & Mechanical Stability at Hi Temps
- Good Thermal Overshoot for Off-Nominal Trajectories
- High Emittance Surface
- Resistance to Water Pickup During Launch & Ground Ops (Rain & Moisture Humidity Cycling)
- Resistance to High Velocity Gas Erosion
- Good Handling Characteristics
- Resistance to Vibration & Acoustic Noise
- Resistance to Aero & g-loads
- Sufficient Mechanical Strength for Direct Attachment to Primary Structure
- Ease of NDT Inspection, Removal & Replacement
- Ease of Scale-up & Fabrication
- Design Flexibility
- Good Reliability & Predictability

at 1700 K) results in their expansion to cenospheres. It is believed that the formation of the hollow sphere is due to the presence of  $\text{Fe}_2\text{O}_3$  and unburned carbon in the fly ash particle. In this mechanism, the carbon dioxide produced by the reduction of  $\text{Fe}_2\text{O}_3$  to  $\text{FeO}$ , combined with the reaction of the alumina and silica to form an alumino-silicate glass, expands the glassy particle into a hollow sphere against the viscous forces in the glass and atmospheric pressure. The rapid passage of the fly ash particles through the steep temperature gradients causes the glass to "freeze" into the range of particle sizes observed.

Although cenospheres come from many different sources, their chemical compositions are quite similar; this may indicate that their formation occurs only under a rather stringent set of conditions, perhaps favoring some particular quasi-equilibrium state.

Cenospheres are obtained from a domestic source (West Virginia) and an imported source (England). The spheres are collected by "skimming" them off the surface of lagoons into which the fly ash residues are pumped. Table 4-2 gives the chemical analysis of the major constituents of cenospheres from both sources.

An X-ray analysis of the as-received cenospheres indicates the presence of a primary silicate glass phase with a small amount of mullite. Heating the cenospheres above 1500 K results in a significant crystallization of the glass into the mullite phase with a subsequent reduction in the amount of glassy phase. Since the cenospheres contain a large amount of silica (60 wt. %), it was expected from the alumina-silica equilibrium diagram that crystallization of the glass would lead to the formation of some cristobalite (or possibly quartz). This would lead to serious problems with the thermal stability of the material as the phase inversions associated with cristobalite or quartz formation would lead to a destruction of the material on thermal cycling; however, none of the crystalline forms of silica were observed during any subsequent heat treatments. Apparently



Table 4-2 Chemical Analysis of Cenospheres

<u>Compound</u>	<u>Wt %</u>
$\text{Al}_2\text{O}_3$	30.2
$\text{SiO}_2$	59.9
$\text{Fe}_2\text{O}_3$	3.7
$\text{K}_2\text{O}$	3.9
$\text{Na}_2\text{O}$	1.2
$\text{TiO}_2$	1.8
$\text{CaO}$	0.9
$\text{MgO}$	0.3

Table 4-3 Typical CPI Data Sheet

Initial Dimensions (cm)	22.8x22.8x1.9 (8 in. X 8 in X 1 in)
Initial Density ( $\text{kg/m}^3$ )	430 (27 pcf)
Final Dimensions (cm)	19.5x19.5x1.25 (7.6 in. X 7.6 in. x .5 in.)
Final Density ( $\text{kg/m}^3$ )	720 (45 pcf)
Wt % Water Absorption	2.05
Appearance of Tile	Square, uniform texture and appearance, no cracks, monolithic

the alumino-silicate equilibrium reactions are sufficiently sluggish to make the appearance of these phases unlikely.

The effect of high emittance additives such as cobalt oxide was investigated and led to the development and characterization of two CPI compositions; CPI-4 and CPI-8, with CoO being 4 and 8 wt %, respectively.

#### 4.1.2 Processing of CPI Compositions

The successful production of CPI materials is closely related to the processing procedures and firing schedules. Figure 4-1 indicates, by means of a diagram, the processes involved in producing 23cmx23cmx3cm CPI tiles.

The as-received cenospheres\* are placed in stainless steel trays and decrepitated at 800K for 8 hrs to remove any absorbed water entrapped in the glassy shell. Decrepitation is accompanied by a crackling sound associated with the rapid evolution of gas from the glassy sphere.

The decrepitated spheres are placed in a large glass beaker (3000ml) containing a low density fluid such as hexane or heptane (S.G.=0.66), and the floating fraction of the of the spheres are recovered. This procedure, which was found to eliminate the dense, cloudy, carbonaceous material and broken spheres, leaves a floating layer of transparent, lightweight, perfect, spheres. Figure 4-2 shows the spheres after recovery in the fluid.

The as-beneficiated spheres are then mixed with a fugitive organic binder, such as glycerin, and blended with a pre-weighed quantity of cobalt carbonate powders in a Hobart-type blender. The mixture is then placed into a mold and pressed into a block. The block is removed from the mold, dried at 300K, and is then placed into a silica muffle and fired in either a gas fired or an electric kiln in air.

\* Source: Appalachian Power Company, Glasgow, West Virginia

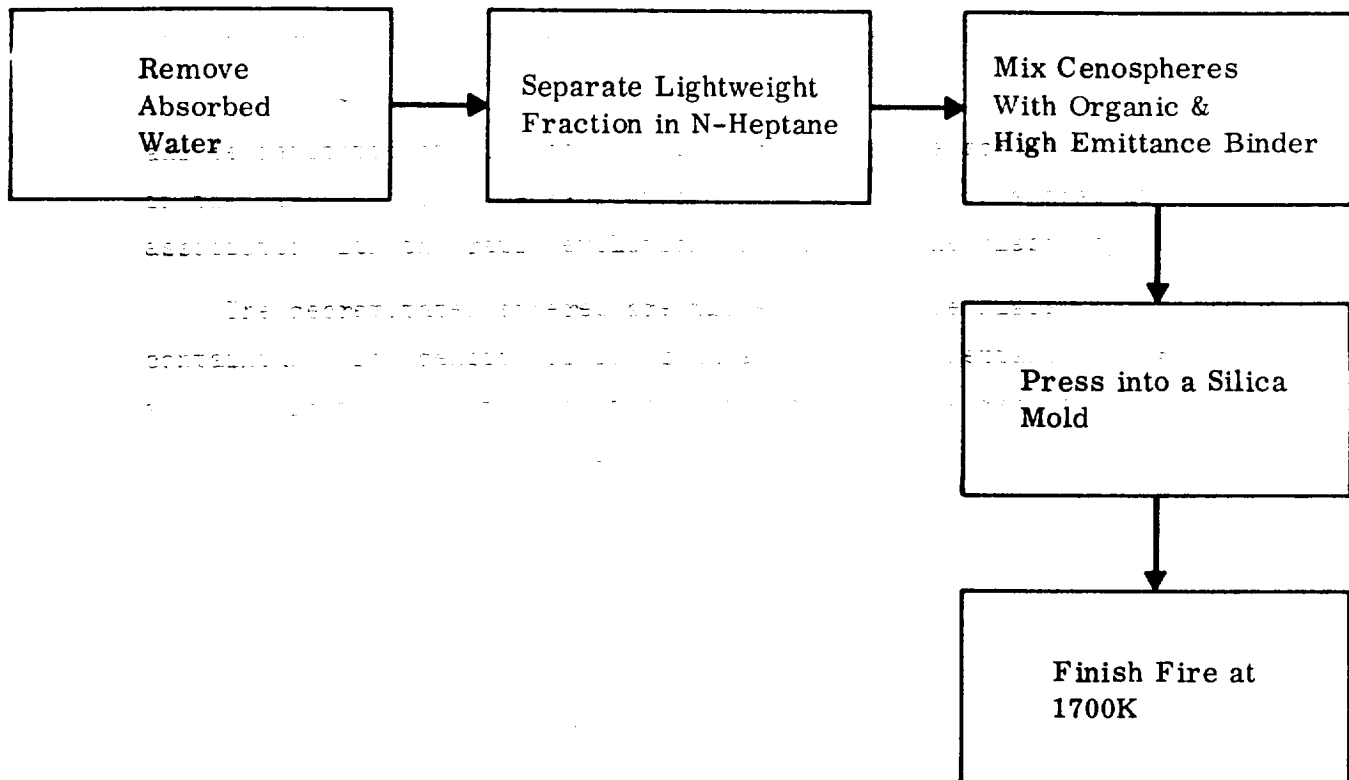
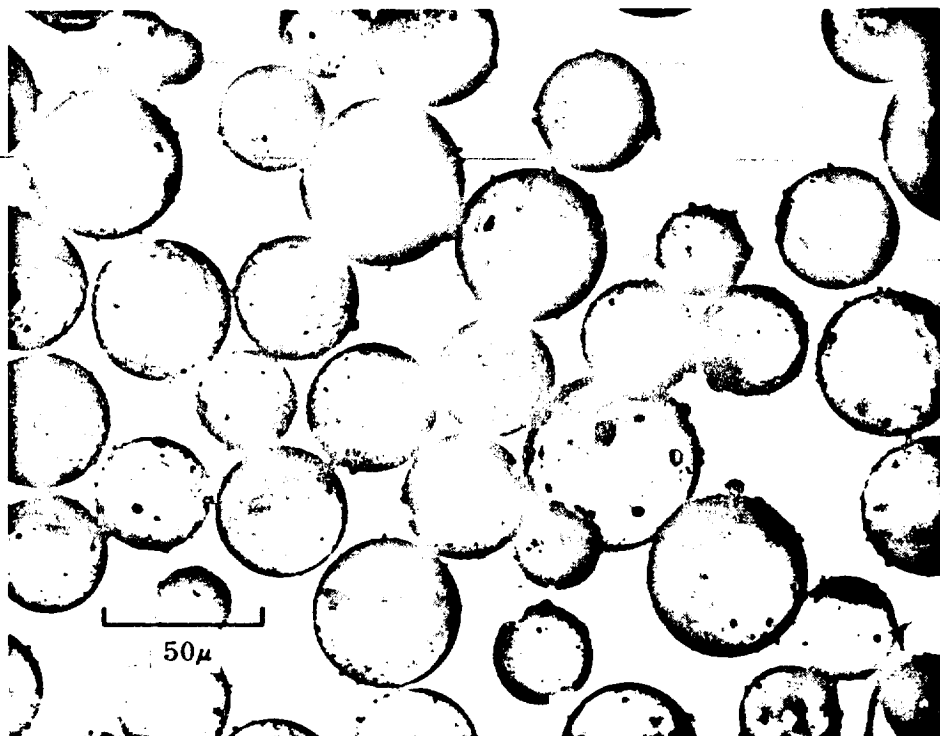


Figure 4-1 CPI Process Development



**Figure 4-2** Photomicrograph of Cenospheres

Two critical temperatures ranges in the firing process have been identified: (1) below 800K where the organics burn off and (2) above 1400K where rapid sintering and densification occur. Firing rates and times must be carefully controlled to ensure a monolithic, closed cell tile. In addition, the hot zone uniformity and the thermal mass of the tiles and muffles have been shown to have a significant effect on the tile quality and firing cycle. All of these parameters have been optimized to produce tiles with the desired properties for the design studies.

Initially CPI-8 was baselined for this study (Ref. 1). However, as the designed requirements were firmed up, it became clear that improvements in mechanical properties of the first generation CPI materials were necessary. Further development work identified CPI-4 as a significantly superior material in terms of mechanical properties.

This new composition was optimized, scaled-up and characterized for this program. The thermo-physical properties of these two materials are described in the following paragraphs.

#### 4.1.3 Physical Properties of CPI Tiles

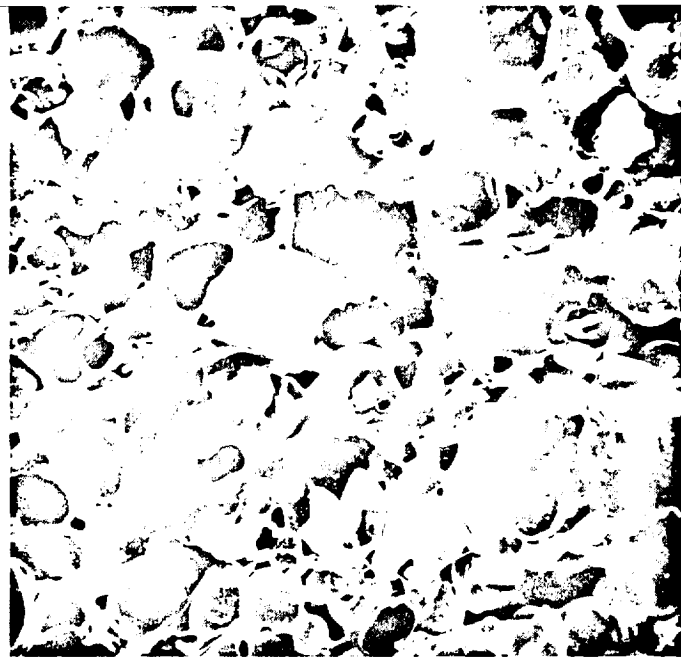
##### 4.1.3.1 Density and Physical Dimensions

Table 4-3 gives the typical dimensions and densities of unfired and fired CPI tiles used for the test program. Densities were measured by weighing pre-dried tiles (400K) and recording the dimensions of pre-cut and ground blocks as measured with a Vernier caliper.

In order to assure uniformity of properties, the dimensions of the fired tile were as close to the required tile size as possible. Machining operations accounted for a 5-10% loss of material.

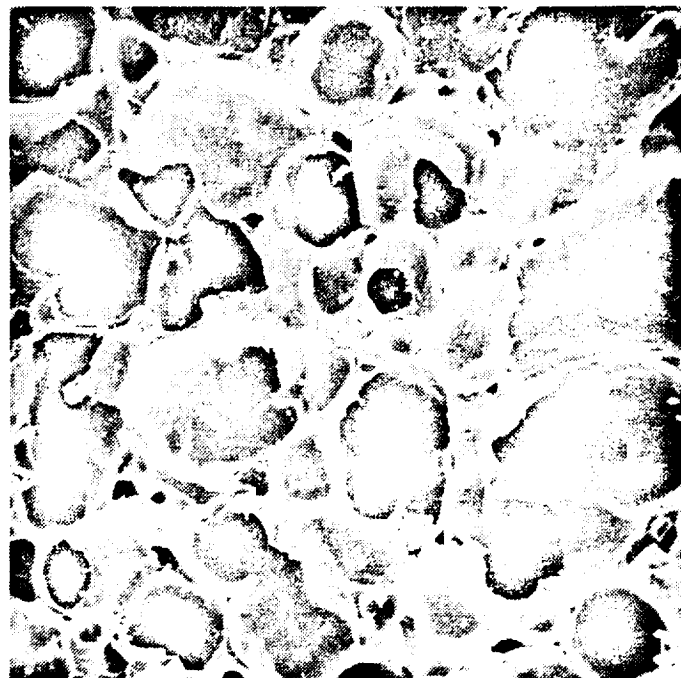
##### 4.1.3.2 Microstructures of CPI Tiles

The fired tiles had a foam-like appearance and closed pores. Figure 4-3 shows scanning electron micrographs of typical CPI-4 and CPI-8 compositions. The average pore size of the CPI-4 samples was 80 micrometers and that of the CPI-8 samples was 170 micrometers. These values are averages of measurements made on 10 micrographs for each series. The difference in pore size between the CPI-4 and CPI-8 materials is consistent with



(100X)

(a) 4 Wt. % CoO Additive



(100X)

(b) 8 Wt. % CoO Additive

Figure 4-3 Scanning Electron Microscope Photographs of Sintered Cenosphere Bodies Fired at 1650° K for One Hour

the effect of cobalt additions in this system. The general microstructure of fired CPI depends on the action of the expanding gas entrapped in the cenospheres and the viscosity of the glassy cenosphere shell at the firing temperature. By adding cobalt oxide to the cenospheres, the viscosity of the glassy shell is decreased at the firing temperature. Thus, larger pore sizes are encountered with increasing cobalt oxide content due to the fluxing action of the cobalt. It should be noted that the average pore size of the fired CPI without cobalt additions is about 75 micrometers. The decrease of viscosity with increasing cobalt is also shown in the softening point data that are discussed later in this report.

#### 4.1.3.3 Crystallography of CPI Materials

The X-ray diffractograms of CPI blocks indicate the presence of mullite ( $3\text{Al}_2\text{O}_3 \cdot 2\text{SiO}_2$ ), cobalt aluminate ( $\text{CoAl}_2\text{O}_4$ ) and a glass phase. In general, as the cobalt addition increased, the amount of cobalt aluminate present increased while the amount of mullite decreased. Preliminary X-ray results indicate that the solubility of the cobalt oxide in the cenospheres is about 4 wt. %. At higher cobalt oxide additions, crystallization of cobalt aluminate occurs. As-fired tiles of CPI-4 have been observed to show further crystallization of cobalt aluminate upon heat treatment in the 1200-1500 K range. This phenomenon is related to the increasing solubility of  $\text{CoO}$  in the glass phase at the formation temperature of the foam and the nucleation and growth of the glass-ceramic at the lower temperatures.

4.1.3.4 Water Absorption. Measurements were made by a simple immersion test. Samples (nominally 0.23 cm x 0.23 cm x 0.3cm) were weighed and then immersed in a beaker of water at room temperature for 96 hours. The samples were removed from the beaker, dipped in alcohol to remove any water just held into the surface pores, and were then reweighed. The change in weight was recorded and the water absorption was calculated according to the following formula:

$$\% \text{ WA} = \text{Wt gained/Dry Wt of Block} \times 100 \quad (1)$$

Table 4-4 summarizes the water absorption data. These low values of water absorption are consistent with a closed cell foam.

Figure 4-4  
Blocks Fired at 1000°C

Table 4-4 PHYSICAL PROPERTIES OF CPI

PROPERTY	4% CoO	8% CoO
MICROSTRUCTURE	NETWORK OF CLOSED CELLS	
COLOR	BROWN-BLUE	DARK BLUE
DENSITY ( $\text{kg/m}^3$ )	630-770 (39-48 pcf)	530-670 (33-42 pcf)
WT % WATER ABSORPTION	0.5-4	0.5-4
AVERAGE PORE SIZE	80 $\mu\text{m}$	170 $\mu\text{m}$
AVAILABLE SIZES	23cmx23cmx 3 cm	23cmx23cmx X 3 cm
AVAILABLE SHAPES	FLAT TILE	FLAT TILE
MACHINABILITY	MACHINABLE CERAMIC WITHIN 0.005 CM TOLERANCE	



#### 4.1.3.5 Machinability of CPI Materials

CPI materials are nonfriable and can be easily machined into any size and shape with conventional carbide tooling; however, the abrasive nature of the material reduces tool lifetime and tolerances and diamond tooling is the preferred drilling and cutting medium. CPI plates have good handleability. However, the brittle nature of the material requires some care, as with any glass body. The materials can be scaled up into larger and more complex components with minimum tooling problems.

#### 4.1.4 Thermal Properties of CPI Materials

##### 4.1.4.1 Thermal Expansion

Linear thermal expansion measurements were made on CPI-4 and CPI-8 samples. A fused quartz dilatometer was used and the slope of the percent linear expansion versus temperature curve in the temperature region of 298 K (room temperature) to 1073 K was taken as the average linear coefficient of thermal expansion. It should be noted that all traces were linear in this temperature region so the slope approximation is valid. A heating rate of 473 K per hour was used on all runs. Softening points of the glassy phase in the CPI samples were also extrapolated from the curves. Table 4-5 shows the results of this study. It can be seen from these data that as the cobalt content is increased in this system, the thermal expansion increases and the softening point decreases. Figure 4-4 shows the normalized expansion of the CPI-4 and CPI-8 material versus temperature.

4.1.4.2 Differential Thermal Analysis. DTA runs were made on the CPI-4 and CPI-8 materials to verify their thermodynamic stability. Powdered samples were used in all runs and the reference material was alumina. Two typical DTA traces are shown in Figure 4-5. It can be seen from these traces that there were no phase change or crystallization heat effects evident from room temperature to about 1500 K. The broad endothermic

**Table 4-5 THERMAL AND CHEMICAL PROPERTIES OF CPI**

PROPERTY	4% CoO	8% CoO
THERMAL EXPANSION (RT-1370K)	$5.2 \times 10^{-6}/K$ ( $2.9 \times 10^{-4}/^{\circ}F$ )	$5.4 \times 10^{-6}/K$ ( $3.0 \times 10^{-6}/^{\circ}F$ )
HEAT CAPACITY RT-725K (JOULE/kg-K)	8-9	7.1-8.4
CRYSTALLOGRAPHY	MULLITE COBALT ALUMINATE GLASS	
DILATOMETRIC SOFTENING POINT	1300K	1250K
TOTAL NORMAL EMISSION RT-1500K	0.63-0.65	0.75-0.78
TOTAL NORMAL EMISSION OF COATED SAMPLE	0.82-0.88	
THERMAL STABILITY (DTA)	FURTHER CRYSTALLIZATION OF COBALT ALUMINATE AT 1300-1500K	NO CHANGES
CHEMISTRY	$Al_2O_3$ , $SiO_2$ $Fe_2O_3$ , $CoO$ , $TiO_2$ , $Na_2O$	
CHEMICAL RESISTANCE	NOT ATTACKED BY MOST ACIDS, OR ORGANIC MATERIALS	

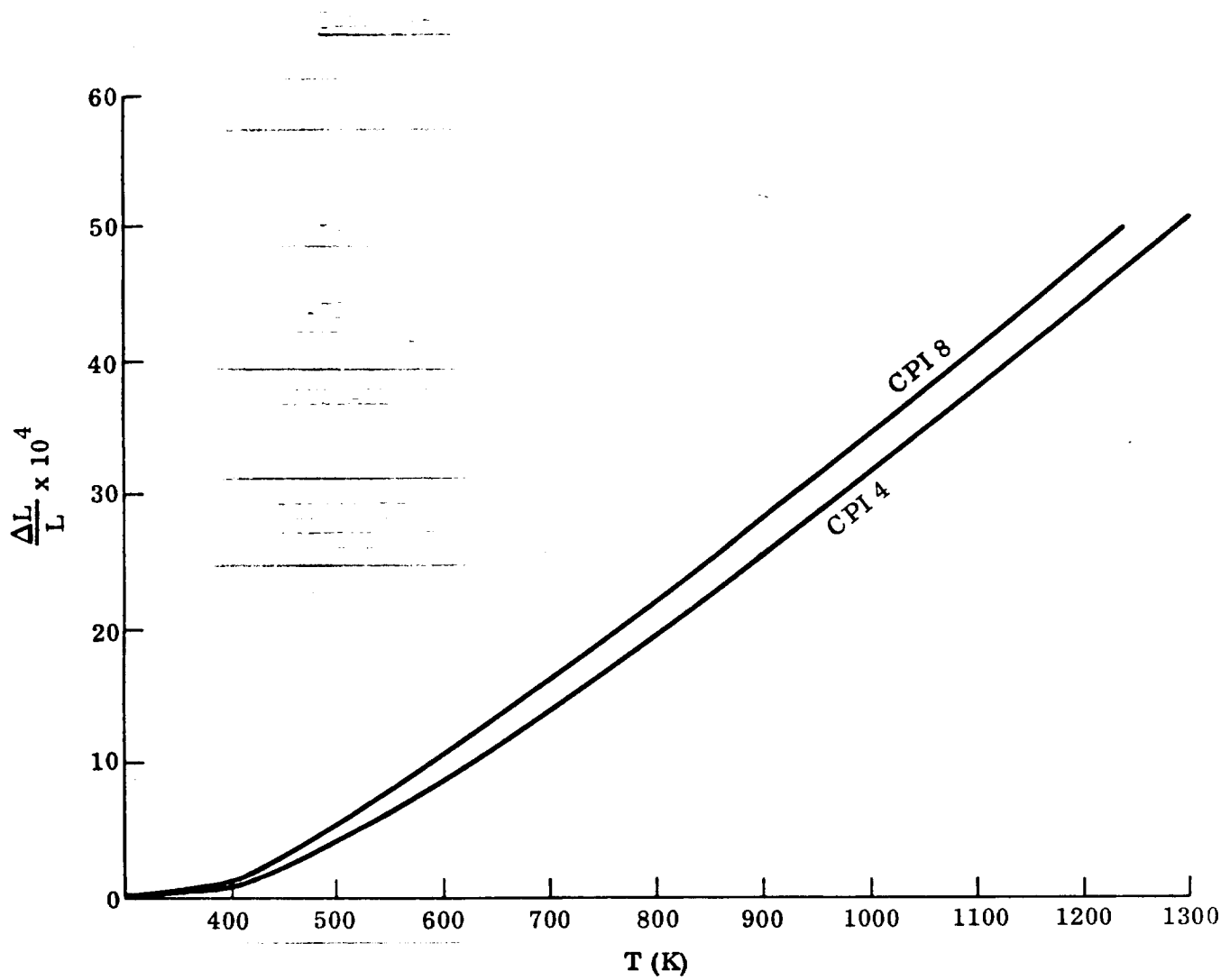


Figure 4-4 Thermal Expansion of CPI Materials vs. T(K)

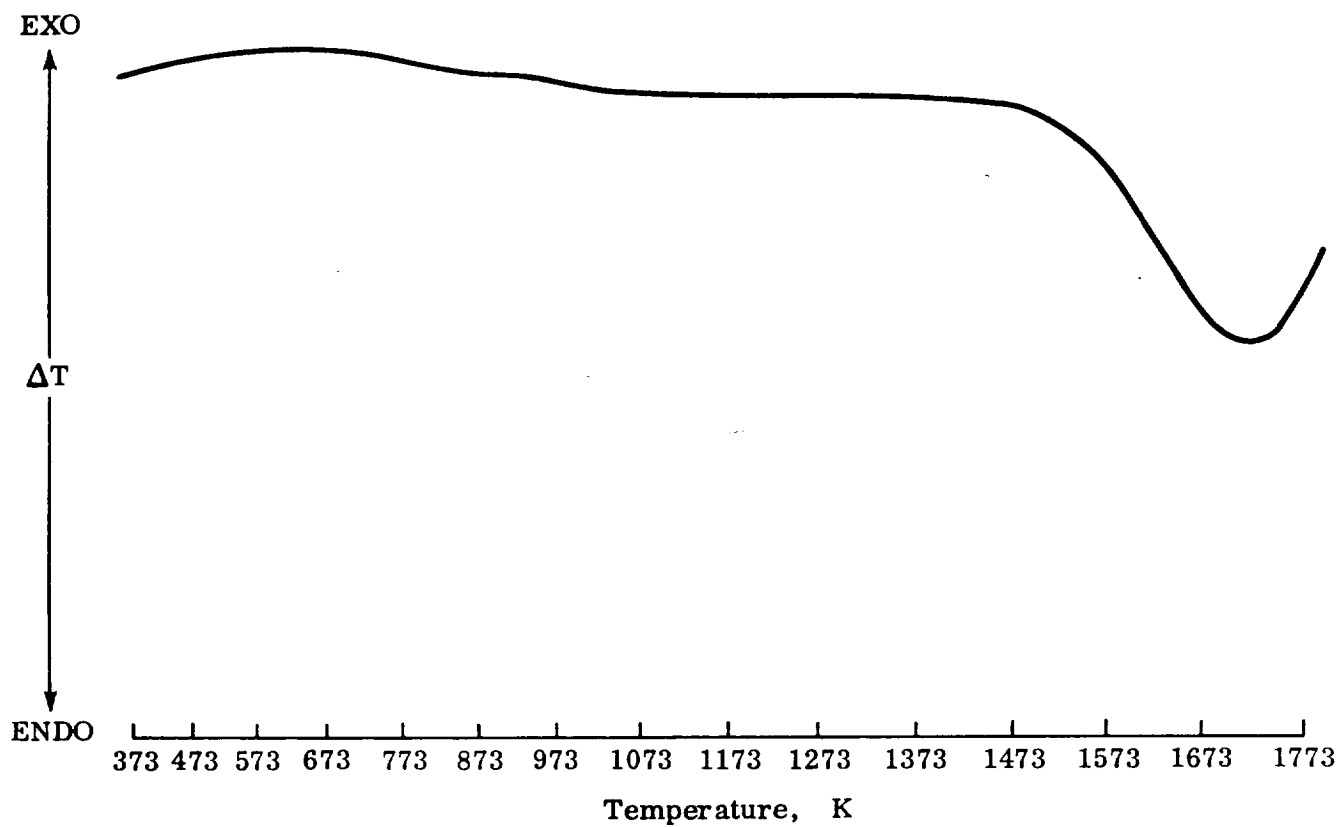


Figure 4-5 Typical Differential Thermal Analysis Traces of Scaled-Up CPI-4 and CPI-8 Tiles

peaks at about 1700K are associated with the melting of the crystalline phases in the CPI with the aid of the fluid glassy phase. X-ray diffractograms of CPI powdered samples quenched from 2073 K showed no evidence of crystalline phases, i.e., the quenched material formed a stable glass.

4.1.4.3 Specific Heat. These values were measured on the CPI-4 and CPI-8 series materials from room temperature to 723 K using a differential scanning calorimeter. It appears that as the amount of cobalt additive is increased, the specific heat decreases. The values for mullite, obtained from the literature (Ref. 2), are plotted for comparison in Figure 4-6. As the cobalt content is increased in the CPI, more cobalt aluminate is formed at the expense of mullite. Because specific heat is generally considered an additive function, it was expected that as the amount of mullite present decreased, the specific heat should decrease, which was the observed effect.

4.1.4.4 Total Normal Emittance Measurement. The total normal emittance, in the temperature range 750-1533 K, was measured in a universal high temperature emissometer (Ref. 2). The experimental setup and measurement procedures are presented in Ref. 2. Emittance measurements were made to verify the projected use of these CPI tiles in a re-radiative-type heat shield. Total normal emittances greater than 0.75 are necessary to allow CPI to be considered as a candidate heat shield material. Figure 4-7 is a plot of the emittance data. For comparison, the emissivity of CPI with no additive is given. The straight lines drawn on this graph are a least squares fit of the data and are an indication of the trend.

It is not clear from these experimental results whether the emittance-temperature behavior shown is indeed real; the maximum experimental error for a particular emittance value is 7 percent, which is larger than the percent differences between the emittance values obtained. Future work, wherein the temperature dependence of the spectral emissivity is measured, should help resolve this point. To enhance the emissivity of CPI-4 a diffusion coating of CoO was developed by spraying a coat of a cobalt-organo-metallic compound followed by burn-off at 1500K to remove the organic material and fuse the thin CoO into the glassy surface. (See Fig. 4-7)

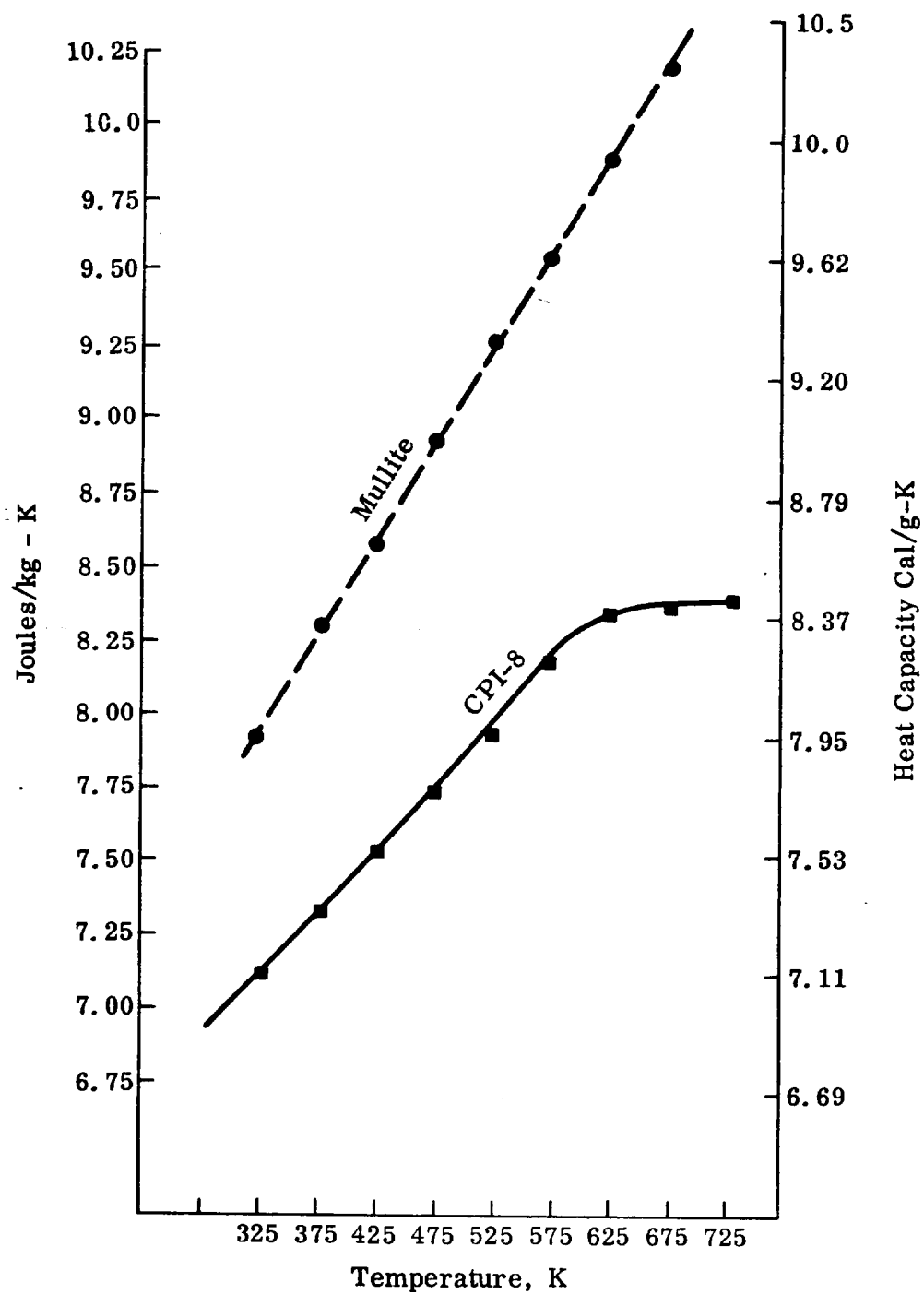


Figure 4-6 Heat Capacity versus Temperature of Scaled-Up CPI-8 Tiles and Mullite

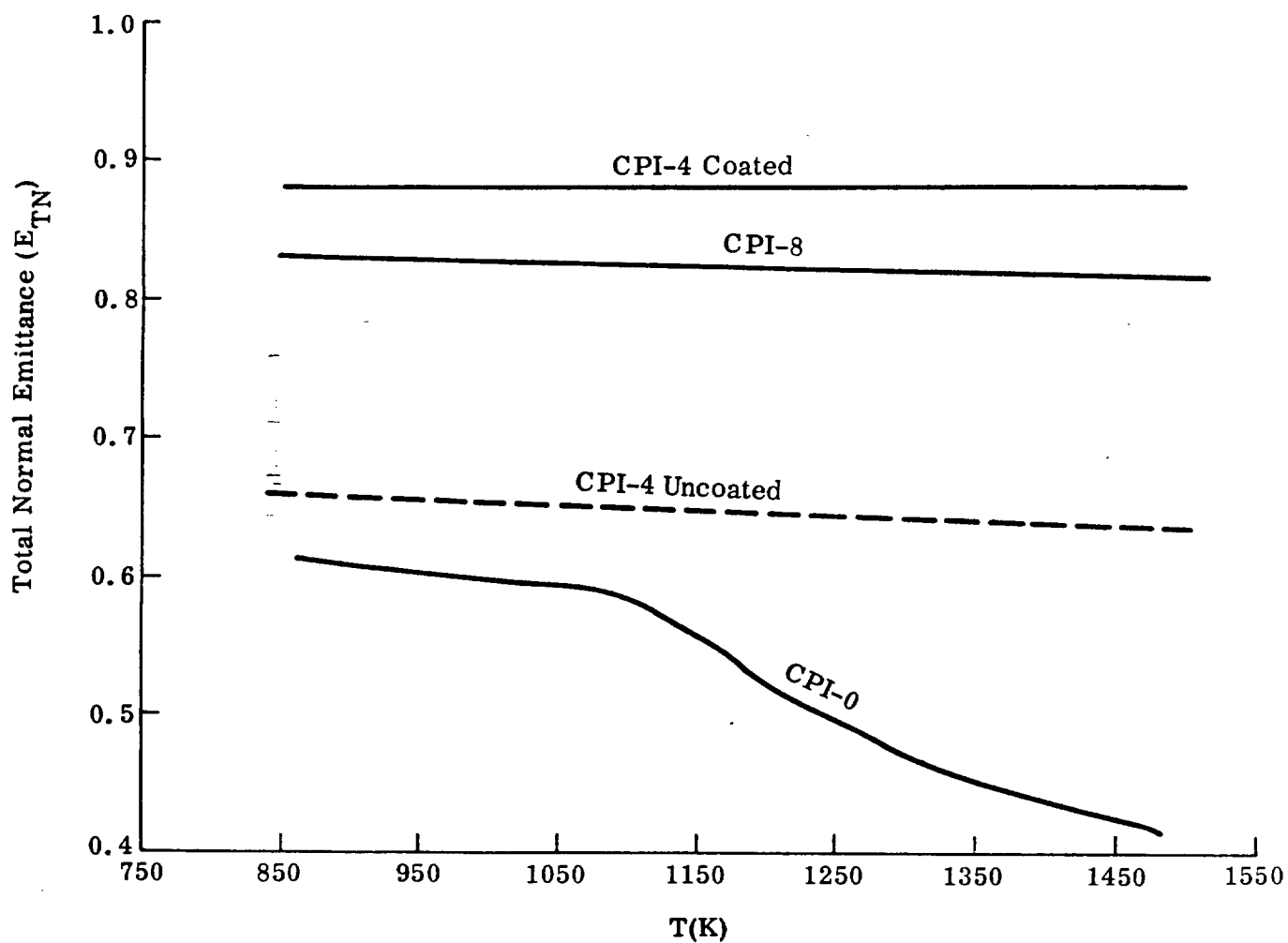


Figure 4-7 Total Normal Emittance ( $E_{TN}$ ) for CPI-4, CPI-8 (Coated and Uncoated) and CPI-0 vs. Temperature (K)

4.1.4.5 Thermal Conductivity Measurements. These measurements were made on the CPI-4 and CPI-8 series materials from 368 to 1478 K. The measuring system employed a radial heat flow across a hollow cylindrical sample. The experimental setup and measurement procedures are described in detail in Ref. 1. Thermal conductivity at elevated temperatures is a measure of the heat transfer by solid conduction and radiation. All of the samples tested had approximately the same density, so that the contribution of the solid heat conduction was fairly constant. Due to the smaller pore size of the CPI-4 material, it was expected that these samples would scatter the radiation component of the heat transfer to a greater extent resulting in a lower over-all thermal conductivity. However, because of this smaller pore size (at the same density as the CPI-8 samples), the walls between pores were thinner. This fact, combined with the lower cobalt content of the CPI-4 series materials, accounted for a lower absorption capability. The CPI-8 has a larger pore size and is thus a less efficient scatterer. It has thicker walls between pores and a higher cobalt content causing their absorption to be greater (as can be seen in the emissivity data). As a result of the compensating effects of the competing scattering and absorption mechanisms described above, the thermal conductivity values of the CPI-4 and CPI-8 materials were similar. These data are presented in Figure 4-8.

#### 4.1.5 Characterization of Fibrous Materials

##### 4.1.5.1 Introduction

Although materials characterization program concentrated on CPI it became apparent early in the program that composite heat shield designs involving CPI and ceramic fibrous insulators offered the greatest potential for a low cost, weight competitive TPS. Since time did not permit detailed studies of fibrous insulation, it became necessary to consider commercially available materials. Only minor modifications of these materials were made, as needed, to simplify their integration with CPI or with the attachment system.



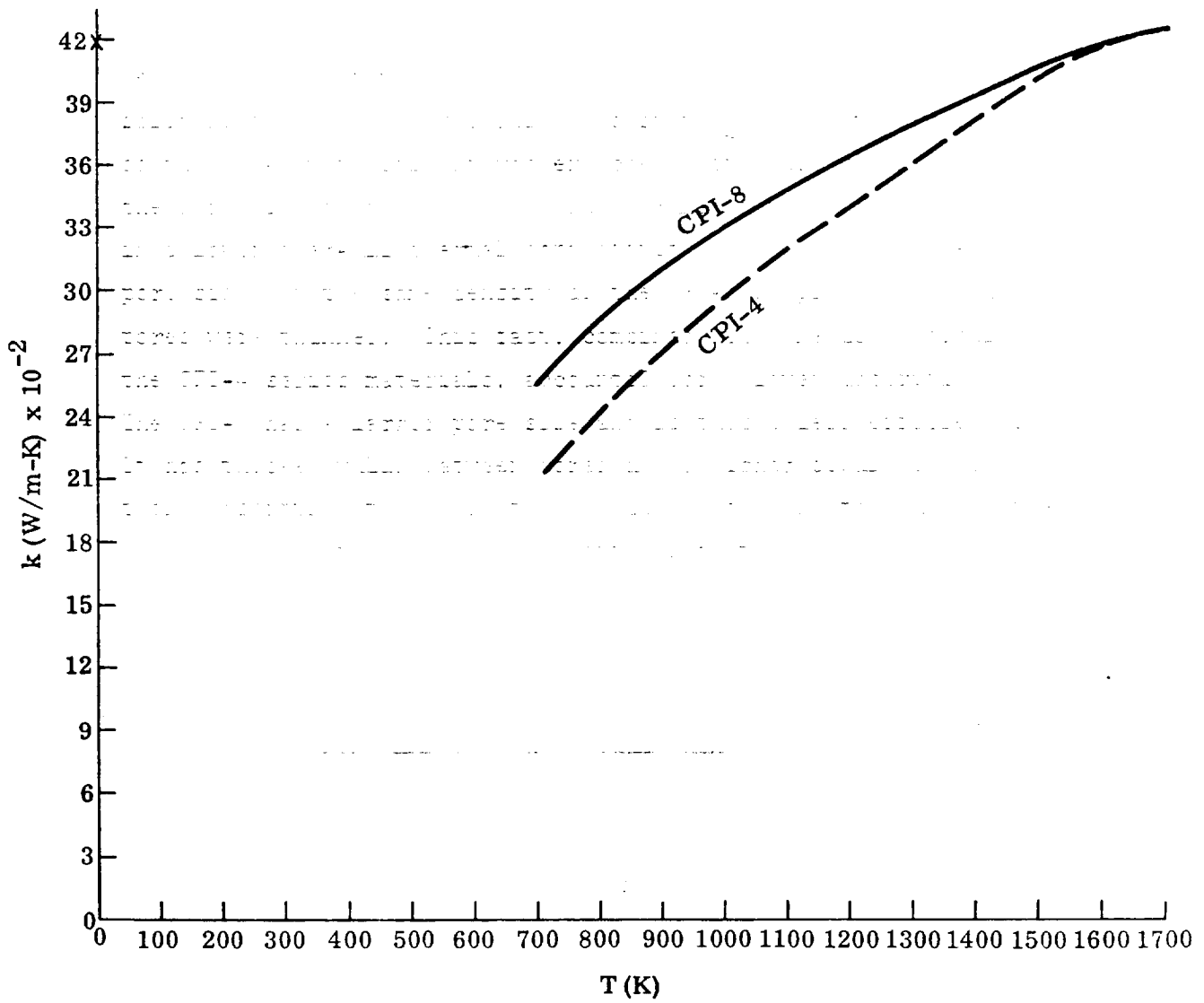


Figure 4-8 Thermal Conductivity of CPI-4 and CPI-8 vs. T ( K)

Two classes of commercially available insulators were considered: (1) low density fibrous blankets with densities in the range of 48-96 kg/m<sup>3</sup> and (2) rigidized fibrous boards with densities in the range of 192-288 kg/m<sup>3</sup>.

#### 4.1.5.2 Low Density Blankets

Low density fibrous blankets have the following advantages: (1) well characterized thermal properties, (2) excellent thermal shock resistance, (3) highest thermal efficiency per unit weight, (4) readily available, at low cost. They have the disadvantage in that they are not load bearing and must be handled carefully to avoid compaction. These fibers find applications in mechanically supported design applications of CPI and serve as a secondary insulations system.

Among the fibers selected from considerations were Microquartz\* Refrasil\*\* and Fiberfrax H\*\*\*. Figure 4-9 compares the thermal properties of these materials vs. temperature at one atmosphere. These data were taken from the manufacturer's handbook (Ref. 2-5). Table 4-6 lists the range of use temperatures for each insulation and the problems encountered with respect to Shuttle application.

#### 4.1.5.3 Rigidized Fibrous Insulations

The selection of industrial fibrous insulations was based on a design in which CPI is employed as a surface material and is directly bonded to the rigidized block. Selection of materials was based on (1) thermal stability of the fiber due to phase changes on cycling, (2) low shrinkage, (3) thermal shock resistance of the fibers, (4) thermal expansion match between CPI and the fibers and (5) availability and cost.

Based on these considerations, two basic rigidized fibrous insulations were selected for evaluation: (1) Kaowool Ceramic Fiber Block\* and (2) Mullite fibers\*\*. Fiberfrax H\*\*\* became available during the course of this investigation; however, insufficient time was available to evaluate

\* Product of Babcock and Wilcox Co.

\*\* Product of Babcock and Wilcox Co.

\*\*\* Product of Carborundum Co.

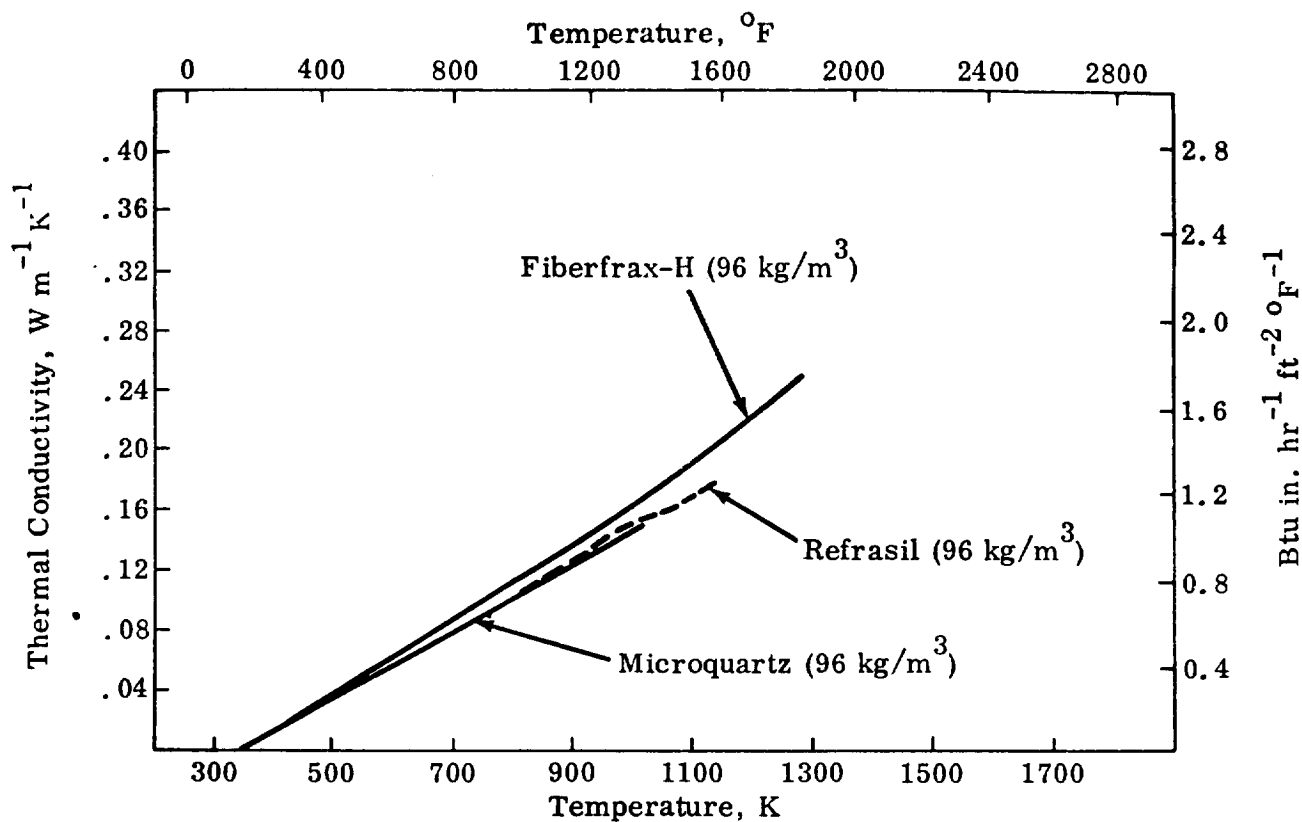
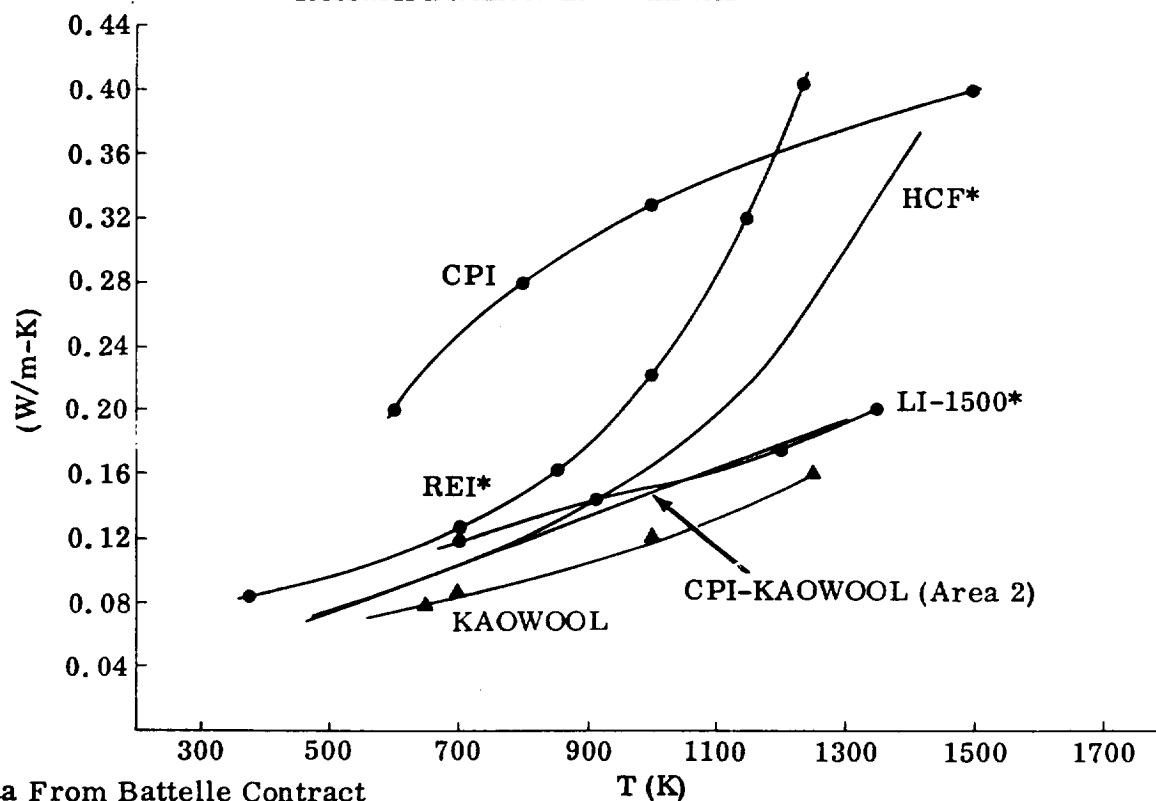


Figure 4-9 Thermal Conductivity of Microquartz, Fiberfrax-H and Refrasil Blankets in 1 Atm Air



\*Data From Battelle Contract  
NAS 9-10853

Figure 4-10 Thermal Conductivity (W/m-K) of Candidate TPS Insulation Materials vs T (K)

Table 4-6 CHARACTERISTICS OF LOW DENSITY FIBROUS INSULATIONS

TYPE	CHEMISTRY	AVAILABLE DENSITIES (kg/m <sup>3</sup> )	MAXIMUM USE TEMPERATURE (K)	MAJOR PROBLEMS
MICROQUARTS	99.5% SiO <sub>2</sub>	48-96	1300	SETTLING SHRINKAGE DEVITRIFICATION
REFRASIL	98% SiO <sub>2</sub>	48-96	1500	SETTLING SHRINKAGE
FIBERFRAX H	62% Al <sub>2</sub> O <sub>3</sub> 38% SiO <sub>2</sub>	96	1700	SETTLING SHRINKAGE

Table 4-7 PHYSICAL PROPERTIES OF KAOWOOL FIBERS

COLOR	WHITE
FIBER DIAMETER (MICROMETERS)	2.8
SPECIFIC GRAVITY	2.56
MEAN SPECIFIC HEAT	0.255 BTU/lb/F
TENSILE STRENGTH FIBER	1.9x10 <sup>5</sup> psi
TENSILE MODULUS FIBER	17x10 <sup>6</sup> psi
MELTING POINT	2000 K
KNOOP HARDNESS	700

rigidized blocks of this material). All of these materials are aluminosilicate fibers and should be chemically and thermally compatible with CPI aluminosilicate foams.

#### 4.1.5.4 Kaowool Block

Major emphasis was placed on this material as it offered the greatest potential in terms of thermal properties, availability, and low cost. Tables 4-7 and 4-8 give the principal properties of Kaowool ceramic fiber block. The thermal conductivity of this material is given in Fig. 4-10 along with other RSI materials, for comparison.

To assess this material's thermal stability, a study was conducted to identify the effect of isothermal heat treatment on the fibers' crystallinity. Table 4-9 summarizes these results which indicate that (1) the fiber is essentially glassy as-received; (2) at temperatures below 1300K the primary crystallization product is mullite; (3) at temperatures above 1320K the onset of crystallization of cristobalite is detected; (4) by 1400K significant cristobalite formation is observed.

#### 4.1.5.5 High Purity Kaowool Fibers

Although it was not possible to evaluate a new high purity fiber developed by the Babcock and Wilcox Co., a thermal stability study showed no evidence of cristobalite formation after 16 hrs at 1400K. Only mullite was observed. Table 4-10 gives the chemistry of these high purity fibers. Future in-house work will examine these materials' compatibility with CPI, for Area 2 and Area 2P exposures.

#### 4.1.5.6 Mullite Fibers

Mullite fibers were rigidized by a vacuum forming process using colloidal silica and starch binders. A total of six rigid blocks was fabricated for this study. Table 4-11 summarizes their physical properties. Table 4-12 gives the chemistry and physical properties of the mullite fibers. Although no thermal and mechanical property measurements were made on these fibers, it is believed that they should not differ significantly

Table 4-8 PROPERTIES OF KAOWOOL CERAMIC FIBER BLOCK

SERVICE TEMPERATURE	1300K
DENSITY ( $\text{kg/m}^3$ )	208-272 (13-17 ref)
MAXIMUM LINEAR SHRINKAGE (%)	0 AT 1270K 0.5 AT 1400K 1.00 AT 1500K
THERMAL	
CHEMISTRY OF BLOCK	
CERAMIC FIBER	90
INORGANIC BINDER	5
ORGANIC BINDER	5
CHEMISTRY OF KAOWOOL FIBER	
(WT %)	
$\text{SiO}_2$	51.6
$\text{Al}_2\text{O}_3$	41.8
$\text{TiO}_2$	1.6
$\text{Fe}_2\text{O}_3$	0.90
$\text{Cr}_2\text{O}_3$	0.08
$\text{MgO}$	0.30
$\text{Na}_2\text{O}$	0.006
CHEMISTRY OF INORGANIC BINDER	
(WT %)	
$\text{SiO}_2$	50
$\text{Al}_2\text{O}_3$ WATER	40
	10
CHEMISTRY OF ORGANIC BINDER	
CARBON	70
HYDROGEN	10
OXYGEN	20
MODULUS OF RUPTURE	55 psi
COMPRESSIVE STRENGTH (5% DEFORMATION)	24 psi
(10% DEFORMATION)	28 psi
PRICE	\$2.00/BOARD FOOT

Table 4-9 THERMAL STABILITY OF KAOWOOL CERAMIC FIBER BLOCK

DESCR	TEMPERA- TURE (K)	TIME	PHASES PRESENT	AREA MULLITE PEAK (ARBI- TRARY UNITS)	AREA CRISTOBALITE PEAK (ARBI- TRARY UNITS)
K	1220	1 HR 15 MIN	MULLITE	60	0
K	1220	2 HR 15 MIN	MULLITE	80	0
K	1220	3 HR 15 MIN	MULLITE	90	0
K	1220	15 HR	MULLITE	110	0
K	1280	2 HR 15 MIN	MULLITE	135	0
K	1280	24 HR	MULLITE	150	0
K	1280	6 HR	MULLITE	125	0
K	1280	3 HR 35 MIN	MULLITE	110	0
K	1370	3 HR	MULLITE $\alpha$ -CRISTOBA- LITE	160	108
K	1370	9 HR	MULLITE $\alpha$ -CRISTOBA- LITE	300	100
KR	1370	20 HR	MULLITE $\alpha$ -CRIST.	275	>400
K	1370	5 HR 30 MIN	MULLITE $\alpha$ -CRIST.	225	105
K	1370	1 HR 45 MIN	MULLITE $\alpha$ -CRIST.	192	66
K	1280	1 HR 30 MIN	MULLITE	125	0
K	1330	3 HR	MULLITE $\alpha$ -CRIST.	108	12
KR	1370	2 HR 20 MIN	MULLITE $\alpha$ -CRIST.	88	180
KR	1370	20 HR	MULLITE $\alpha$ -CRIST.	275	>400

Table 4-9 THERMAL STABILITY OF KAOWOOL CERAMIC FIBER BLOCK (Cont.)

DESCR	TEMPERA- TURE (K)	TIME	PHASES PRESENT	AREA MULLITE PEAK (ARBI- TRARY UNITS)	AREA CRISTOBALITE PEAK (ARBI- TRARY UNITS)
K	1330	19 HR	MULLITE $\alpha$ -CRIST.	170	40
KR	1260	4 HR	MULLITE	80	0
KR	1260	6 HR	MULLITE	80	0
KR	1260	17 HR	MULLITE	80	0
KR	995	1 HR	MULLITE	20	0
KR	995	3 HR	MULLITE	20	0
KR	995	68 HR	MULLITE	20	0

NOTE: K = KAOWOOL BLOCK  
 KR = KAOWOOL BLOCK & KAOWOOL RIGIDIZER



Table 4-10 CHEMISTRY OF HIGH PURITY KAOWOOL FIBERS

COMPOUND	WT %
$Al_2O_3$	47.0
$SiO_2$	52.9
$Fe_2O_3$	0.05
$TiO_2$	0.07
MgO	
CaO	
$Na_2O$	
$B_2O_3$	

Table 4-11 PROPERTIES OF RIGIDIZED MULLITE FIBERS

DENSITY ( $kg/m^3$ )	160-230 (10 - 15 pcf)
DIMENSIONS (cm)	35 x 35 x 8
BINDER	COLLOIDAL SILICA & STARCH
FORMING TECHNIQUE	VACUUM

Table 4-12 B&W EXPERIMENTAL MULLITE FIBER

- CHEMISTRY (WEIGHT PERCENT)

$\text{Al}_2\text{O}_3$	$77 \pm 1\%$
$\text{SiO}_2$	$17 \pm 1\%$
$\text{B}_2\text{O}_3$	$4.5 \pm 0.5\%$
$\text{P}_2\text{O}_5$	$1.5 \pm 0.25\%$
Trace Impurities - Less Than 0.5%	

- FIBER DIAMETER

4.7 microns - Average of 100 individual counts on random sample

- Crystalline Phases (X-Ray Diffraction)

Mullite - Major  
 $\text{YAl}_2\text{O}_3$  - Minor

- Grain Size (X-Ray Diffraction Line Broadening Analysis)

250 - 400A° for mullite constituent

- Fiber Length (Judgement Factor - No Tests Available)

4 - 5 inches

- Tensile Strength

100,000 to 200,000 psi

- Young's Modulus of Elasticity

18 - 22 x 10<sup>6</sup> psi

- Fiber Density (Pycnometer With  $\text{H}_2\text{O}$  or Kerosene)

2.9 to 3.1 g/cc

from the HCF mullite as fabricated by McDonnell Douglas Corp. (Ref.6)

#### 4.1.5.7 Fiberfrax-H

Although rigidized boards of Fiberfrax H were not fabricated, it is believed that this material should offer excellent compatibility with CPI materials. Fiberfrax H is thermally stable up to 1700K. Future work should examine this possibility for Area 2P exposures. Table 4-13 gives the properties of Fiberfrax H fibers.

#### 4.1.5.8 Kaowool Cement

Kaowool cement, a specially formulated cement for Kaowool fiber materials was found to be the most successful adhesive for bonding CPI to Kaowool ceramic fiber blocks. This material, an air-setting ceramic fiber cement, is applied by spraying or brushing. The cement sets up with a strong hard film at 410K and develops a ceramic bond at temperatures above 1100K. It is mildly alkaline and after air set, is insoluble in most chemical reagents. Table 4-14 gives this cement's physical and chemical properties.

#### 4.1.5.9 Kaowool Rigidizer

Kaowool rigidizer was used to control fiber block surfaces so that precision cutting and grinding operations could be performed. Kaowool rigidizer, a colloidal silica fluid, was applied by dipping the rough cut block into a solution (diluted to 3 parts H<sub>2</sub>O to 1 part rigidizer)

The wet block was dried for 16 hrs at 400K and fired 1 hr at 1100K. The surface hardened block was then dry ground and cut to exact dimensions. Table 4-15 gives the properties of Kaowool rigidizer solution.

Table 4-13 PROPERTIES OF FIBERFRAX H

Color	White
Fiber Length (cm)	2.54
Fiber diameter (micrometer)	2-4
Fiber density ( $\text{gm}/\text{cm}^3$ )	2.6
Maximum Use temperature (K)	1700
Melting Point (K)	2200
Chemistry (wt%)	
	$\text{Al}_2\text{O}_3$ 62
	$\text{SiO}_2$ 38

Table 4-14 PHYSICAL AND CHEMICAL PROPERTIES OF KAOWOOL CEMENT

Appearance	White paint
Density ( $\text{kg}/\text{m}^3$ )	1840-1950 (115 pcf)
Melting temperature ( $^{\circ}\text{F}$ )	3200
Compressive Strength	6500 psi
Specific Heat	0.24-27
(400K-800K)	
Chemistry	
$\text{SiO}_2$	57.0
$\text{Al}_2\text{O}_3$	41
$\text{Na}_2\text{O}$	0.8
$\text{B}_2\text{O}_3$	0.6
$\text{MgO}$	0.4
Inorganics	0.2
Coverage (0.025 cm film)	$1.1 \times 10^5 \text{ cm}^2/\text{gallon}$
Price (gallon)	\$20.00

Table 4-15 PHYSICAL AND CHEMICAL PROPERTIES OF KAOWOOL RIGIDIZER

Color	Bluish-white
Solids Content	28-29% SiO <sub>2</sub>
Density	75 pcf
Specific gravity	1.2
PH	9.7
Viscosity	4x10 <sup>-2</sup> poise

## 4.2 Material Property Data

### 4.2.1 General

The determination of the design allowables of the materials used in any structural component is vital to a design integration effort. These allowables must satisfy the environmental conditions that the vehicle will experience, and they must be determined with the degree of accuracy so as to confer confidence in the complete structure's ability to perform successfully.

An experimental program was therefore devised to determine the basic strength characteristics for a design in which the CPI material is used as the primary aerodynamic surface of a thermal protection system (TPS).

Characterization of the CPI class of materials was in progress prior to this effort, under Grumman IRAD and NASA/Langley funding. More extensive property evaluations of the most applicable CPI compositions were made, however, under the present effort. This section presents the CPI materials' basic mechanical properties. Both virgin (as fired) and thermally-exposed materials were evaluated. A basic objective in these tests was the determination of strength as a function of temperature and simulated exposure time.

All test data for the two CPI compositions (CPI-4 and CPI-8) most applicable to TPS design are summarized in Table 4-16. The complete test data are given in Appendix A.

### 4.2.2 Flexural Strength

The CPI's flexural strength was deemed of primary importance because, in the various design concepts proposed, the CPI will be used as a plate to transmit external pressures to the primary structure. The CPI's flexural strength was determined first, since the flexural strength test of a brittle material such as CPI is relatively easier to perform than a uniaxial tension test. The flexural test used two types of test specimens which were subjected to room and elevated temperatures. Both

TABLE 4-16 SUMMARY OF AVERAGE MECHANICAL

PROPERTY	CPI-8 MATERIAL							
	UNEXPOSED							
	TEST TEMPERATURE (°F)							
	R.T.	1,148	1,400	1,562	1,700	1,832	2,000	2,100
1. SINGLE PT. FLEXURE								
STRENGTH (PSI)	863	1,010	-	815	-	836	-	-
MOD. $\times 10^5$ (PSI)	.90	.89	-	.34	-	.11	-	.0
2. FOUR PT. FLEXURE								
STRENGTH (PSI)	1,150	-	-	-	-	-	-	-
MOD. $\times 10^6$ (PSI)	1.18	-	-	-	-	-	-	-
3. DIAMETRAL COMPRESSION								
STRENGTH (PSI)	466	-	554	-	-	-	-	-
MOD. $\times 10^6$ (PSI)	-	-	-	-	-	-	-	-
POISSON'S RATIO( $\mu$ )	-	-	-	-	-	-	-	-
4. UNCONFINED COMPRESSION								
STRENGTH (PSI)	2,800	-	1,750	-	1,650	-	172	-
MOD. $\times 10^6$ (PSI)	1.14	-	-	-	-	-	-	-
5. AXIAL TENSILE								
STRENGTH (PSI)	355	-	-	-	-	-	-	-
MOD. $\times 10^6$ (PSI)	1.12	-	-	-	-	-	-	-
6. JOHNSON SHEAR								
STRENGTH (PSI)	1,100	-	-	-	-	-	-	-
7. BOND STRENGTH (PSI)	-	-	-	-	-	-	-	-

(1) - EXPOSURE CONSISTED OF 19 HOURS AT 2,050°F. IN A  $10^{-5}$  TORR VACUUM OVEN.

(2) - SUSTAINED STRESS, NO CATASTROPHIC FAILURE.

(3) - ALL RESULTS ARE THE AVERAGE OF 3 TO 10 TEST SPECIMENS

PROPERTIES OF CPI-4 AND CPI-8 MATERIAL

		CPI-4 MATERIAL					
	EXPOSED (1)	UNEXPOSED					EXPOSED (1)
	TEST TEMP. (°F)	TEST TEMPERATURE (°F)					TEST TEMP. (°F)
92	R.T.	R.T.	1,400	1,700	2,000	2,192	R.T.
25	720	1,218	1,490	1,537	441	64	1,135
	.79	1.35	.91	.25	.07	.02	1.30
	1.094	1,864	-	-	-	-	1,672
	1.46	1.84	-	-	-	-	1.95
	416	903	876	-	-	-	817
	1.04	-	-	-	-	-	1.65
	.225	-	-	-	-	-	.191
	2,310	7,010	3,470	3,990	616	-	6,680
	1.02	1.87	-	-	-	-	1.72
	-	629	-	-	-	-	-
	-	1.41	-	-	-	-	-
	754	1400	-	-	-	-	1600
	-	-	-	-	-	-	-
	-	489	-	-	-	-	-

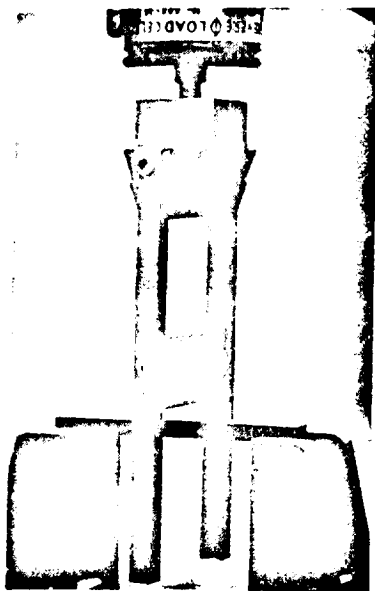


strains and deflection were carefully measured at the critical mid-span section.

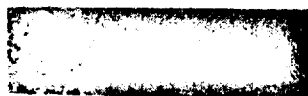
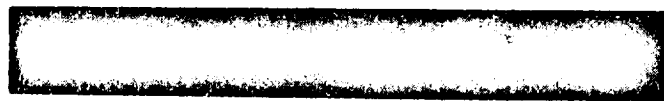
The most extensive series of flexural strength (modulus of rupture) tests were performed using a 0.25 in. (0.63 cm) X 0.5 in. (1.25 cm) X (15.2 cm) specimen on its flat side and loaded by a single point load at mid-span, as shown in Figure 4-11 (a). Failure in all cases occurred in the critical zone, as shown in Figure 4-11 (b). For elevated temperature testing, the beam specimen was supported on an alumina pedestal and loaded through an alumina rod. The entire assembly was heated by means of a cylindrical furnace which was lowered over the specimen, as illustrated in Figure 4-11 (c). A closeup of the high temperature test specimen is shown in Figure 4-11 (d). A total of over 40 specimens were tested in single point flexure. Results are summarized in Table A-1 of the Appendix A. Temperature variations of the flexural strength (modulus of rupture) for CPI-4 and CPI-8 materials are shown in Figure 4-12. The effect of temperature on the elastic modulus determined from the single point flexure specimens is shown in Figure 4-13. As can be seen in Figure 4-13, the elastic modulus of CPI-4 and CPI-8 remains essentially constant up to a temperature of approximately 1200°F and starts to decrease dramatically at about 1500°F.

No significant degradation of flexural strength was observed after CPI-4 and CPI-8 were exposed for 19 hours at 2050°F in a vacuum furnace ( $10^{-5}$  torr) and then tested.

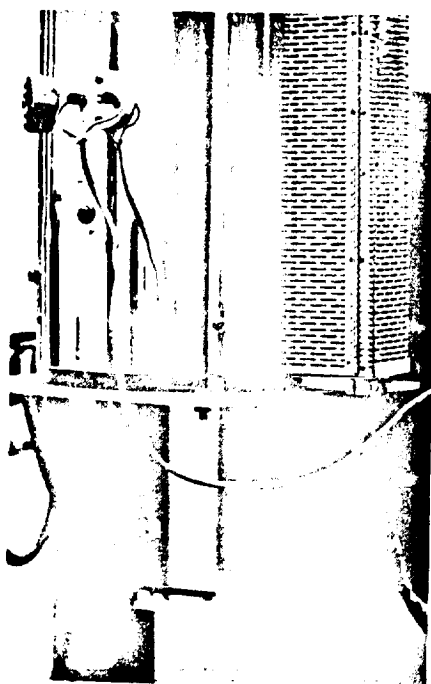
Another series of approximately 40 flexural specimens was tested by loading at two centrally located points, thus creating a section of constant moment. The set-up for room temperature strength tests is shown in Figure 4-14(a). Typical specimens are shown in Figure 4-14(b). All failures occurred within the constant moment region. Exposure for 19 hours at 2050°F, in vacuum and air, had no apparent degrading effect on the flexural strength of the CPI-4 and CPI-8 materials, as can be seen from the results shown in Table A-2, Appendix A.



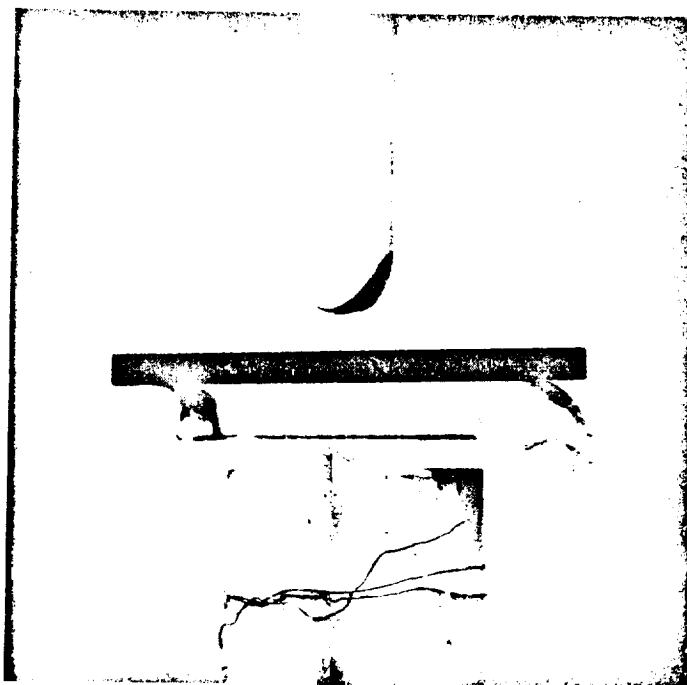
(a) Room Temperature  
Fixture



(b) Typical Specimen Before (Top) and After (Bottom) Test



(c) High Temperature  
Testing Method



(d) Close Up of High Temp Test Specimen

Figure 4-11 Single Load Point Flexural Testing

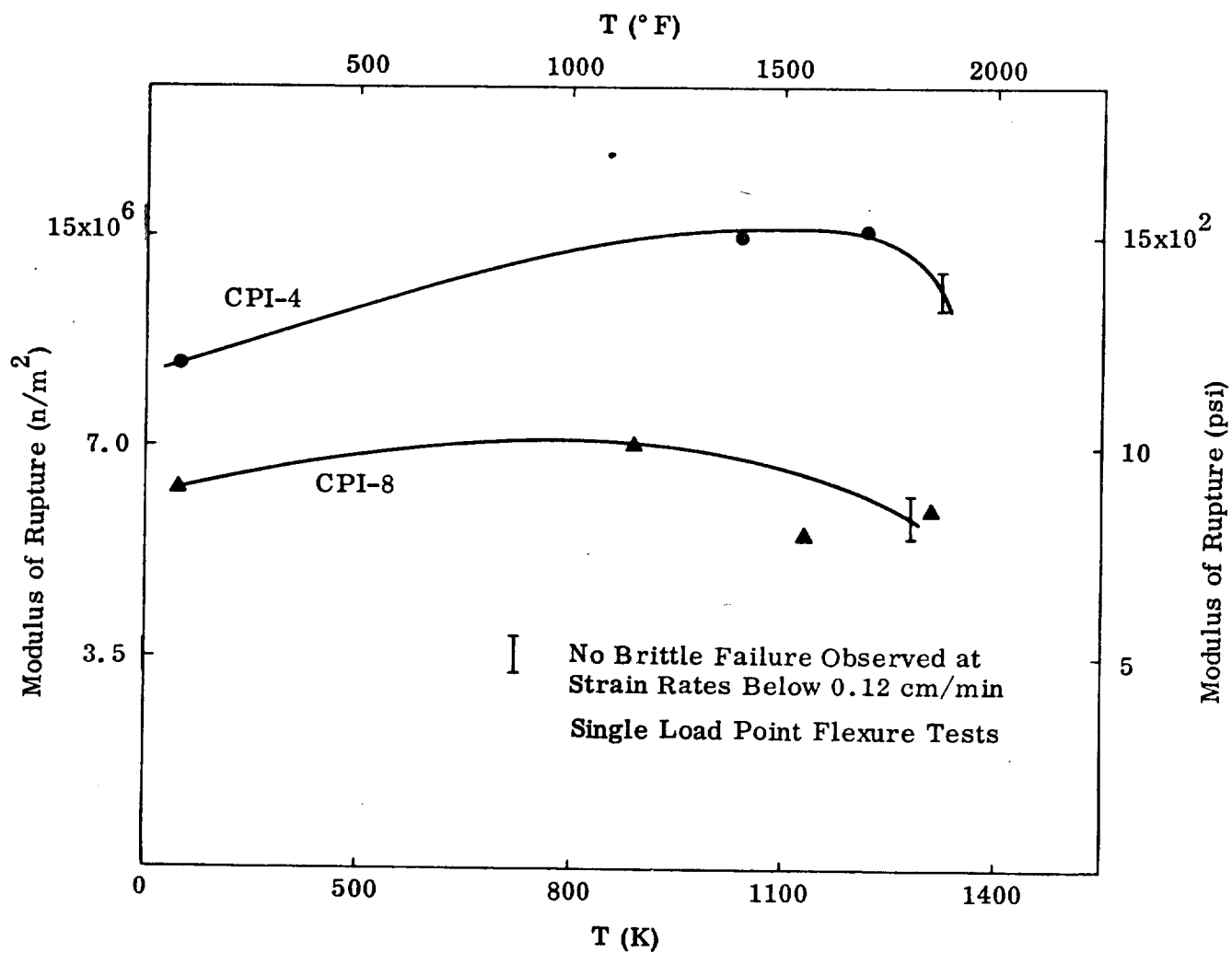


Figure 4-12 Modules of Rupture (Flexure) vs. Temperature

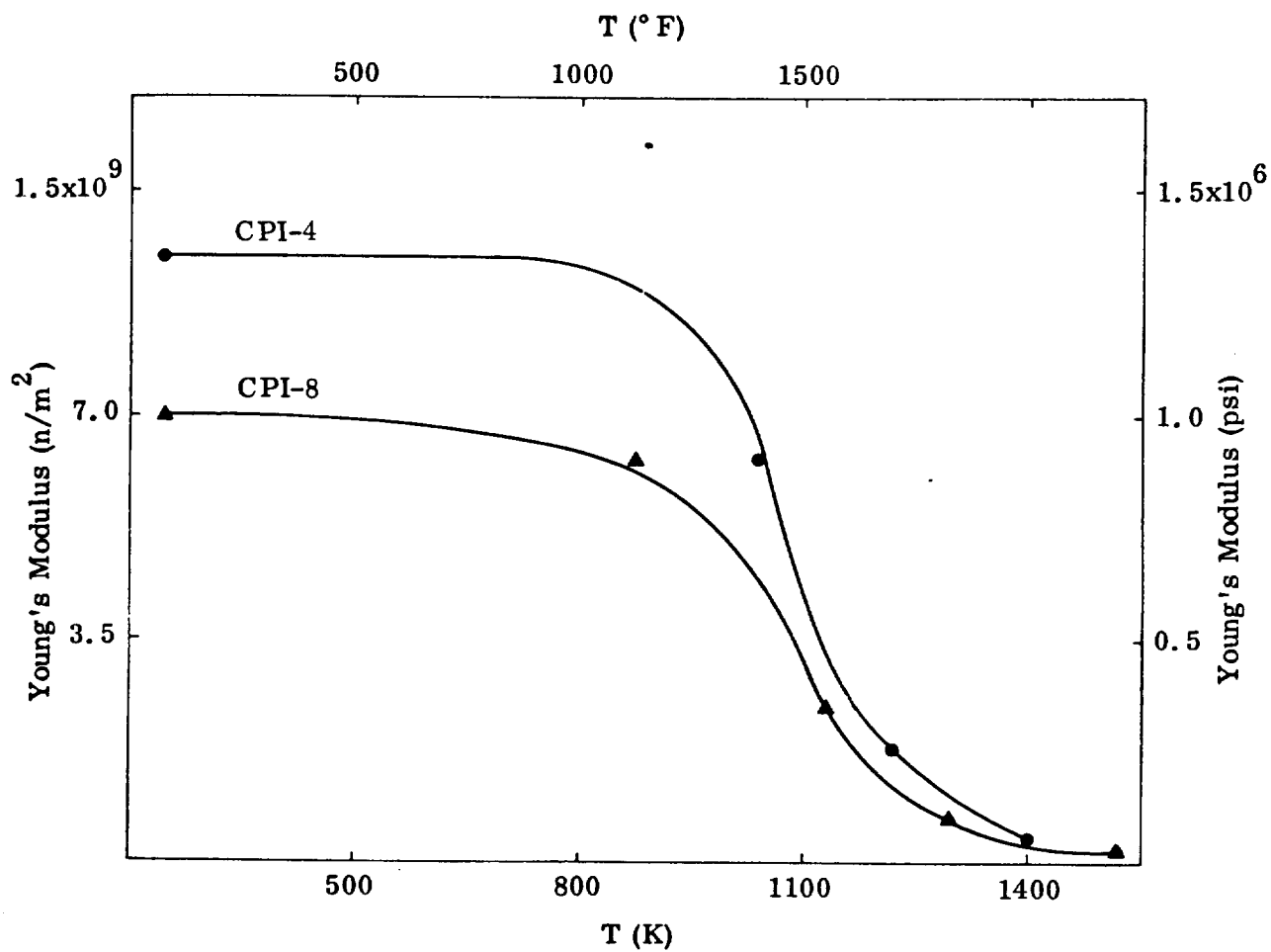
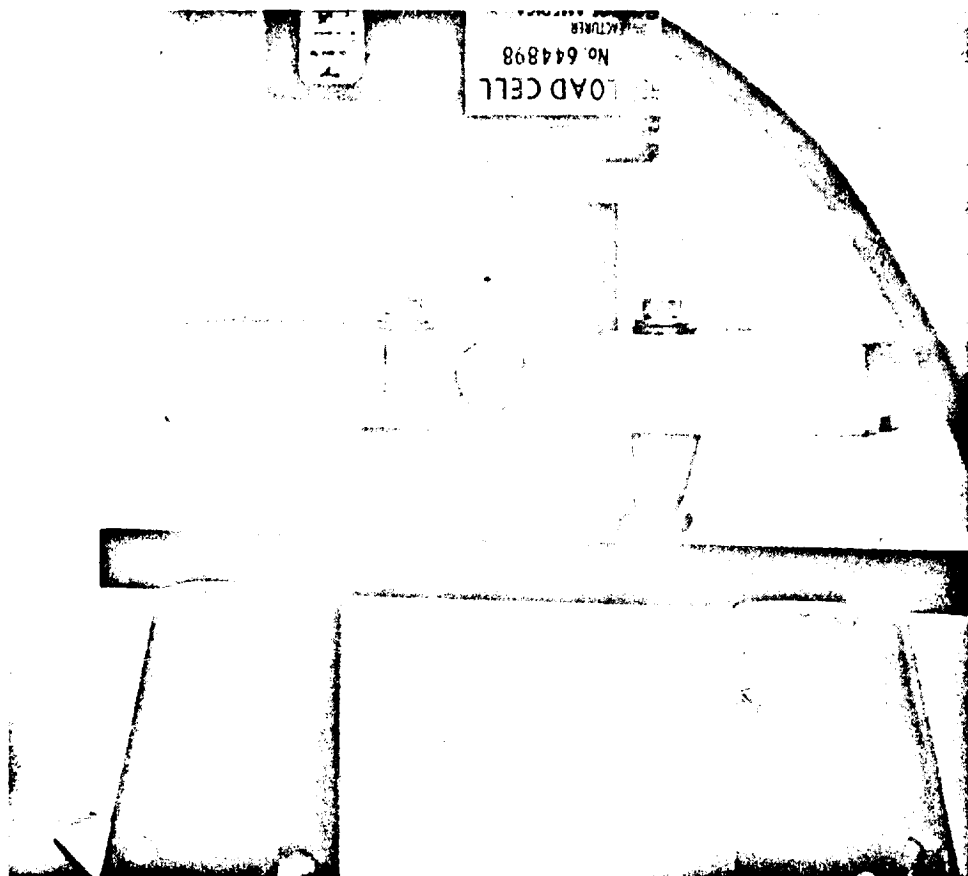
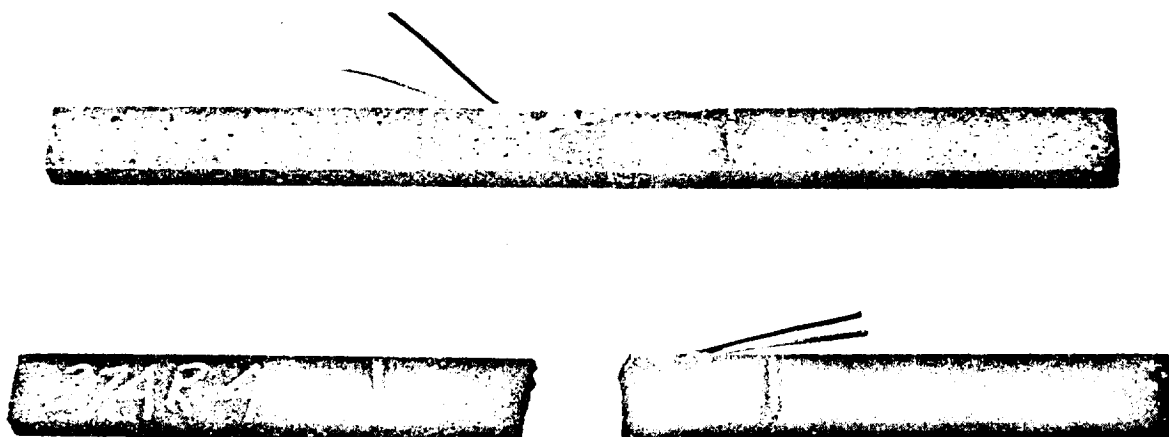


Figure 4-13 Elastic Modulus vs Temperature of CPI Materials



(a) Loading Fixture



(b) Test Specimen Before and After Test

Figure 4-14 Two Load Point Flexural Testing

#### 4.2.3 Tensile Strength

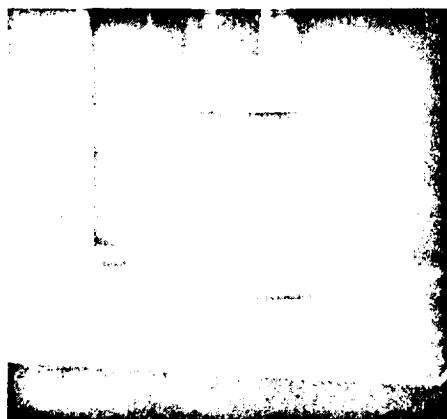
Since the determination of brittle material's uniaxial tensile strength is difficult, costly and unreliable, other methods have been developed for determining their approximate tensile strength. One of the simplest - the diametrical compression or "split cylinder" test - was used in the CPI tests cited herein. In this test, a solid cylindrical specimen of the material was compressed on opposite generators (see Figures 4-15 (a), (b)), causing a uniform tensile state of stress along the plane of symmetry, except in the vicinity of the two points of contact. The specimen usually splits down the plane of symmetry, as shown in Figure 4-15(c). The elevated temperature test is accomplished by loading the cylinder through an alumina rod, as shown in Figure 4-15(b).

The variation of the "split cylinder" tensile strength as a function of temperature is shown in Figure 4-16. As can be seen in Figure 4-16, the CPI-4 shows a much higher tensile strength than CPI-8, due to its higher refractoriness. No significant degradation was observed after the test samples were exposed to a temperature of 2050°F for 19 hours, as shown in Table A-3, Appendix A.

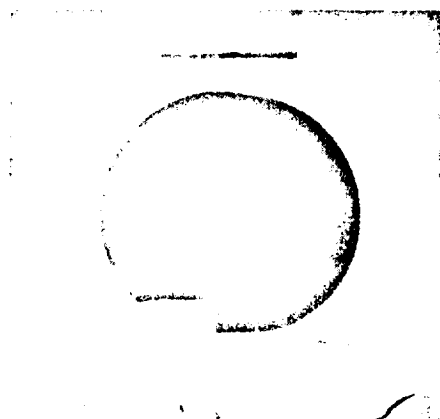
The "split cylinder" test specimens were instrumented with strain gages on their flat ends in order to measure the Poisson's ratio of the CPI material. In table A-3 of Appendix A the strains and the computed Poisson's ratio using theory of elasticity relationships are presented. This is permissible because the stress vs. strain relationships of the cylinder are linear up to failure.

#### 4.2.4 Compressive Strength

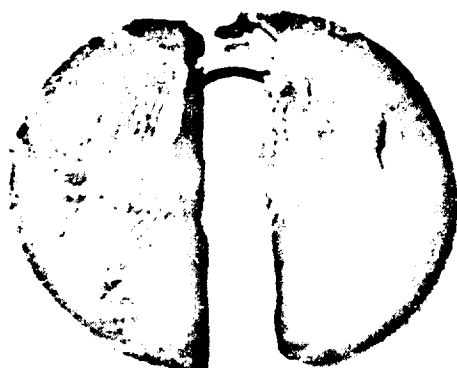
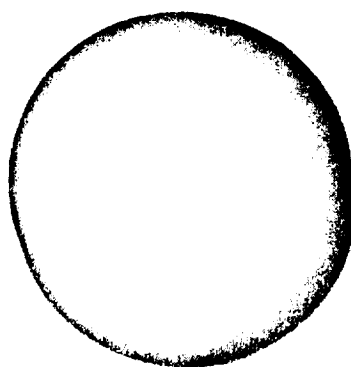
The uniaxial compressive strength of the CPI material was determined using prisms of 3/8" X 3/8 in. X 1 in. nominal. Figures 4-17(a), (b) show the room and elevated temperature test set-up, respectively. Two typical compressive failure modes of the specimens are shown in Figure 4-17(c). The CPI uniaxial compressive strength variation with temperature is shown in Figure 4-18. As can be seen from Figure 4-18, the



(a) Room Temperature Fixture



(b) High Temperature Test



(c) Cylindrical Specimens Before and After Test

Figure 4-15 Split Cylinder Test as a Measure of Tensile Strength

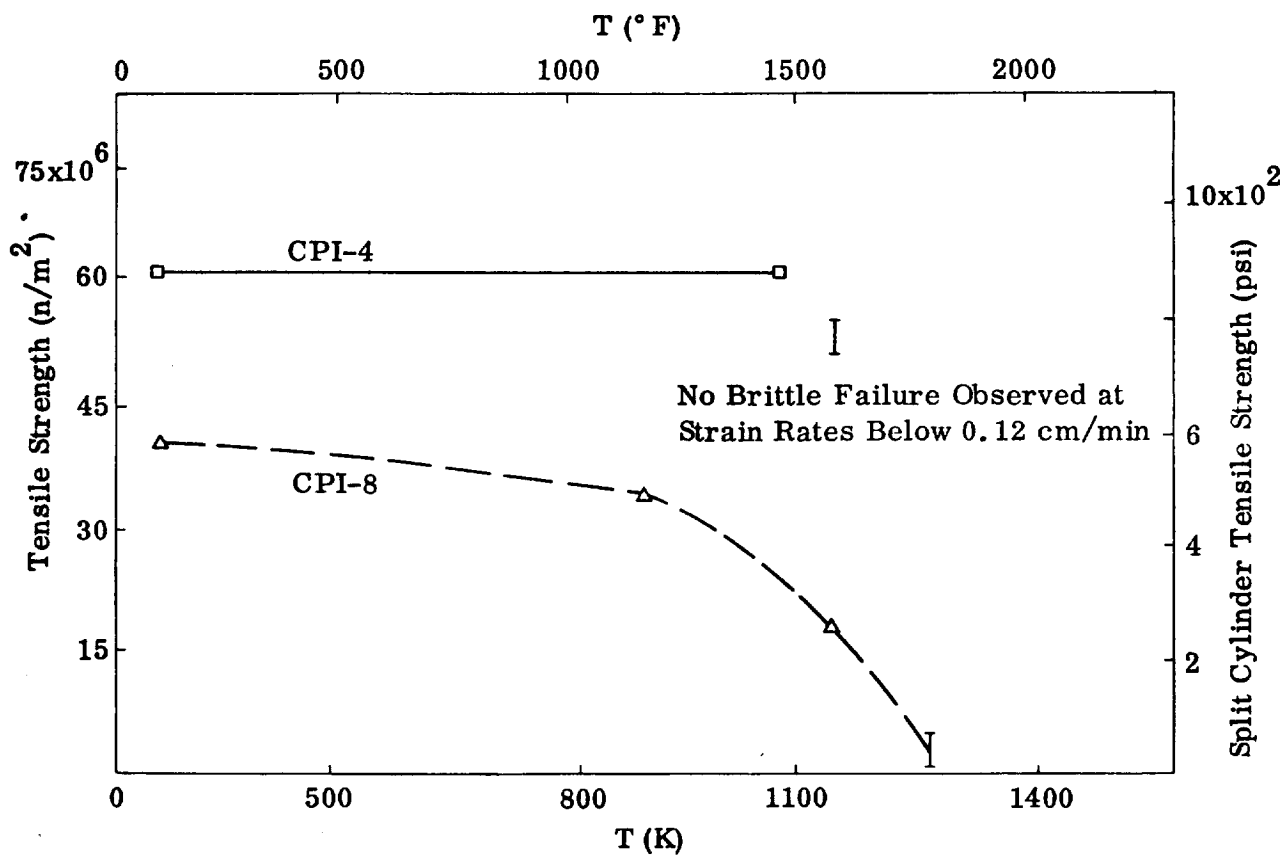
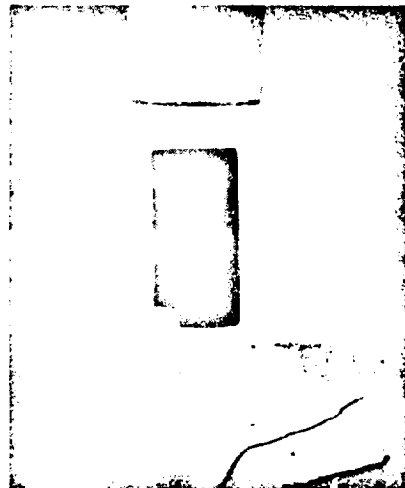


Figure 4-16 Split Cylinder Tension Strength vs Temperature for 2 CPI Compositions

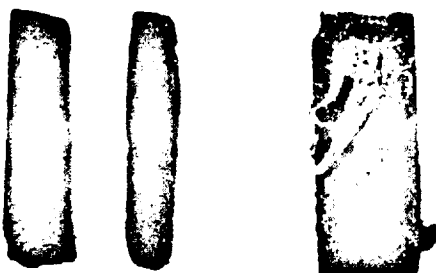




(a) Room Temperature Fixture



(b) High Temperature Test



(c) Typical Specimens

Figure 4-17 Unconfined Compressive Strength Testing

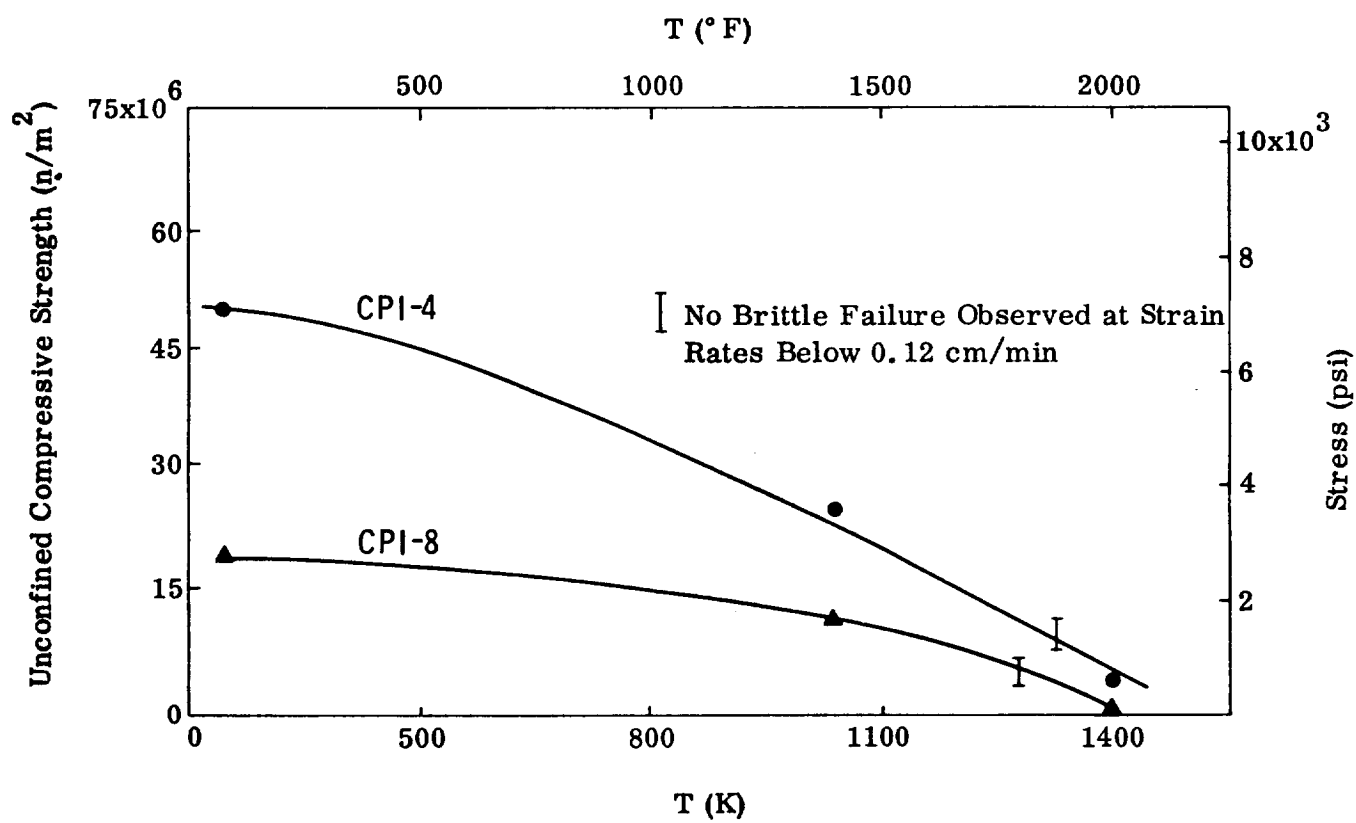


Figure 4-18 Compressive Strength vs Temperature of CPI

CPI-4 material is considerably stronger than the CPI-8 material, over the entire range of temperatures, although they tend to approach each other at temperatures greater than 2000°F. A complete tabulation of the compressive strength test program is shown in Table A-4, Appendix A. As can be seen from the results, which are plotted in Figure 4-19, no significant degradation was observed following the samples' exposure to a temperature of 2050°F for 19 hours in a vacuum furnace.

#### 4.2.5 Uniaxial Tensile Strength

A somewhat limited test program was conducted to determine the uniaxial strength of the CPI-4 and CPI-8 material. A schematic drawing of the tensile specimen is shown in Figure 4-20. The test set-up and a typical failed specimen are shown in Figures 4-21(a), (b). CPI-4 material had almost twice the tensile strength of the CPI-8 materials. The instrumentation of the tensile specimens consisted of strain gages mounted on both faces, which were monitored throughout the test, indicated some bending due to the loading fixtures. However, as indicated in Table A-5, Appendix A, the amount of bending was not excessive, as shown by the final strain readings at failure.

#### 4.2.6 Bond Strength

The machined CPI surfaces' bond strength, an important parameter, had to be evaluated early in the program. Some of the design details called for CPI-to-CPI bonding of small details in order that the TPS panel could be effectively supported on the primary structure. The specimen used for the bond test is shown in Figure 4-22. Figure 4-23(a) shows the specimen ready for test; Figure 4-23(b) shows a failure through the CPI, indicating a bond strength greater than the tensile strength. Table A-6, Appendix A, summarizes the various compounds used in efforts to determine the strongest bonding material. Test results shows that

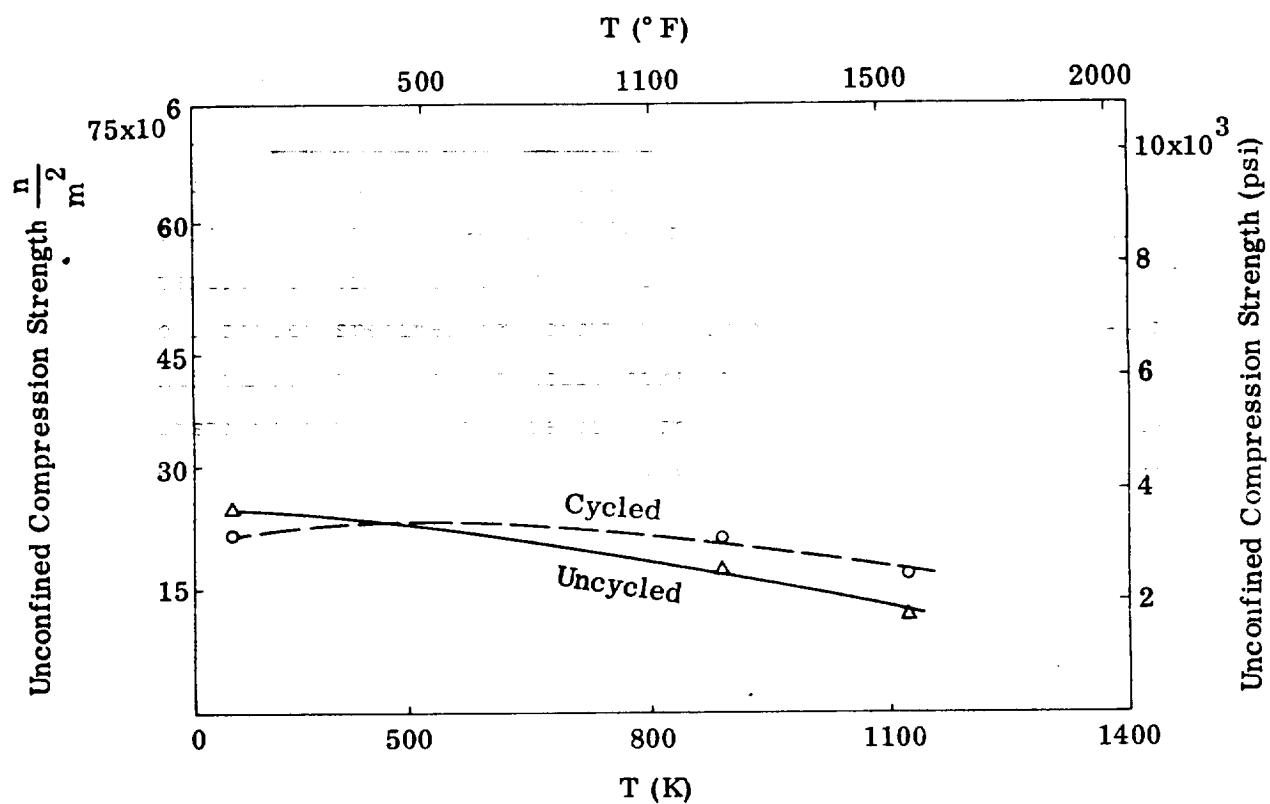


Figure 4-19 Compression Strength vs Temperature of CPI-8 for Cycled and Uncycled Material

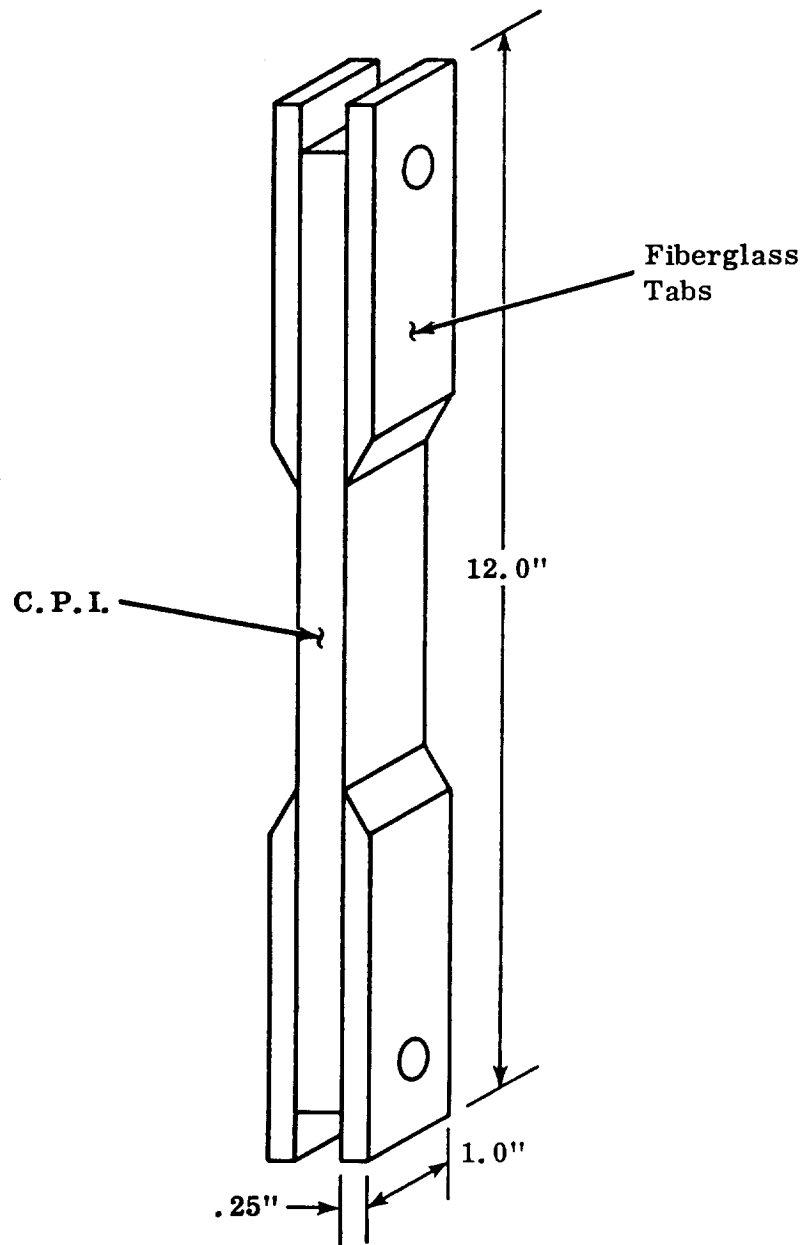
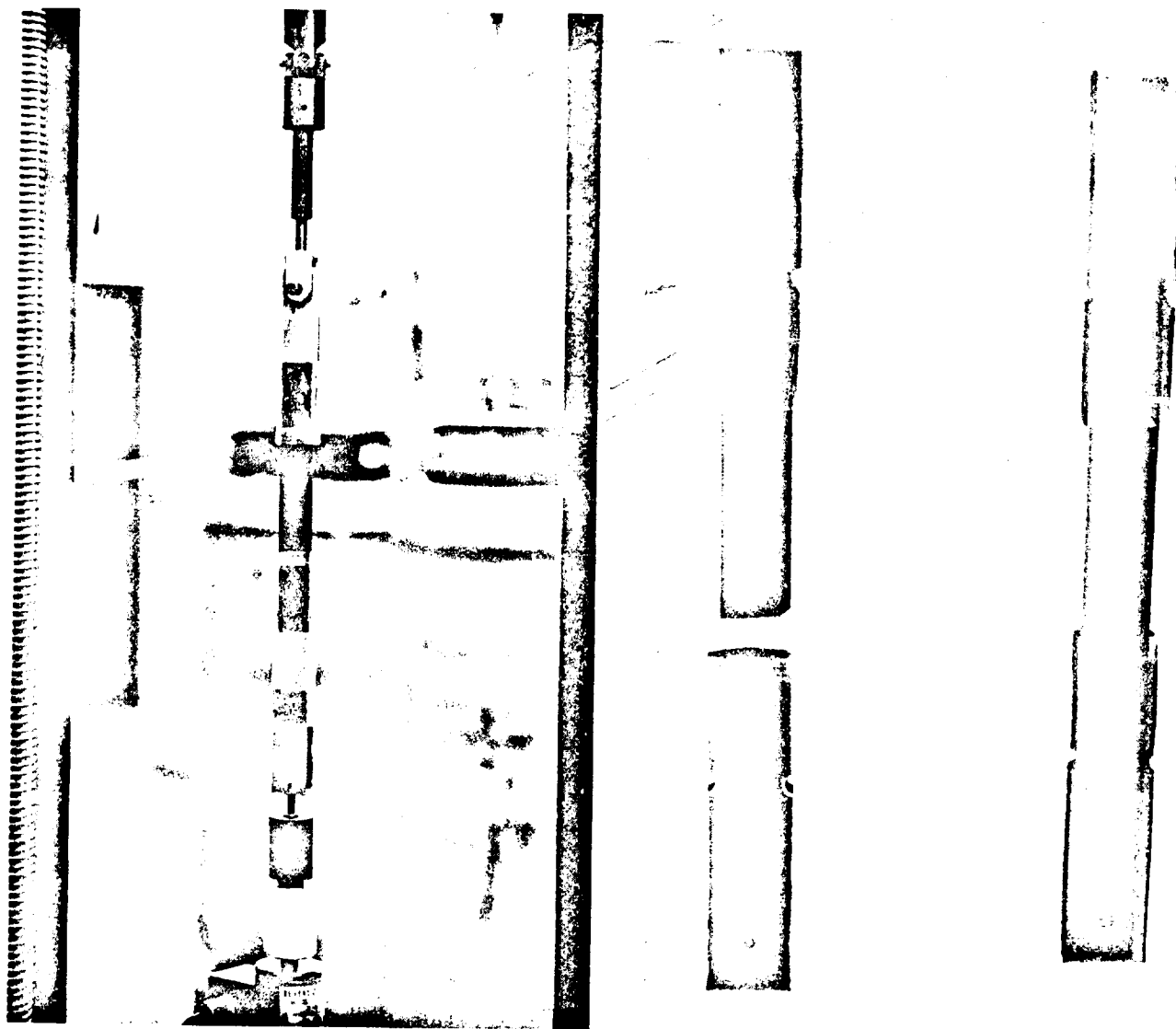


Figure 4-20 Uniform Axial Tensile Specimen



(a) Test Set up

(b) Typical Specimens

Figure 4-21 Uniaxial Tension Test of CPI Material

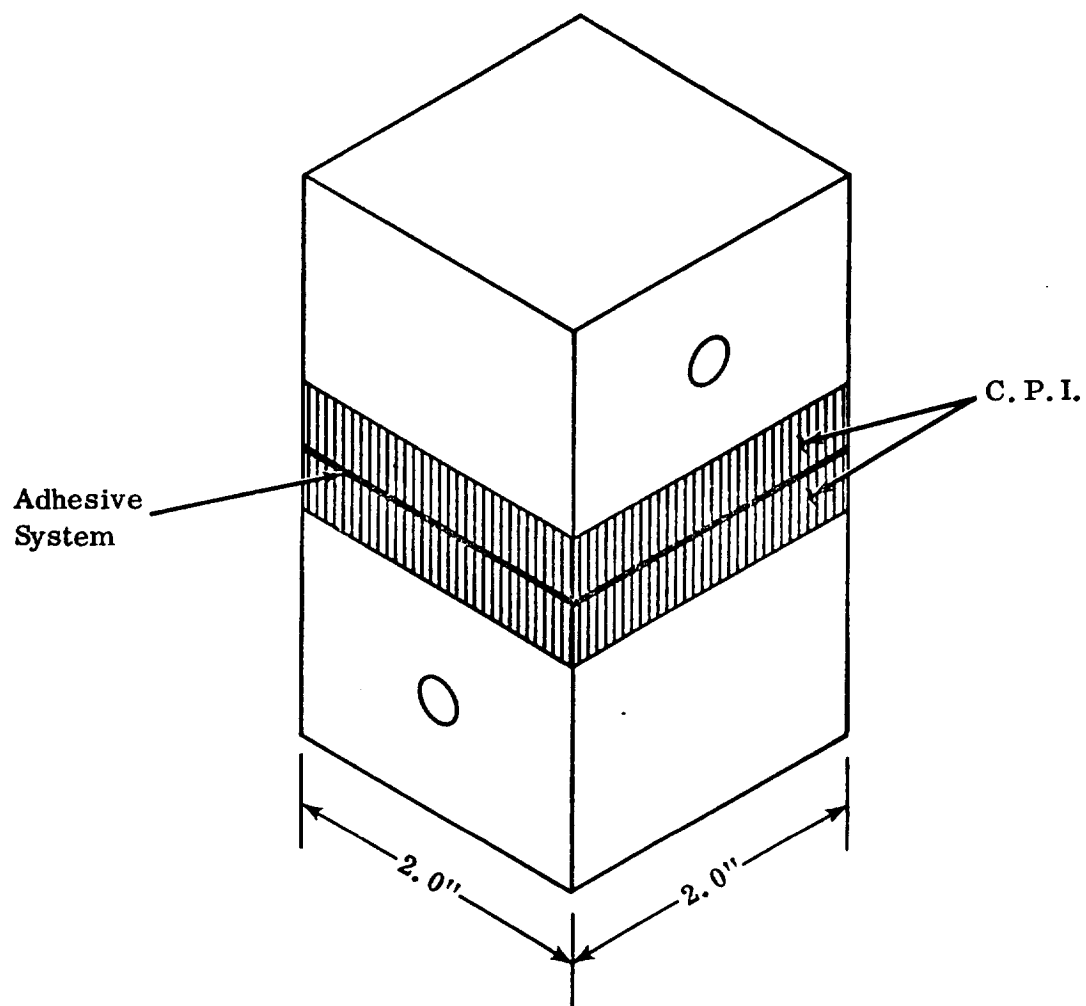
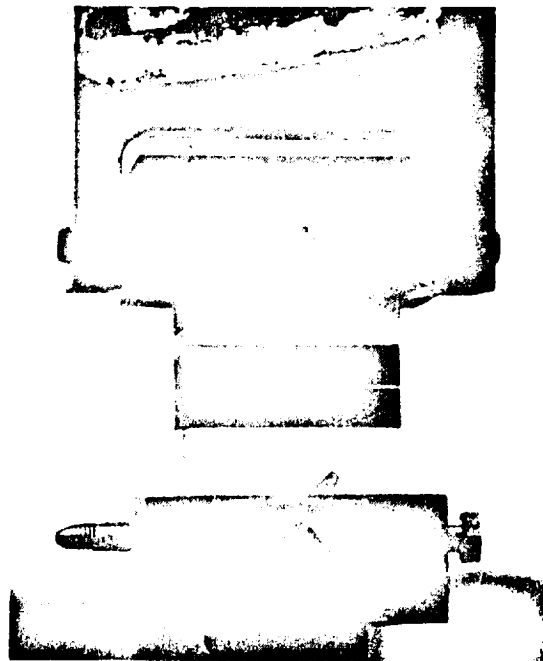
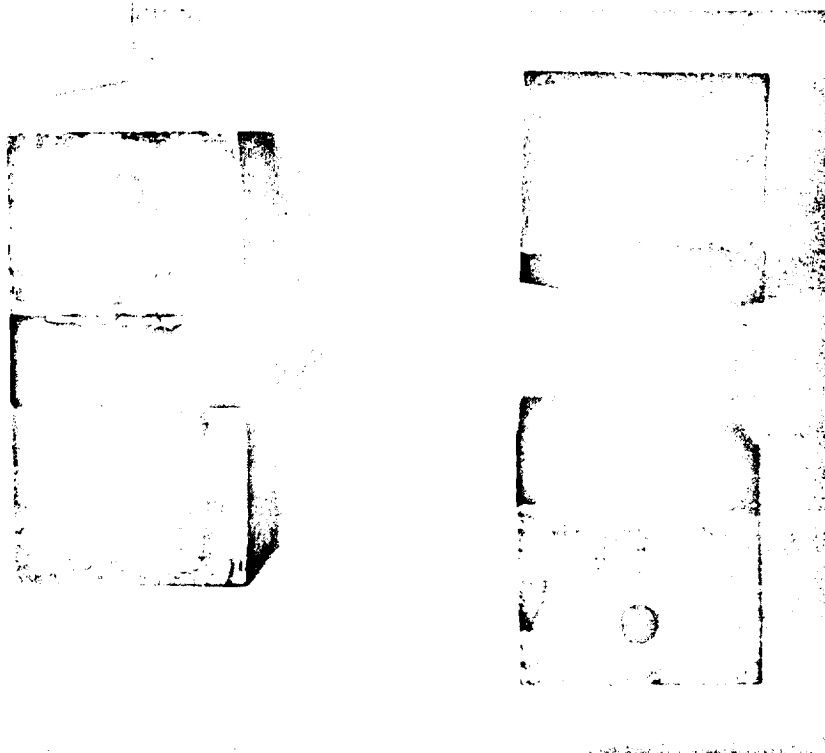


Figure 4-22 Bond Strength Specimen



(a) Test Set up



(b) Typical Specimens

Figure 4-23 Bond Testing of the CPI Material



a CPI-4 powder, mixed with colloidal silica HS \* in the ratio of two to one, was the best bonding agent for this application. This compound was used in the manufacture of the test panels.

#### 4.2.7 Shear Strength

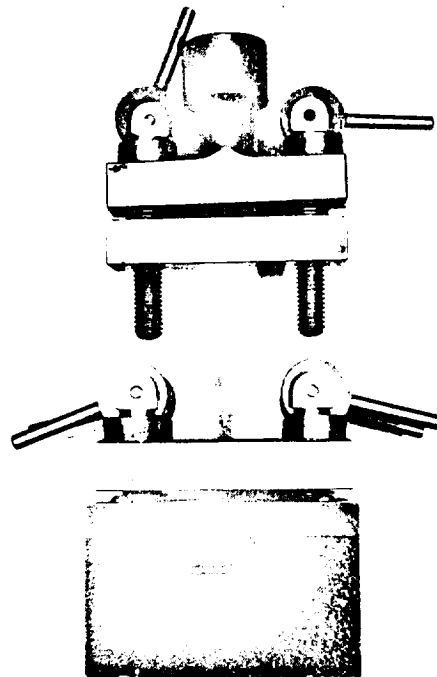
A series of tests was conducted to determine the shear strength of the CPI material. The Johnson Shear Test was used; it employed a prismatic beam, sheared on two faces, using a clamping fixture, as shown in Figure 4-24(a). The test set-up is shown in Figure 4-24(b). Table A-7, Appendix A, summarizes all the shear strength results. Typical specimens, before and after testing, are shown in Figure 4-25.

#### 4.2.8 Creep Properties of CPI

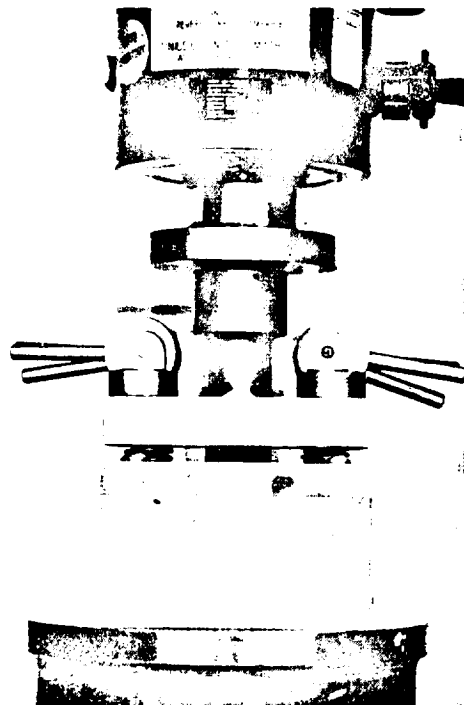
During reentry, the materials composing the external TPS surface will be subjected to surface pressures and high temperatures. For this reason, sustained loading tests of the TPS material are mandatory. Small flexural specimens, subjected to steady state creep tests, served to provide an indication of the cumulative effects of temperature and load on the CPI. Beams, fabricated from the same batch of material, were loaded with small alumina rods and held by special fixtures in a furnace which was operated at various elevated temperatures. Figure 4-26 shows a beam series of three specimens ready for testing. The beams' deflections were measured photographically over a period of 18 hours.

Beam deflection data was used to compute the extreme fiber creep strains for the CPI-4 and CPI-8 material at the critical mid-span section. Figure 4-27 shows the creep strain versus time curves for the CPI-4 at 1368K and CPI-8 at 1253K. Creep strains of the CPI-4

\* Product of Dupont, Wilmington, Delaware



(a) Clamping Fixture



(b) Test Set up

Figure 4-24 Johnson Shear Test

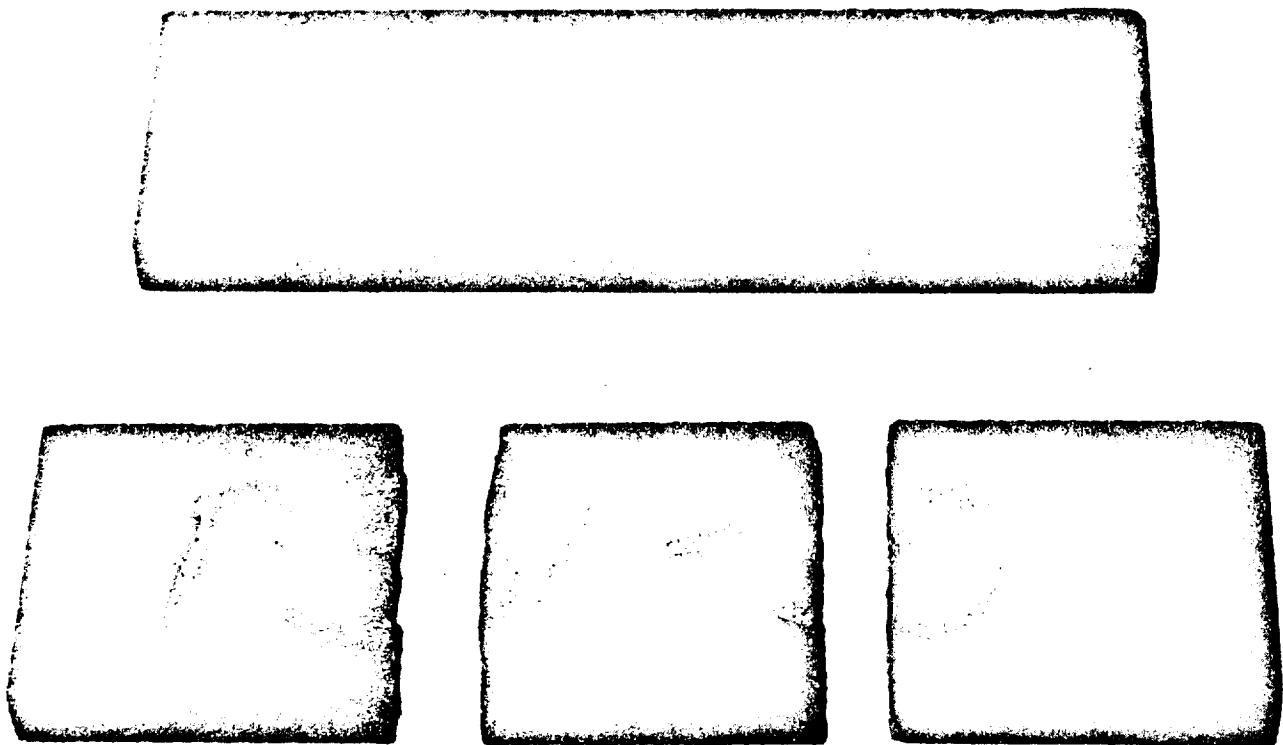
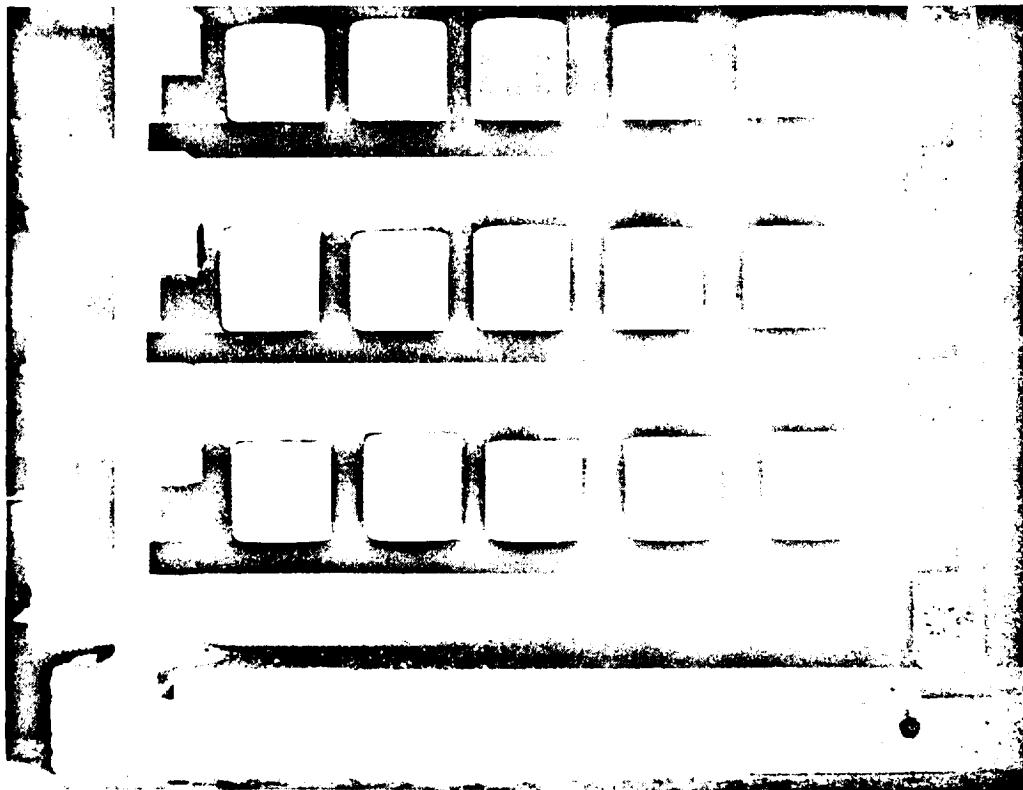
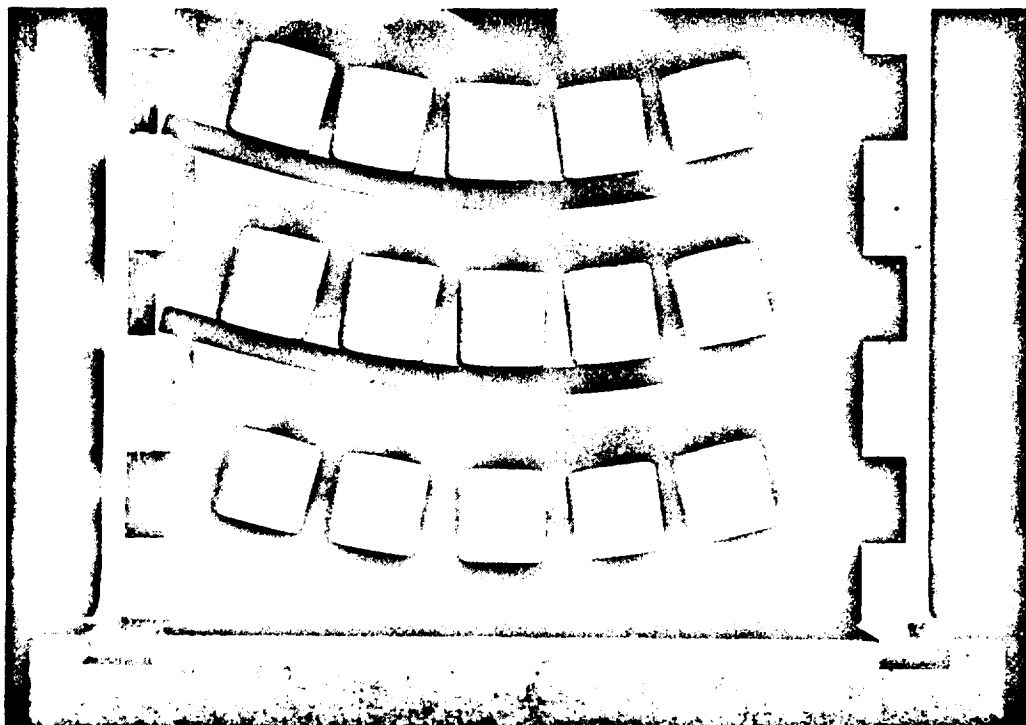


Figure 4-25 Typical Test Specimens From Johnson Shear Test



(a) Before Test - CPI-8



(b) After Test - CPI-8 @ 1253K After 18 Hrs Heating

Figure 4-26 Creep Tests of CPI Beams

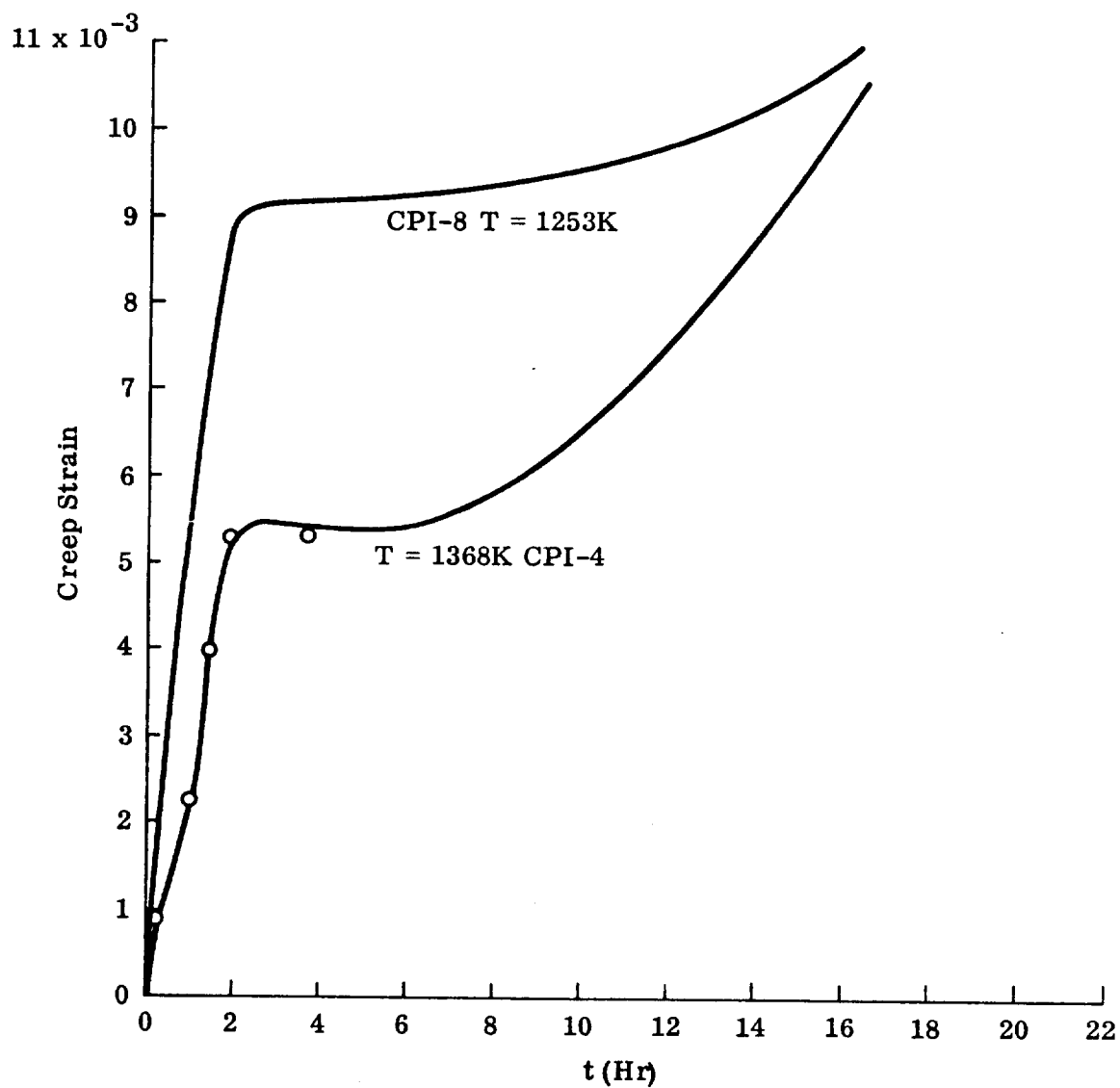
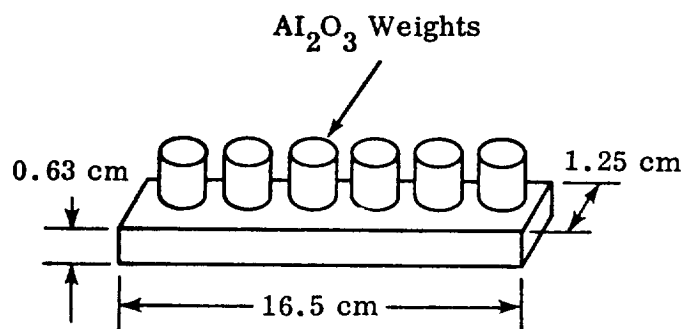


Figure 4-27 Flexural Creep Strain Vs Time For CPI-4 and CPI-8 At Two Different Temperatures

material were found to be considerably less than those of the CPI-8 material. This indicated again the CPI-4's higher refractoriness.

#### 4.3 Environmental Testing of CPI Subelements

A radiant heat lamp facility, described in Appendix B, was used to evaluate the thermal performance of CPI tiles, bonded composites and mechanically-attached heat shields. To evaluate the thermal shock associated with the re-entry maneuver, the facility was programmed to simulate Areas 1, 2 and 2P of the Shuttle re-entry profiles. (See Fig. 4-28) All tests were performed at one atmosphere. Drive thermocouples, installed into CPI ground guard plates adjacent to the CPI "Test Section", facilitated removal of the test section for inspection after each cycle and minimized handling damage to the drive and measurement thermocouples. The facility was previously calibrated by inserting thermocouples into the test section and guard tiles. The variation of temperature in the test section was less than 20K.

##### 4.3.1 CPI Tiles

The CPI's thermal shock resistance and cyclic re-use capability are of major importance. An extensive program was therefore initiated to establish the effect of tile dimensions and tile composition on the CPI materials' capability to sustain repeated use. Table 4-17 summarizes these results.

For CPI plates of up to 1.25cm thickness, no thermal stress failures were observed after 25-40 cumulative cycles in Areas 2 and 2P heating. Some distortion of CPI-8 tiles was observed in Area 2P cycling, while only minor distortion was observed in CPI-4 after 25 cycles of Area 2P. The amount of distortion depended on plate size and thickness. No distortion was observed in CPI-4 after Area 2 cycling. It is believed

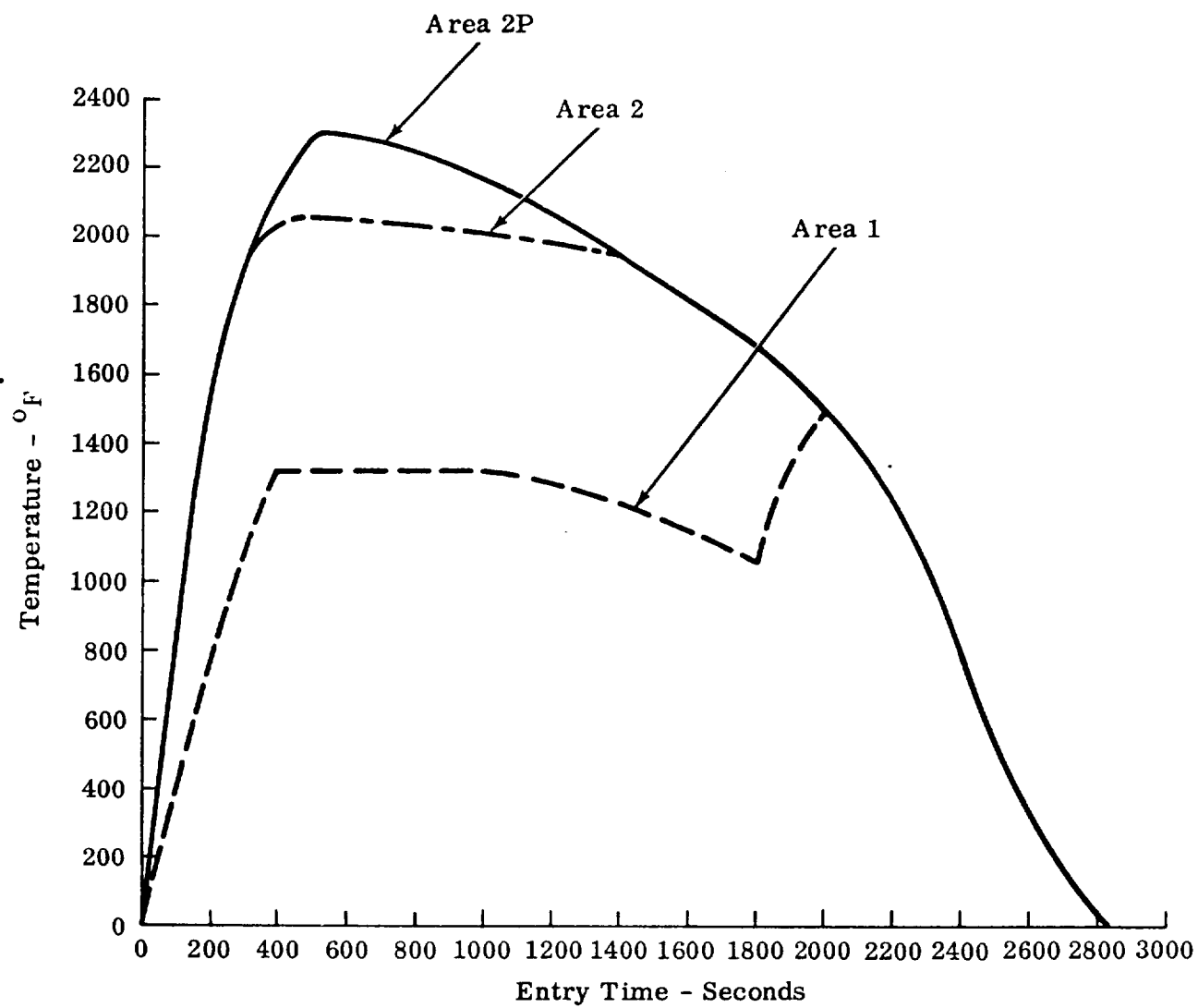


Figure 4-28 Temperature vs. Time Variation of Areas 1, 2 and 2P

Table 4-17 SUMMARY OF THERMAL CYCLING TEST RESULTS ON  
INDIVIDUAL CPI TILES (UNRESTRAINED)

SPECIMEN DESIGNATION	% Co O	SPECIMEN DIMENSIONS	RE-ENTRY SIMULATION	NUMBER OF CYCLES	SPECIMEN CONDITION
X	8	15.2cm x 15.2cm	Area 2	25	No changes
1	8	15.2cm x 15.2cm x .32cm	Areas 2-2P	3	Cracks on Cycle #2 Handling crack on Cycle #3
2	8	15.2cm x 15.2cm x .475cm	Areas 2-2P	25	No Changes
3	8	15.2cm x 15.2cm x .64cm	Above 2P (>1650K)	2	Specimen partial melted due to operational failure of thermocouples
4	8	15.2cm x 15.2cm x .79cm	Above 2P (>1650K)	2	Specimen partial melted due to operational failure of thermocouples
15	8	10cm x 10cm x 1.25cm	Area 1	25	No Changes
1A	8	15.2cm x 15.2cm x .32cm	Area 2	25	No Changes
2A	8	15.2cm x 15.2cm x .475cm	2	25	No Changes
3A	8	15.2cm x 15.2cm x .64cm	2	3	No Changes
4A	8	15.2cm x 15.2cm x .79cm	Area 2	25	No Changes Slight Bow at center after cycle #3 No other changes



Table 4-17 (Continued)

SPECIMEN DESIGNATION	% Co O	SPECIMEN DIMENSIONS	RE-ENTRY SIMULATION	NUMBER OF CYCLES	SPECIMEN CONDITION
P46	8	20.4cm x 20.4cm x .95cm	Area 2	25	No changes
248R	4	16.8cm x 16.8cm x .95cm	Area 2	10 15	No changes Slight Bow
SP26	4 (Coated)	16.8cm x 16.8cm x .79cm	Area 2P	25	Slight bow. Surface glazed due to fluxing action of Co O coating on CPI glass
SP43	4 (Coated)	16.8cm x 16.8cm x .95cm	Area 2P	25	Partial surface crack developed at end of cycle #25 due to fluxing action of coating
10	4	7.62cm diameter x 1.2cm	Area 1 (Arc Jet)	25	No Changes
11	4	7.62cm	Area 2P (Arc Jet)	25	No Changes

that tile distortion is related to thermal stresses incurred when the tile is cycled through the glass transition point in the material. The tile can then flow to accommodate the stresses. The CPI-4 material's reduced tendency to flow is related to its higher softening point. The reduction in distortion with increasing plate thickness is related to the lowered average temperature level in the CPI plate due to the plate's finite thermal conductivity.

#### 4.3.2 CPI/Fiber Composites

An extensive thermal screening program was initiated to assess the feasibility of a suitable bonded scheme. Small composite specimens were fabricated (7cm x 7cm), using various adhesive formulations between the CPI and the rigidized fibers. These specimens were subjected to thermal cycling in Areas 2 and 2P heating.

##### 4.3.2.1 CPI/Kaowool Composites

Table 4-18 summarizes the effects of thermal cycling on bonded CPI/Kaowool composites. In general, it was observed that attempts to bond the CPI to Kaowool by diffusion bonding led to considerable shrinkage and devitrification of the fibers and delamination upon subsequent thermal cycling.

Secondary bonding processes, using commercially available inorganic adhesives, proved to be the most successful although delamination problems were encountered with these materials. Secondary bonding operations, however, permit a lower curing cycle and eliminate overheating of the fibers. Kaowool cement\* proved to be the most successful inorganic adhesive for this application.

\* Babcock and Wilcox Co.

Table 4-18 SUMMARY OF THERMAL CYCLING RESULTS ON  
CPI/RIGIDIZED FIBER COMPOSITES (CPI THICKNESS  
= .25cm)

SPECIMEN DESIGNA- TION	% Co O	FIBROUS SUBSTRATE	BONDING TECHNIQUE	SPECIMEN DIMEN- SIONS (Overall)	RE-ENTRY SIMULA- TION	NUMBER OF CYCLES	CONDITION OF SPECIMEN
16	8	KAOWOOL	Diffusion at 1600K 1 hr at .1 psi	6.2cm x 7.6cm x 3.8cm	Area 2	49	Surface crack after Cycle #3. No subse- quent changes
17	8	Kaowool	Diffusion at 1650K 1 hr at .1 psi	6.2cm x 7.6cm x 3.8cm	Area 2	39	Surface crack Cycle #1 Enlarged after Cycle #17 Partial delamination after Cycle #21
18	8	Mullite	Diffusion at 1600K 1 hr at .1 psi	5.0cm x 7.6cm x 3.2cm	Area 2	5	Complete delamination
19	8	Mullite	Diffusion at 1650K 1 hr at .2 psi	7.6cm x 7.6cm x 3.2cm	Area 2	21	No change
20	8	Kaowool	Diffusion at 1700K 1 hr at .2 psi	5.0cm x 7.6cm x 3.2cm	Area 2- 2P	2	Partial delamination

Table 4-18 (Continued)

SPECIMEN DESIGNATION	% Co O	FIBROUS SUBSTRATE	BONDING TECHNIQUE	SPECIMEN DIMENSIONS (Overall)	RE-ENTRY SIMULATION	NUMBER OF CYCLES	CONDITION OF SPECIMEN
21	8	Kaowool	Diffusion at 1500K 1 hr at .1 psi	5.0cm x 7.6cm x 5.0cm	Area 2	17	Crack in CPI after Cycle #9, Corner delamination after Cycle #16. Complete delamination after Cycle #17
23	8	Kaowool	Ground up CPI powders + colloidal silica	7.6cm x 7.6cm x 5.0cm	Area 2	14	Crack after cycle #8; Partial delamination after Cycle #13
24	8	Mullite	Ground up CPI powders + colloidal silica	7.6cm x 7.6cm x 5.0cm	Area 2	12	Crack in CPI after Cycle #7; Delamination after Cycle #12
25	8	Mullite	Diffusion at 1700K 1 hr at .1 psi	7.6cm x 7.6cm x 5.0cm	Area 2	2	Delamination
A	8	Kaowool	Chromium Based Commercial Adhesive*	7.6cm x 7.6cm x 5.0cm	Area 2	32	Cracks in CPI after Cycle #2. Cracks after Cycle #27 extended

Table 4-18 (Continued)

SPECIMEN DESIGNATION	% Co O	FIBROUS SUBSTRATE	BONDING TECHNIQUE	SPECIMEN DIMENSIONS (Overall)	RE-ENTRY SIMULATION	NUMBER OF CYCLES	CONDITION OF SPECIMEN
LC-42	4	Kaowool	Kaowool Cement**	15.2cm x 15.2cm x 5.0cm	Area 1	25	No Changes small
26	4	Kaowool	Kaowool Cement	15.2cm x 15.2cm x 5.0cm	Area 2	25	Crack in Kaowool Fibers about 1cm below CPI/Fiber inter- face after Cycle #5 No further changes

\* Industrial Infra-Red Products

\*\* Babcock & Wilcox

#### 4.3.2.2 CPI/Mullite Fiber Composites

Since mullite fibers have a much higher temperature capability than Kaowool fibers, it was decided that a diffusion bonding would produce a good bond between these two materials. To effect a good contact between the CPI and mullite surfaces, both materials were machined flat (to within 0.01 cm). Diffusion bonding temperatures of 1530K-1670K were used at pressures of 0.2 - .4 psi. The bonding process lasted for one hour. Table 4-18 summarizes the effects of thermal cycling on the integrity of the CPI/mullite fiber bond. In general it was found that a one hour heat treatment at 1600K at a pressure of .2 psi is sufficient to effect a bond that will survive re-entry cycling.

#### • 4.3.2.3 CPI/CPI Bonds

One promising concept for a mechanically fastened heat shield, which eliminates surface fasteners (See Sec. 5.1), employs a CPI washer to retain the fastener to the tile lower surface. A CPI-to-CPI bond development program was initiated to verify this design concept. Adhesives composed of powders obtained from CPI fired tiles mixed with colloidal silica, as the inorganic binder, and commercially available inorganic adhesives, were evaluated. Table 4-19 summarizes the results of thermal cycling on the most promising compositions. Mechanical property data on these adhesive formulations are presented in Sec. 4.2.6. It was found that the ground CPI powders and colloidal silica binder were best suited for bonding CPI-to-CPI. This composition was used for this study. These adhesives were cured by drying for one hour at 400K and firing for one hour at 1400K.

#### 4.3.3 Salt Spray Testing

TPS material must have the ability to resist chemical degradation due to sea salt spray during the Space Shuttle's pre-launch and ground

Table 4-19

SUMMARY OF THERMAL CYCLING RESULTS ON CPI/CPI  
BONDING EXPERIMENTS (TORUS ASSEMBLY)

SPECIMEN DESIGNA- TION	% CoO	BONDING TECHNIQUE	SPECIMEN DIMEN- SIONS	RE-ENTRY SIMULA- TION	NUMBER OF CYCLES	SPECIMEN CONDITION
LC-4	4	Ground up CPI pow- der with colloidal silica† binder (cement)	10cm x 10cm x 0.62cm	Area 1	17	No change
				Area 2	25	No change
				Area 2P	3	No change
LC-46	4	Kaowool Cement**	10cm x 10cm x 0.62cm	Area 2	25	No change
				Area 2P	3	No change
LC-48A	4	Ground up CPI pow- der with colloidal silica†† binder	10cm x 10cm x .62cm	Area 2	16	No change
LC-48B	4	Ground up CPI pow- der with colloidal silica binder†††	10cm x 10cm x .62cm	Area 2	16	No change

††† - Ludox Positive Sol

† - Dupont Ludox LS

†† - Ludox HS

operations. Sea water normally contains various alkali and alkaline earth elements (Li, Na, K, Mg, etc.), all of which may act as a fluxing agent to any silicate glass. It was decided therefore to determine the effects produced by salt water mist after deposition of these elements and subsequent re-entry cycling.

CPI-4 test specimen discs (3.0cm X 1.0cm) were exposed to salt water mist\* sprayed from a conventional atomizer. The specimens were dried at 370K. Salt deposition measured 0.05-0.08 mg/cm<sup>2</sup>. Three specimens were coated, a fourth was used as a control. Samples were placed in a muffle furnace\*\* with a fast firing cycle to simulate the re-entry condition of Area 2P. The samples' temperatures were monitored by a thermocouple placed near the specimens. All test specimens were re-coated after each of the 25 cycles completed.

The control and the CPI-4 test specimens had a pre-coat of cobalt oxide fused into the surface layer. It was observed that the slight glazing of the surface that occurred was more pronounced on the samples sprayed with the salt mist. However, no cracking or specimen degradation was apparent. An X-ray examination of the sprayed and unsprayed specimen surfaces revealed a higher concentration of cobalt aluminate in the surface layers than in the bulk material. However, the salt spray did not have any significant effect on this precipitation process. This is consistent with earlier observations, (see Sec. 4.1).

Finally, the salt spray did not affect density or water absorption in the CPI-4 specimens.

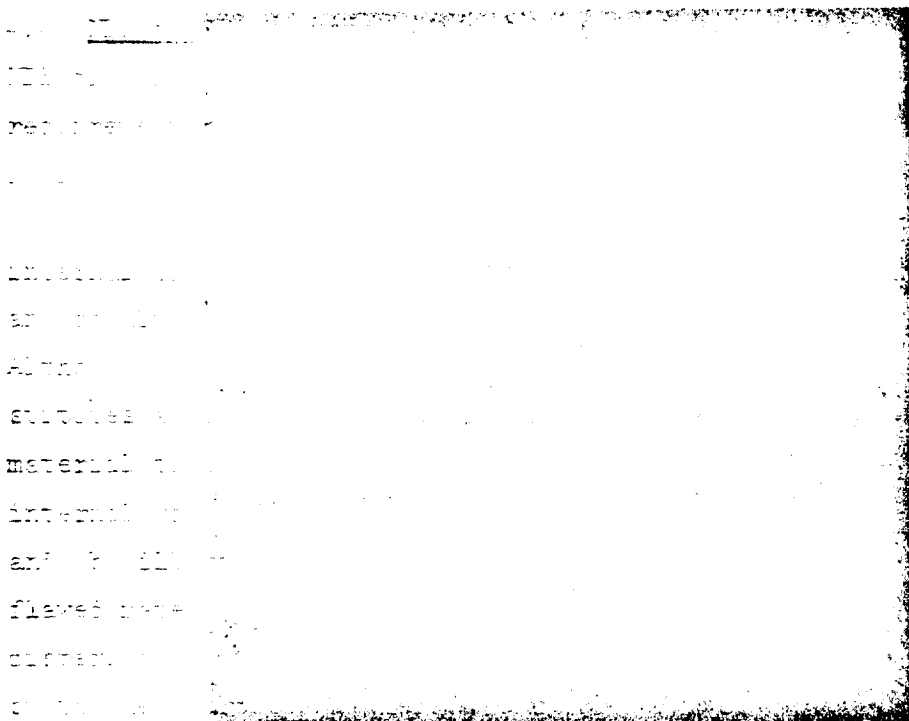
\*Salt water obtained off Fire Island

\*\*Rapid-Temp Lab Furnace - Model 1700M



#### 4.4 NDE of CPI Materials

NDE of candidate materials for heat shield applications becomes a major requirement where reliability and reusability are essential. X-ray radiography has been found to be a useful technique for the inspection of CPI materials. This technique has successfully detected voids, internal cracks and cracks due to thermal cycling, density variations and cobalt oxide rich inclusions, due to improper mixing procedures. Although standards have not as yet been established as to what constitutes a critical flaw, the technique has been used to reject any material that shows gross inhomogeneities, due to poor mixing, or internal voids or cracks invisible to the naked eye. Figure 4-29 (a) and (b) illustrates typical examples of good quality material and flawed material, respectively. These photographs show that complete dispersion of the cobalt oxide into the cenosphere system is possible by the heat treatment used to form the CPI tile. The agglomerations were produced by incomplete dispersion. Density variations may be due to pressing non-uniformities in the pre-fired tile or to non-uniform shrinkage during firing operations. Off-center flexural failures and low strength values were traced to poor quality materials. In Figure 4-30, a CPI tile is shown that appeared good to the naked eye, but its X-ray showed a large internal crack, as can be seen lower part of the photograph.



(b) With Large Number of Agglomerations



(a) Homogeneous

Figure 4-29 X-Ray Pictures of CPI Tiles



Figure 4-30 X-Ray Picture of CPI Tile With Internal Crack

## SECTION 5

### TPS CONCEPT DEVELOPMENT

#### 5.1 CPI Material Design Characteristics

CPI is a unique closed-pore ceramic foam insulation material which offers design flexibility. The material's outstanding characteristics are:

- Rigidity - The material's rigid nature renders it easy to handle and offers a hard durable surface for the vehicle exterior.
- Machineable - The material is easily machineable. Complex shapes, steps and grooves, edge members can be incorporated.
- Water Repellent - The ceramic foam material can be fabricated to provide negligible water absorption. (1 to 3% by Weight).
- Mechanical Attachment Feasibility - Mechanical attachments are feasible with CPI. This feature has potential for the elimination of bonding and/or use of a carrier panel which can significantly reduce total TPS weight and simplify integration with the vehicle primary structure.
- Use as a Coating Material - CPI's rigid water repellent, high emissivity and high erosion resistance characteristics serve to make it useful as a coating material to enclose a core of fibrous insulation.

#### 5.2 Conceptual Design Studies

##### 5.2.1 General

A comparison of thermal conductivities of the various TPS candidate materials is shown in Figure 4-10. The CPI's high conductivity requires that it be used in a way significantly different than existing reusable external insulation systems. It was concluded that:

- CPI must be used in conjunction with other low density thermally efficient insulators, i.e., Kaowool, Mullite or Dyna-quartz, in order for the total system to be thermally competitive.
- The CPI's higher density requires that it be used as a thin plate, i.e., either as a coating on rigidized fibrous insulations, or as an independently-supported surface tile in order to be weight competitive with other TPS systems.

Many CPI TPS concepts were examined in an effort to select those most eligible for in-depth design and analysis. Each concept has certain desirable features in addition to problem areas which require further study. Essentially, two basic approaches emerged which indicated promise for study in the program. These are CPI/Bonded Concepts and CPI/Mechanically Fastened Concepts.

The vehicle design criteria, environments and requirements outlined in Subsection 3 were used as the basis for the concept development. Two regions of uniform heating on the lower surface of a typical Shuttle Orbiter, Areas 1 and 2P, were evaluated. Area 1, a typical region on the vehicle lower surface, receives moderate heating (1500°F). Area 2P, close to the leading edge, experiences higher entry temperatures (2300°F).

The concepts to be presented were selected on the basis of low weight, low cost and maximum reliability. Strain isolation techniques and minimal heat shorts to the primary structure were accorded primary attention.

#### 5.2.2 Bonded Concepts

The bonded concepts were studied first because of their inherent lightness and simplicity. With these concepts, the CPI is used as a coating material. The approach is similar to existing RSI systems in that a thin layer of CPI is employed over the primary rigidized fibrous insulations. The CPI material appears very attractive in these concepts because it has greater strength and strain to failure than existing coatings and because of its high emissivity, erosion resistance and water repellency.

With these concepts, the CPI is assumed to carry no differential pressure loads. All these loads are carried by the primary structure.

With the bonded concepts, two designs were developed, both very similar, but tailored to each of the Area 1 and Area 2P requirements. This was done to provide a minimum cost system to meet each environment. The bonded systems consist of four elements; surface tile, primary insulation, strain isolator, and the seal, if used. The overall concept is illustrated in Figure 5-1.

#### 5.2.2.1 CPI Surface Tile

In this application, the CPI is used solely as a surface material. The CPI tile thickness is determined by minimum machining requirements. Although with more advanced machining techniques the CPI could be machined to a thinner thickness, 0.120 inch thickness was used for the test panels. This thickness provided a tile that is easy to inspect and handle, especially during the subsequent bonding process.

#### 5.2.2.2 Primary Insulation

Two types of fibers, Kaowool and Mullite, were considered for the bonded concept. The properties of these fibers are discussed in Section 4.1.5 of this report.

The newly developed 10 pcf Johns-Manville Rigidized Dynaquartz fibers were considered for use with CPI. These fibers are pure amorphous silica and exhibit short term stability to 2500°F. They offer the lowest conductivity of all the fibers and therefore would provide the lowest weight system. Attempts of bonding CPI to Dynaquartz however have proved difficult. This is the result of the large difference in thermal expansion between the two materials. In addition, the Dynaquartz block of greater than 1 inch thickness tended to form large through-the-thickness cracks on thermal cycling to the area 2 or 2P heating. Within the limited program time therefore, Dynaquartz was eliminated from study in the program.

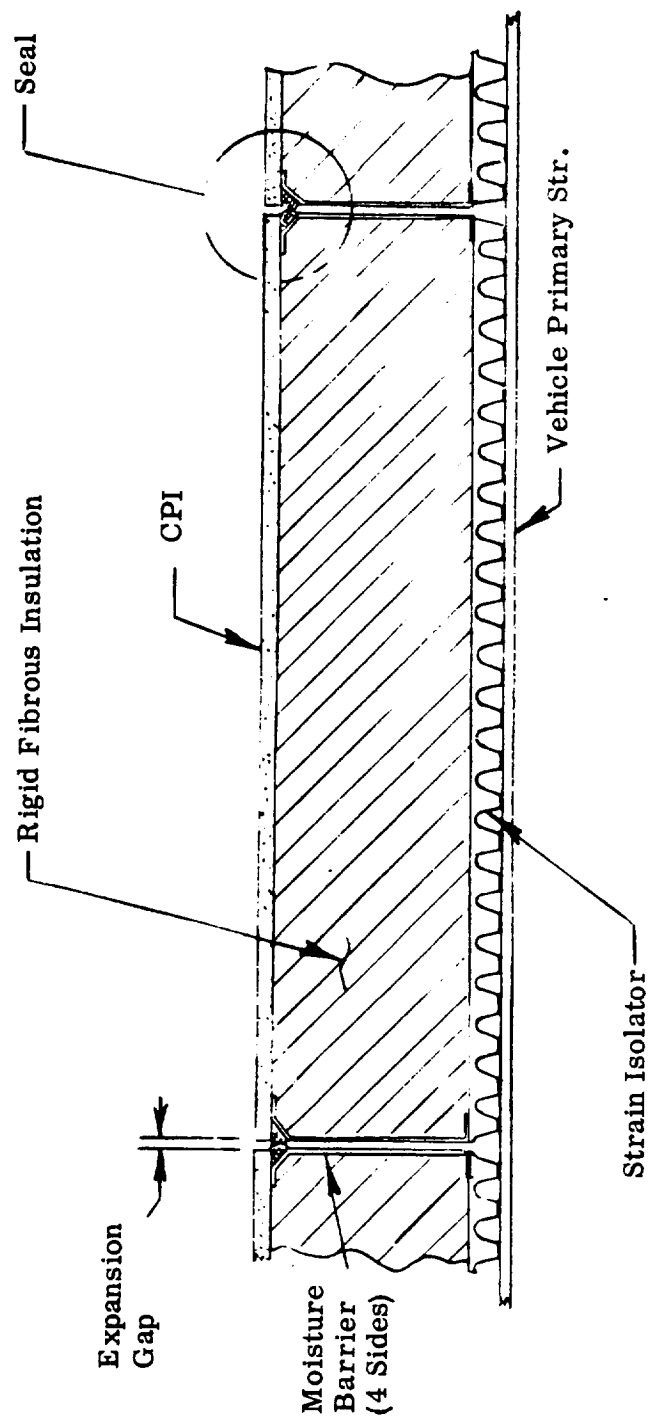
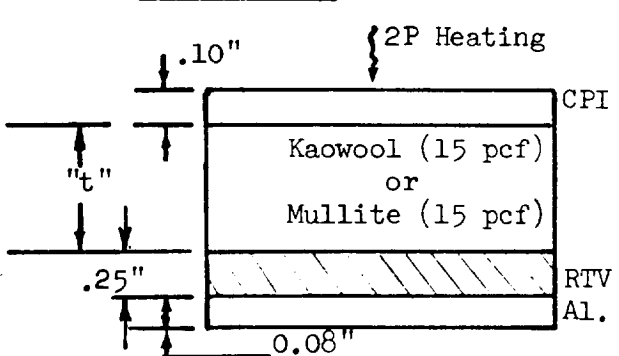


Fig. 5-1 CPI Bonded Concept

Temperature analysis of the two most promising bonded schemes using mullite and Kaowool fibers were made and the results are shown below:

Construction	Fiber	Required Thickness ("t")
	Mullite	2.49"
	Kaowool	2.10"

This comparison gives an indication of the higher thermal efficiency of the Kaowool fibers. However, these low cost fibers cannot be properly used in all areas because the highest temperature stability of the Kaowool fibers is 1950°F. This then precludes their use in designs that can accommodate an area 2P heating. For an area 2P application, a two-layered composite is used, as described in a later section. A thin mullite layer, 0.30" thick, is used to drop the peak temperature in the Kaowool to a safe 1700°F.

#### 5.2.2.3 Moisture Barrier

As illustrated in Figure 5-1, the rigid fibrous insulation is protected from moisture absorption by the CPI on the top, and the RTV rubber strain isolator on the bottom. Only the sides therefore require a barrier. The CPI cannot be used to seal the sides because of the large thermal gradient which would develop. A metallic foil barrier was investigated for sealing the four sides because metallic foils have been successfully used to seal low density fibrous insulations employed with metallic thermal protection systems.

The foil system is simple to fabricate. The foil is folded around the four sides of the fibers prior to installation of the CPI surface tile. The foil is folded with return lips around the block; the lips are overlapped



and subsequently spotwelded at the corners. Figure 5-2 shows the foil enclosed block prior to bonding of the CPI and the strain isolator. Subsequent bonding of the CPI and the strain isolator also contribute to foil retention.

The type of foil used is determined by the operating temperature required for the system. For Area 1, where a 1500°F peak temperature is reached, Inconel 600 or 702 can be used. For Area 2P, where a 2300°F peak temperature is reached TD-Ni 20 Cr foil is employed. The use of TD-Ni 20 Cr metallic foil as a moisture barrier was validated by McDonnell-Douglas in their NASA funded (Contract NAS 8-26115), High Temperature Insulation Materials for Reradiative TPS program. Venting of the assembly is accomplished through holes in the strain isolator, which because of its finger-like configuration, permits good venting.

#### 5.2.2.4 Edge Seal Development

The CPI material is exceptionally suited for development of unique boundary layer gas seals. Figure 5-3 illustrates seven designs which could be used with the thin tiles typical of the bonded concepts. Design "A" offers a good seal but requires the fabrication of a separate assembly, including the foil, and strain isolator. Assembly problems are increased because of the need to locate the seal strip between the panels prior to panel installation. Design "B" provides a positive seal but requires the bonding of a CPI seal member to one CPI surface tile. This design also requires a "male" and "female" tile arrangement complicating assembly and removal. Designs "C" and "D" are positive but require additional machining of the CPI surface tile. Design "E" eliminates the male-female requirement but requires the installation of the silica rope seal during tile in-

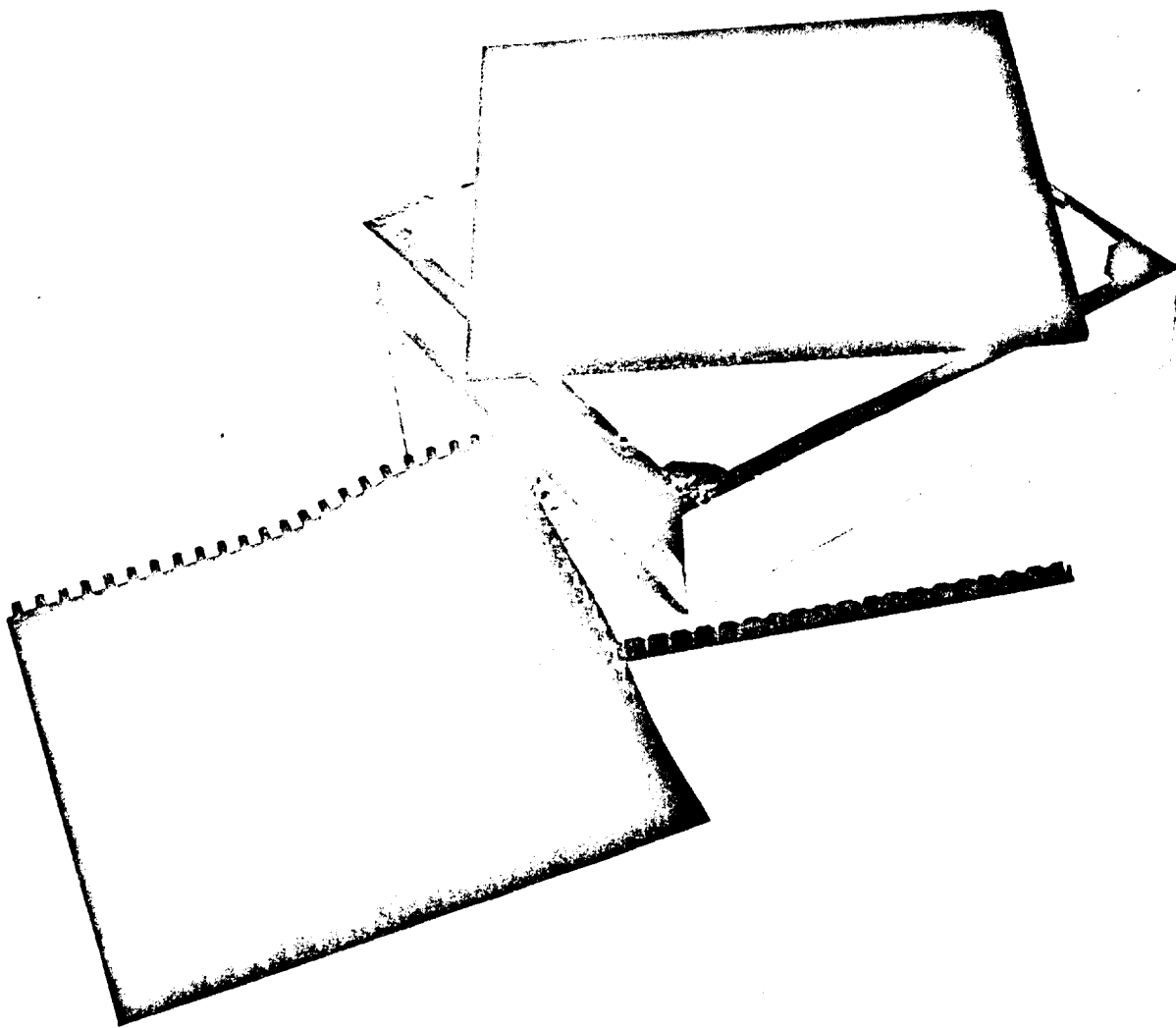
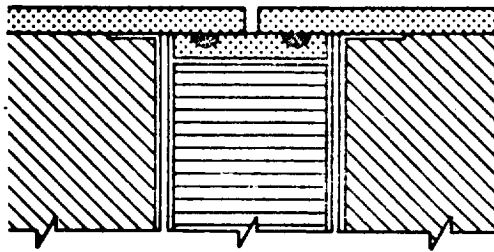
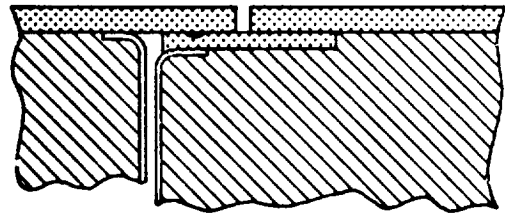


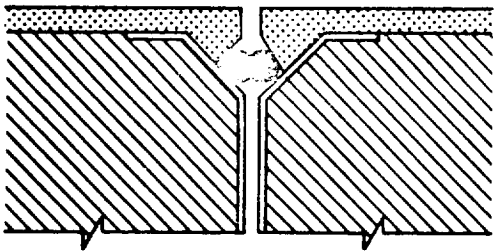
Figure 5-2 CPI/Bonded - Area 1 Test Component Prior To Assembly



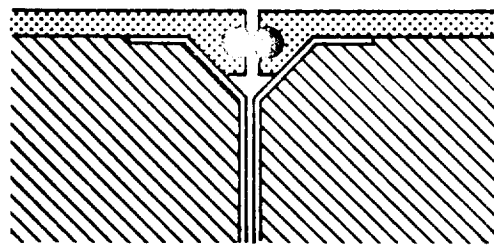
A



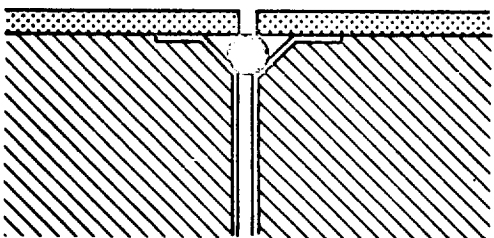
B



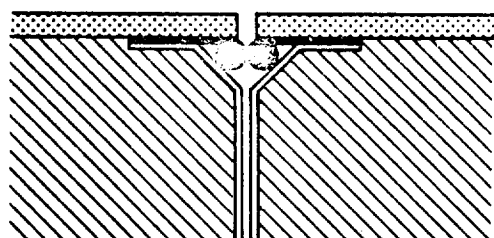
C



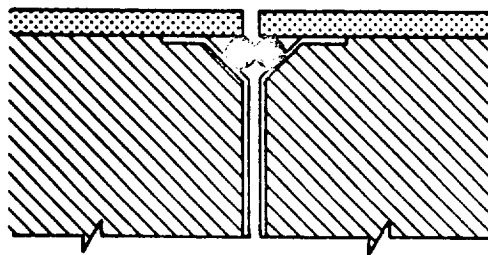
D



E



F



G

Figure 5-3 Bonded Concept - Edge Seal Designs

Installation. The design offers poor sealing at the corners because the seal is not continuous around the corners. Design "F" and "G" are very similar. Both designs permit individual tile removal and require no additional machining of the CPI surface tile. Moisture and thermal sealing is accomplished by the compression of adjacent seals. The rigidized primary insulation is fabricated with a chamfer as illustrated. The foil moisture barrier is folded around the chamfer and forms a cavity for the rope seal. The seal is bonded in place using refractory Kaowool cement. Design "F" utilizes a tadpole shaped seal for maximum retention. The tadpole could be fabricated using a silica cloth covering around the braided silica cord, and bonded between the CPI tile and foil enclosed insulation block as shown. Design "G" was baselined for fabrication in the program. The 1/8" diameter ceramic cord was purchased from Gaskets, Inc. of Rio, Wisconsin 53960.

### 5.2.3 Mechanically Fastened Concepts

In contrast to the bonded concepts, the mechanically fastened concepts take maximum advantage of the CPI material and its ability to carry pressure loads without the use of a substrate. A surface tile is employed to beam the pressure loads to the standoffs which transmit them to the primary structure. The advantages of these approaches are that no bonding is required, and that efficient low density insulations can be used. Of significant importance is the fail-safe nature of these concepts wherein a separate, packaged insulation system is employed which is independent of the CPI surface tile, and can resist the reentry environment in the event of surface tile failure. The standoffs serve as strain isolators with these concepts and greatly simplify integration with the vehicle.

Five mechanically fastened concepts are presented. Each offers a different approach to the total TPS. Each of the concepts contain certain desirable features in addition to problem areas.

#### 5.2.3.1 CPI/Web Standoff Concept

An early mechanically supported concept is shown in Figure 5-4. A 15.2 x 25.4 cm (6.0 x 10.0 in.) CPI surface tile is used, supported on metallic web type standoffs which are insulated from and mechanically attached to the primary structure. The CPI support clips are designed to permit the tile to expand and contract as required, while still resisting vertical loads. This is achieved by orienting the clips, and the supporting post, along radial lines emanating from the panel's geometric center. Three additional clips are used along the longitudinal edges to keep the CPI bending stresses within acceptable limits. As illustrated, the webs are located to pickup the vehicle stringers. TD-Ni20Cr screws are used, through holes in order to retain the tile. The screws are covered with CPI plugs as shown.

Some advantages of the concept include:

- Positive tile retention. Screws are positive and easy to inspect. Additionally the web standoff transfers normal and in-plane loads directly to the primary structure
- Support clips permit tile expansion and contraction
- Independent, foil enclosed insulation package which is fail-safe in the event of tile failure

Some disadvantages of the concept include:

- Holes are required in the CPI tile, which causes stress concentrations. Additionally, bonded plugs are required on installation.
- Excessive heat shoring occurs through the web-standoffs
- Four very complex, packaged insulation elements are required for each panel
- Screws are close to the hot surface and are prone to oxidation
- Concept is not weight competitive with later systems

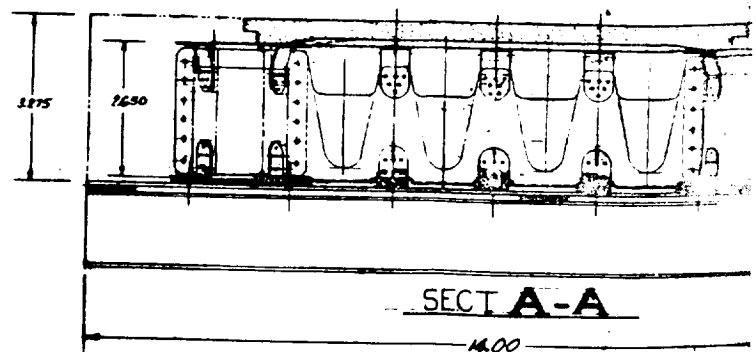
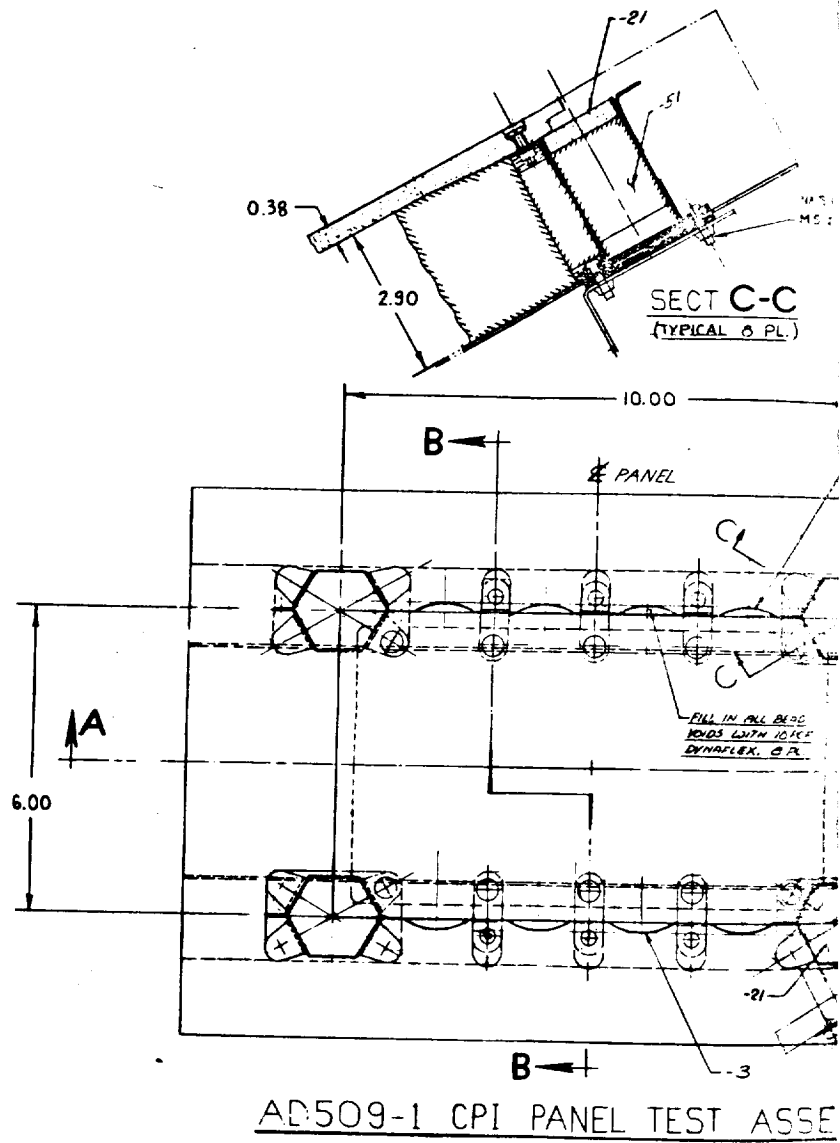
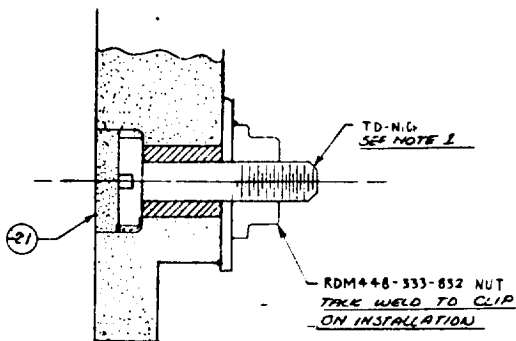
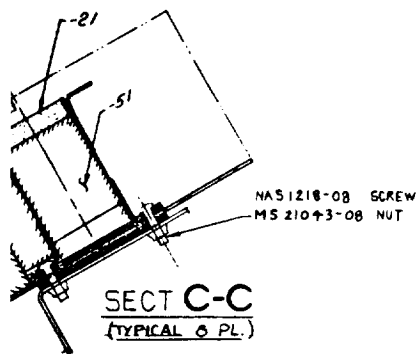
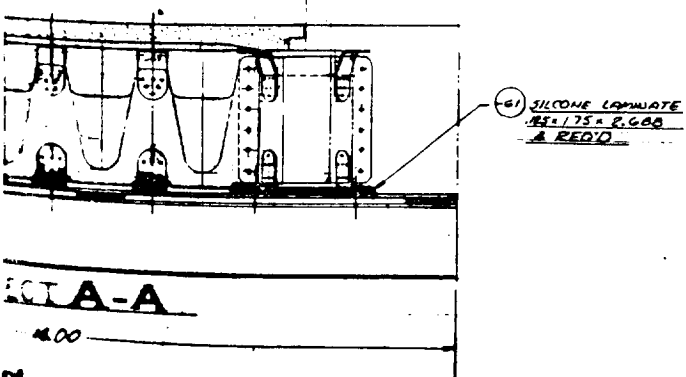
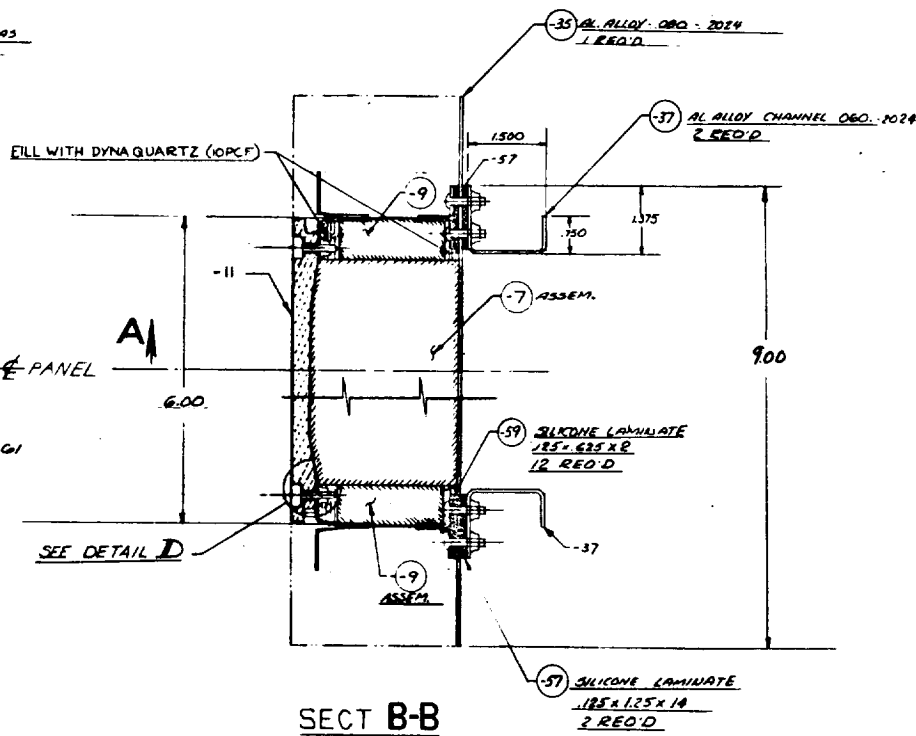
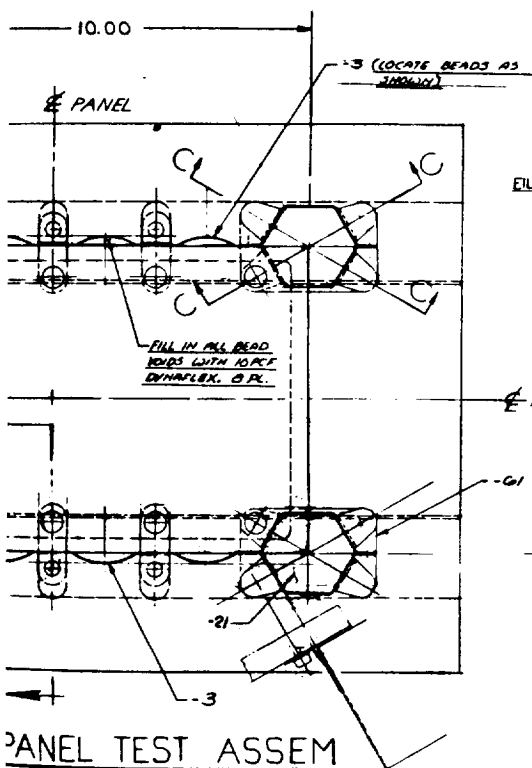


Figure 5-4 CPI/Web Support Concept



**NOTE 1**  
HI-TEMP ANTISEIZE LUBRICANT LF 97-66-1  
IN ACCORDANCE WITH M80 MATERIALS ENG'R  
DIRECTIONS.  
(CONTACT A. FLESCHER X1874 FOR  
LUBRICANT & DIRECTIONS.

**DETAIL D**  
(SCALE: 5/1)



Although this concept offers some interesting fail-safe features, it is not weight competitive. Weights of 4.57 lbs/ft<sup>2</sup> for Area 1 and 5.58 lbs/ft<sup>2</sup> for Area 2P were estimated. The concept was not optimized further. A test component was fabricated to evaluate the CPI tile retention details and the CPI surface plug performance. The component is shown in Figure 5-5. Because of the tight program schedule and other component priorities, the component was not tested.

#### 5.2.3.2 CPI/Square Plug Concept

This concept which is illustrated in Figure 5-6 employs a metallic post standoff which offers minimum weight and heat shorting, since each post supports four surface tiles. Special, dish-shaped metallic retainers are employed which are designed to support the tiles as illustrated and are positively retained by a special screw which threads into the post. The entire support assembly is protected by a CPI plug which is retained by a pin fixed to the plug with a bonded CPI torus shaped boss. A seal is incorporated in each tile to prevent leakage.

Some advantages of the concept include:

- Easily inspectable and positive primary retention system - with plug removed
- Relative ease of assembly and removal. Only one plug required with a simple push-in installation
- Simple large size independent insulation package possible, with minimal post penetrations
- Minimal weight and heat shorting of support posts which are easily integrated to the vehicle and provide very good strain isolation

Some disadvantages of the concept include:

- No positive lateral restraint of the CPI tile is possible because the retainers must be designed to permit the tile to expand and contract. (Restraint occurs when the tile "bottoms")



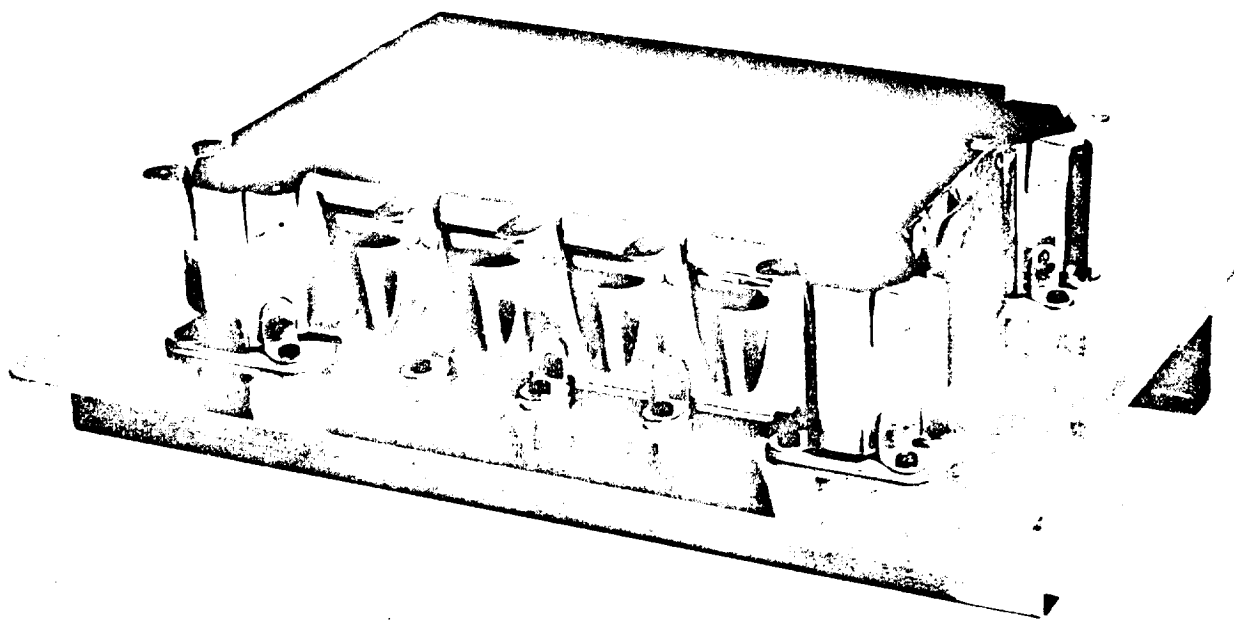


Figure 5-5 CPI/Web Standoff Test Component (6 x 10 Tile Size)

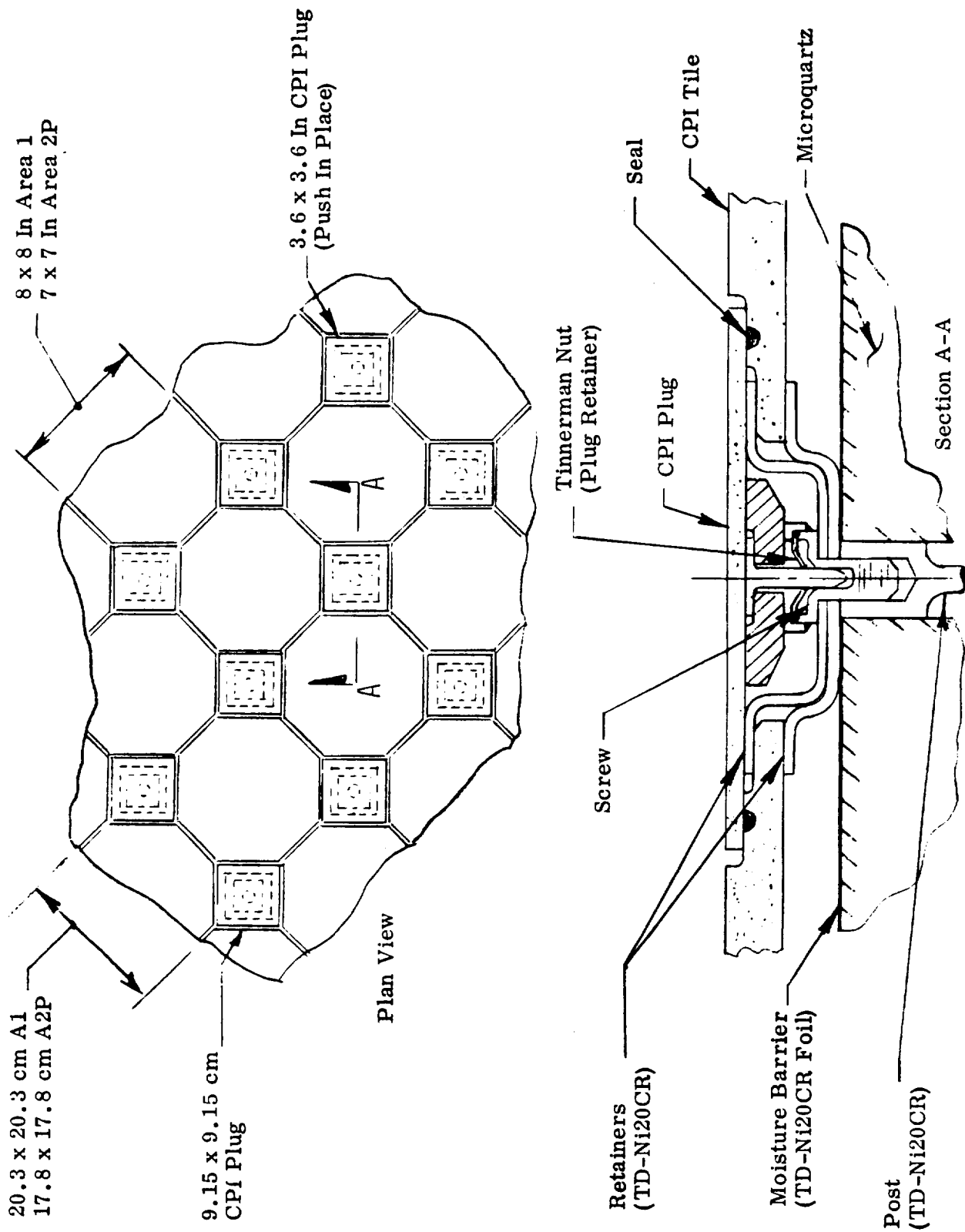


Fig. 5-6 CPI/Post Square Plug Concept

- Redundant up-load path. It is possible to overload the CPI plug retainer for negative pressure conditions.
- Close tolerances are required between metallic retainers to insure in-plane expansion without excessive looseness. The various elements accumulate too many tolerances in addition to tolerances developed with the three adjacent tiles

The weight of this concept was estimated at 3.82 lbs/ft<sup>2</sup> for Area 1 and 5.63 lbs/ft<sup>2</sup> for Area 2P which is somewhat heavier than other designs. The redundant up-load aspect and the difficulty of meeting the tolerance requirements were considered such difficult problems that the concept was not developed further.

#### 5.2.3.3 CPI/Post-Snap Washer Concept

A promising concept is illustrated in Figure 5-7. The concept employs a metallic post standoff which offers minimum weight and heat shorting, since each post supports four surface tiles. A flat star shaped metallic support plate is used which is screwed into and supported by the post. Four specially notched pins are welded to the plate as illustrated in the enlarged detail. The pins are designed to fit into oversized holes in the CPI tile and the tile is retained by a special snap-washer type nut, which is designed to permit tile expansion and contraction. The pin and washer is protected by a CPI plug which is bonded in place after installation. The concept permits use of a lap interpanel seal as illustrated and an independent insulation package which can use more efficient low density insulations.

A 20.3 x 20.3 cm (8 x 8 in.) tile size is used in Area 1 and a 17.8 x 17.8 cm (7 x 7 in.) size is used in Area 2P. Tile size was determined by holding tile thickness to .76 cm (.375 in.) and keeping within material allowable strengths as measured in a material evaluation program.

Some advantages of the concept include:

- No bonding is required with the primary fastening system

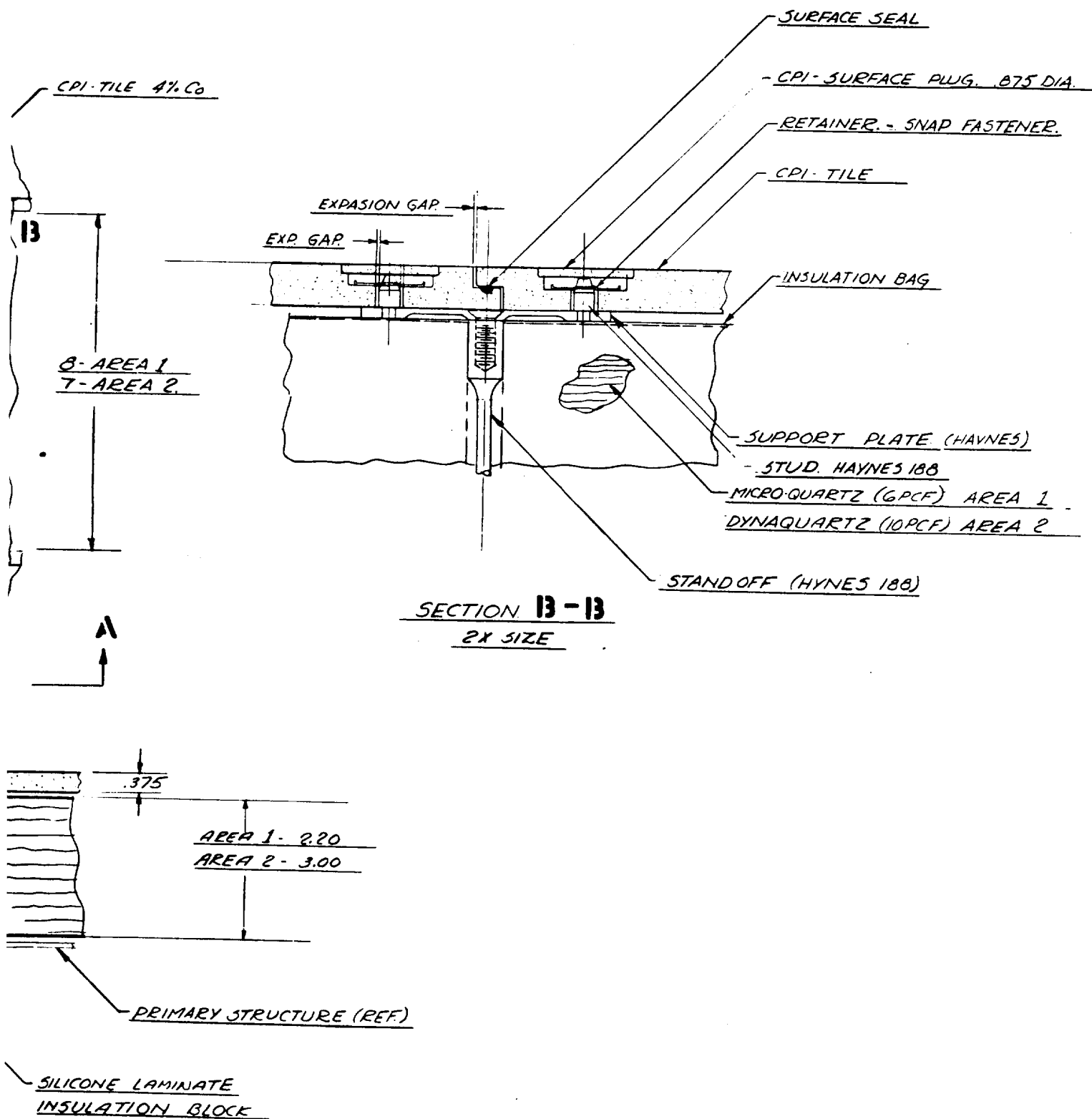


Figure 5-7 CPI/Post - Snap Washer Concept

- Simple snap-in tile retention with simple inspection of the fasteners prior to plug installation
- Minimal weight and heat shorting of the support posts which are easily integrated with the vehicle and provide good strain isolation
- An independent low density insulation package can be used providing fail-safe capability
- Adaptability to curved surfaces

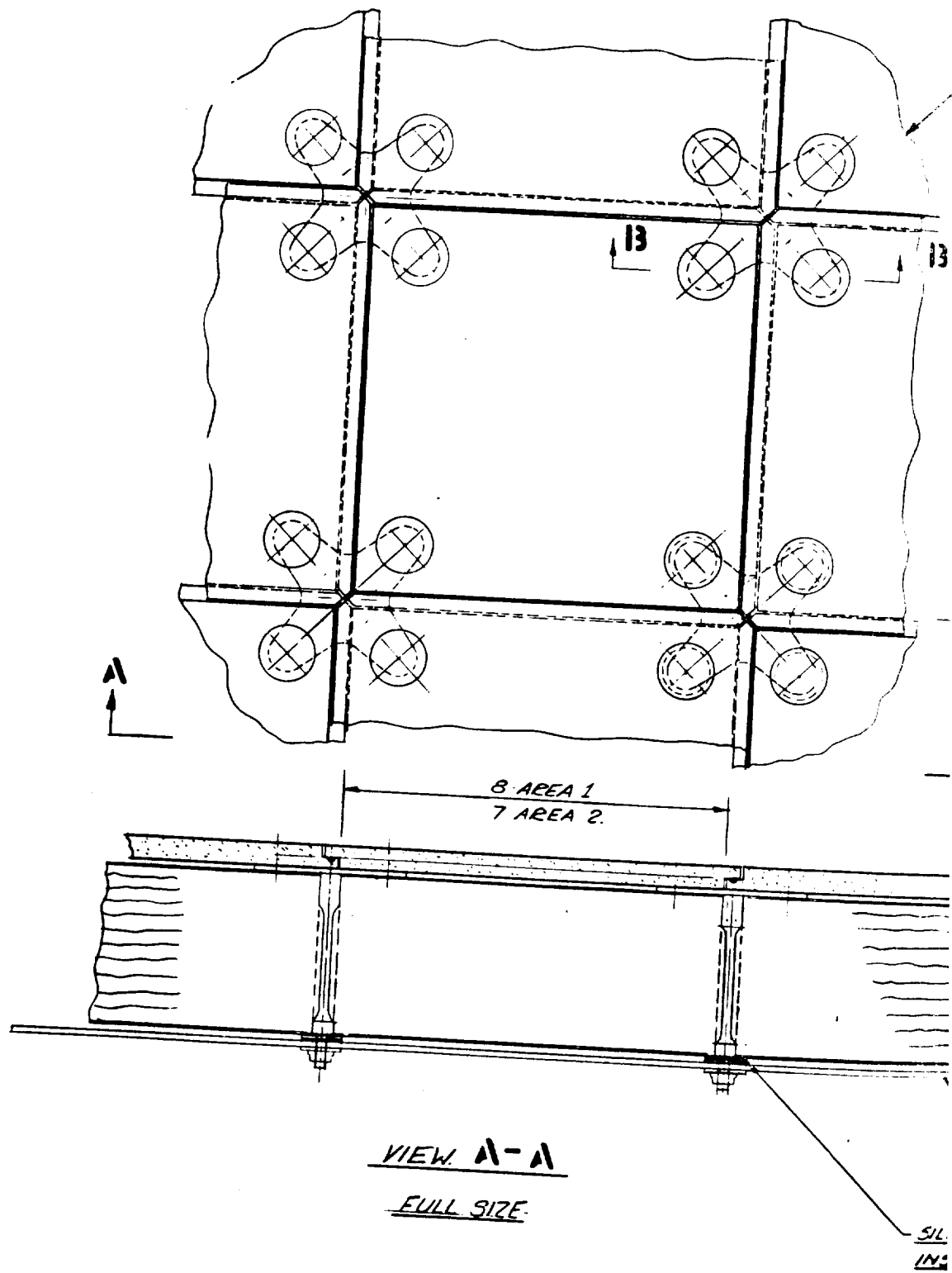
Some disadvantages of the concept include:

- Holes are required in the CPI tile which causes stress concentrations. Additionally, plugs are required on installation and must be broken for panel removal
- Snap-washers are located close to the hot surface with possible degradation of spring action
- Movement of tiles occurs during lateral loading as a result of oversize holes required for in-plane tile expansion

The CPI/Post - Snap Washer concept offers the lightest system of all the post supported schemes and was extensively tested in the program.

#### 5.2.3.4 CPI/Sandwich Concept

A concept that received study in the program is shown in Figure 5-8. The concept was developed to utilize the efficiency of sandwich construction to fabricate large TPS panels. The sandwich includes an upper and lower CPI face plate which is diffusion bonded to a regidized mullite fiber core. The upper face plate is machined with thick boss areas so that a Haynes-188 screw can be buried below the surface. The screw is protected from the environment by means of a CPI surface plug, as illustrated. The



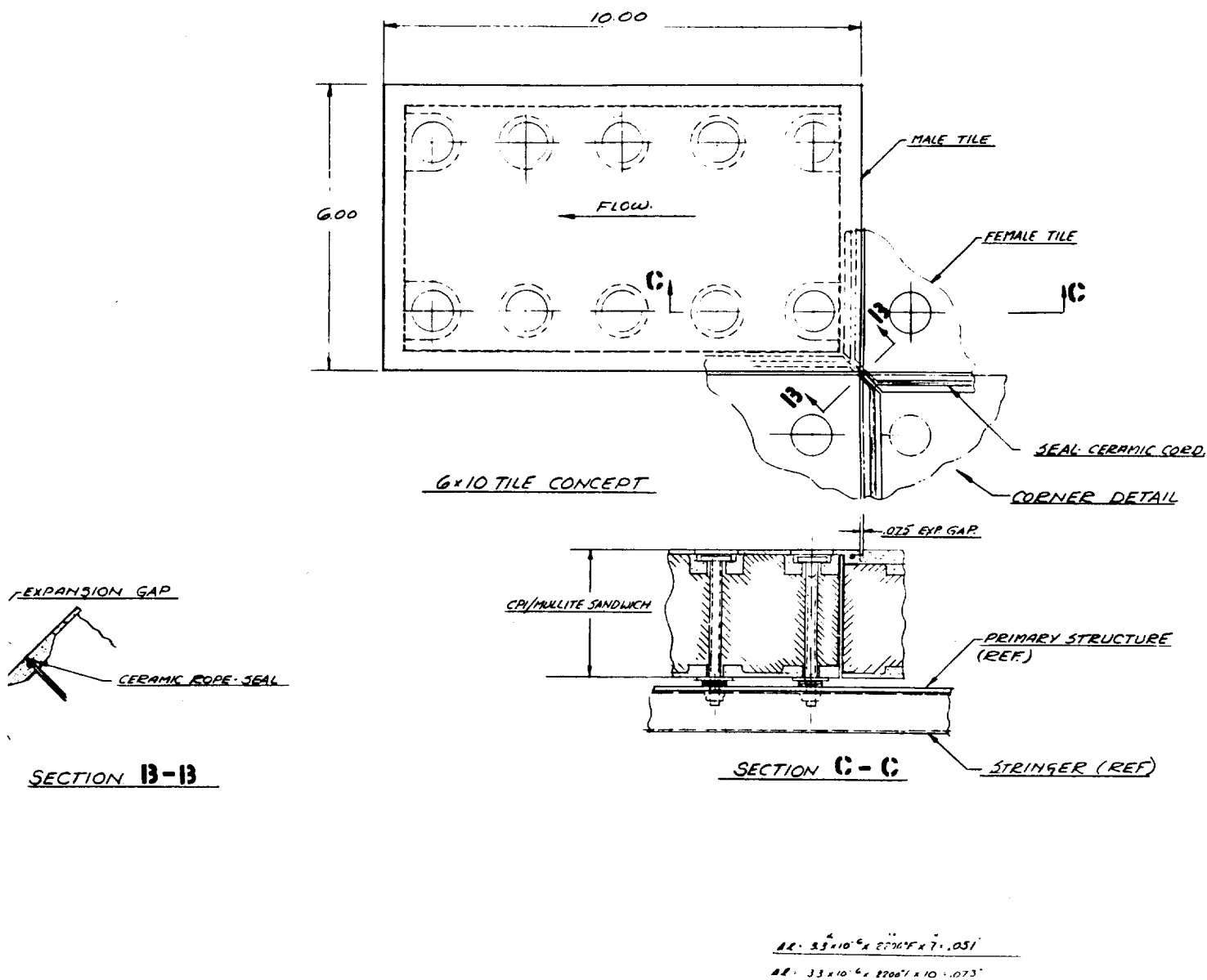


Figure 5-8 CPI/Sandwich Concept

lower face plate is held above the primary structure by use of silicone laminate spacers, as shown. The panel is supported by special Haynes-188 posts which are designed to include a shoulder and threaded stud for assembly to the primary structure which includes an anchor nut. The upper end of the post is threaded to retain the Haynes-188 screw which retains the panel.

Two different bolt patterns were studied to determine the lightest design. The four (4) bolt pattern design is shown in the left of Figure 5-8 and a ten (10) bolt pattern design is shown on the right. The four bolt design assumes panel plate action and is a more efficient approach.

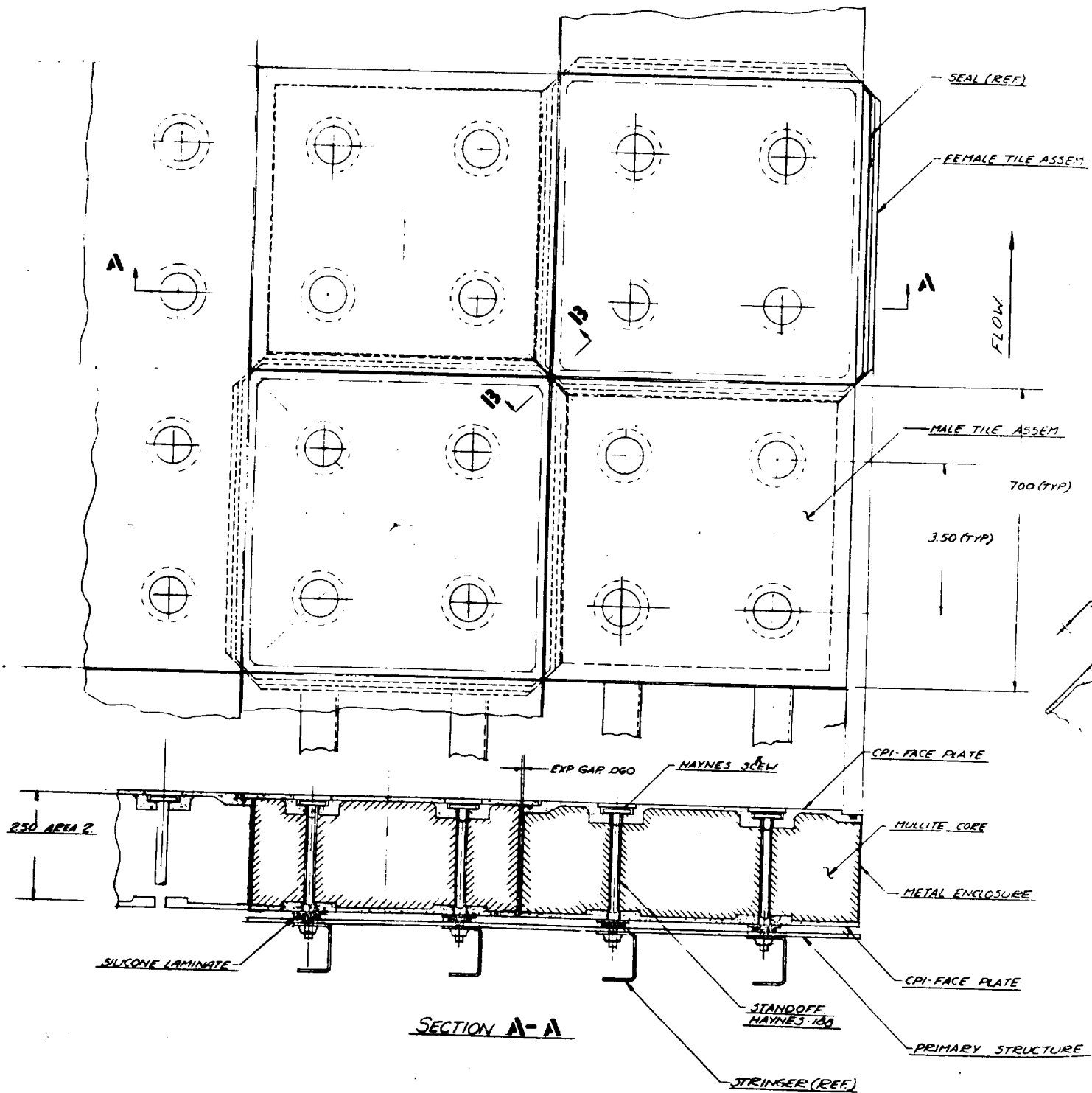
The concept was not pursued in depth because the initial objective was not met. Large panels were not possible with the concept because relatively high shear stresses were developed in the mullite core material. Some additional disadvantages of the concept include:

- Holes and bosses required in the CPI tiles, cause stress concentrations. Additionally, bonded plugs are required on installation.
- CPI tiles require more machining than other concepts.
- Screws are close to the hot surface and are prone to oxidation.
- Panel expansion is difficult to accommodate because of different temperatures across the panel
- Concept is not weight competitive with other systems

#### 5.2.3.5 CPI/Post-Sliding Bushing Concept

The development of this concept evolved during the process of eliminating certain shortcomings of the CPI/Post-Snap Washer Concept. The concept is very similar in that the post support is employed, which offers minimum weight and heat shorting, provides good strain isolation, and is easily integrated with the vehicle. The concept differs in that the star-shaped support plate incorporates a slot which is used to support a special bushing, which retains the CPI surface tile and permits thermal expansion





and contraction. The versatility of the sliding bushing design is described in more detail in paragraph D of this section wherein three alternate designs for tile retention are discussed.

In addition to tile retention versatility, the concept is adaptable for use with various tile configurations. Each is described in the following paragraphs.

(a) Hexagonal Tile Design

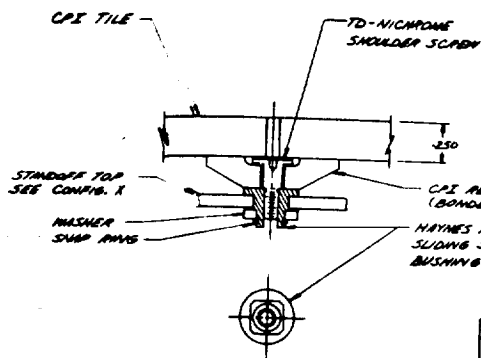
This design was developed as a result of failures developed during thermal cycling of the early CPI material and is shown in Figure 5-9. The failures occurred in the corners of square shaped specimens as a result of tile warping, and efforts were directed at the development of concepts which provided more circular tiles. The hexagonal design offers a more nearly circular tile configuration thereby reducing corner stresses. Some additional advantages of the concept include:

- Minimum corner stresses as a result of CPI out-of-plane warping due to thermal gradients
- Radial in-plane expansion accommodated by sliding bushing design
- More uniform tile support which lowers the stress level in the CPI

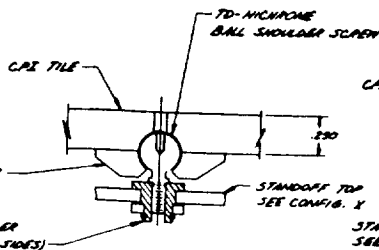
Some disadvantages of the concept include:

- Hexagonal tile is more difficult to manufacture with increased tolerance buildup
- Unconventional tile shape. Edge treatment is difficult and special tiles would be required
- Concept is slightly heavier than an identical system using a square tile

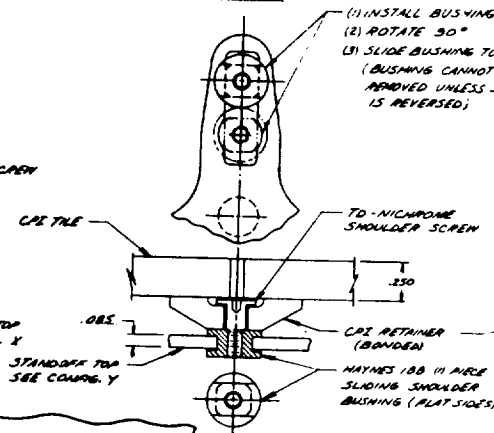
**OPTION A**  
SHOULDER SCREWS  
SLIDING SHOULDER BUSHING ASSY.  
2 x SIZE



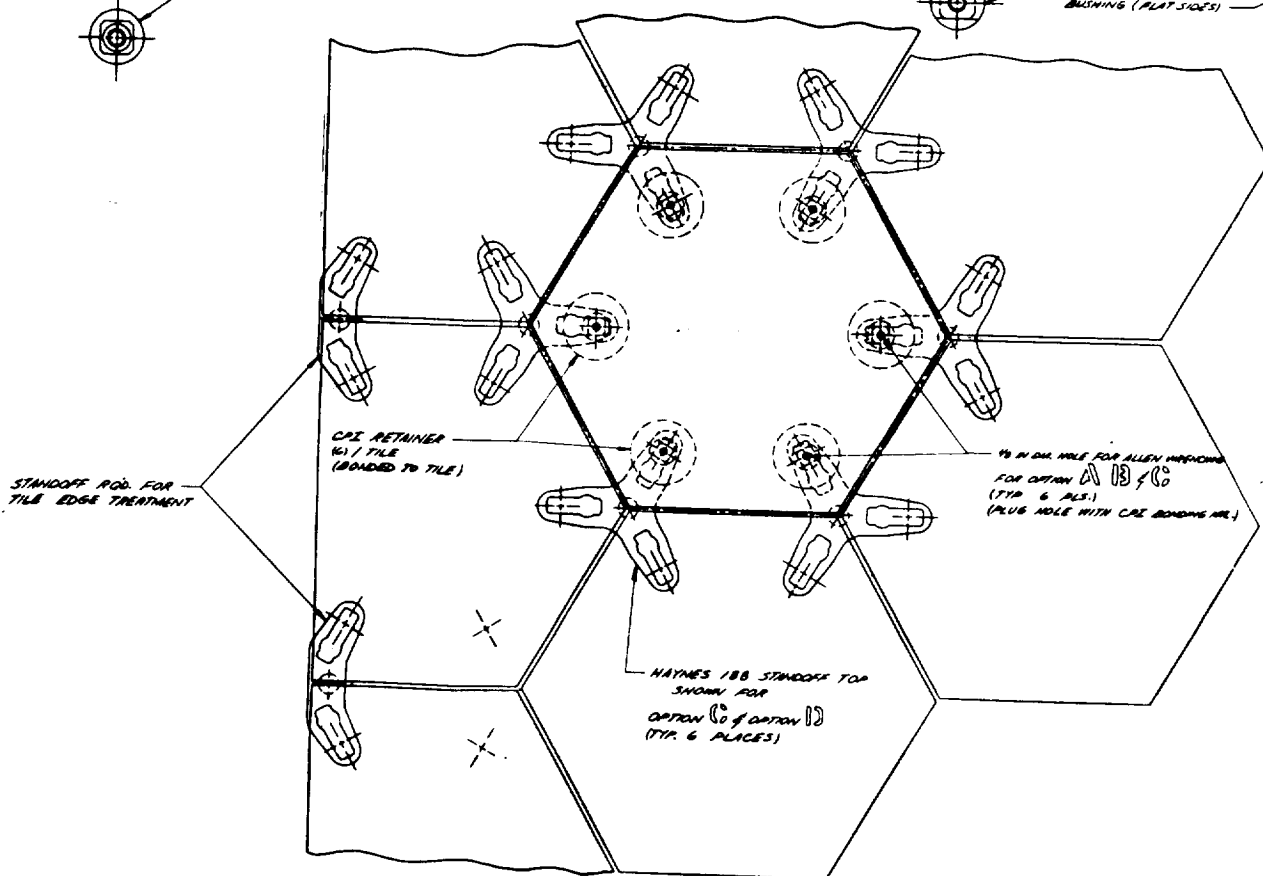
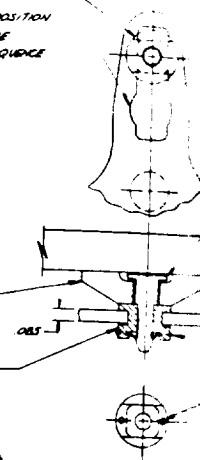
**OPTION B**  
BALL SHOULDER SCREW  
SLIDING SHOULDER BUSHING ASSY.  
2 x SIZE



**OPTION C**  
SHOULDER SCREWS  
11 PIECE SLIDING SHOULDER BUSHING  
2 x SIZE

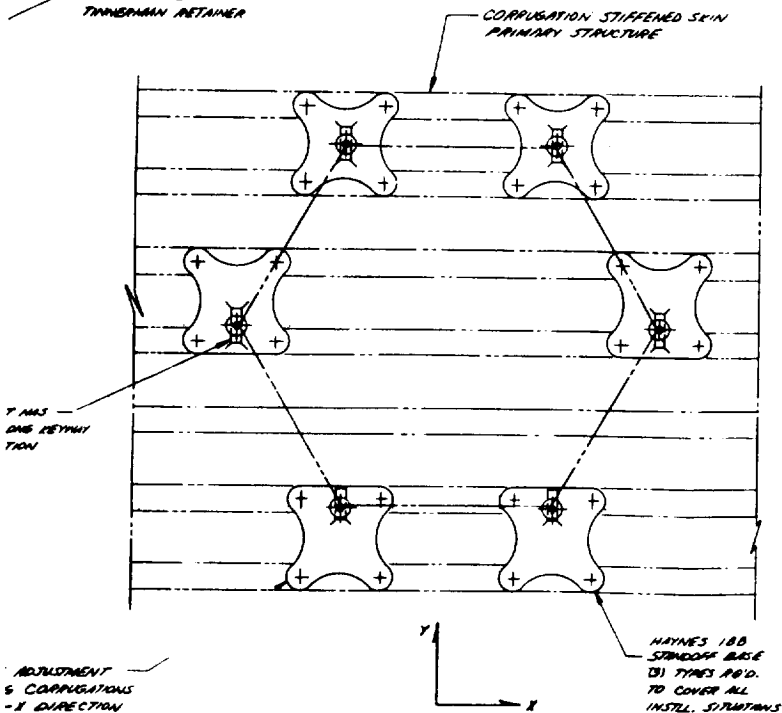
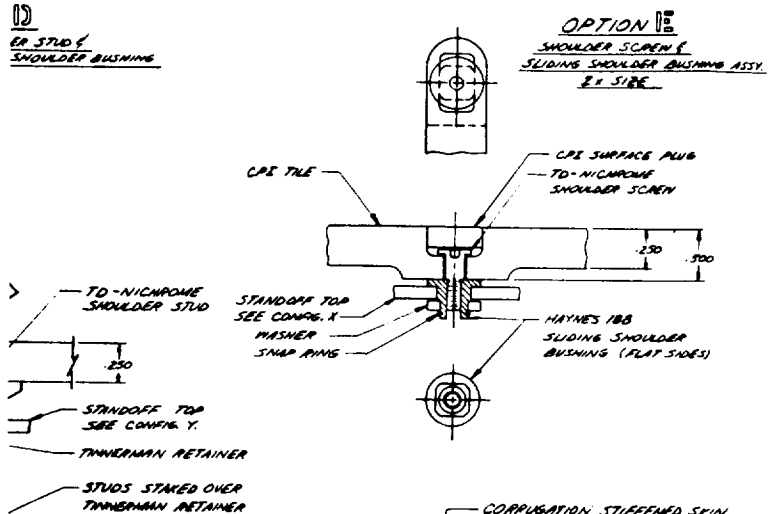


**OPTION D**  
BLIND  
11 PIECE

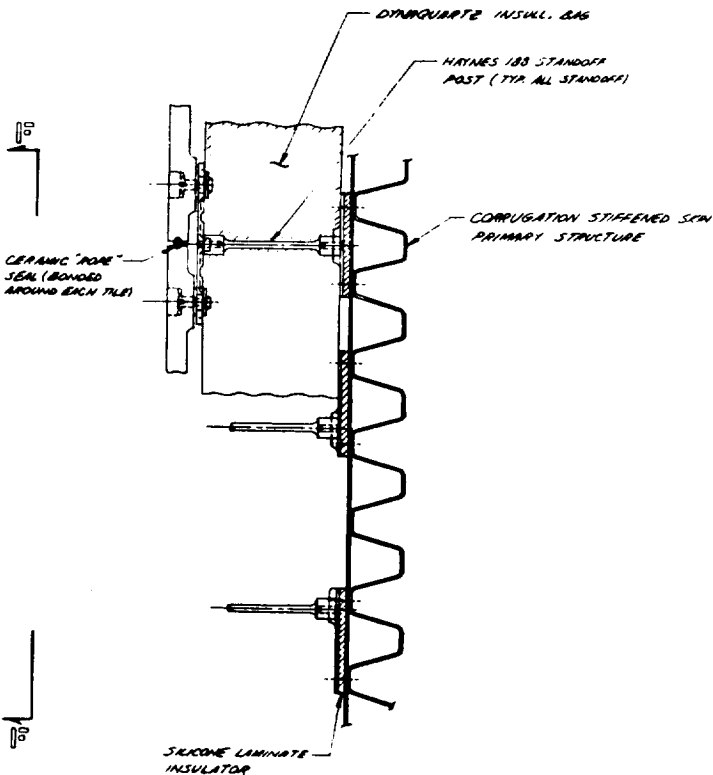


**CONFIGURATION Y**  
UTILIZES CPI BONDED RETAINERS  
SEE OPTIONS A, B, C & D

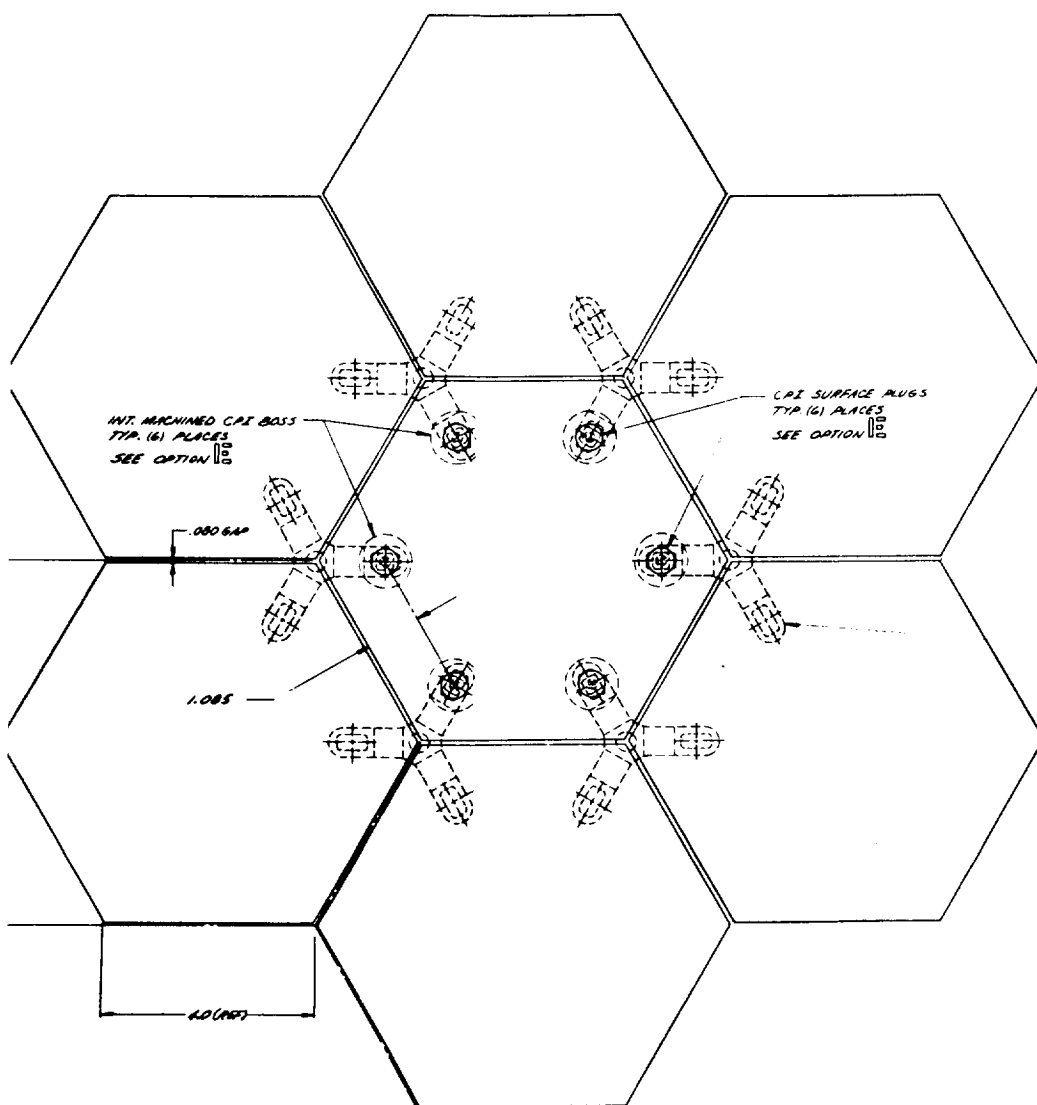
ED STUDS  
SHOULDER BUSHING



STANDOFF PRIMARY STRUCTURE  
ATTACHMENT  
FOR  
CONFIGURATION X & Y



SECTION 10-10  
STANDOFF PRIMARY STRUCTURE  
ATTACHMENT FOR  
CONFIGURATION X & Y



HAYNES 188 STANDOFF TOP  
SHOWN FOR OPTION 1E

CONFIGURATION X  
UTILIZES HOLES IN CPI TILE  
SEE OPTION 1E

Figure 5-9 CPI/Post - Sliding Bushing Concept  
Hexagonal Tile Design

Also illustrated in Figure 5-9 are five optional tile retention designs which are possible with the sliding bushing. Also shown is a standoff base plate which can adapt the TPS to the corrugation stiffened primary structure, if it is used.

Development of the 4% cobalt oxide material (CPI-4) eliminated tile warping thereby eliminating the primary need for the hexagonal design and it was not pursued further in the program.

(b) Rectangular Tile Design

This design which is shown in Figure 5-10, employs the sliding bushing concept and makes use of a 6 X 10 inch tile size. The design was developed to increase tile size, thereby reducing tile quantity. To permit thermal expansion and contraction, the standoff support plate is designed to permit expansion from the geometric center of the tile. The plate is supported by a two-piece conical standoff which is shown in detail "A". The concept is shown with the surface screw and CPI plug retention design, although the blind designs could be used.

Although offering a larger tile size, the design is slightly heavier than the square tile design and was not pursued further in the program.

(c) Square Tile Design

Figure 5-11 illustrates the sliding bushing concept with a square tile which is the concept finally baselined in the program. The concept employs the post type standoff which has been previously described. A star shaped support plate is used which is stamped with slotted holes. A special bushing is used, which is designed to fit the slotted opening without the use of any tools. The bushing supports a blind, Tinnerman type nut as illustrated in Detail "D". A simple flat .375 in. CPI tile is used which supports a CPI stud retainer which retains a straight shanked TD-Ni20Cr shoulder pin. The CPI stud retainer is bonded to the surface tile

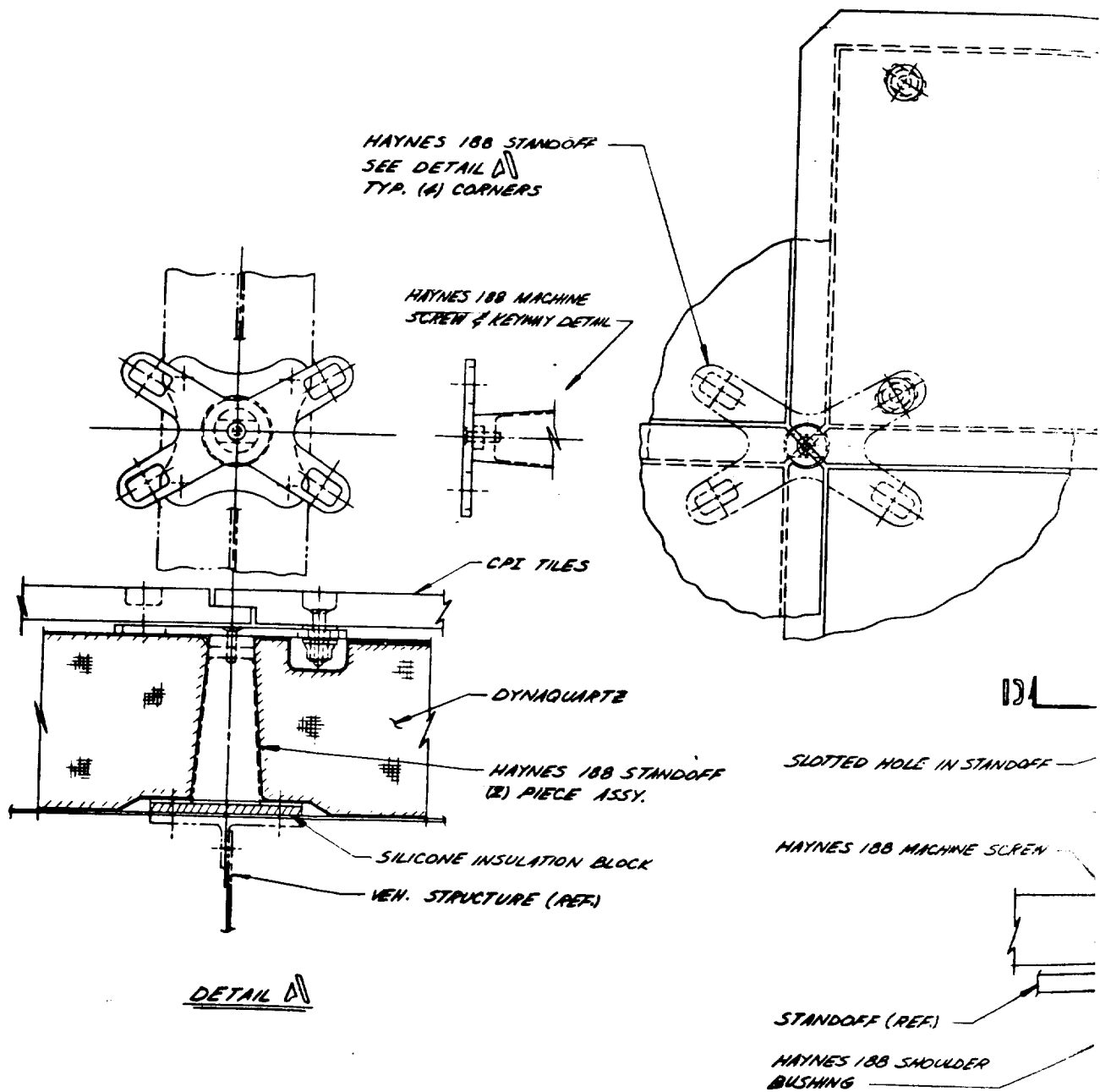
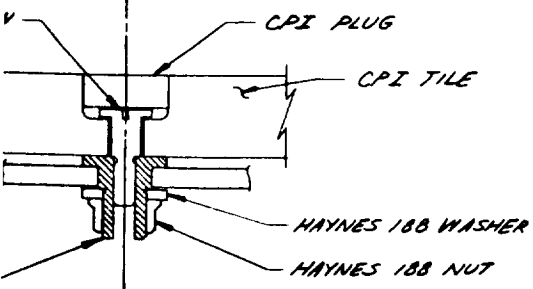
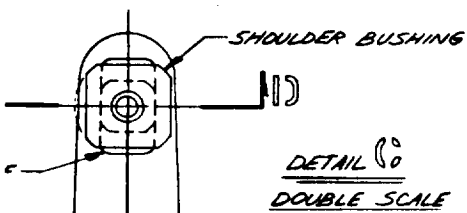
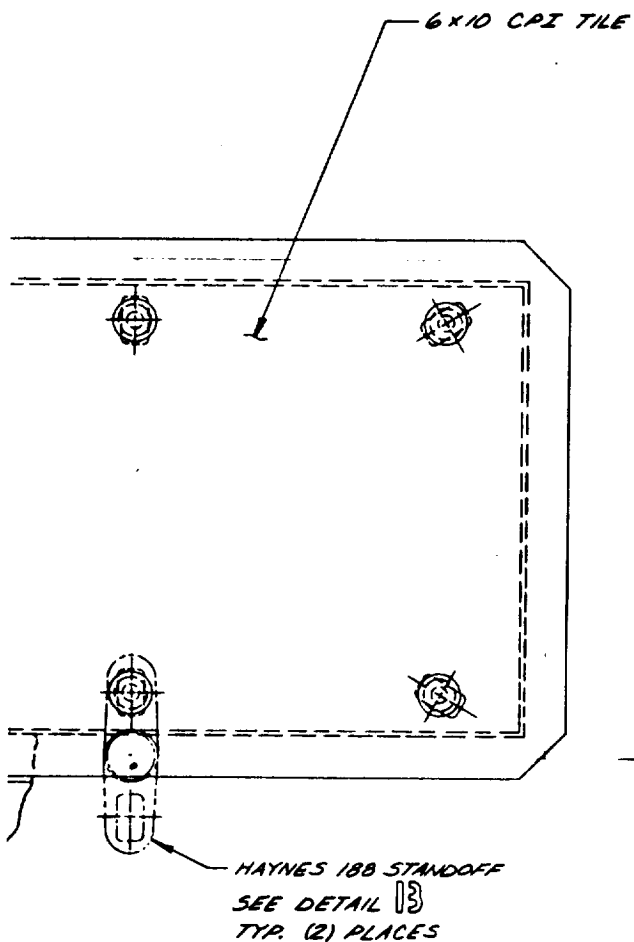
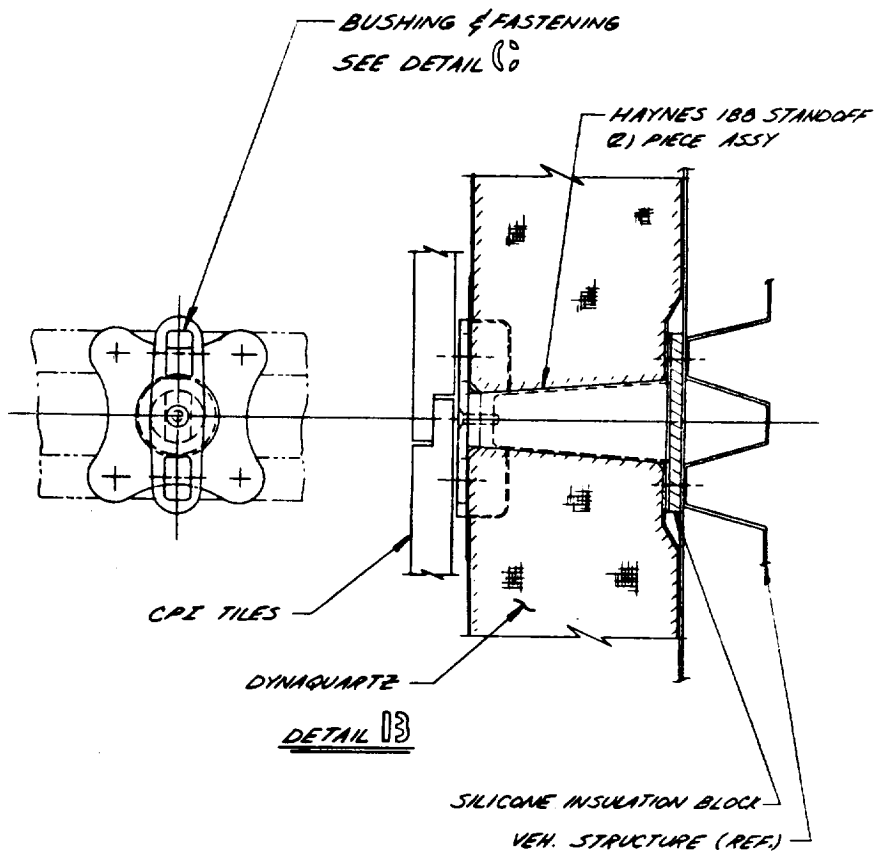


Figure 5-10 CPI/Post - Sliding Bushing Concept Rectangular Tile Design

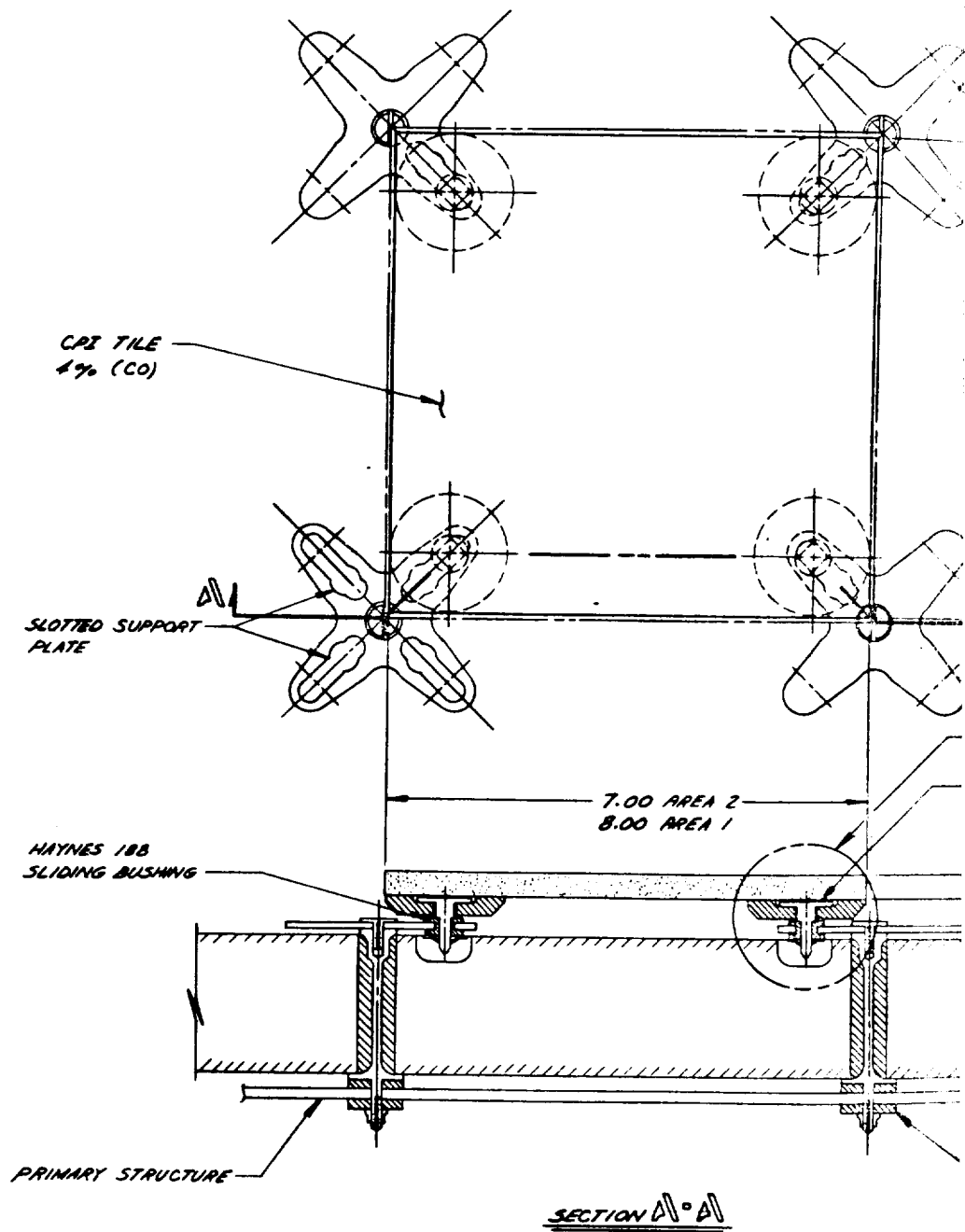


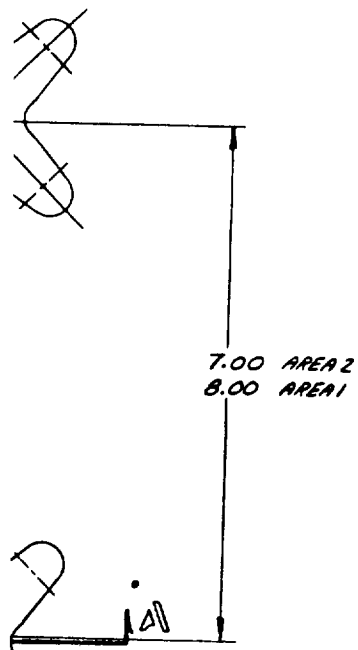
SECTION 10-10

CPI FASTENING METHOD  
"ANCHOR NUT" CONCEPT  
DOUBLE SCALE

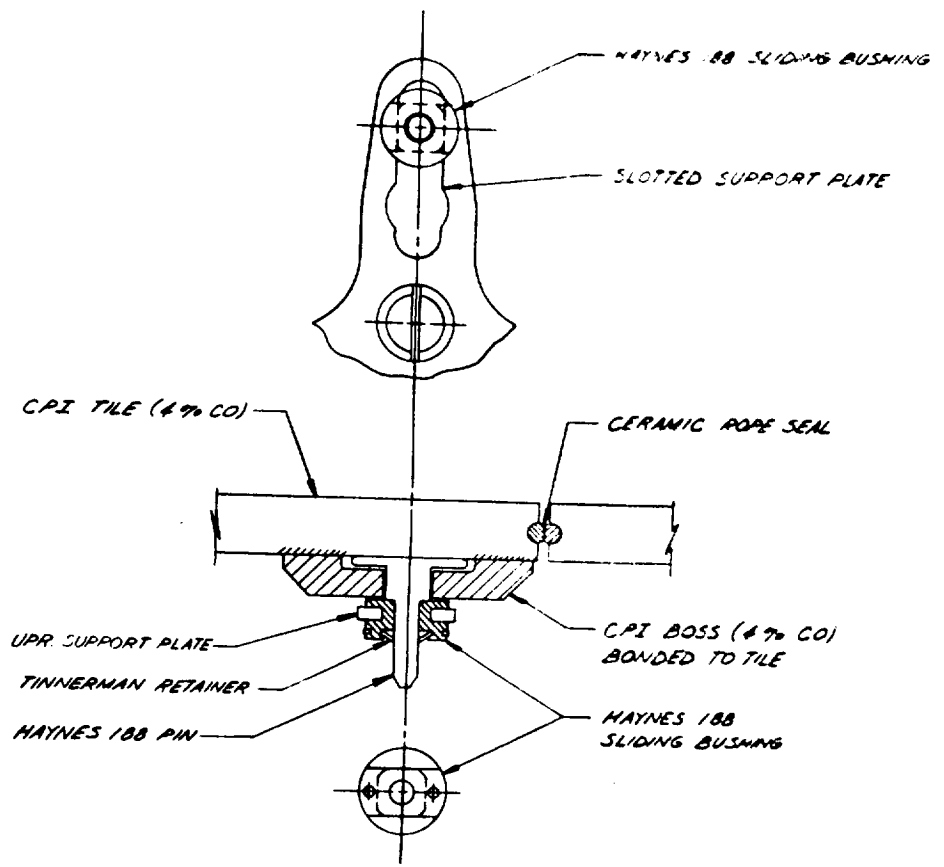
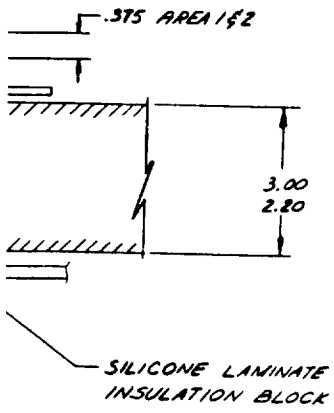








SEE DETAIL 13  
HAYNES 188 PIN



DETAIL 13  
2x SCALE

Figure 5-11 CPI/Post - Sliding Bushing Concept Square Tile Design

and is described later.

Engagement of the four pins into the bushing-nut assembly insures a secure simple push in installation of the tile assembly. The bushings slide within the slots and permit tile thermal expansion. The various seal concepts possible with this concept are described in Section 5.2.3.6. A 20.3 X 20.3 cm ( 8 X 8 in) tile size is used in Area 1 and a 17.8 X 17.8 cm (7 X 7 in) size is used in Area 2P.

Some advantages of this concept include:

- An independent, low density insulation package can be used providing fail-safe capability in the event of tile failure
- Concept permits simple push-in installation
- With the concept illustrated (blind nut) no holes are required in the CPI surface tile
- Post standoffs provide minimum weight and heat shorting. Additionally, they are easily integrated with the vehicle and provide good strain isolation from the primary structure
- The concept offers alternate retention concepts as illustrated in (D) below.
- The surface tile has positive restraint in all directions

Some disadvantages of the concept include:

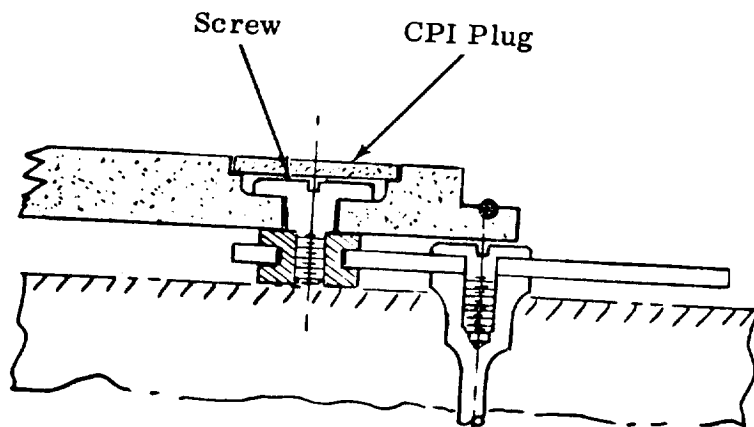
- More detail parts are required
- A CPI to CPI joint is required for pin retention with the blind design
- A small increase in total TPS depth is required to clear the pin retainer

The concept offers the most advantages of all the approaches studied and is very close to the lowest weight system. This concept was therefore baselined, and received extensive testing in the program.

#### (d) Sliding Bushing Alternate Retention Designs

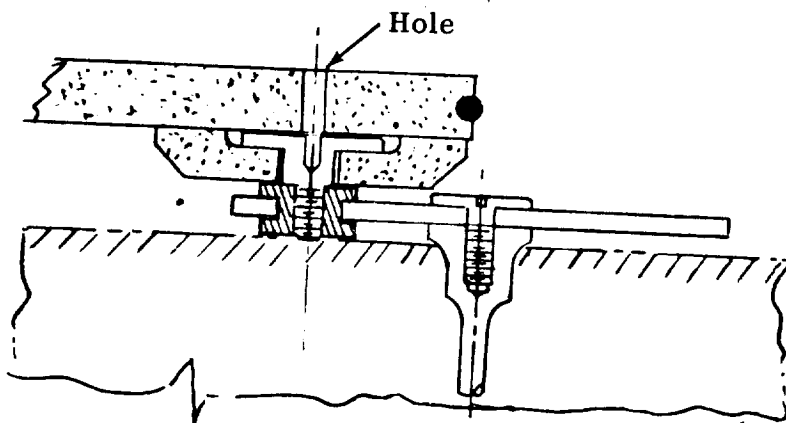
The versatility of the sliding bushing concept is illustrated in Figure 5-12 wherein three alternate designs are possible.

The screw-down concept illustrated in the upper portion of the



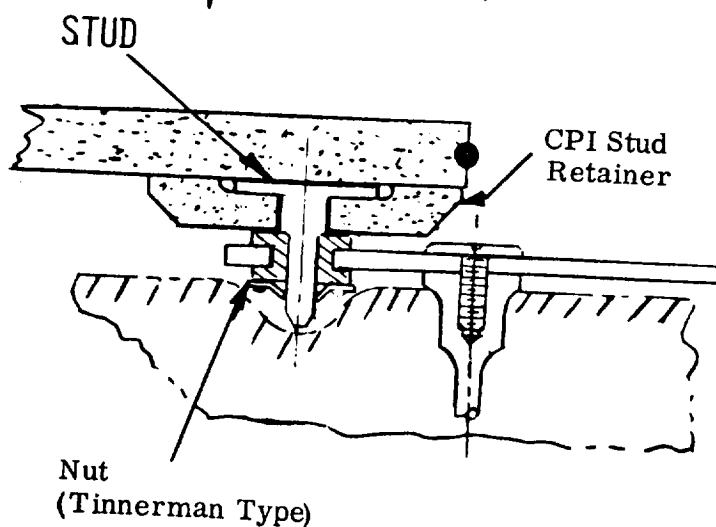
#### Screw-Down Concept

- Surface Plug Req'd
- Max Positive Retention
- Simple Inspection



#### Screw-Down Concept (Surface Hole)

- Max Positive Retention
- Bonded CPI Screw Retainer Req'd



#### Blind Concept

- No Surface Holes
- Simple Push-Down Installation
- Bonded CPI Stud Retainer Req'd

Figure 5-12 CPI/Post Sliding Bushing - Retention Concepts

figure offers a design with maximum positive retention. A bonded surface plug is required to protect the screw after installation. Panel removal is achieved by breaking the plug and removing the screw. This design could be employed where frequent access behind the TPS is required.

The screw-down concept with a surface hole eliminates the need for a surface plug, but still provides positive retention. A surface hole is provided to permit allen wrenching of the shoulder screw. The hole could be filled with a room temperature setting Kaowool cement. A bonded CPI screw retainer is required with this design.

The blind design is shown in the lower illustration. This design could be used in areas where access is not required. No surface holes are necessary and a simple push-down installation is possible. A bonded CPI screw retainer is required with this design. Removal of the tile however, requires panel destruction.

#### 5.2.3.6 Boundary Layer Gas Seal Designs

Figure 5-13 illustrates three seal designs which can be used with the mechanically fastened concepts. The lap butt design offers a good redundant design but requires male and female tiles which is not desirable. The lap design offers a good seal but also suffers from needing male and female tiles. The straight butt was the design chosen to baseline. It offers redundancy because it permits the use of two silica or Refrasil rope seals. Additionally, male and female tiles are not required because all tiles are identical.



Lap Butt



Lap



Straight Butt

Figure 5-13 Boundary Layer Gas Seal Concepts for Mechanically Fastened Panels

## 5.3 CONCEPT SELECTION

### 5.3.1 General

As described in Sections 5.2.2 and 5.2.3, the conceptual design studies identified two basic TPS approaches with CPI: CPI/Bonded Concepts and CPI/Mechanically fastened concepts. With the bonded concepts, the Area 1 design and the Area 2P design were chosen for in-depth design and analysis. With the mechanically fastened concepts two designs were chosen for in-depth design and analysis; CPI/Post-Sliding Bushing Concept and CPI/Post-Snap Washer Concept. The four designs are discussed in detail in the following sections.

### 5.3.2 CPI/Bonded Concepts

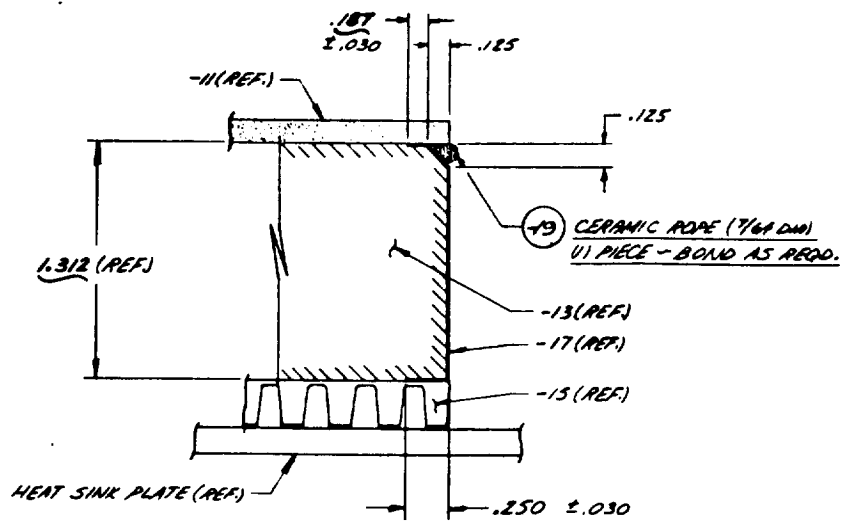
#### 5.3.2.1 Design Description

##### (a) Area 1 Design

The CPI/Bonded Concept for Area 1 is illustrated in Figure 5-14. The concept employs a thin .305 cm (.120 in.) CPI tile which basically acts as a coating. The CPI is bonded to a block of rigidized Kaowool using refractory Kaowool cement. Kaowool is a commercially available alumino-silicate fiber which is thermally stable to 1313°K (1900°F) easily meeting the Area 1 environment. The cost of a rigidized Kaowool block is approximately \$3.00/ft<sup>2</sup> in the 3.33 cm (1.31 in.) thickness illustrated. Additionally, the Kaowool fibers offer good thermal expansion match with the CPI.

Strain isolation for the system is provided by a molded silicone rubber mat which is bonded to the Kaowool. Holes are incorporated in the mat-Kaowool joint and the configuration of the mat permits good venting. Although the strain isolation system was not optimized, it was included for thermal representation. The isolator design, however, does simplify panel removal and permits larger panels to be used.

As illustrated, the four sides of the Kaowool fibers are sealed from moisture absorption by use of an Inconel foil enclosure. This concept eliminates the need for coated sides and all the associated inspection problems.



DETAIL 13  
SCALE: 2x SIZE

NOTES:

1. WRAP -13 KRODOL WITH -17 AS REQD. (USING 4 PIECES OR MORE OF .00125 INCONEL 600 FOIL) SUCH THAT CORNERS & SIDES OF -13 KRODOL ARE NOT EXPOSED. SPOTWELD FOIL CORNERS (TOP & BOTTOM) AS SHOWN PER 655 6102 CREATING 11 PIECE FOIL ASSY (-17). DO NOT BOND -17 ASSY TO -11 TILE, -13 KRODOL & -15 ISOLATOR.
2. TOLERANCE ON -13 & -15 ±.020

Figure 5-14 Direct Bond Test Article, Area 1



An interpanel seal is incorporated as illustrated in Detail "A". The Kaowool block is chamfered and the silica rope seal is bonded into the cavity as shown.

The actual Area 1 test component is shown in Figure 5-15. The test component is 6.5 x 6.5 inches. As shown, the test component includes a silica rope seal which is bonded in place using Kaowool cement. The seal was included in the component so that it could be evaluated during thermal cycling. The test component also includes the RTV 560 molded strain isolator which is bonded to a .250 in aluminum heat sink plate. The oversize plate represents the heat sink mass required to perform the thermal test under atmospheric conditions while still keeping the same thickness of Kaowool obtained from flight condition thermal properties.

(b) Area 2P Design

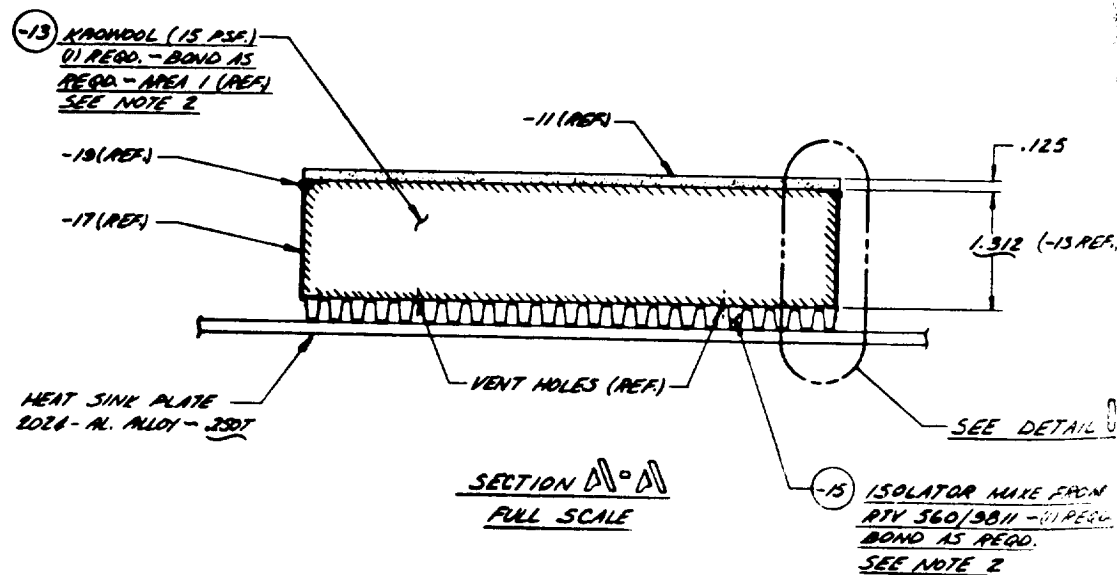
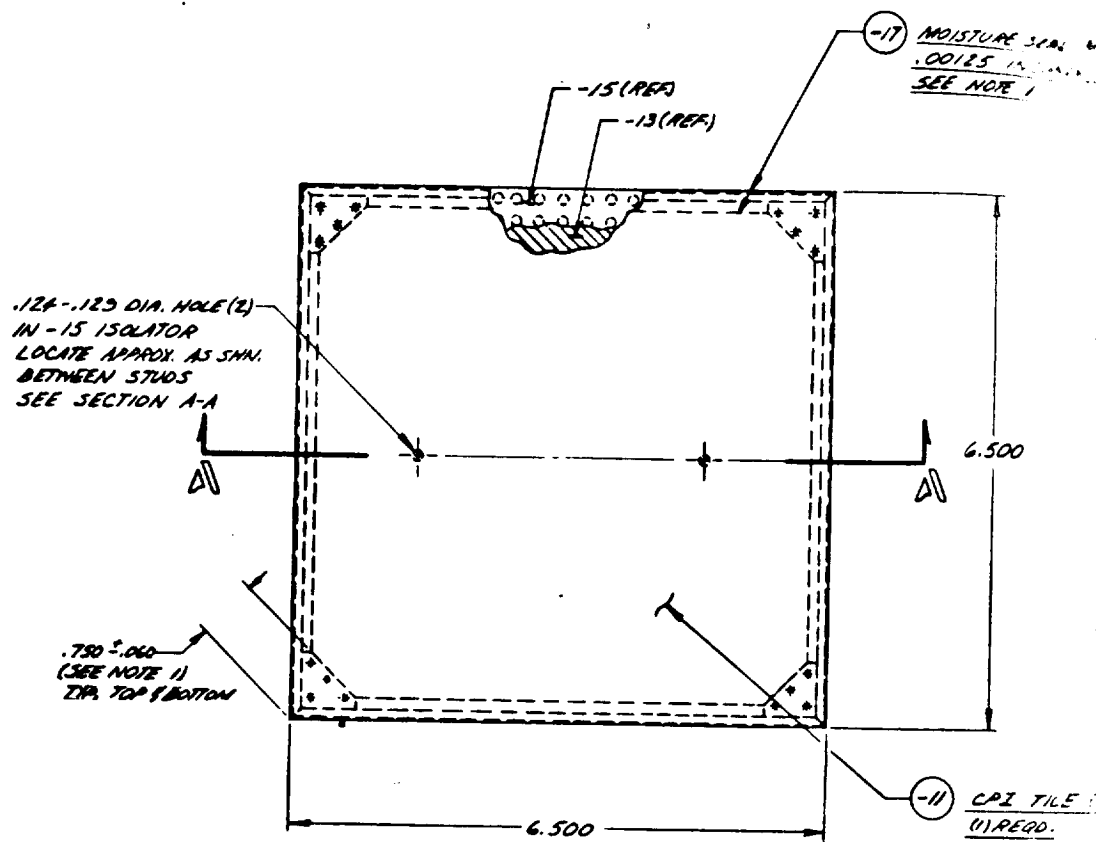
The CPI/Bonded Concept for Area 2P is illustrated in Figure 5-16. The design is generally similar to the Area 1 concept except that mullite is employed to protect the Kaowool fibers from the higher temperature environment. A .30 inches thickness of mullite is adequate to lower the temperature to 1700°F at the Kaowool-mullite interface.

A diffusion bond joint provided the best joining technique for the CPI to mullite interface and was employed in the concept. The diffusion bond was achieved at 2400°F and .20 psi pressure for one hour. This results from good chemical and thermal compatibility between CPI and mullite. Kaowool cement was used at the mullite-Kaowool joint.

Both the RTV rubber strain isolator and the interpanel seal joint are identical to the one employed for the Area 1 concept.

A TD-Ni20Cr foil moisture barrier is employed, because of the higher Area 2P operating temperature.

The actual Area 2P test component is shown in Figure 5-17. A 6.5 x 6.5 inch component was fabricated, although larger panel sizes are possible with these materials. The TD-Ni20Cr foil moisture barrier and silica rope seal were not included in the component so that the edges of the panel could be inspected during thermal cycling. This was considered necessary because thermal analysis indicated high thermal gradients would occur during Area 2P thermal cycling.



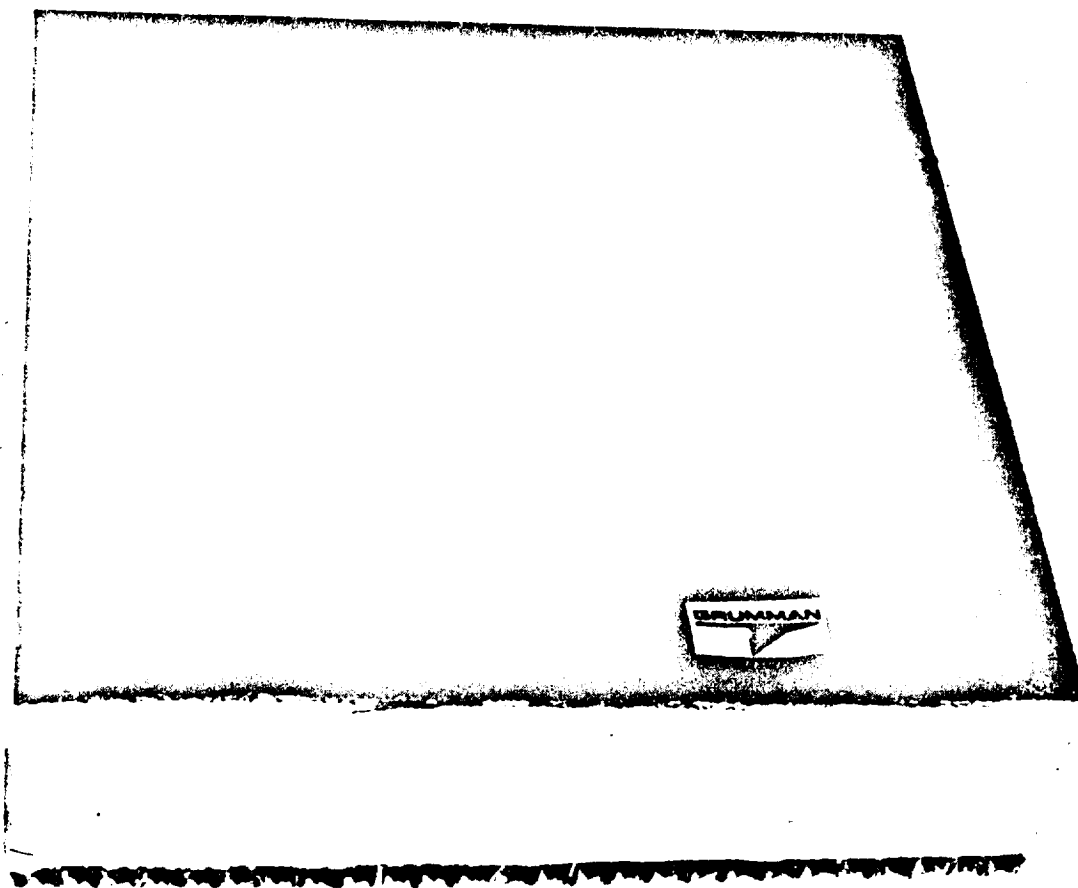


Figure 5-15 CPI/Bonded - Area 1 Test Component  
(6.5 x 6.5 Inch Tile Size)

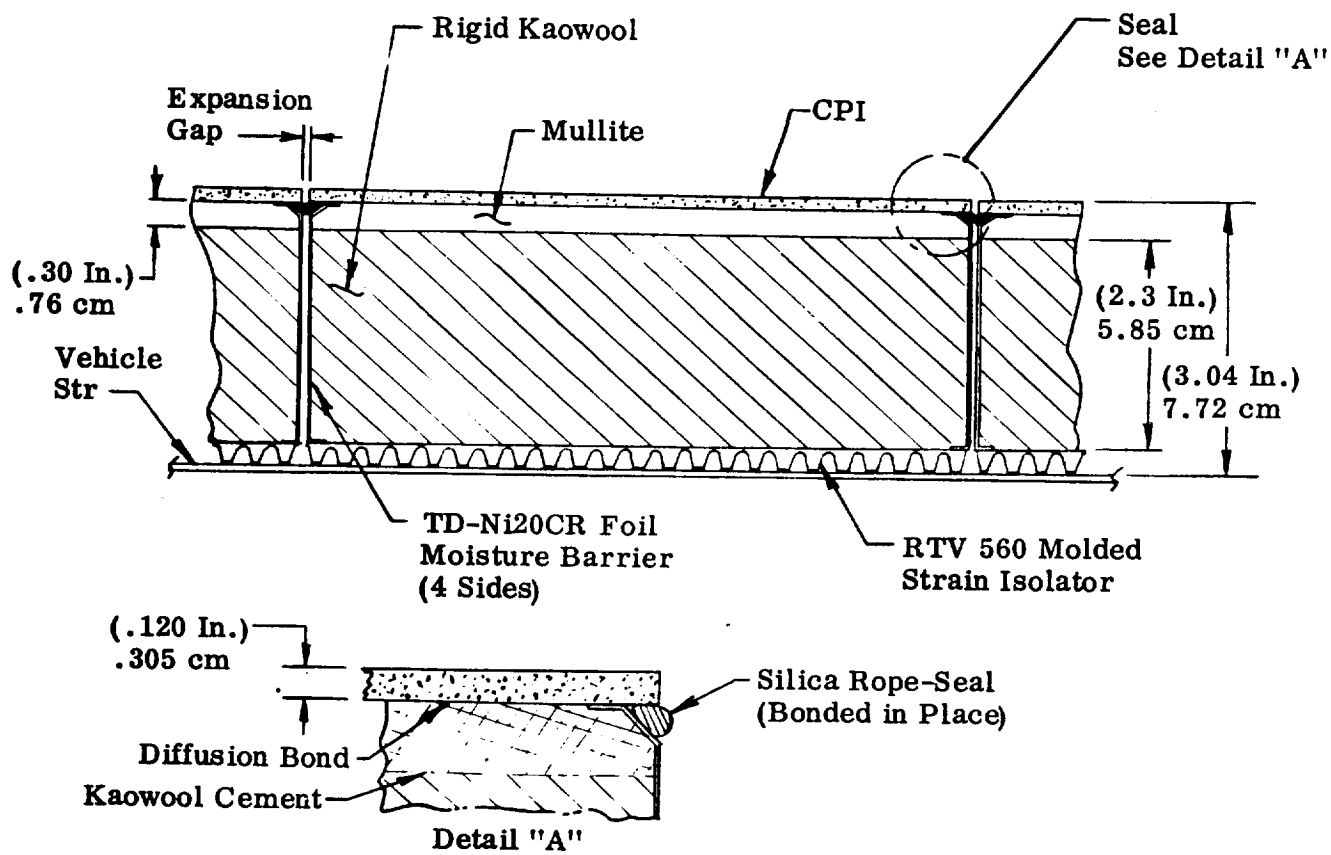


Figure 5-16 CPI/Kaowool - Mullite Bonded Concept Area 2P

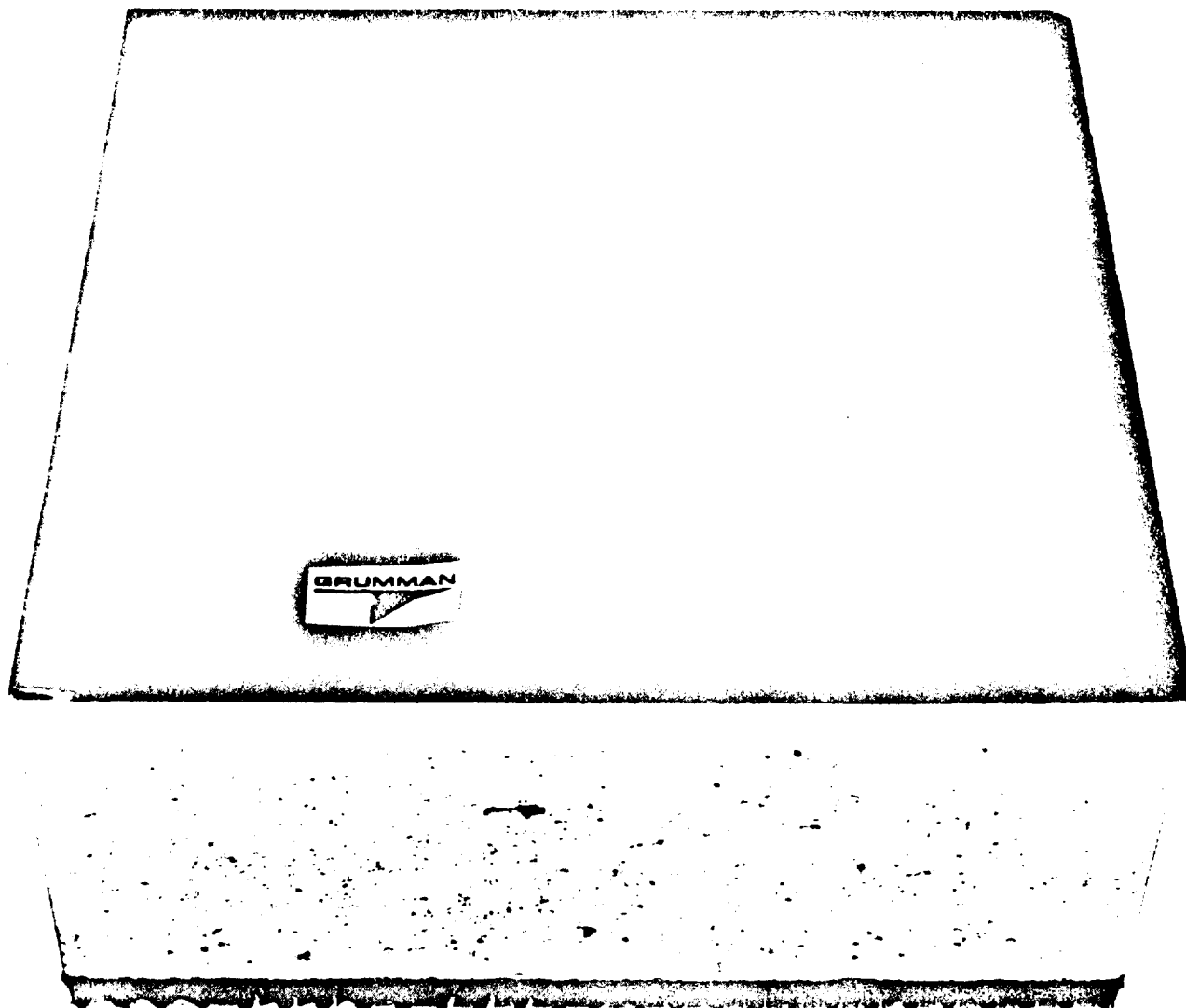


Figure 5-17 CPI/Bonded Area 2P Test Component  
(6.5 X 6.5 Inch Tile Size)

### 5.3.2.2 Structural Analysis

Because of the internal primary structure loads, the TPS composites' in-plane strain compatibility is a primary consideration for the CPI/Bonded scheme. The CPI tile composite must be bonded to a strain isolator, due to the insulating material's low failure strains with respect to the aluminum primary structure's working strains. A shear lag analysis of the bonded concept in which Kaowool is used, appears in Appendix C. This analysis indicates that, for the assumed properties of the materials used, the stresses are less than the allowables.

A check of the stresses in the RTV/9811 rubber strain isolator shows that it has the strength required to transmit the applied surface loads to the primary structure. At Area 1 the isolator is found to be critical in tension for the ultimate negative pressure of 4.5 psi as shown in Appendix C.

Thermal stresses set up during the heat up and cool down phases of each reentry cycle are considered.

### 5.3.2.3 Thermal Stress Analysis

The temperature analyses of the CPI/Bonded concepts were performed using Grumman's 1-D transient thermal analysis program. Figure 5-18 shows the critical temperature distributions for the Area 1 heating using CPI on rigidized Kaowool block. For an Area 2P application, a thin layer of mullite 0.30 inches thick is used on top of the Kaowool which operates at a temperature below 1700°F. The results of a thermal analysis for this design are shown in Figure 5-19. As can be seen from Figure 5-19 the thermal gradients are much larger for the Area 2P heating case than for the Area 1 shown in Figure 5-18.

Using the temperature distributions obtained in the transient temperature analysis a thermal stress computation was made for each case for the completely unrestrained plate. Typical results for the case using all mullite for the insulation layer under the CPI are shown in Appendix D. The results of Appendix D indicate that tensile thermal stresses set up in the mullite are less than 150 psi which are more than the allowable. However, this occurs near the CPI/mullite interface and the material can be strengthened prior to bonding of the CPI. In actual practice if all the precautions are not taken during manufacture, the tendency is for the mullite to delaminate on thermal cycling.

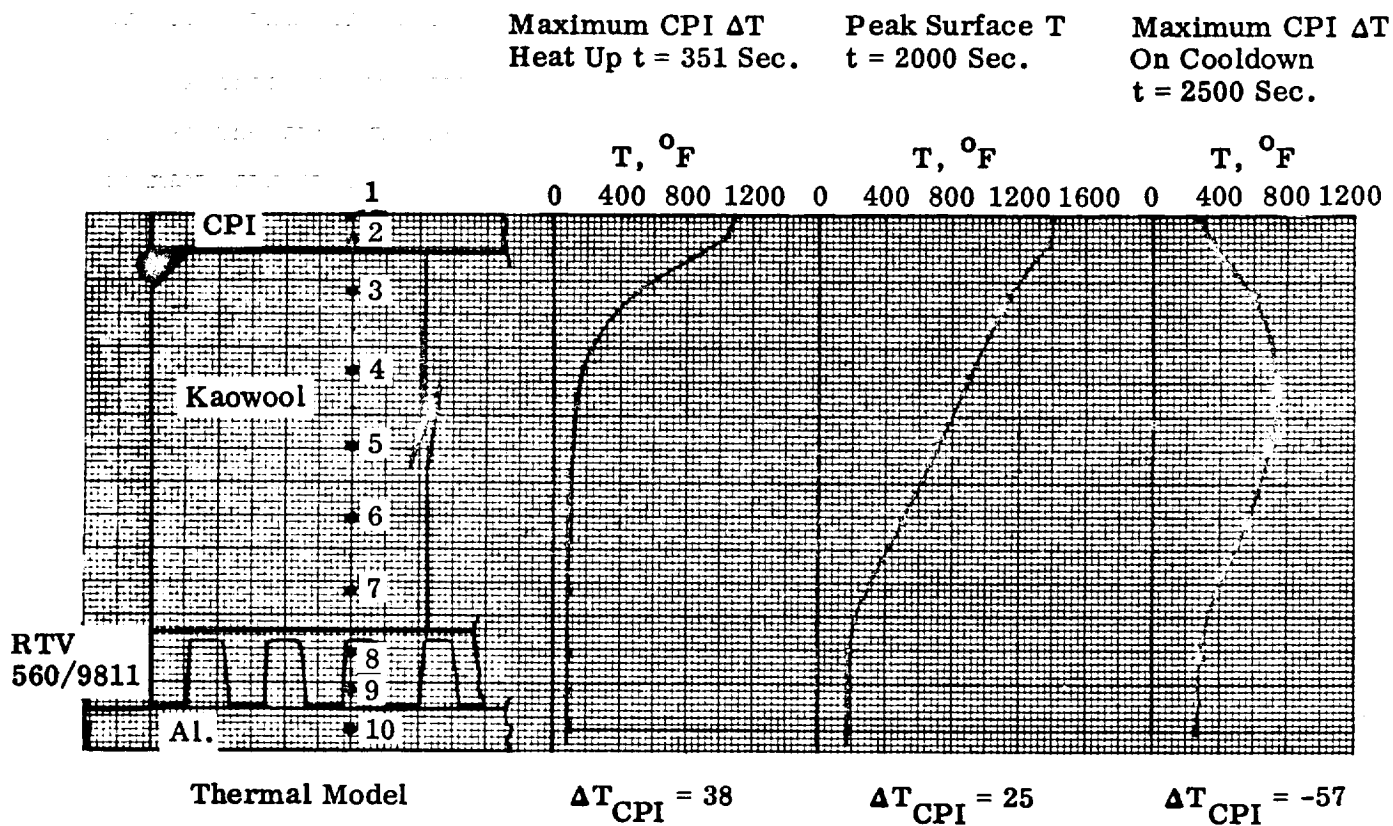


Figure 5-18 Critical Temperature Distributions for Area 1 Heating of CPI/Bonded Concept

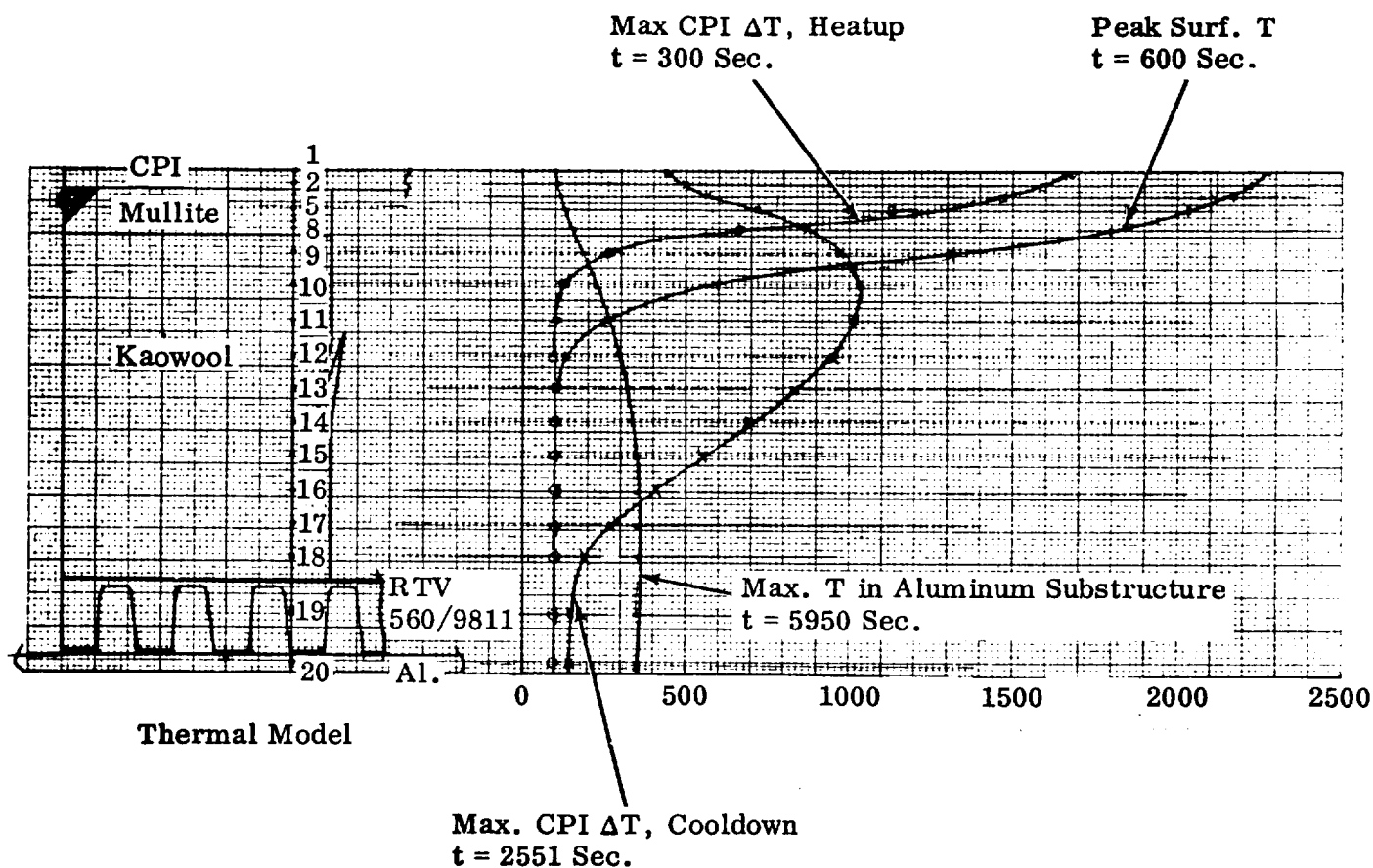


Figure 5-19 Critical Temperature Distributions for Area 2 Perturbed Direct Bond Scheme Kaowool Peak Temp. 1700°F



#### 5.3.2.4 CPI/Bonded Concepts - Weight Breakdown

##### (a) Area 1 Design - Weight Breakdown

The Area 1 design weight breakdown is as follows:

CPI Surface tile	.44
Kaowool (1.31 in.)	1.64
Foil moisture barrier	.06
RTV Strain isolator	.66
RTV bond	.10
<hr/>	
Total Weight	2.90 lbs/ft <sup>2</sup>

As indicated, the RTV strain isolator represents approximately 23 percent of the total system weight. This is an area where weight savings can be made. The strain isolator was not optimized since this was beyond the scope of the program.

##### (b) Area 2P Design - Weight Breakdown

The Area 2P design weight breakdown is as follows:

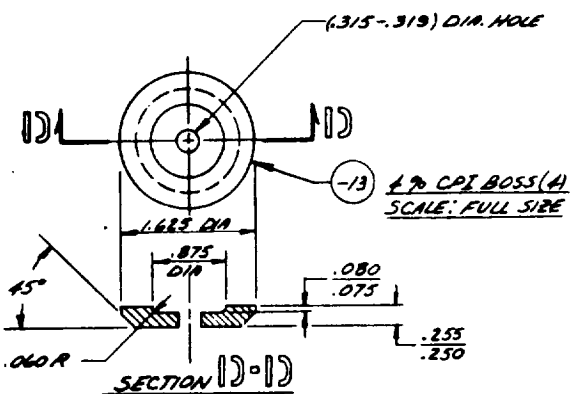
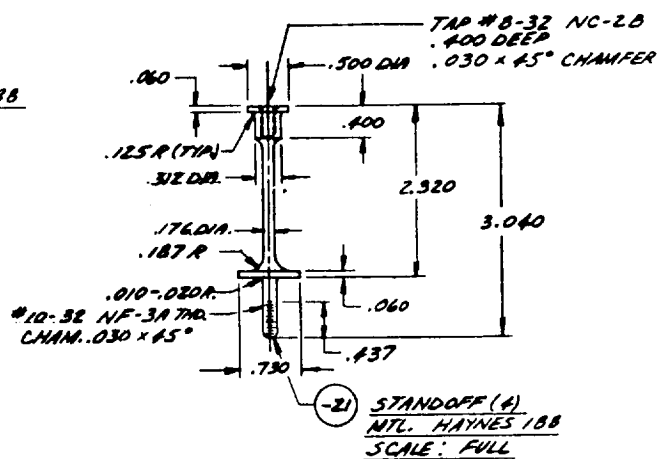
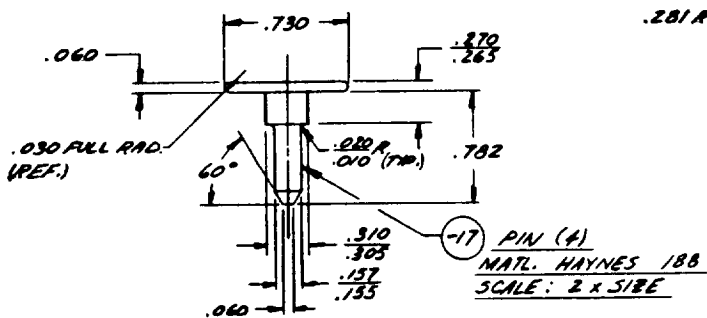
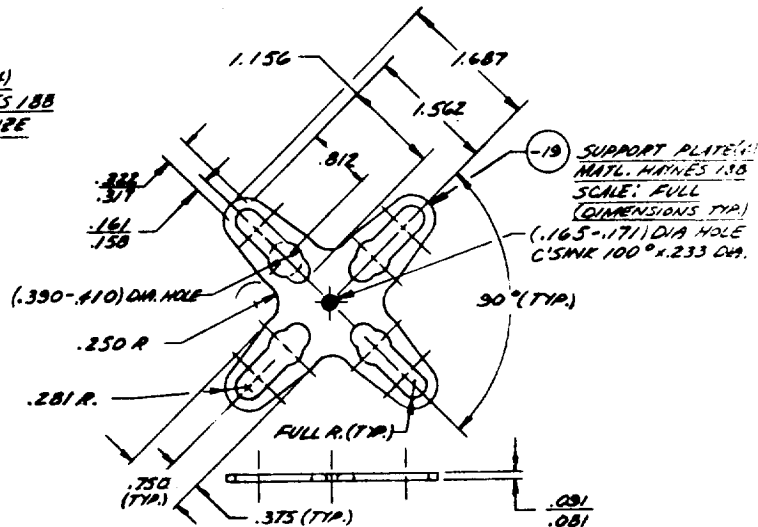
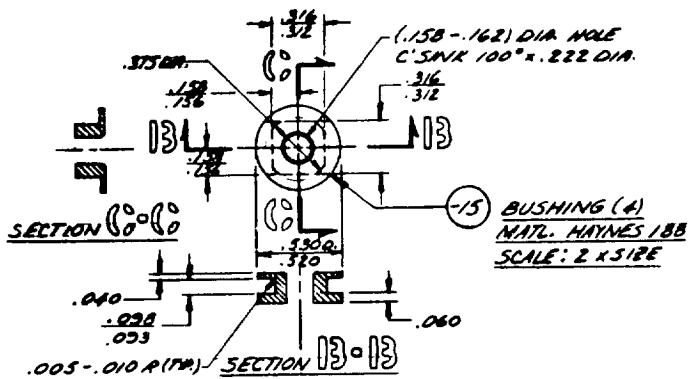
CPI Surface tile	.44
Mullite (.30 in.)	.38
Kaowool (2.3 in.)	2.88
Foil moisture barrier	.16
RTV strain isolator	.66
RTV Bond	.10
<hr/>	
Total Weight	4.62 lbs/ft <sup>2</sup>

#### 5.3.3 Mechanically Fastened - CPI/Post-Sliding Bushing Concept

##### 5.3.3.1 Design Description

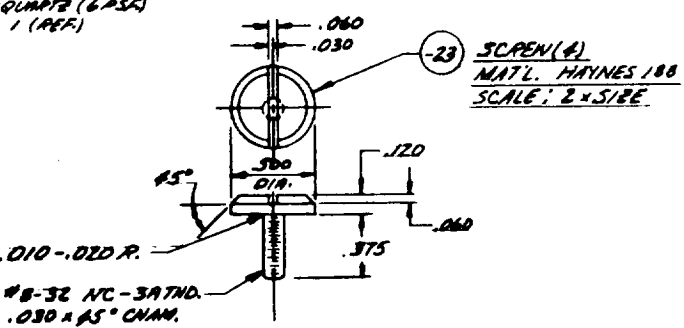
The most promising mechanically fastened concept identified in the program is the CPI/Post-Sliding Bushing Concept. The manufacturing drawing generated to fabricate the test component is shown in Figure 5-20. The concept is fully described in Section 5.2.3.5. The square tile design was chosen for testing since it was lighter and was simpler than the hexagonal tile and rectangular tile designs. The inter-tile silica rope seal was not included in the test component to save time. As shown in Figure 5-20, the blind retention design was chosen for the component. A C967-017 steel Tinnerman nut retainer was used,





- NOTES:
1. -13, -15, -17, -21 & -23 CONCENTRICITY WITHIN .004 TIR
  2. -21 & -23 THREADS SHALL BE FREE OF BURRS & SLIVERS - THDS IN ACCORDANCE WITH MK-S-7742
  3. -FINISH - 125 RMS FOR -15 THRU -23

MICROQUANTE (6 PSC)  
AREA 1 (REF)



which was staked to the sliding bushing. A Haynes or TD-Ni20Cr Tinnerman nut could not be obtained from Tinnerman in time. It is expected that the steel nut will oxidize during testing. A 12 x 12 inch insulation package was fabricated so that it would extend past the 7.375 x 7.375 in tile. The insulation material used in the component is 6 lbs/ft<sup>3</sup> microquartz, which is protected from moisture by a TD-Ni20Cr foil package. TD-Ni20Cr foil was used so that Area 2P thermal testing could be performed with the same component. Additional aluminum will be added to the heat sink plate to compensate for the higher heating levels during Area 2P testing. The actual test component is shown in Figure 5-21.

#### 5.3.3.2 Structural Analysis - Sliding Bushing Concept

The analysis of the mechanically fastened-sliding bushing concept uses a static structural analysis solution for sizing. The first part of this analysis consists of representing the area within the four support points as a square plate uniformly loaded and supported only at the corners. This yields a maximum moment at a point midway between the supports, at the edge of the plate. The remaining pressure loading acting on the overhanging portion of the panel is idealized as a double overhanging beam of unit width in the vicinity of the supports. The two solutions yield a maximum panel moment equal to the following:

$$M_{\max} = 0.1527 qa^2 - 0.500 qx^2$$

where

$q$  = uniform pressure (psi)

$a$  = edge distance between supports (in.)

$x$  = length of overhanging portion of panel (in.)

The CPI-4 tile is critical for an ultimate negative pressure equal to 4.5 psi at Area 1 and an ultimate positive pressure equal to 5.0 psi at Area 2. The tile thickness must satisfy a bending stress which is equal to or less than  $F_{bu} = 1,200$  psi. The CPI bonded on boss is analyzed as a circular plate with a concentric circular hole. The outer edge is assumed fixed, the inner edge free with a uniform load on a concentric circular ring. The nominal bending stress due to the maximum radial moment acting along the fixed edge is increased by the stress concentration factor caused by the transition of the flat circular plate to the cylindrical portion. The bond stress between the basic

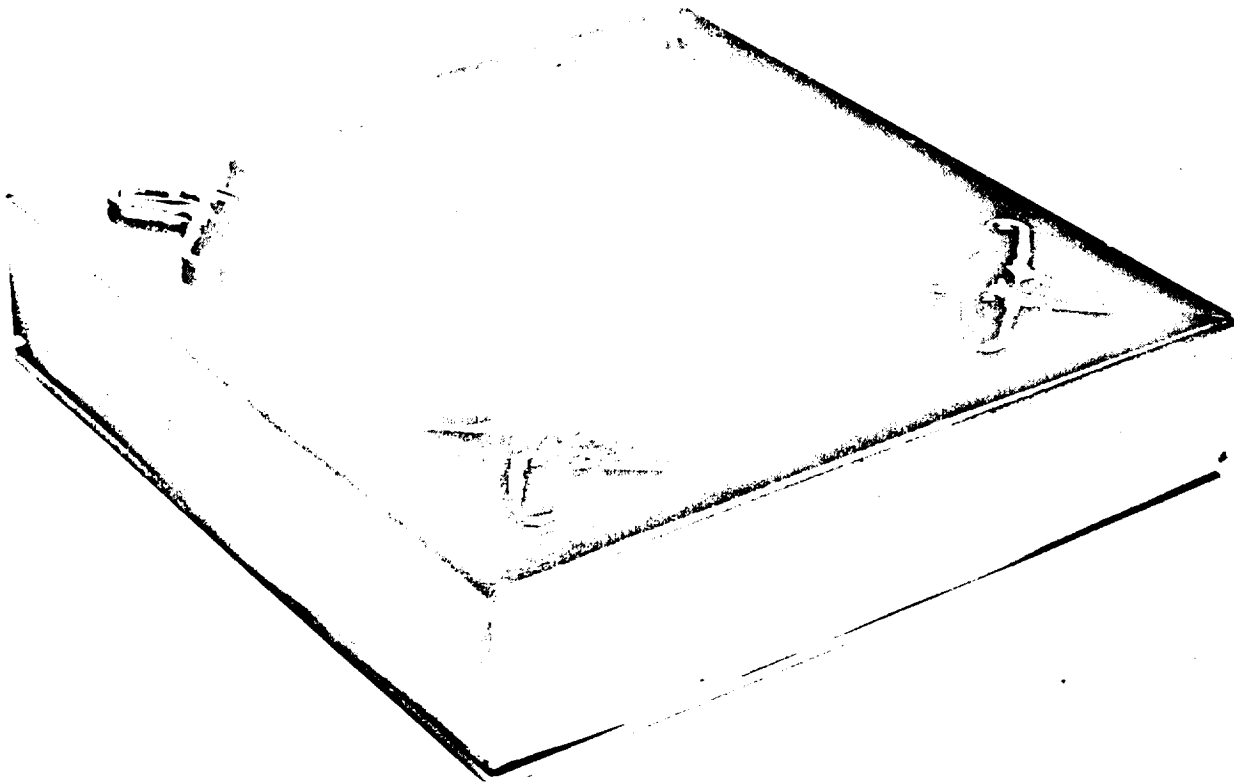


**Figure 5-21 CPI/Post - Sliding Bushing Test Component  
(6.5 x 6.5 Inch Tile Size)**

CPI panel and the boss is limited to  $F_{tu} = 250$  psi. The boss is critical for an ultimate negative pressure equal to 4.5 psi at both Area 1 and Area 2. The primary consideration in analyzing the Haynes-188 support is to restrict the bending stress level due to cantilever action to less than  $F_{ty} = 53,000$  psi. The critical condition for the Haynes-188 support is a limit negative pressure equal to 3.0 psi at both Area 1 and Area 2.

The main consideration in analyzing the Haynes-188 standoff is to restrict the bending stress level due to cantilever action to less than  $F_{ty} = 45,000$  psi. The Haynes-188 standoff is critical for the limit in-plane vibration loadings equal to 20 g's at both Area 1 and Area 2. The stress analysis of the mechanically fastened-sliding bushing concept for both Area 1 and Area 2 is contained in Appendix E.

#### 5.3.3.3 Thermal Stress Analysis

A temperature analysis of the mechanically fastened concept using a sliding bushing support was made using the thermal model shown in Figure 5-22. As can be seen from Figure-22 the critical thermal gradients are not very large through the CPI tile and therefore thermal stress problems in the interior of the tile do not exist. However, at the four corners where supports must be provided the restraint to the tile caused by the thermal expansions and rotations must be minimized. A three-dimensional temperature and structural analysis is required to determine the nature of the thermal stress problem in this region. Since time did not allow for such an extensive analysis, the approach taken in this program was essentially a semi-empirical one. It consisted of a phased designed-test-analysis and redesign procedure in evaluating the more critical design details such as the supports.

#### 5.3.3.4 Concept Weight

The CPI/Post-Sliding Bushing Concept weight breakdown is as follows:

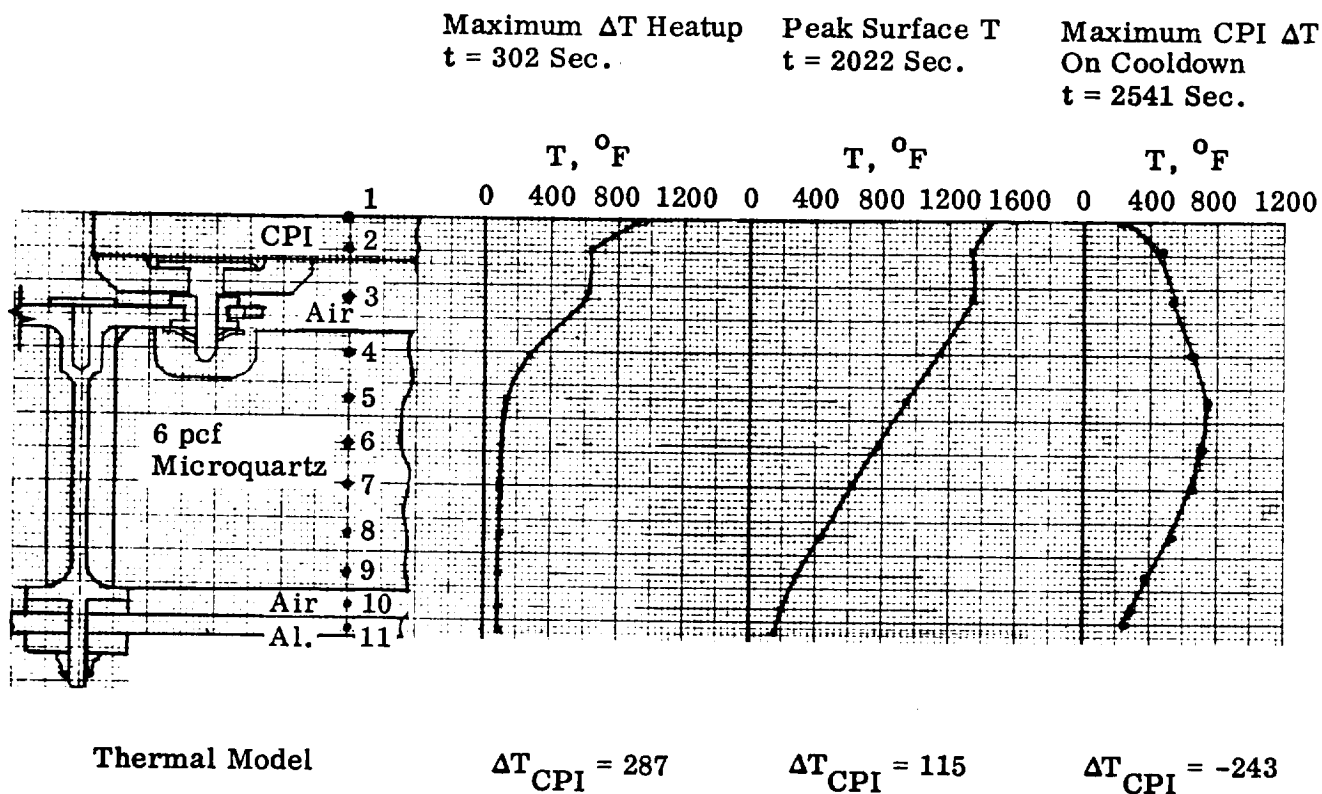


Figure 5-22 Critical Temperature Distributions for Area 1 Heating - Sliding Bushing Concept

(a) Area 1 Design

CPI Tile (8 x 8 x .375)	1.400
Standoff, plate, screws, etc.	.618
Insulation (Microquartz 6 lb/ft <sup>3</sup> )	1.110
Foil moisture barrier	<u>.108</u>
	3.236
(Plus 5%) =	<u>.164</u>
	3.400 Lbs/Ft <sup>2</sup>

(b) Area 2P Design

CPI Tile (7 x 7 x .375)	1.400
Standoff, plate, screws, etc.	.805
Insulation (10 lb/ft <sup>3</sup> )	2.500
Foil moisture barrier	<u>.108</u>
	4.813
(Plus 5%) =	<u>.240</u>
	5.053 Lbs/Ft <sup>2</sup>



### 5.3.4 Mechanically Fastened - CPI/Post-Snap Washer Concept

#### 5.3.4.1 Design Description

The manufacturing drawing generated to fabricate the CPI/Post-Snap Washer Panel is illustrated in Figure 5-23. The concept is fully described in Section 5.2.3.3. The actual test component fabricated is shown in Figure 5-24.

It is important to note that when the concept was in detail design only the 8 percent cobalt oxide CPI material allowables were available. The panel therefore was designed with 4 x 4 x .375 inch tiles. Two CPI panels were included in the test component. A silica rope seal was included at the inter-tile joint for evaluation during thermal testing. The insulation package was fabricated using 10 lbs/ft<sup>3</sup> Dynaquartz protected from moisture by a TD-Ni20Cr foil moisture barrier so that Area 2P thermal testing could be performed with the same component.

#### 5.3.4.2 Structural Analysis - Snap Washer Concept

The analysis of the mechanically-fastened snap washer supported concept is almost identical to the mechanically fastened - sliding bushing concept (Section 5.3.3) analysis. The primary exception is the replacement of the bonded on boss with supports which are an integral part of the basic tile. This eliminates the analysis of the adhesive.

The stress analysis of the mechanically-fastened snap washer support concept for both Area 1 and Area 2 is contained in Appendix F.

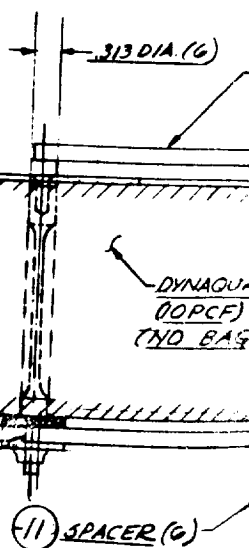
#### 5.3.4.3 Thermal Stress Analysis

Apart from the support detail of the snap washer concept, the thermal stress problems in this design are the same as those of the sliding bushing concept. Since a three-dimensional thermal analysis was not possible, the same semi-empirical approach used in the previous designs was taken in the case of the snap washer support concept also.

AD 517-23 RETAINER (2) -  
AD 517-31 CPI PLUG (6)  
SEE SECTION FF ON  
AD 517 FOR DETAIL.

A

2024 AL ALLOY - 180t.  
70.25 x 6.375  
DRILL #19 (165-171) 6 HOLES



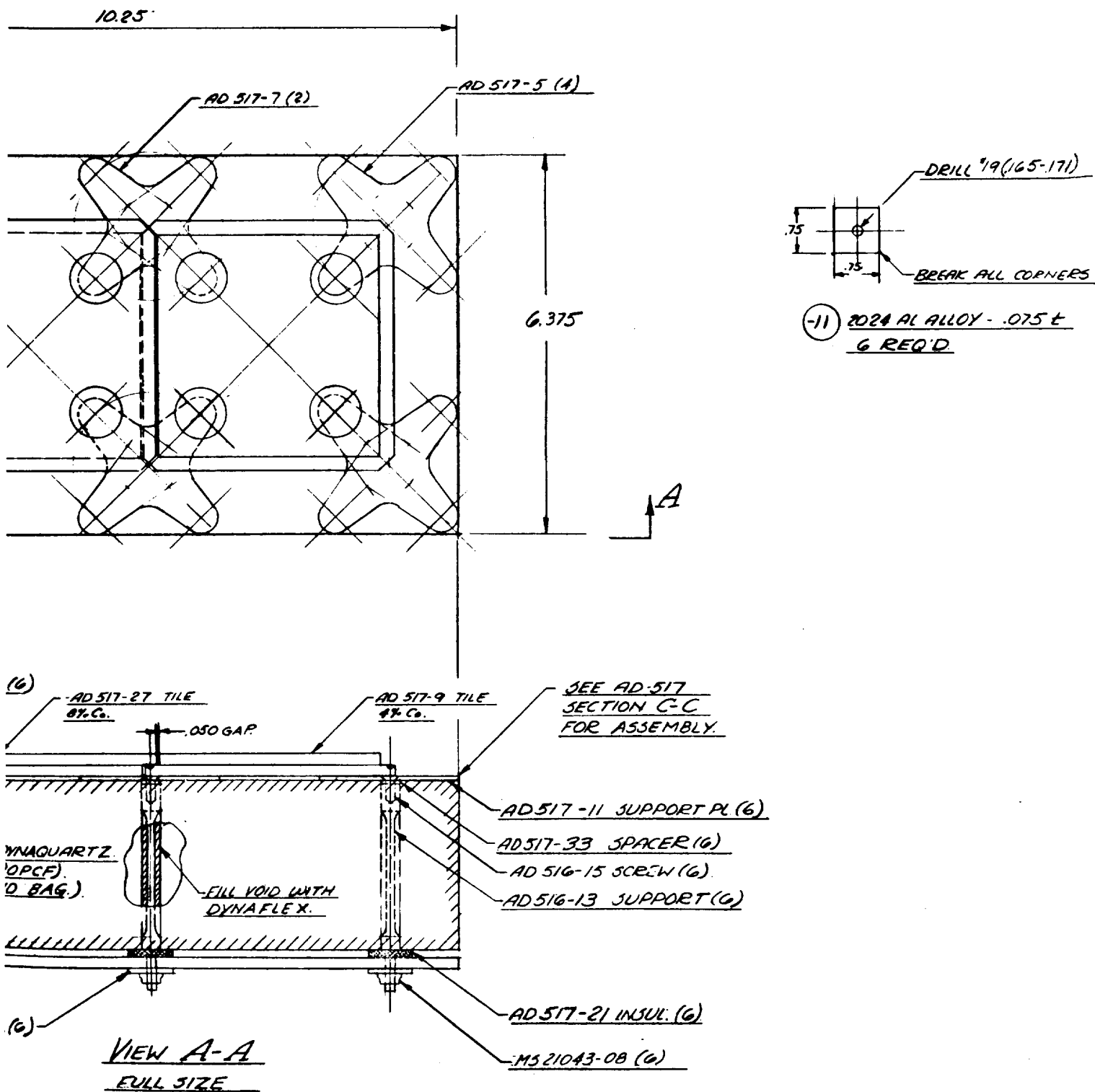


Figure 5-23 CPI/Post - Snap Washer Test Component

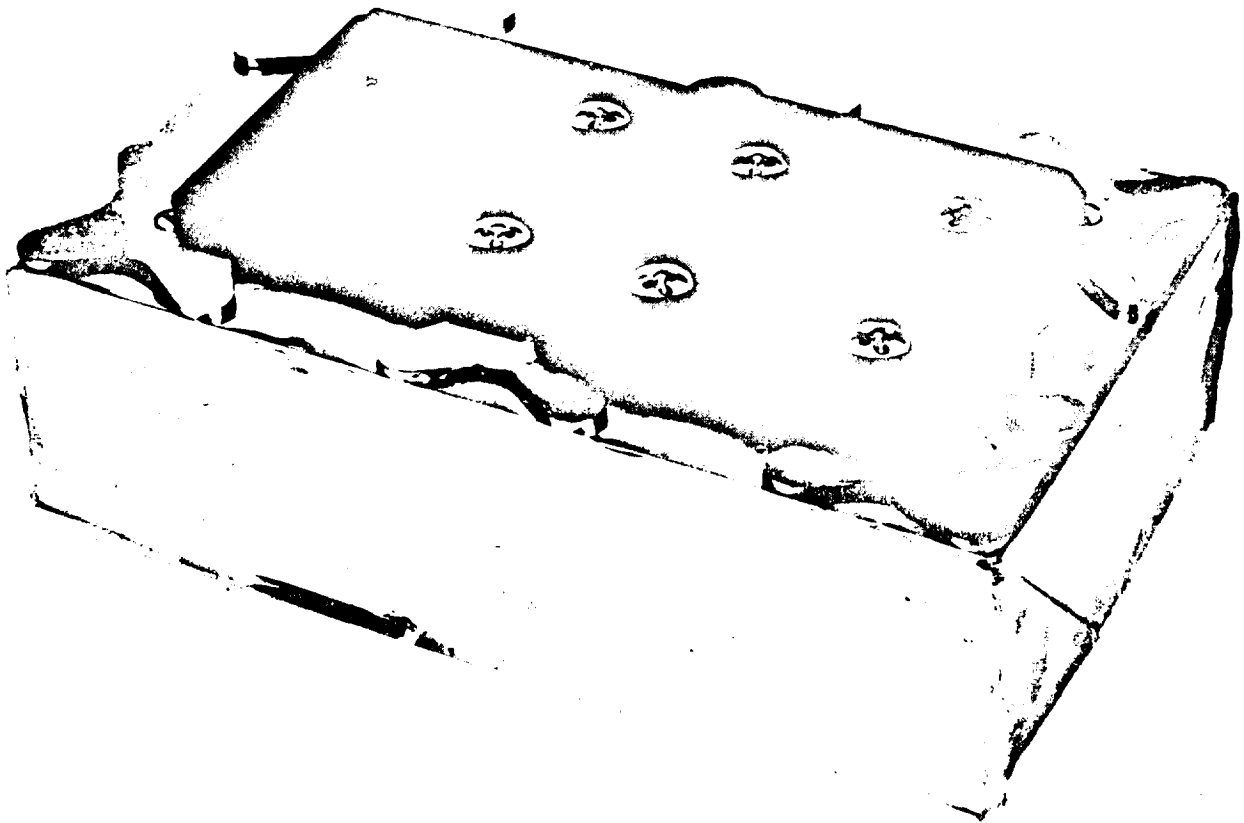


Figure 5-24 CPI/Post - Snap Washer Test Component  
(4 x 4 Inch Tile Size)

#### 5.3.4.4 CPI/Post-Snap Washer Weight Breakdown

The CPI/Post-Snap Washer weights are as follows:

- (a) Area 1 3.09 lbs/ft<sup>2</sup> (including 5% factor)
- (b) Area 2P 4.63 lbs/ft<sup>2</sup> (including 5% factor)

Section 6  
DESIGN DETAILS - DEVELOPMENT/EVALUATION

6.1 CPI/Bond Joint Development

The various experimental techniques used to effect adhesive bonds between CPI and the rigidized fibrous insulation (Kaowool and mullite) are described in Section 4.1.6.2.

Table 4-16 lists the major experimental results of the bond development program. The following bonding schedules for the scaled-up components are based on these results.

6.1.1 CPI/Mullite Bond Joint Development

The diffusion bonding schedules selected for scaled-up components (6" X 6") consisted of a machined CPI plate (6" x 6" x 3" rigidized mullite block. A weight corresponding to 0.1 psi ( $700 \text{ n/m}^2$ ) was placed on the CPI plate and the assembly was fired to 2450°F for one hour and furnace cooled. Microscopic examination of the interfacial region showed intimate contact between the two materials and some flow of the glassy CPI material into the fibers' surface pores. No interfacial failures occurred when the composite was subjected to thermal cycling (Area 2).

6.1.2 CPI/Kaowool Bond Joint Development

Kaowool cement was found to be the optimum bonding agent for this composite (See Table 4-16). Components (6" X 6" X 2") were fabricated using the following procedures:

- (1) As-received, rough cut, Kaowool blocks were fired to 1500°F for one hour to remove organic binders.
- (2) The blocks were immersed in a solution of Kaowool rigidizer (diluted 2.5 HgO: 1 rigidizer by volume) and dried at 200°F for 16 hours.

- (3) The dried and rigidized blocks were ground flat on the surface to be bonded.
- (4) A thin layer of Kaowool cement was applied to the CPI surface and the Kaowool block and the surface were mated (excess cement was squeezed out).
- (5) The composite was dried at room temperature for 16 hours and fired to 1600°F for one hour.

Microscopic examination of the interfacial region showed excellent adherence and contact between the two materials. Examination following 25 thermal cycles (Area 1 and Area 2) showed no interfacial failures. Figure 6-1 shows two typical CPI tiles after 25 thermal cycles at Area 2 heating. Note the thermal stress crack in the larger of the two composite tiles shown in Figure 6-1. This type of failure occurs at the point of maximum thermal stress, as verified by analysis. The smaller size tile showed no cracking.

#### 6.1.3 CPI/CPI Bond Joint Development

The results of thermally cycling CPI/CPI bonds, using a bonding agent consisting of ground CPI powders mixed with colloidal silica (Astrocera<sup>m</sup> and Kaowool cement), are described in Section 4.1.6.2.

A mechanical property screening program was initiated to verify the strength of bonds in which CPI powder/colloidal silica cement was used. Four CPI powder/colloidal silica combinations were examined:

1. CPI-0 powders with colloidal silica\*
2. CPI-4 powders with colloidal silica
3. CPI-8 powders with colloidal silica
4. Astrocera<sup>m</sup>\*\*.

\* Ludox-HS, Dupont Corp. Wilmington, Delaware

\*\* Granite State Machine Co.

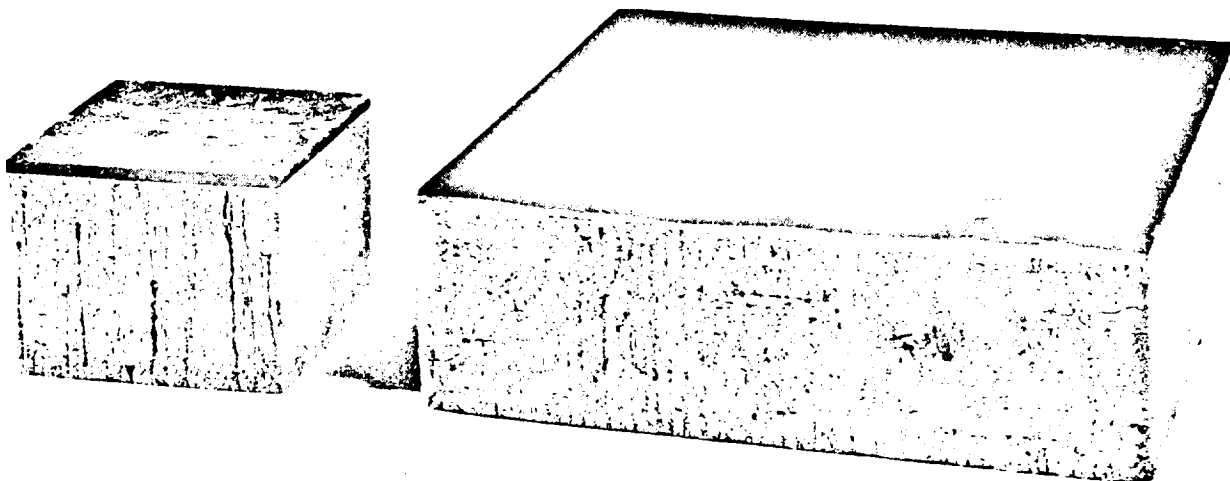


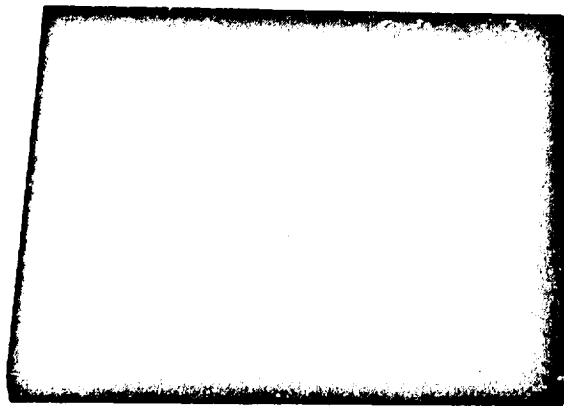
Figure 6-1 CPI/Kaowool Bonded Tiles After Thermal Cycling



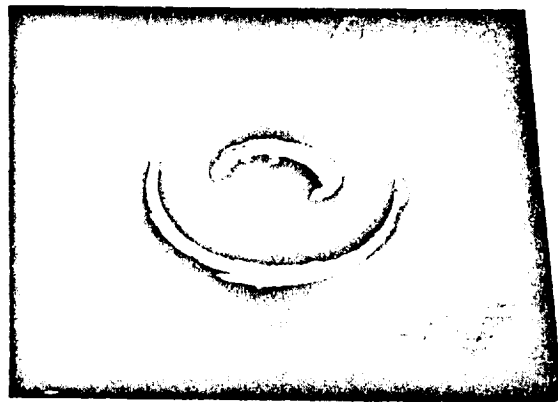
All powders were produced by ball-milling precrushed pieces of CPI for 24-48 hrs. Cement combinations were produced by mixing with one part colloidal silica binder.

Two flat ground CPI plates (2" x 2" x .375") were bonded together by painting the adhesive on both surfaces and squeezing out the excess. Samples were dried at room temperature for 16 hours and fired to 2000°F for one hour and furnace cooled. The bonded specimens were then bonded to two aluminum blocks (2" x 2" x 2") using an epoxy adhesive. Each block contained a machined hole for mounting into the tensile fixture. The tensile fixture allowed for free rotation of the specimen, thus minimizing misalignment problems. All specimens were pulled to failure and the breaking strength and nature of the failure were noted. Table A-6 of Appendix A summarizes these results. We found that the most consistently high breaking strengths were achieved using the CPI-4 powders/colloidal silica combination. In all cases no interfacial failures were observed.

This indicates that the bond strength exceeded the CPI-4's tensile strength. This adhesive was baselined for use in the CPI/Sliding Bushing Concept. Test specimens used to evaluate the effect of thermal cycling on the bonded CPI torroidal retainer are shown in Figure 6-2. These test specimens have undergone 25 cycles of Area 1 heating, 25 cycles of Area 2 heating, 3 cycles of Area 2P heating and 3 cold soak cycles at -200°F with no failures.



CPI Cement



Kaowool Cement

Figure 6-2 CPI/CPI Bond Test Specimens

## 6.2 CPI/Mechanically Attached Element Tests

### 6.2.1 CPI/Post Supported Concept With Snap Washer-Panel Test

The assembly for this test panel consisted of 2 - 4" x 4" tiles as shown in Figure 6.3, which was taken after the first thermal cycle. The panel received a total of 58 thermal cycles: 29 cycles at Area 1 heating, 24 cycles at Area 2 and 5 cycles at Area 2P. The first crack occurred in one corner of one of the two tiles on the first Area 2P heating. Additional cracks occurred during subsequent Area 2P cycling, as shown in Figure 6-4.

It is our belief that the cracks are a result of stress concentrations around the holes in the tile.

### 6.2.2 CPI/Sliding Bushing Concept Panel Test

A test component using the sliding bushing corner attachment concept was tested to a total of 29 thermal cycles: 12 Area 1 and 17 at Area 2. At the first cycling to Area 2 there was a noticeable bow at the center of the panel. An examination of the results and subsequent retesting of a similar panel without the sliding bushings indicated that no bowing occurs when the corners of the tile are freed to distort. Thus it appears that a partial undesirable restraint was present in the tile with the sliding bushings in place. Examination of the failed tile revealed that a series of cracks formed in the 4 torus-shaped support retainers at the bottom of the tile. Figure 6.5 shows the failed specimen.

Post failure inspection of the assembly revealed that the Haynes plate and bushing were oxidized. Attempts to slide the bushing in the slot required excessive load to overcome the increased friction resulting from the oxidation. This restraint may have caused excessive stresses in the retainers causing cracking.

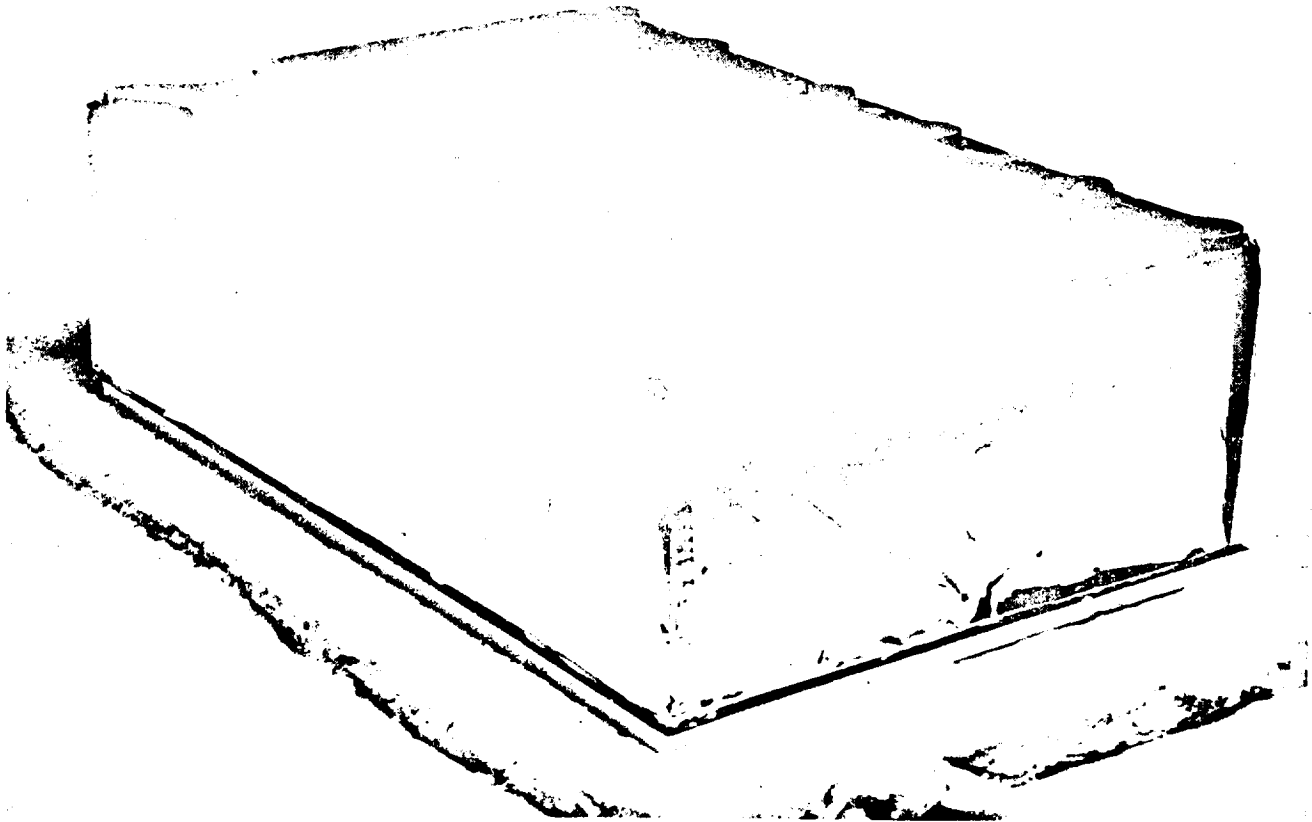


Figure 6-3 CPI/Post With Snap Washers Concept - After One Thermal Cycle

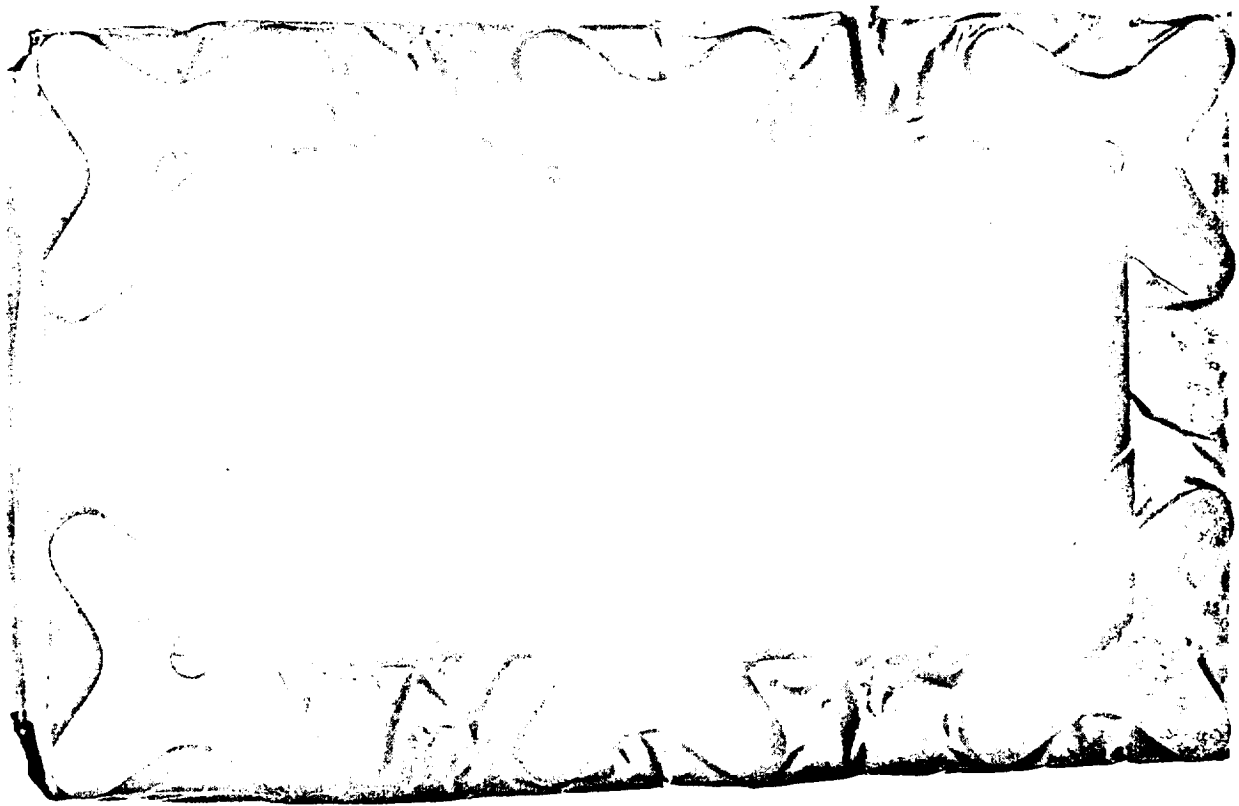
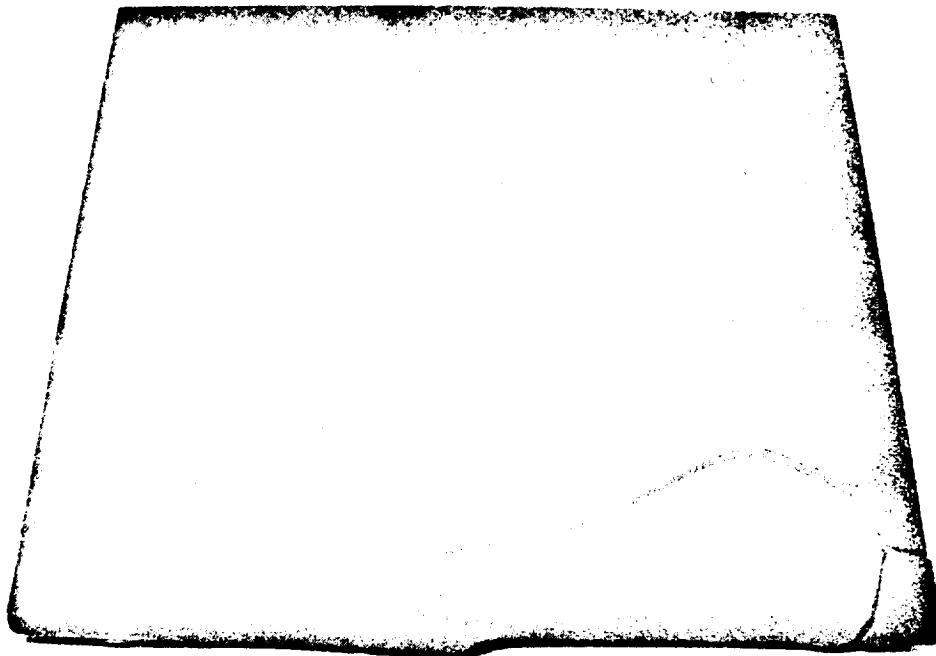
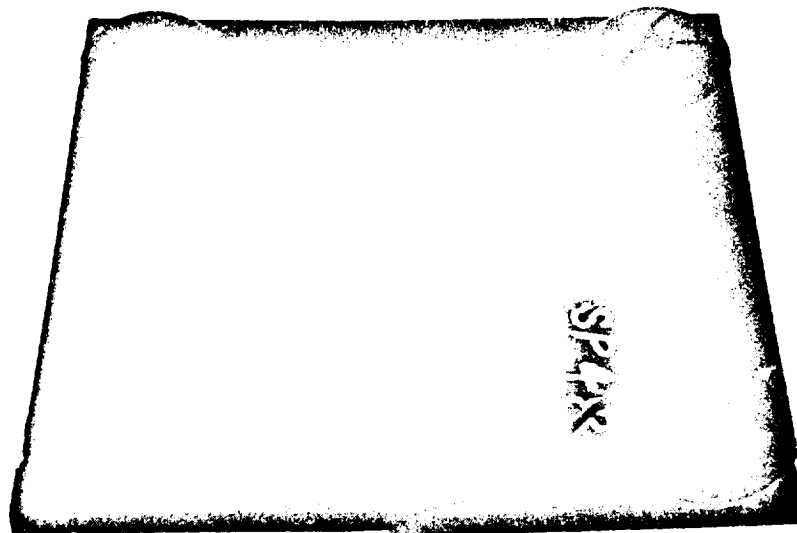


Figure 6-4 CPI/Snap Washer Test Article After 58 Thermal Cycles.



(a) Top Surface



(b) Bottom Surface

Figure 6-5 CPI/Sliding Bushing Concept Test Article After 29 Thermal Cycles

## SECTION 7

### CONCLUSIONS AND RECOMMENDATIONS

#### 7.1 CONCLUSIONS

##### 7.1.1 Material Development

(a) This effort has successfully developed and optimized a new, reusable class of low cost materials for the Space Shuttle Orbiter's external thermal protection system. These materials which consist of 20-30 percent dense closed cell high emittance, glass-ceramic foams produced by sintering a mixture of fly ash cenospheres with 4 and 8 weight percent cobalt oxide offers the following advantages:

- Non-interconnecting cell network obviates the need for any waterproof coating.
- Built-in high emissivity
- Can withstand space shuttle's thermal environment for at least 25 missions, without impairing reuse capability.
- Excellent machinability. Capable of being worked to the close tolerances required for an integrated TPS.

(b) The CPI-4's and CPI-8's thermal, physical and mechanical properties over the temperature range pertinent to Shuttle application showed that CPI-4 had superior mechanical properties, (see Table 4-5, and 4-16).

(c) The CPI-4's emissivity was enhanced by applying a thin coating of CoO, which diffuses into and becomes integral with the surface.

(d) The CPI thermal stability, has been demonstrated.

(e) Softening of CPI glass-ceramic at temperature above 1300K, and a strain rate dependence of mechanical properties were observed.

(f) CPI's higher density and thermal shock characteristics requires that it be used in relatively thin sections.

##### 7.1.2 Inspection

NDE inspection of CPI materials, using X-ray radiography for detection of flaws such as cracks, voids, inclusions and density variations, has been demonstrated.

### 7.1.3 Concept Development

In the design concept development task, two basic approaches were identified. CPI/Bonded Concepts and CPI/Mechanically fastened concepts. With the CPI/Bonded Concepts, two panels were designed and fabricated. One was designed to meet Area 1 requirements, and one to meet Area 2P requirements.

Direct adhesive bonding of CPI to rigidized fibrous materials such as Kaowool and Mullite have demonstrated survival capability to at least 25 thermal cycles. Of the CPI/Mechanically fastened concepts, two were designed and fabricated: the CPI/Post-Sliding Bushing Concept and the CPI/Post-Snap Washer Concept. The panels were tested under Area 1 and Area 2 conditions. The CPI/Post-Sliding Bushing Concept proved to be the superior design although more refinements of the design details are necessary.

### 7.2 RECOMMENDATIONS

It is our conviction that further investigation of CPI as a TPS material is warranted. The effort reported herein represents a highly accelerated six months program wherein the material's potential was demonstrated.

It should be noted that the special properties of CPI, such as its hard wear-resistant surface, machinability and ability to be mechanically fastened to the substructure make it attractive in conjunction with other systems. For example, there are areas where present RSI systems are not suitable. Doors will require hard edge members for sealing and handling. The interface with carbon/carbon leading edges, if used, will require a transition area to the basic RSI panels. Areas thermally isolated from the basic structure, such as the cabin and cargo doors, where extreme cold soak temperature could preclude the use of the bonded joints, are natural areas for CPI. The evaluation of these "special use" areas for CPI, however, was beyond the scope of this program.

In the area of material's improvement it is recommended that the following areas be investigated:

of flow and crack growth under  
been demonstrated



- Optimization of coating thickness of CoO required to give maximum surface emissivity to CPI-4 without degrading surface strength.
- Investigation of other high emissivity surface additives that will not compromise refractoriness of CPI-4. Optimization of optical properties of the CPI surface to produce the lowest solar absorptance to emittance ratio.
- Investigation of more efficient methods of achieving intimate dispersions of cenospheres and the high emissivity additives such as spray drying, electrostatic methods etc.
- Investigations of techniques to increase production rates (and decrease costs) for producing fired CPI tiles i.e., continuous firing kilns.
- Investigate new CPI compositions which will increase refractoriness (creep properties) of CPI without compromising other desirable properties.

# APPENDIX A MATERIAL STRENGTH DATA

TABLE A-1 SINGLE POINT FLEXURAL PROPERTIES OF CPI  
MATERIAL WITH 8 AND 4%  
COBALT ADDITIVE

SPEC. IDENT.	DENSITY (#/FT <sup>3</sup> )	TEST TEMP (°F)	THICK (IN.)	WIDTH (IN.)	FAIL LOAD	ULT. STRESS (PSI)	MOD. X 10 <sup>6</sup> (PSI)	LOCATION OF FAILURE
GROUP I - 8% COBALT								
A-UNEXPOSED								
SB-7	37.0	RT	.250	.460	5.37	840	.92	CENTER ↓
-8	↓	↓	.244	.493	5.36	822	.88	
-9	↓	↓	.246	.484	5.60	861	.93	
-10	↓	↓	.245	.480	5.36	837	.85	
-11	↓	↓	.246	.485	5.74	880	.84	
-12	↓	↓	.243	.494	6.07	937	.99	
					AVG.	863	.90	
U -4	37.0	1148	.250	.520	7.40	1,020	.95	CENTER ↓
-5	↓	↓	.250	.520	7.40	1,020	.90	
-6	↓	↓	.250	.519	7.22	1,000	.82	
					AVG.	1,010	.89	CENTER ↓
U -1	37.0	1562	.250	.520	5.95	824	.35	
-2	↓	↓	.250	.519	6.08	843	.33	
-3	↓	↓	.250	.519	5.62	780	.35	
					AVG.	815	.34	CENTER ↓
U -1	37.0	1832	.251	.540	6.55	866	.10	
-2	↓	↓	.251	.540	6.15	814	.11	
-7	↓	↓	.251	.526	6.10	828	.11	
					AVG.	836	.11	NO FAILURE ↓
U-10	37.0	2192	.250	.520	-	-	.025	
-11	↓	↓	.250	.517	-	-	.023	
-12	↓	↓	.250	.513	-	-	.026	
					AVG.	-	.025	
B-EXPOSED-(19 HRS, 2,050°F @ 10 <sup>-5</sup> TORR)								
SB-17	37.0	RT	.243	.493	4.06	628	.83	CENTER ↓
-18	↓	↓	.245	.485	4.74	733	.71	
-19	↓	↓	.245	.488	5.20	799	.83	
					AVG.	720	.79	

TABLE A-1 (Continued)

SPEC. IDENT	DENSITY (#/FT <sup>3</sup> )	TEST TEMP (°F)	THICK (IN.)	WIDTH (IN.)	FAIL LOAD	ULT. STRESS (PSI)	MOD. X 10 <sup>6</sup> (PSI)	LOCATION OF FAILURE
<u>GROUP II - 4% COBALT</u>								
A-UNEXPOSED								
SB-13	52.5	RT	.243	.493	8.18	1,270	1.40	CENTER ↓
-14	↓	↓	.243	.496	7.48	1,150	1.30	
-15	↓	↓	.243	.514	8.79	1,300	1.20	
-16	↓	↓	.243	.500	7.56	1,153	1.50	
					AVG.	1,218	1.35	
P33-1	52.5	1400	.256	.498	10.27	1,420	.93	CENTER ↓
-2	↓	↓	.256	.498	10.54	1,450	.87	
-3	↓	↓	.256	.498	11.64	1,600	.94	
					AVG.	1,490	.91	CENTER ↓
P33-4	52.5	1700	.256	.498	9.79	1,350	.26	
-5	↓	↓	.256	.498	10.71	1,480	.25	
-6	↓	↓	.256	.498	12.91	1,780	.24	
					AVG.	1,537	.25	CENTER ↓
P33-7	52.5	2000	.256	.498	3.12*	431	.07	
-8	↓	↓	.256	.498	3.20*	442	.07	
-9	↓	↓	.256	.498	3.25*	450	.07	
					AVG.	441	.07	CENTER ↓
P33-10	52.5	2192	.256	.498	.48*	66	.01	
-11	↓	↓	.256	.498	.47*	65	.02	
-12	↓	↓	.256	.498	.45*	62	.02	
					AVG.	64	.02	
B-EXPOSED-(19 HRS., 2,050°F @ 10 <sup>-5</sup> TORR)								
SB-20	52.5	RT	.250	.487	7.55	1,110	1.30	OFF CENTER
-21	↓	↓	.243	.509	7.16	1,075	1.31	OFF CENTER
-22	↓	↓	.243	.507	8.12	1,220	1.30	CENTER
					AVG.	1,135	1.30	

\* - SUSTAINED LOAD, NO CATASTROPHIC FAILURE

TABLE A-2 FOUR POINT FLEXURAL PROPERTIES OF CPI MATERIAL WITH  
8 AND 4% COBALT ADDITIVE

SPEC. IDENT.	DENSITY (#/FT <sup>3</sup> )	TEST TEMP (°F)	THICK (IN.)	WIDTH (IN.)	FAIL LOAD (LBS)	ULT. STRESS (PSI)	MOD. X 10 <sup>6</sup> (PSI)	STRAIN AT FAILURE	LOCATION OF FAILURE
<u>GROUP I - 8% COBALT</u>									
A-UNEXPOSED									
236R-1	41.2	RT	.547	.251	22.6	903	1.26	-	CENTER
-2	↓	↓	.563	.251	21.3	803	.93	-	↓
-3	↓	↓	.559	.251	31.7	1,210	1.27	-	↓
P14-1	43.0	↓	.579	.251	41.4	1,480	1.35	-	↓
-2	↓	↓	.579	.250	39.8	1,430	1.23	-	↓
-3	↓	↓	.580	.251	39.9	1,420	1.12	-	↓
P45 <sub>3</sub> -1	38.7	↓	.500	.252	21.4	1,020	1.25	-	↓
-2	↓	↓	.499	.252	26.7	1,280	1.16	-	↓
-3	↓	↓	.498	.251	21.3	1,025	1.27	.00070 <sup>(1)</sup>	↓
-4	↓	↓	.498	.251	19.3	925	.97	.00062 <sup>(2)</sup>	↓
AVG.						1,150	1.18		
B-EXPOSED-(19HRS, 2,050°F @ 10 <sup>-5</sup> TORR)									
8-1	38.7	RT	.413	.252	11.0	775	1.10	-	CENTER
-2	↓	↓	.413	.255	14.6	1,000	1.45	-	↓
-3	↓	↓	.426	.255	22.0	1,430	2.10	-	↓
-5	↓	↓	.414	.255	14.0	964	1.43	.00071 <sup>(1)</sup>	↓
-6	↓	↓	.504	.255	28.8	1,300	1.21	.00086 <sup>(2)</sup>	↓
AVG.						1,094	1.46		
<u>GROUP II - 4% COBALT</u>									
A-UNEXPOSED									
4-8	48.0	RT	.503	.249	49.6	2,360	1.80	-	LOAD POINT
-9	↓	↓	.503	.248	46.6	2,230	1.50	-	CENTER
-10	↓	↓	.504	.247	51.8	2,480	2.00	-	CENTER
-12	↓	↓	.504	.249	40.6	1,930	1.60	-	CENTER
274-1	43.7	↓	.504	.252	30.3	1,420	1.92	-	CENTER
-2	↓	↓	.475	.251	32.0	1,690	1.98	-	LOAD POINT
-3	↓	↓	.478	.252	26.8	1,400	1.86	-	CENTER
-4	↓	↓	.474	.253	33.8	1,781	1.70	-	CENTER
-5	↓	↓	.477	.252	32.0	1,670	2.06	.00069 <sup>(1)</sup>	LOAD POINT
-6	↓	↓	.475	.252	31.8	1,675	1.98	.00075 <sup>(2)</sup>	CENTER
AVG.						1,864	1.84		

TABLE A-2 (Continued)

SPEC. IDENT.	DENSITY (#/FT <sup>3</sup> )	TEST TEMP	THICK (IN.)	WIDTH (IN.)	FAIL LOAD (LBS)	ULT. STRESS (PSI)	MOD. <sup>6</sup> X 10 <sup>6</sup> (PSI)	STRAIN AT FAILURE	LOCATION OF FAILURE
B-EXPOSED-(19 HRS. 2,050°F @ 10 <sup>-5</sup> TORR)									
0-1	43.7	RT	.477	.252	30.7	1,603	1.97	-	CENTER
-2	↓	↓	.479	.252	30.7	1,590	1.97	-	CENTER
-3	↓	↓	.479	.252	30.0	1,560	2.07	-	LOAD POINT
-4	↓	↓	.479	.252	33.1	1,720	2.00	-	CENTER
-5	↓	↓	.477	.257	38.0	1,940	1.79	.00073 <sup>(1)</sup>	OUTSIDE GAGE
-6	↓	↓	.480	.251	31.1	1,620	1.89	.00067 <sup>(2)</sup>	CENTER
AVG.						1,672	1.95		
C-EXPOSED-(19 HRS. 2,050°F IN AIR)									
A-1	43.7	RT	.499	.252	30.9	1,480	1.48	-	CENTER
-2	↓	↓	.499	.251	36.9	1,760	2.04	-	CENTER
-3	↓	↓	.476	.252	30.6	1,610	1.77	-	LOAD POINT
-4	↓	↓	.499	.252	39.6	1,890	1.87	-	CENTER
-5	↓	↓	.498	.252	36.6	1,740	1.55	.00072 <sup>(1)</sup>	LOAD POINT
-6	↓	↓	.499	.252	31.1	1,490	1.32	.00062 <sup>(2)</sup>	CENTER
AVG.						1,662	1.67		

(1) - TENSION FACE STRAIN

(2) - COMPRESSION FACE STRAIN

**TABLE A-3 - DIAMETRAL COMPRESSION PROPERTIES OF CPI MATERIAL  
WITH 8 AND 4% COBALT ADDITIVE**

SPEC. IDENT.	DENSITY (#/FT <sup>3</sup> )	TEST TEMP (°F)	THICK (IN.)	DIA. (IN.)	FAIL LOAD (LBS)	ULT. STRESS (PSI)	STRAIN AT FAILURE (IN./IN.)		POISSON'S RATIO (μ)	MOD. X 10 <sup>6</sup> (PSI)	MODE OF FAILURE
							+Ex	-Ex			
GROUP I: 8% COBALT											
A - UNEXPOSED											
ST-6	37.0	RT	.592	1.278	558	470	-	-	-	-	TENSION
-7	↓	↓	.593	1.278	580	487	-	-	-	-	TRIPLE CLEFT
-8	↓	↓	.591	1.275	525	444	-	-	-	-	TENSION
-9	↓	↓	.592	1.275	546	461	-	-	-	-	TENSION
AVG.						466					
ST-16	37.0	1400	.499	1.274	520	520	-	-	-	-	TRIPLE CLEFT
-17	↓	↓	.497	1.275	560	562	-	-	-	-	TENSION
-21	↓	↓	.510	1.282	650	632	-	-	-	-	TRIPLE CLEFT
-22	↓	↓	.485	1.282	490	500	-	-	-	-	TRIPLE CLEFT
AVG.						554					
B - EXPOSED - (19 HRS., 2,050°F @ 10 <sup>-5</sup> TORR)											
ST-13	37.0	RT	.493	1.268	394	402	.00064	.00118	.258	1.10	TENSION
-14	↓	↓	.499	1.284	462	470	.00064	.00130	.187	1.13	TENSION
-15	↓	↓	.491	1.278	370	376	.00072	.00137	.230	.90	TRIPLE CLEFT
AVG.						416	.00067	.00128	.225	1.04	
GROUP II: 4% COBALT											
A - UNEXPOSED											
ST-10	52.5	RT	.523	1.281	952	905	-	-	-	-	TRIPLE CLEFT
-11	↓	↓	.509	1.281	944	922	-	-	-	-	↓
-12	↓	↓	.526	1.281	932	881	-	-	-	-	
AVG.						903					

TABLE A-3 - DIAMETRAL COMPRESSION PROPERTIES OF CPI MATERIAL  
WITH 8 and 4% COBALT ADDITIVE (Continued)

SPEC. IDENT.	DENSITY (#/FT <sup>3</sup> )	TEST TEMP (°F)	THICK (IN.)	DIA. (IN.)	FAIL LOAD (LBS)	ULT. STRESS (PSI)	STRAIN AT FAILURE (IN./IN.)		POISSON'S RATIO (μ)	MOD. X 10 <sup>6</sup> (PSI)	MODE OF FAILURE
							+Ex	-Ex			
A - UNEXPOSED (Continued)											
P34 <sub>3</sub> -1	40.0	1400	.503	1.280	914	895	-	-	-	-	TRIPLE CLEFT
-2	↓	↓	.499	1.281	785	783	-	-	-	-	TRIPLE CLEFT
-3	↓	↓	.497	1.280	950	950	-	-	-	-	TENSION
AVG.						876					
B-EXPOSED - (19 HRS., 2,050°F @ 10 <sup>-5</sup> TORR)											
ST-37	52.5	RT	.511	1.287	750	726	.00070	.00142	.193	1.63	TRIPLE CLEFT
-38	↓	↓	.520	1.282	885	845	.00072	.00164	.140	1.62	TENSION
-39	↓	↓	.508	1.281	900	880	.00088	.00165	.240	1.70	TRIPLE CLEFT
AVG.						817	.00077	.00157	.191	1.65	

TABLE A-4 - UNCONFINED EDGE COMPRESSION PROPERTIES OF CPI  
MATERIAL WITH 8 AND 4% COBALT ADDITIVE

SPEC. IDENT.	DENSITY (#/FT <sup>3</sup> )	TEST TEMP (°F)	THICK (IN.)	WIDTH (IN.)	LENGTH (IN.)	FAIL LOAD (LBS)	ULT. STRESS (PSI)	STRAIN AT FAILURE (IN./IN.)		MOD. X 10 <sup>6</sup> (PSI)	MODE OF FAILURE
								SIDE 1	SIDE 2		
GROUP I: 8% COBALT											
A - UNEXPOSED											
SC-1	37.0	RT	.374	.373	.998	432	3,090	.00254	.00265	1.27	CENTER EDGE COMP. CENTER
-2	↓	↓	.362	.357	.998	296	2,300	.00204	.00242	1.02	
-3	↓	↓	.370	.361	.990	400	3,000	.00248	.00284	1.13	
						AVG.	2,800	.00235	.00264	1.14	
SC-4	37.0	1400	.361	.371	.991	240	1,710	-	-	-	EDGE COMP.
-5	↓	↓	.368	.357	.988	242	1,850	-	-	-	EDGE COMP.
S12-8	↓	↓	.376	.370	.996	215	1,550	-	-	-	CENTER
-9	↓	↓	.376	.370	.996	260	1,870	-	-	-	CENTER
						AVG.	1,750				
S12-1	37.0	1700	.376	.370	.996	231	1,660	-	-	-	CENTER
-2	↓	↓	.377	.370	.996	187	1,350	-	-	-	↓
-3	↓	↓	.376	.370	.996	271	1,950	-	-	-	
						AVG.	1,650				
S12-4	37.0	2000	.377	.370	.996	23.0	164	-	-	-	BUCKLING
-5	↓	↓	.378	.370	.996	22.0	157	-	-	-	↓
-6	↓	↓	.376	.370	.996	27.0	194				
						AVG.	172				
B - EXPOSED - (19 HRS., 2,050°F @ 10 <sup>-5</sup> TORR)											
SC-18	37.00	RT	.372	.364	.988	296	2,190	.00204	.00255	1.08	EDGE COMP.
-19	↓	↓	.355	.369	.989	278	2,120	.00241	.00266	.96	CENTER
-20	↓	↓	.354	.356	.985	276	2,190	.00244	.00208	1.02	EDGE COMP.
-21	↓	↓	.378	.370	.989	384	2,740	.00268	.00298	1.02	CENTER
						AVG.	2.310	.00239	.00257	1.02	
GROUP II: 4% COBALT											
SC-7	43.0	RT	.387	.362	.989	824	5,890	.00320	.00288	1.85	CENTER
-8	↓	↓	.384	.361	.990	975	7,010	-	-	-	↓
-9	↓	↓	.383	.360	.988	1,042	7,550	.00400	.00373	1.85	
-10	↓	↓	.386	.358	.990	1,050	7,600	.00357	.00430	1.90	
						AVG.	7,010	.00359	.00364	1.87	



TABLE A-4 (Continued)

SPEC. IDENT.	DENSITY (#/FT <sup>3</sup> )	TEST TEMP (°F)	THICK (IN.)	WIDTH (IN.)	LENGTH (IN.)	FAIL LOAD (LBS)	ULT. STRESS (PSI)	STRAIN AT FAILURE (IN./IN.)		MOD. X 10 <sup>6</sup> (PSI)	MODE OF FAILURE	
								SIDE 1	SIDE 2			
GROUP II: 4% COBALT (Continued)												
SC-12	43.0	1400	.358	.385	.990	453	3,300	-	-	-	CENTER EDGE COMP. CATA- STROPHIC CENTER	
P33-18	52.5	↓	.360	.380	.996	518	3,780	-	-	-		
SC-18	43.0	↓	.376	.370	.994	454	3,260	-	-	-		
-19	43.0	↓	.376	.370	.996	490	3,530	-	-	-		
						AVG.	3,470					
P33-1	52.5	1700	.376	.371	.996	547	3,940	-	-	-	CENTER ↓	
-2	↓	↓	.376	.370	.996	550	3,960	-	-	-		
-3	↓	↓	.376	.370	.996	566	4,070	-	-	-		
						AVG.	3,990	-	-	-		
P33-4	52.5	2000	.376	.371	.998	74	532	-	-	-	BUCKLING ↓	
-5	↓	↓	.376	.371	.996	83	597	-	-	-		
-6	↓	↓	.376	.371	.996	100	719	-	-	-		
						AVG.	616					
B - EXPOSED -(19 HRS. 2,050°F @ 10 <sup>-5</sup> TORR												
SC-14	43.0	RT	.362	.379	.990	834	6,090	.00420	.00209	1.67	EDGE COMP. CATA- STROPHIC CATA- STROPHIC EDGE COMP.	
-15	↓	↓	.363	.389	.989	983	6,980	.00434	.00360	1.70		
-16	↓	↓	.392	.361	.990	1,084	7,630	.00460	.00385	1.83		
-17	↓	↓	.361	.385	.989	832	6,000	.00388	.00326	1.68		
								AVG.	6,680	.00426	.00320	1.72

TABLE A-5 AXIAL TENSILE PROPERTIES OF CPI MATERIAL WITH  
8 AND 4% COBALT ADDITIVE

SPEC IDENT	DENSITY (#/FT <sup>3</sup> )	TEST TEMP (°F)	THICK (IN.)	WIDTH (IN.)	AREA (IN) <sup>2</sup>	FAIL LOAD (LBS)	ULT. STRESS (PSI)	STRAIN AT FAILURE (IN./IN.)		MOD. X 10 <sup>6</sup> (PSI)	LOCATION OF FAILURE
								SIDE 1	SIDE 2		
GROUP I: 8% COBALT (UNEXPOSED ONLY)											
ST-29	37.0	RT	.246	.940	.231	106	459	-	-	-	EDGE OF TAB ↓
-31	↓	↓	.246	.940	↓	67	290	-	-	-	
-32	↓	↓	.246	.938	↓	79	342	.000295	.000325	1.10	
-33	↓	↓	.245	.941	↓	83	359	.000310	.000310	1.15	
-34	↓	↓	.246	.941	↓	65	281	.000250	.000250	1.12	
-35	↓	↓	.246	.941	↓	92	398	.000400	.000325	1.11	
AVG.						355		.000314	.000303	1.12	
GROUP II: 4% COBALT (UNEXPOSED ONLY)											
P4O <sub>2</sub> -1	43.5	RT	.248	.994	.247	133	539	-	-	-	EDGE OF TAB ↓
-2	↓	↓	.245	.995	.244	177	723	.000600	.000480	1.33	
-3	↓	↓	.248	.993	.246	157	638	.000500	.000400	1.42	
-4	↓	↓	.247	.981	.242	145	599	.000525	.000340	1.50	
-5	↓	↓	.246	.988	.243	142	582	.000425	.000330	1.50	
-6	↓	↓	.255	.995	.254	151	593	.000415	.000415	1.40	
-8	↓	↓	.255	.995	.254	151	595	.000400	.000485	1.35	
-9	↓	↓	.255	.995	.253	191	755	.000630	.000480	1.36	
-10	↓	↓	.256	.996	.255	164	642	.000385	.000497	1.43	
AVG.						629		.000485	.000428	1.41	

TABLE A-6 BOND STRENGTH PROPERTIES OF 4% COBALT ADDITIVE CPI

SPEC. IDENT.	TEST TEMP (°F)	NOMINAL AREA (IN) <sup>2</sup>	FAIL LOAD (LBS)	ULT. STRESS (PSI)	MODE OF FAILURE
A - 4% CPI - NO BOND					
1	RT	4.0	1,126	282	CPI ↓ ADH.-CPI FIXTURE ↓
2	↓	↓	1,460	365	
3	↓	↓	1,940	485	
4	↓	↓	990	248	
5	↓	↓	790	190	
6	↓	↓	750	188	
			AVG.	293	
B - 8% CPI POWDER/PVA, 50/50 SOLUTION					
LC32-1	RT	4.0	1,804	451	100% COHESIVE ↓
-2	↓	↓	70	18	
-3	↓	↓	64	16	
-5	↓	↓	192	48	
-6	↓	↓	400	100	
			AVG.	127	
C - 8% CPI POWDER/CS,* HS 2:1 SOLUTION					
LC35-1	RT	4.0	85	21	100% ADH. TO CPI 100% ADH. TO CPI CPI ↓
-2	↓	↓	130	36	
-3	↓	↓	1,580	395	
-4	↓	↓	1,400	350	
-6	↓	↓	1,748	437	
			AVG.	248	
D - ASTROCERAM, A-LP					
LP-1	RT	4.0	960	240	* 100% COHESIVE 100% ADH. TO CPI 100% ADH. TO CPI * 100% ADH. TO CPI
-2	↓	↓	616	154	
-3	↓	↓	196	49	
-4	↓	↓	48	12	
-5	↓	↓	932	233	
-6	↓	↓	388	97	
			AVG.	131	
E - 4% CPI POWDER/CS,* HS 2:1 SOLUTION					
LC36-1	RT	4.0	1,920	480	CPI ↓
-2	↓	↓	1,706	427	
-3	↓	↓	1,984	496	
-4	↓	↓	1,465	366	
-5	↓	↓	2,575	644	
-6	↓	↓	2,080	520	
			AVG.	489	

\* CS = Colloidal Silica, Ludox HS

TABLE A-6 (Continued)

SPEC. IDENT.	TEST TEMP (°F)	NOMINAL AREA (IN) <sup>2</sup>	FAIL LOAD (LBS)	ULT. STRESS (PSI)	MODE OF FAILURE
F - PURE CENOSPHERE POWDER/C.S., H.S., 2:1 SOLUTION					
LC37-1	RT	4.0	1,860	465	CPI
-2	↓	↓	780	195	10% ADH., 90% CPI
-3	↓	↓	1,670	418	CPI
-4	↓	↓	1,060	265	10% ADH., 90% CPI
-5	↓	↓	1,060	280	CPI
-6	↓	↓	1,450	363	CPI
			AVG.	331	

\* - ADHESIVE FAILURE THAT PROPAGATED INTO THE CPI BLOCK

TABLE A-7 JOHNSON SHEAR PROPERTIES OF CPI MATERIAL WITH  
8 AND 4% COBALT ADDITIVE

SPEC. IDENT.	DENSITY (#/FT <sup>3</sup> )	TEST TEMP (°F)	THICK (IN.)	WIDTH (IN.)	AREA (IN) <sup>2</sup>	FAIL LOAD (LBS)	ULT. STRESS (PSI)	MODE OF FAILURE
<u>GROUP I: 8% COBALT</u>								
A - UNEXPOSED								
P49 <sub>4</sub> -1	45.0	RT	.253	.995	.252	648	1,286	SHEAR
-2	↓	↓	.253	.995	.252	614	1,218	↓
-3	↓	↓	.252	.994	.251	482	960	↓
-4	↓	↓	.252	.995	.251	562	1,120	↓
-5	↓	↓	.253	.995	.252	492	976	↓
-6	↓	↓	.253	.995	.252	533	1,058	↓
						AVG.	1,100	
B - EXPOSED (19 HRS., 2,050°F @ 10 <sup>-5</sup> TORR)								
P49 <sub>4</sub> -7	45.0	RT	.255	1.002	.255	363	710	SHEAR
-8	↓	↓	.255	.996	.254	520	1,024	↓
-9	↓	↓	.255	.995	.254	270	531	↓
-10	↓	↓	.257	.996	.256	235	459	↓
-11	↓	↓	.255	.994	.253	530	1,047	↓
						AVG.	754	
<u>GROUP II: 4% COBALT</u>								
A - UNEXPOSED								
P31-1	46.0	RT	.249	.994	.248	730	1,471	SHEAR
-2	↓	↓	.250	.994	.249	756	1,581	↓
-3	↓	↓	.249	.997	.248	685	1,381	↓
-4	↓	↓	.250	.994	.249	584	1,173	↓
-5	↓	↓	.250	.995	.249	625	1,255	↓
-6	↓	↓	.250	.996	.249	760	1,526	↓
						AVG.	1,400	

TABLE A-7 (Continued)

SPEC. IDENT.	DENSITY (#/FT <sup>3</sup> )	TEST TEMP (°F)	THICK (IN.)	WIDTH (IN.)	AREA (IN) <sup>2</sup>	FAIL LOAD (LBS)	ULT. STRESS (PSI)	MODE OF FAILURE
B - EXPOSED (19 HRS, 2,050°F @ 10 <sup>-5</sup> TORR)								
P31-7	46.0	RT	.248	.995	.247	824	1,670	SHEAR ↓
-8	↓	↓	.249	.996	.248	745	1,502	
-9			.249	.992	.247	772	1,563	
-10			.249	.995	.248	908	1,830	
-11			.250	.997	.249	665	1,340	
-12	↓	↓	.248	.999	.248	832	1,680	
						AVG.	1,600	

## APPENDIX B

### RADIANT HEAT LAMP RE-ENTRY THERMAL SCREENING TESTS

#### Test Setup

To simulate re-entry temperatures, a quartz lamp array was assembled that is capable of sustained high temperature operation. This array provides the 1500 K-temperature-time profile shown in Figure 4-28. The heating array consisted of a series of six high density radiant heater modules. Each module is designed to accommodate six 3200w quartz lamps side by side. The module reflector and body is water-cooled and the lamps and end seals are air-cooled to prolong their useful life. A clear quartz window enclosed the lamps to prevent the test panel surface from being convection-cooled. The six lamp modules are assembled side by side to give an effective heated area of 0.40 m X 0.46 m, see Figure B-1.

The quartz array was powered by a Thermac-A\* power supply (Figure B-2) and the time temperature profile was programmed on the Thermac data track that took the input from the thermocouple on the front face and automatically followed the preprogrammed time temperature profile.

In the latter stages of the program, a heater bank consisting of silicon carbide heating elements was mounted on a frame and surrounded by Glasrock foam silica, (see Figure B-3). It was found that this facility required less maintenance and suffered fewer breakdowns than the quartz lamp array. To increase the testing rate for the initial thermal screening program. the heater assembly was mounted on rollers which were clamped on a table on which three separate test banks were mounted. Three different specimens could be tested sequentially by rolling the heater assembly over each bank in sequence. Thus, one specimen could be cycled while another

\*Product of R. I. Controls, Minneapolis, Minn.

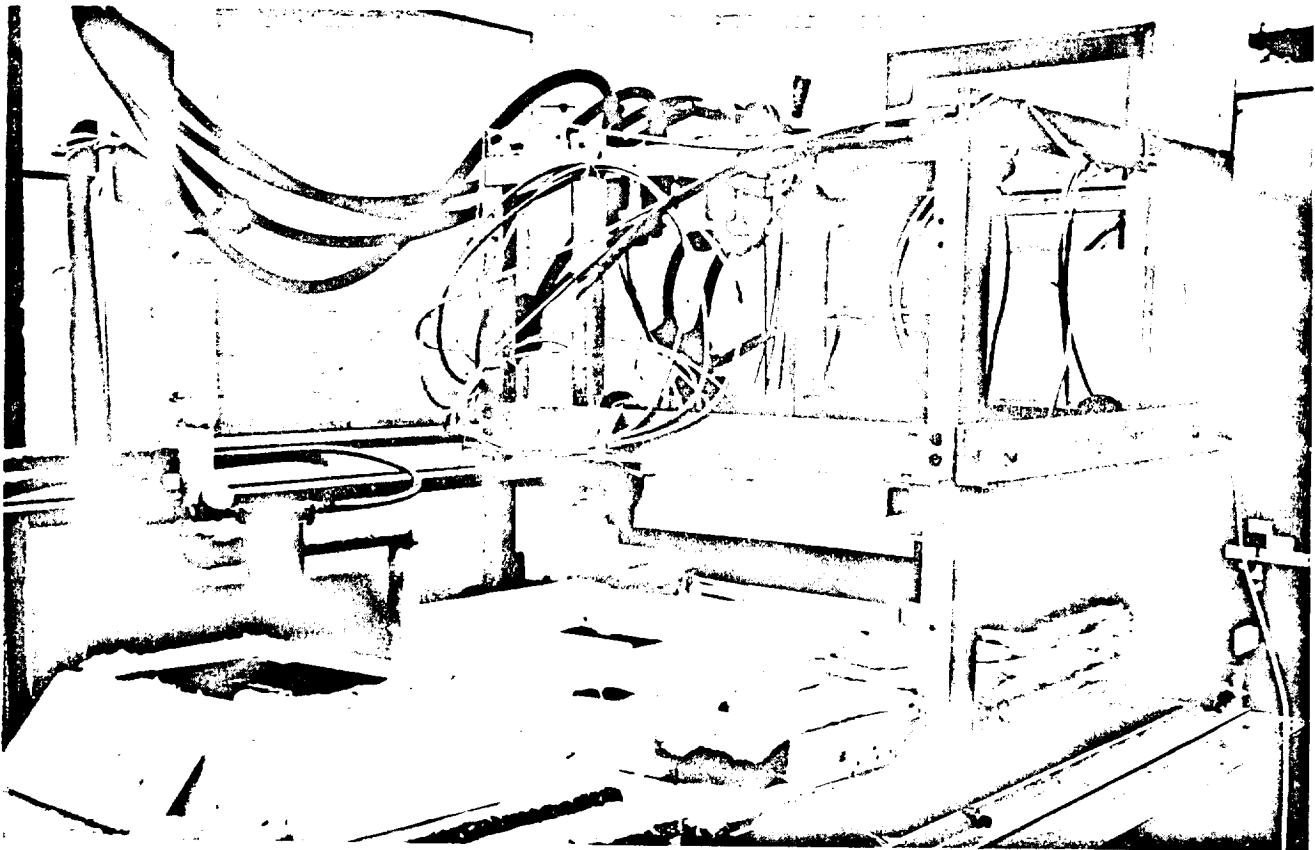


Figure B-1 Radiant Heating Facility



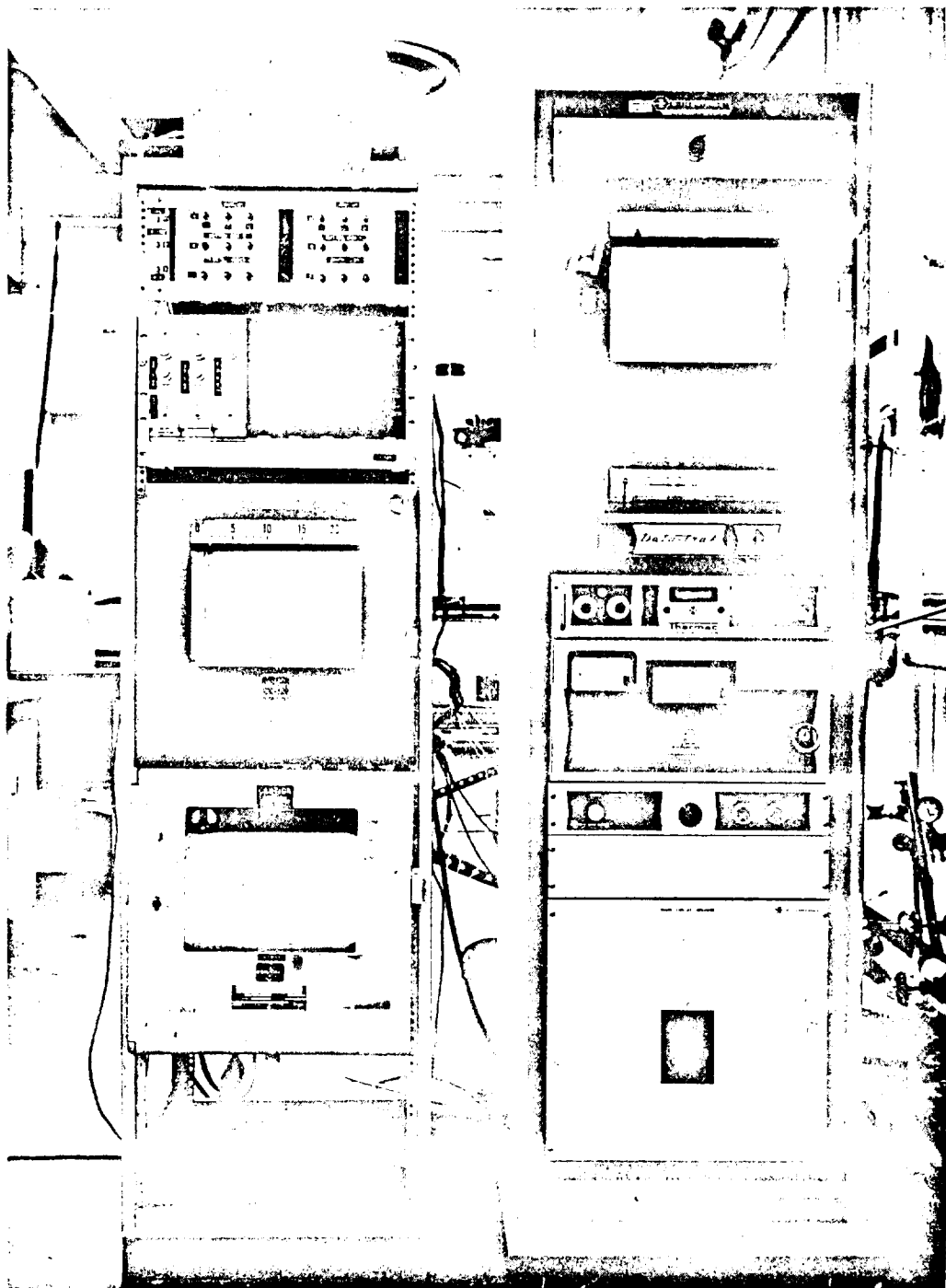


Figure B-2 Thermac-A Controller and Data Track



Figure B-3 CPI Component Ready For Test

was cooling down. During the test, the specimen is placed on a blanket of microquartz insulation and instrumented CPI guard plates are built up around its sides. Below the insulation blanket is an aluminum plate with 0.125 cm microquartz insulation behind it. This acts as the heat sink that represents interior vehicle heat losses.

In the initial stages of the test program, thermocouples were installed using Astroceram. Analysis of test results showed a possible error of approximately 366 K. Therefore, the present method of thermocouple installation evolved. Thermocouples are installed in a small groove made in the specimen. The groove is then covered over using a mixture of the powder from the specimen and a silica binder so that the surface thermal properties are uniform. Test results of surface temperatures are lower than analytical results due to thermocouple installation. The surface thermocouples are slightly below the surface.

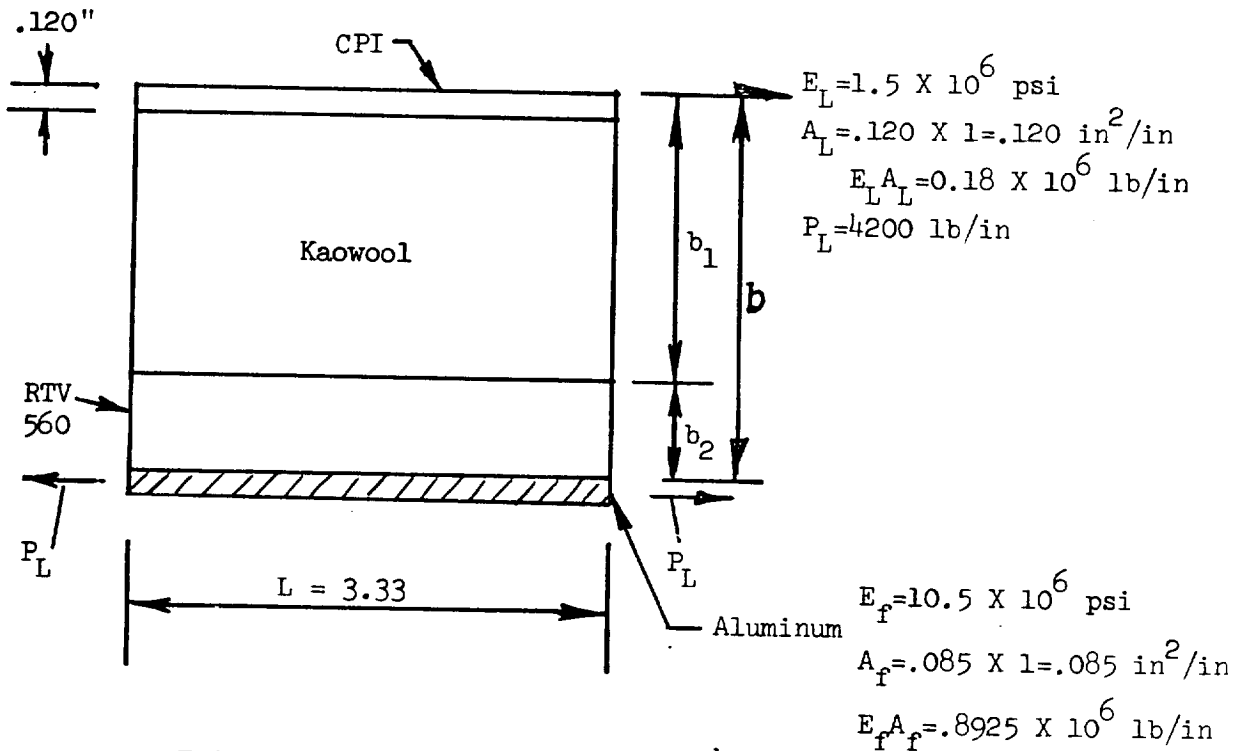
All tests were performed at one atmosphere air pressure so that the fibrous insulations were not vented and thus required a larger thickness than would be necessary to simulate the actual flight conditions.

In those instances where the flight condition thicknesses were used, a larger heat-sink aluminum plate was employed to maintain back face temperature at computed values within the allowable design limits.

## APPENDIX C

### STRESS ANALYSIS OF BONDED CPI DESIGN

#### 1. In plane Stresses



$$\tau = \frac{PK}{t} \frac{E_L A_L}{E_F A_F + E_L A_L} \frac{\sinh KX}{\cosh KL}$$

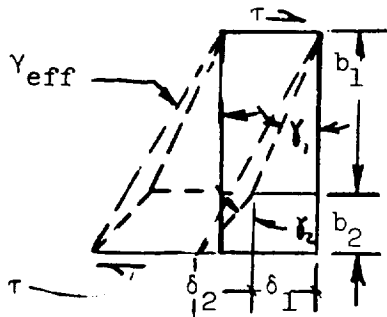
$$\sigma_L = \frac{PE_L}{E_F A_F + E_L A_L} \left( 1 - \frac{\cosh KX}{\cosh KL} \right)$$

$$\sigma_F = \frac{PE_F}{E_F A_F + E_L A_L} \left( 1 + \frac{E_L A_L}{E_F A_F} \frac{\cosh KX}{\cosh KL} \right)$$

where,

$$K = \sqrt{\frac{G_{eff} t}{b} \left( \frac{1}{E_F A_F} + \frac{1}{E_L A_L} \right)}$$

# Effective Shear Modulus



$$\delta_1 = \gamma_1 b_1 = \frac{\tau}{G_1} b_1 \quad \delta_{\text{total}} = \delta_1 + \delta_2 = \delta_{\text{eff}} (b_1 + b_2)$$

$$\delta_2 = \gamma_2 b_2 = \frac{\tau}{G_2} b_2$$

$$G_{\text{eff}} = \frac{\tau}{\gamma_{\text{eff}}} = \frac{\tau (b_1 + b_2)}{\delta_1 + \delta_2} = \frac{b_1 + b_2}{\frac{b_1}{G_1} + \frac{b_2}{G_2}}$$

## Kaowool

$$G_1 = 7000 \text{ psi}$$

$$b_1 = 2.6 \text{ in.}$$

$$\tau_{\text{allow}} = 25 \text{ psi}$$

$$G_{\text{eff}} = \frac{\frac{b_1 + b_2}{\frac{b_1}{G_1} + \frac{b_2}{G_2}}}{\frac{2.6}{7000} + \frac{.25}{100}} = \frac{2.85 \times 1000}{\frac{2.6}{7} + 2.5} = \frac{2850}{.372 + 2.5} = \underline{994 \text{ psi}}$$

## RTV 560 Molded

$$G_2 = 100 \text{ psi}$$

$$b = 0.25 \text{ in.}$$

$$\tau_{\text{allow}} = 50 \text{ psi}$$

$$K = \sqrt{\frac{994 \times 1}{2.85} \left( \frac{1}{.18 \times 10^6} + \frac{1}{.8925 \times 10^6} \right)} = \sqrt{\frac{994}{2.85} \left( \frac{5.56 + 1.12}{6.68} \right) \times 10^{-6}} = \sqrt{2330 \times 10^{-6}} = \underline{0.0483}$$

$$\tau_{\text{max}} @ X = L$$

$$KL = 0.0483 \times 3.33 = .161$$

$$\tanh KL = .15962$$

$$\sigma_{L\text{max}} @ X = 0$$

$$\cosh KL = 1.013$$

$$\tau_{\text{max}} = \frac{Pk}{t} \frac{\frac{E_L A_L}{E_F A_F + E_L A_L} \frac{\sinh KX}{\cosh KL}}$$

$$= \frac{4200 \times .0483}{1} \times \frac{.18 \times 10^6}{.8925 \times 10^6 + .18 \times 10^6} \times .15962$$

## APPENDIX C (Continued)

$$= 4200 \times .0483 \times \frac{.18}{1.0725} \times .15962$$

$$= 5.43 \text{ psi vs. } \tau_{\text{allow}} \approx 25$$

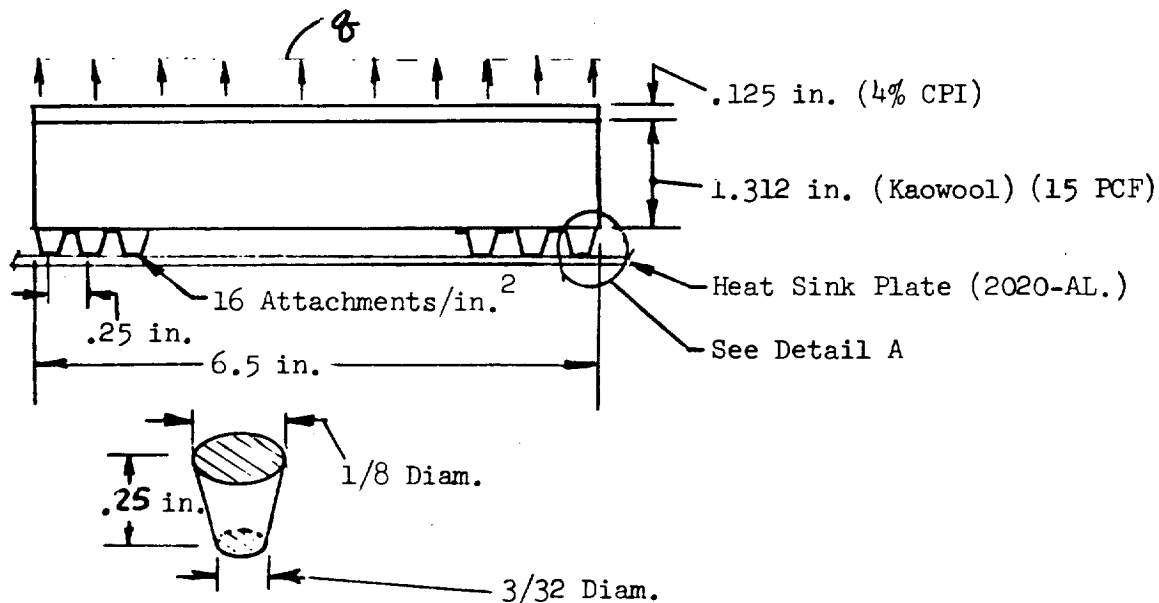
$$\sigma_{L_{\text{max}}} = \frac{4200 \times 1.5 \times 10^6}{.8925 \times 10^6 + .18 \times 10^6} \left( 1 - \frac{1}{1.013} \right) = 70.5 \text{ psi vs. } \sigma_{\text{all.}} = 800 \text{ psi}$$

### 2. Isolator Analysis

Concept (AD - S42)

$$\text{AREA 1 } q_{\text{ult}} = \begin{matrix} +4.0 \text{ psi} \\ -4.5 \text{ psi} \end{matrix} @ \text{ R.T.}$$

$$q_{\text{crit}} = -4.5 \text{ psi, Mat'l. RTV 560/9811}$$



DETAIL A

$$P/\text{Attachment} = \frac{4.5}{16} = .0281 \text{ lb.}$$

Maximum Axial Stress

$$f_t = \frac{P}{A} = \frac{.0281(4)}{\pi(3/32)^2} = 41 \text{ psi}$$

Allowable Stress

$$F_{tu} = 50 \text{ psi}$$

Margin of Safety

$$M.S. = F_{tu}/F_t - 1 = + .22$$

# APPENDIX D

## THERMAL STRESS ANALYSIS OF CPI/MULLITE

### BONDED CONCEPT FOR AREA 2P HEATING

Knowing the temperature distribution and the variation of the elastic properties with temperature we can analyze a slice of the plate assuming that plane sections before bending remain plane during bending. Then,

$$\epsilon = a + by \text{ \& } f = E(a + by - \alpha \Delta T) \text{ where } a \text{ \& } b \text{ are constants.}$$

For the unrestrained case, summing forces and moments on unit section,

$$(1) \quad a \sum EA + b \sum Ay - \sum EA \alpha \Delta T = F = 0$$

$$(2) \quad a \sum E Ay + b \sum Ay^2 - \sum EA \alpha \Delta Ty = M = 0$$

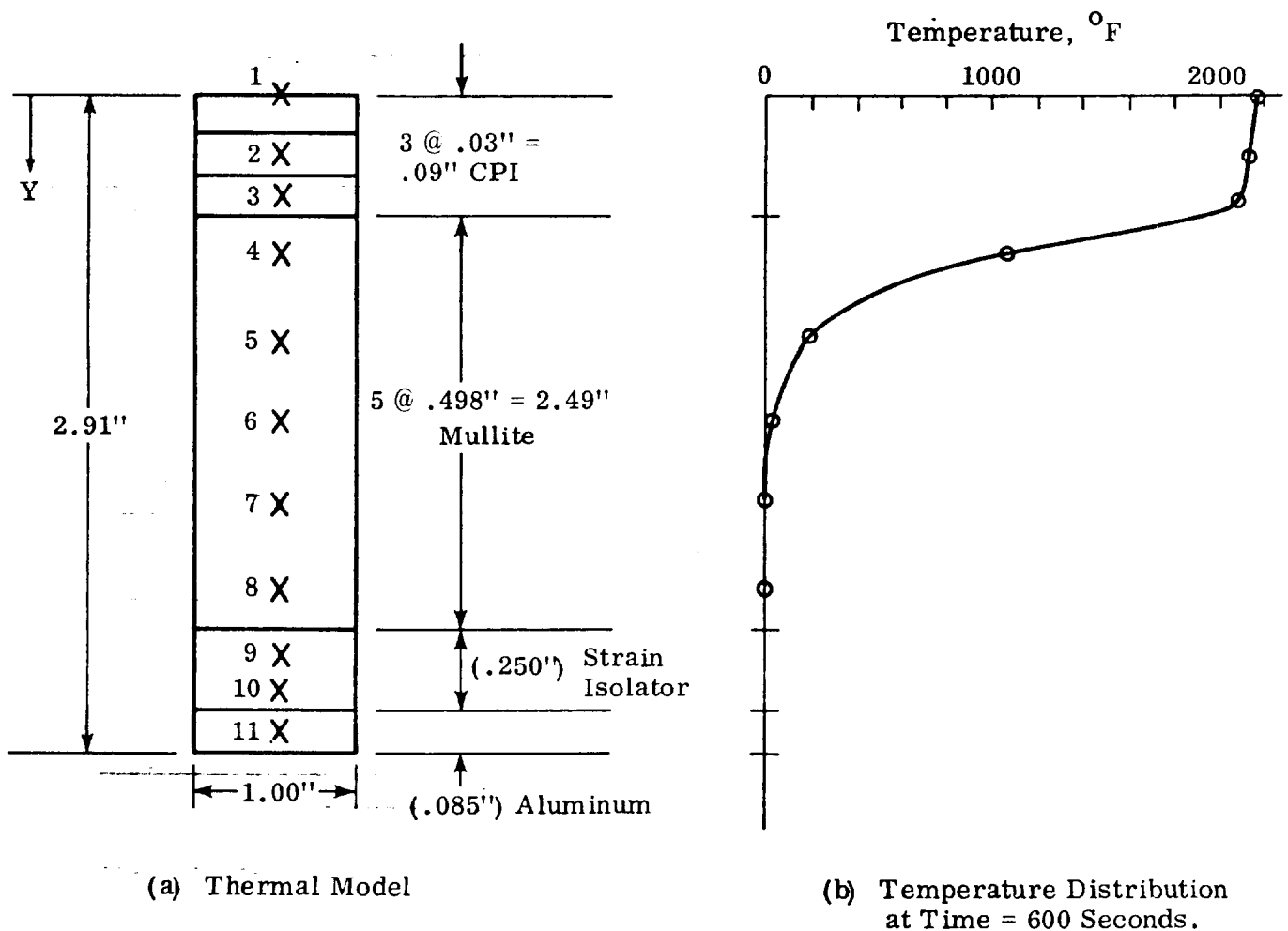


Figure D-1 Thermal Stress Analysis Conditions

Appendix D - THERMAL STRESS ANALYSIS OF CPI/BONDED CONCEPT (Con't)

<u>Node</u>	<u>Area (in<sup>2</sup>)</u>	<u>Y ref.</u>	<u>AY</u>	<u>Ay<sup>2</sup></u>	<u>I<sub>o</sub> x-x</u>	$\left( \frac{Ay^2 + I_{o\ x-x}}{\Sigma Ay^2} \right)$
1	.015625	.0078125	.00012207	.00000095	.00000032	.00000127
2	.046875	.0390625	.00183105	.00007153	.00000858	.00008011
3	.031250	.078125	.00244141	.00019074	.00000254	.00019328
4	.4980	.34275	.17068950	.05850383	.01029217	.06879600
5	.4980	.84075	.41869350	.35201656	.01029217	.36230873
6	.4980	1.33875	.66669750	.89254128	.01029217	.90283345
7	.4980	1.83675	.91470150	1.68007798	.01029217	1.69037015
8	.4980	2.33475	1.16270550	2.71462667	.01029217	2.72491884
$\Sigma$						



CONDITION: MAX. TEMP. GRADIENT THROUGH CPI/MULLITE COMPOSITE

Node	(t = 600 Sec) $\Delta T - O_F$	$\alpha \times 10^6$	$\alpha \Delta T$	$E - \psi_i \times 10^{-6}$	$\Sigma EA \times 10^{-6}$	$\Sigma EAY^2 \times 10^{-6}$	$\Sigma EAY^2 \times 10^{-6}$
1	2178	3.5	.0076230	.020	.00031250	.00000228	.00000003
2	2144		.0075040	.030	.00140625	.00001050	.00000240
3	2111		.0073885	.040	.00125000	.00000924	.00000773
4	1069		.0037415	.0275	.01369500	.00005124	.00189189
5	200		.000700	.029	.014444200	.00001011	.01050695
6	22		.0000770	.030	.014940	.00000115	.02708500
7	2		.0000070	.030	.014940	.00000010	.05071110
8	0		0	.030	.014940	0	.08174757
$\Sigma$					.07592575 $\times 10^6$	.00008462 $\times 10^6$	.17195267 $\times 10^6$

Node	$\Sigma EAY \times 10^{-6}$	$\Sigma EAY \Delta T Y \times 10^{-6}$
1	.00000244	.00000002
2	.00005493	.00000042
3	.00009764	.00000074
4	.00469396	.00001756
5	.01214211	.00000850
6	.02000093	.00000154
7	.02744105	.00000019
8	.03488117	0
$\Sigma$	.09931423 $\times 10^6$	.00002897 $\times 10^6$

Solving for the constants a and b:

$$a = \frac{(\sum EAY^2)(\sum EA\alpha\Delta T) - (\sum EAY)(\sum EA\alpha\Delta Ty)}{(\sum EAY^2)(\sum EA) - (\sum EAY)^2} \quad \& \quad b = \frac{(\sum EA)(\sum EA\alpha\Delta Ty) - (\sum EAY)(\sum EA\alpha\Delta T)}{(\sum EAY^2)(\sum EA) - (\sum EAY)^2}$$

$$a = \frac{(.17195267)(.00008462) - (.09931423)(.00002897)}{(.17195267)(.07592575) - (.09931423)^2} = + \frac{.00001167}{.00319232} = + \frac{.00365565}{.00319232}$$

$$\& \quad b = \frac{(.07592575)(.00002897) - (.09931423)(.00008402)}{.00319232} = - \frac{.000006214}{.00319232} = - \frac{.00194655}{.00319232}$$

Node	E~psi X 10 <sup>-6</sup>	a	b	y	by	αΔT	f~psi
1	.020	.00365565	-.00194655	0	0	.0076230	-79
2	.030			.046875	-.00009124	.0075040	-118
3	.040			.078125	-.00015207	.0073885	-155
4	.0275			.34275	-.00066718	.0037415	-21
5	.0290			.84075	-.00163656	.000700	+38
6	.0300			1.33875	-.00260594	.0000770	+29
7	.0300			1.83675	-.00357533	.0000070	+3
8	.0300	.00365565	-.00194655	2.33475	-.00454471	0	-27

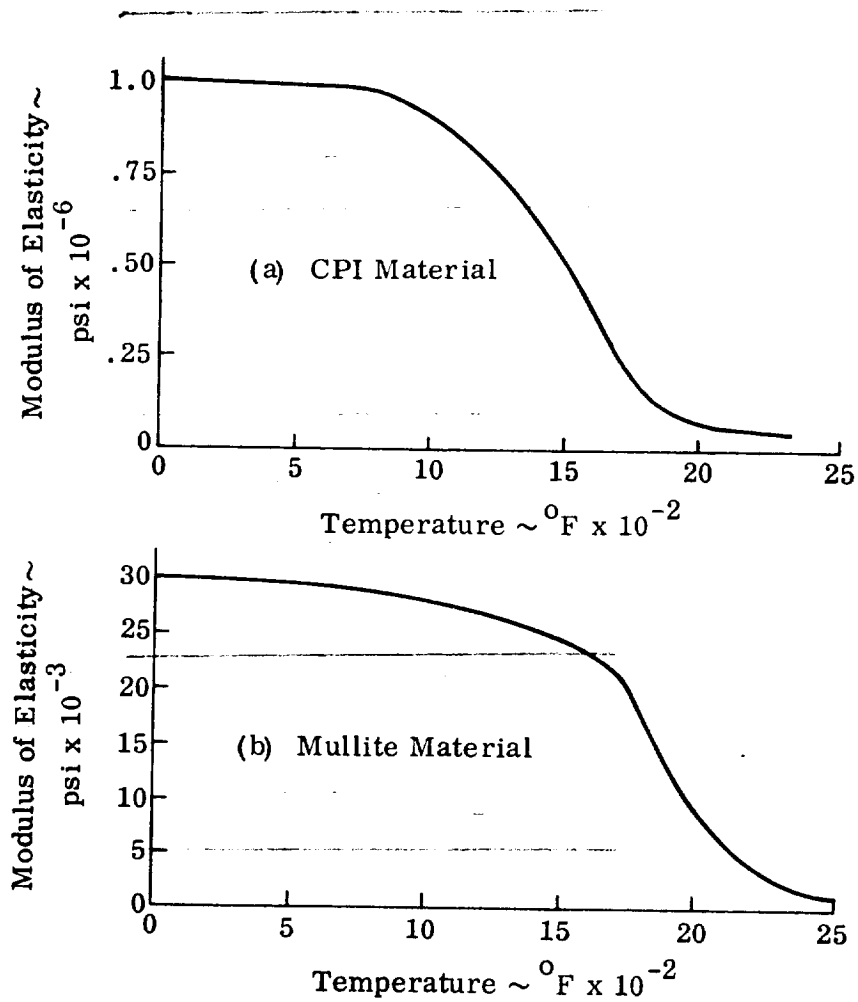


Figure D-2 Modulus vs. Temperature Curves

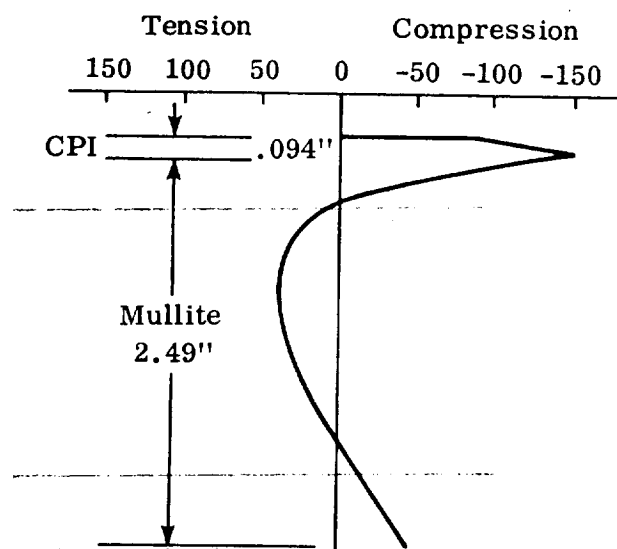


Figure D-3 Thermal Stress Distribution Computed at Time of Maximum Thermal Gradient

## APPENDIX E

### STRESS ANALYSIS OF CPI-4 FOUR SUPPORT CONCEPT - SLIDING BUSHING

CONCEPT: Ref. 5.3.3

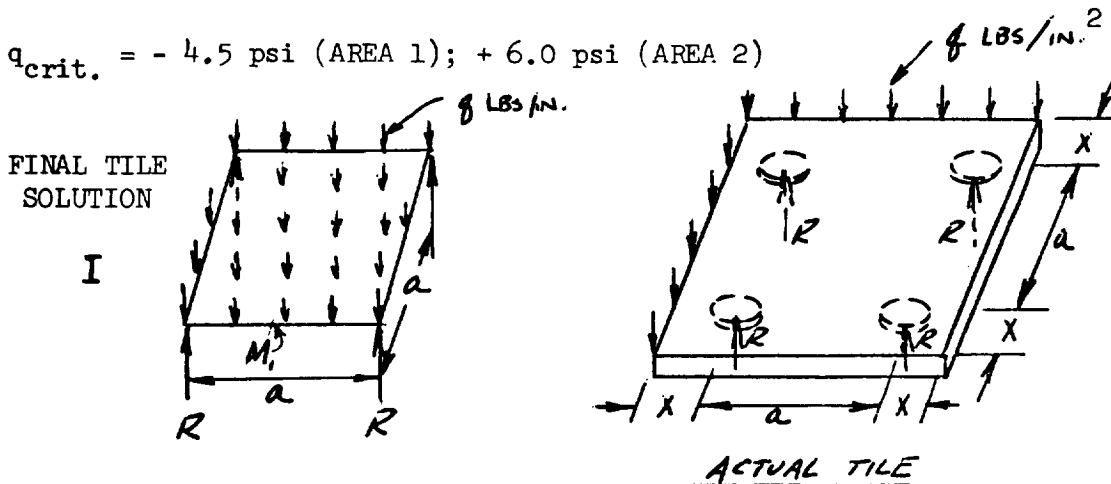
$$\begin{array}{l} \text{AREA 1} \left\{ \begin{array}{l} q_{\text{ult.}} = \begin{cases} +4.0 \text{ psi} \\ -4.5 \text{ psi} \end{cases} @ \text{ R.T.} \\ R = -72.0 \text{ lb.} \\ a = 6.356 \text{ in.} \\ X = 0.822 \text{ in.} \end{array} \right. \quad \text{AREA 2} \left\{ \begin{array}{l} q_{\text{ult.}} = \begin{cases} +6.0 \text{ psi} \\ -4.5 \text{ psi} \end{cases} @ \text{ R. T.} \\ R = 73.4 \text{ lb.} \\ a = 5.356 \text{ in.} \\ X = 0.822 \text{ in.} \end{array} \right. \end{array}$$

$$t = .375 \text{ in.}; I = .0044 \text{ in.}^4/\text{in.}; E = 1.0 \times 10^6 \text{ psi}$$

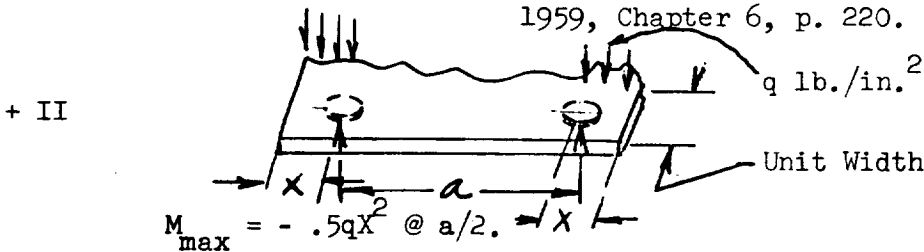
$$F_{\text{bu}} = 1200 \text{ psi}; \nu = .20$$

#### (a) BASIC TILE ANALYSIS

$$q_{\text{crit.}} = -4.5 \text{ psi (AREA 1)}; +6.0 \text{ psi (AREA 2)}$$



$$M_{\text{max.}} = .1527 qa^2 @ a/2, \text{ REF. "Theory of Plates and Shells", by S. Timoshenko and S. Woinowsky-Krieger, 1959, Chapter 6, p. 220.}$$



$$= M_{\text{max.}} = 26.3 \text{ in.-lb (AREA 1)}; 24.3 \text{ in.-lb. (AREA 2)}$$

APPENDIX E (Continued)

MAXIMUM BENDING STRESS

$$f_b = \frac{Mc}{I} = \underline{1120 \text{ psi}} \text{ (AREA 1)}; \underline{1040 \text{ psi}} \text{ (AREA 2)}$$

ALLOWABLE STRESS

$$F_{bu} = \underline{1200 \text{ psi}}$$

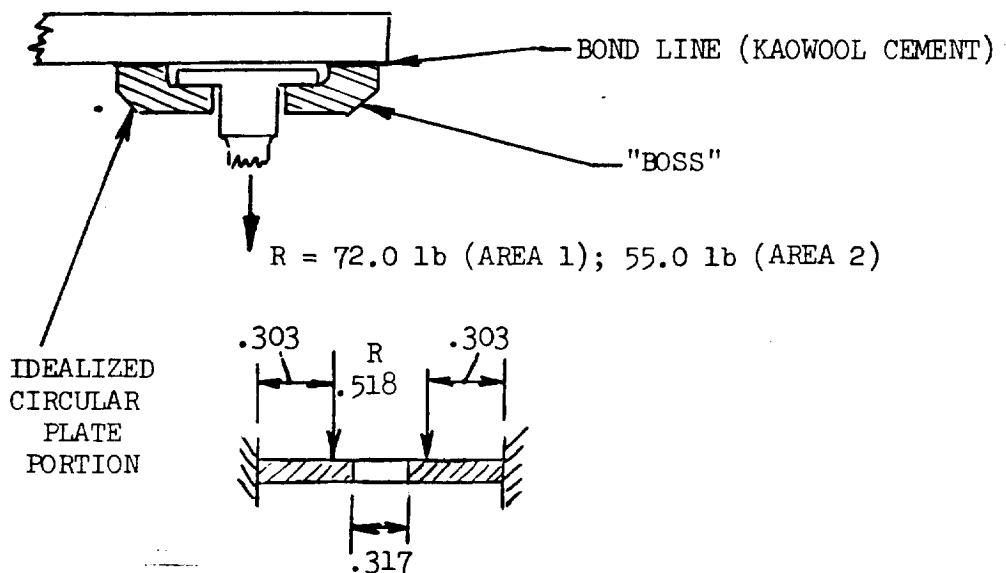
MARGIN OF SAFETY

$$\text{M.S.} = \frac{F_{bu}}{f_b} - 1 = \underline{+.03} \text{ (AREA 1)}; \underline{+.15} \text{ (AREA 2)}$$

(b) BONDED-ON "BOSS" ANALYSIS

$$q_{\text{crit.}} = -4.5 \text{ psi (AREA 1)}; -4.5 \text{ psi (AREA 2)}$$

$$\text{MAT'L CPI-4, } F_{bu} = 1200 \text{ psi}$$



APPENDIX E (Continued)

$$t_{\text{plate}} = .195 \text{ in. (AREA 1); } .175 \text{ in. (AREA 2)}$$

$$I = 0.000616 \text{ in.}^4/\text{in. (AREA 1); } 0.00045 \text{ in.}^4/\text{in. (AREA 2)}$$

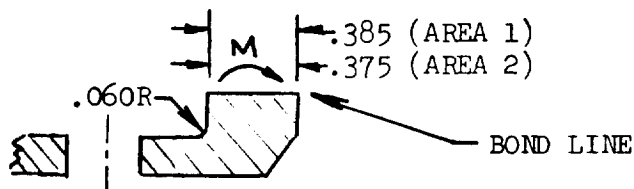
$$M_{f.e.} = 4.90 \text{ in.-lb/in. (AREA 1); } 3.74 \text{ in.-lb./in. (AREA 2)}$$

REF. "Formulas for Stress and Strain", by R. J. Roark,  
1954, Table X,  
"Formulas for Flat Plates", Case No. 60, page 210.

(1) "BOSS"

MAXIMUM BENDING STRESS

$$f_{b \text{ nominal}} = \frac{Mc}{I} = 775 \text{ psi (AREA 1); } 730 \text{ psi (AREA 2)}$$



REF. "Structural Design Data", Grumman Aircraft Engineering Corporation,  
"Stress Concentration Factors For Angle in Bending", page 3.1.6.

$$\frac{r}{t} = .308 \text{ (AREA 1); } .343 \text{ (AREA 2); } K = 1.52 \text{ (AREA 1); } K = 1.46$$

$$f_{\text{max.}} = kf_{\text{nom.}} = \underline{1180 \text{ psi}} \text{ (AREA 1); } \underline{1165 \text{ psi}} \text{ (AREA 2)}$$

ALLOWABLE STRESS

$$F_{\text{bu}} = \underline{1200 \text{ psi}}$$

MARGIN OF SAFETY

$$M.S. = F_{\text{bu}}/f_b - 1 = + \underline{.01} \text{ (AREA 1); } + \underline{.03} \text{ (AREA 2)}$$

APPENDIX E (Continued)

(2) BOND LINE

MAXIMUM BENDING STRESS

$$I = .00475 \text{ in.}^4/\text{in. (AREA 1)}; .00440 \text{ in.}^4 \text{ (AREA 2)}$$

$$f_b = \frac{Mc}{I} = \underline{198 \text{ psi}} \text{ (AREA 1)}; \underline{160 \text{ psi}} \text{ (AREA 2)}$$

MAXIMUM AXIAL STRESS

$$P = \frac{R}{HD} = \frac{R}{H(1.25)} = 18.3 \text{ lb/in. (AREA 1)}; 14.0 \text{ lb./in. (AREA 2)}$$

$$f_a = \frac{P}{A} = \underline{48 \text{ psi}} \text{ (AREA 1)}; \underline{37 \text{ psi}} \text{ (AREA 2)}$$

ALLOWABLE STRESS

$$F_{tu} = 250 \text{ psi}$$

MARGIN OF SAFETY

$$M.S. = \frac{F_{tu}}{f_b + f_a} - 1 = \underline{+.01} \text{ (AREA 1)}; \underline{+.27} \text{ (AREA 2)}$$

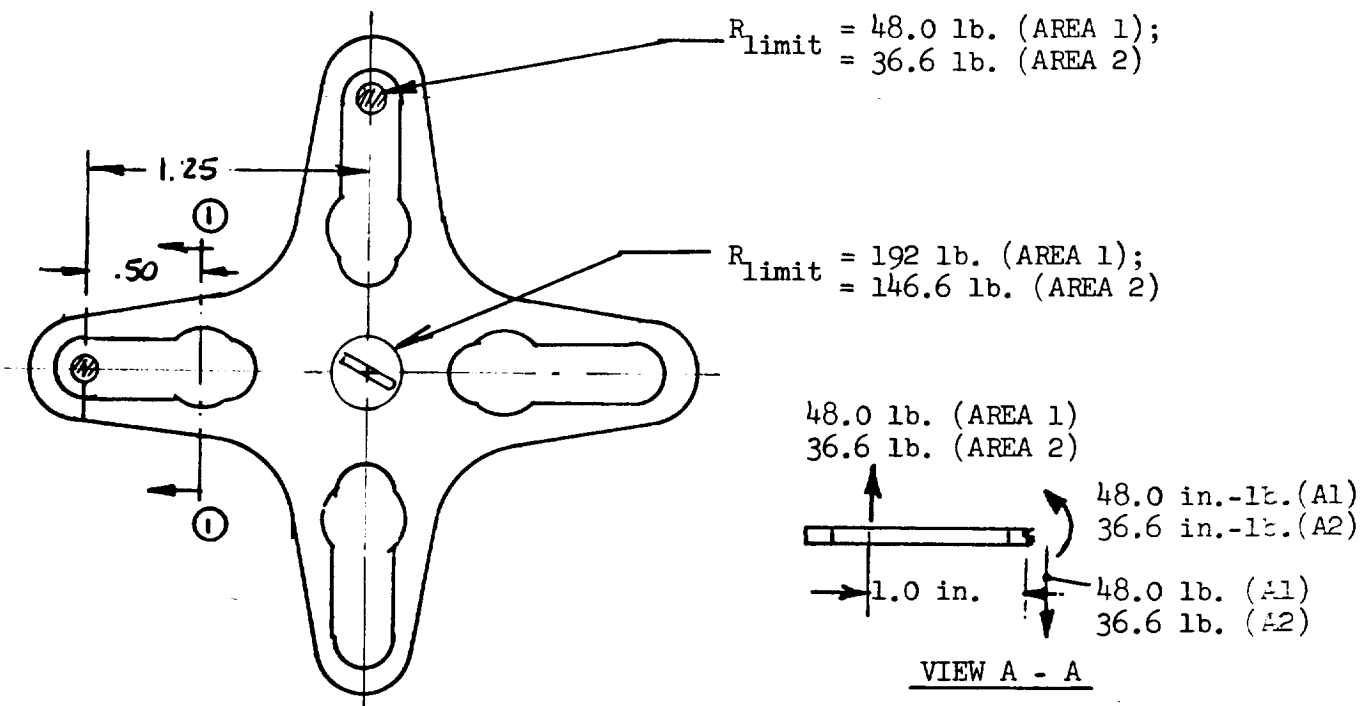
(c) HAYNES 188 SUPPORT PLATE

$$q_{\text{limit}} = -3.0 \text{ psi (AREA 1)}, -3.0 \text{ psi (AREA 2)}$$

$$F_{ty} = 53000 \text{ psi}$$

$$t = \begin{cases} .090 \text{ (AREA 1)} \\ .086 \text{ (AREA 2)} \end{cases}$$

APPENDIX E (Continued)



$$M_{\text{Section } \textcircled{1} - \textcircled{1}} = 24.0 \text{ in.-lb. (AREA 1); } 18.3 \text{ in.-lb. (AREA 2)}$$

MAXIMUM BENDING STRESS

$$f_b = \frac{6M}{bt^2} = \underline{52300 \text{ psi}} \text{ (AREA 1); } \underline{43600 \text{ psi}} \text{ (AREA 2)}$$

ALLOWABLE STRESS

$$F_{ty} = \underline{53000 \text{ psi}}$$

MARGIN OF SAFETY

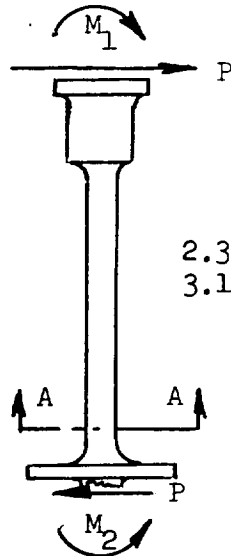
$$M.S. = \frac{F_{ty}}{f_b} - 1 = \underline{+.01} \text{ (AREA 1); } \underline{+.21} \text{ (AREA 2)}$$



# APPENDIX E (Continued)

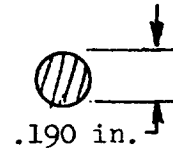
## (d) HAYNES 188 STANDOFF

n(IN-PLANE VIBRATION LOADING) = 20 g's (LIMIT)



$P^* = 12.5 \text{ lb. (AREA 1); } 9.6 \text{ lb. (AREA 2)}$   
 $M_1 = 2.5 \text{ in.-lb. (AREA 1); } 1.9 \text{ in.-lb. (AREA 2)}$   
 $M_2 = 31.5 \text{ in.-lb. (AREA 1); } 31.8 \text{ in.-lb. (AREA 2)}$

\* Assume Load Evenly Distributed Among Standoffs



SECTION A - A

$M_{\text{section A - A}} = 29.5 \text{ in.-lb. (AREA 1); } 29.8 \text{ in.-lb. (AREA 2)}$

## MAXIMUM BENDING STRESS

$$f_b = \frac{M_c}{I} = \underline{43900 \text{ psi}} \text{ (AREA 1); } \underline{44200 \text{ psi}} \text{ (AREA 2)}$$

## ALLOWABLE STRESS

$$F_{ty} = \underline{45000 \text{ psi}}$$

## MARGIN OF SAFETY

$$\text{M.S.} = \frac{F_{ty}}{f_b} = \underline{+0.02} \text{ (AREA 1); } \underline{+0.02} \text{ (AREA 2)}$$

## APPENDIX F

### STRESS ANALYSIS OF CPI-4 FOUR SUPPORT CONCEPT - SNAP WASHERS

CONCEPT Ref. 5.3.4

$$\begin{array}{l} \text{AREA 1} \left\{ \begin{array}{l} q_{ult.} = \begin{cases} +4.0 \text{ psi} \\ -4.5 \text{ psi} \end{cases} @ \text{ R. T.} \\ R = -72.0 \text{ lb.} \\ a = 6.5 \text{ in.} \\ X = 0.75 \text{ in.} \end{array} \right. \quad \text{AREA 2} \left\{ \begin{array}{l} q_{ult.} = \begin{cases} +6.0 \text{ psi} \\ -4.5 \text{ psi} \end{cases} @ \text{ R. T.} \\ R = 73.4 \text{ lb.} \\ a = 5.5 \text{ in.} \\ X = 0.75 \text{ in.} \end{array} \right. \end{array}$$

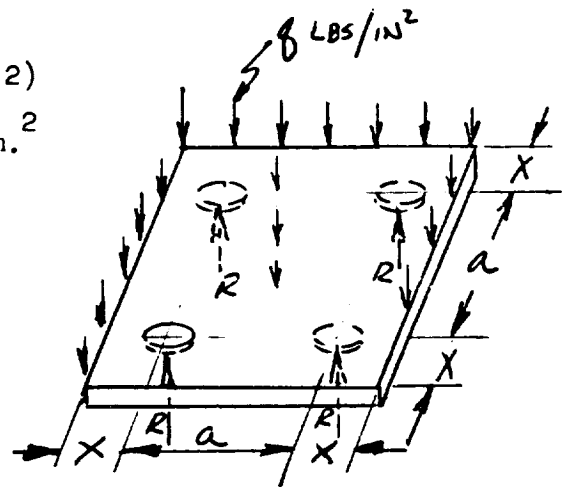
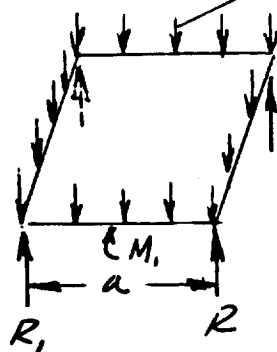
$$\begin{aligned} t &= 0.375 \text{ in.}; I = .0044 \text{ in.}^4/\text{in.} \\ E &= 1.0 \times 10^6 \text{ psi}; F_{bu} = 1200 \text{ psi}; V = 0.20 \end{aligned}$$

#### (a) BASIC TILE ANALYSIS

$$q_{crit.} = -4.5 \text{ psi (AREA 1)}; +6.0 \text{ psi (AREA 2)}$$

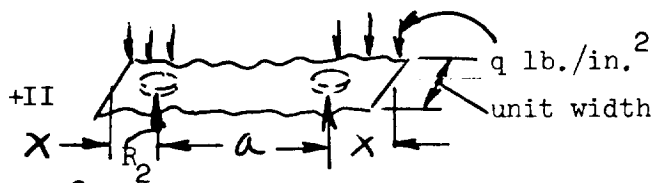
FINAL TILE SOLUTION =

I .



ACTUAL TILE

$$M_1 = .1527 q a^2 @ a/2 \text{ REF. "Theory of Plates and Shells", by S. Timoshenko and S. Woinowsky-Krieger, 1959, Chapter 6, p. 220}$$



$$M_1 = -.5q X^2 @ a/2$$

$$M_{max.} = 27.8 \text{ in.-lb. (AREA 1)}; 26.0 \text{ in.-lb. (AREA 2)}$$

## APPENDIX F (Continued)

### MAXIMUM BENDING STRESS

$$f_b = \frac{Mc}{I} = \underline{1185 \text{ psi}} \text{ (AREA 1)}; \underline{1110 \text{ psi}} \text{ (AREA 2)}$$

### ALLOWABLE STRESS

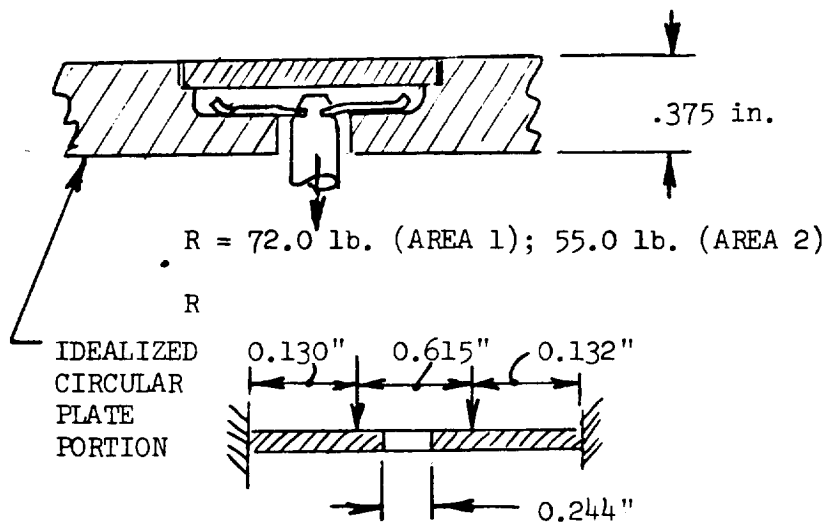
$$f_{bu} = \underline{1200 \text{ psi}}$$

### MARGIN OF SAFETY

$$M.S. = F_{bu}/f_b - 1 = \underline{0.0} \text{ (AREA 1)}, + \underline{.08} \text{ (AREA 2)}$$

### (b) TILE SUPPORT DETAIL

$$q_{crit} = -4.5 \text{ psi (AREA 1)}; -4.5 \text{ psi (AREA 2)}$$



$$t_{plate} = 0.175 \text{ in.}; I = .00045 \text{ in.}^4 / \text{in.}$$

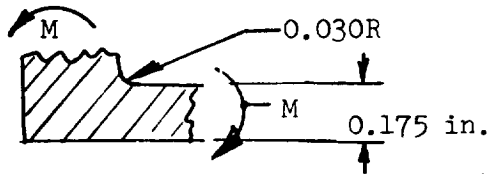
$$M_{F.E.} = 3.0 \text{ in.-lb./in. (AREA 1)}; 2.30 \text{ in.-lb./in. (AREA 2)}$$

REF. "Formulas for Stress and Strain", by R. J. Roark, 1954,  
Table X, "Formulas for Flat Plates", Case No. 60, page 210.

APPENDIX F (Continued)

MAXIMUM BENDING STRESS

$$f_{b \text{ nominal}} = \frac{Mc}{I} = 583 \text{ psi (AREA 1); } 447 \text{ psi (AREA 2)}$$



REF. "Structural Design Data, "Grumman Aircraft Engineering Corporation," Stress Concentration Factors For Angle in Bending", page 3.1.6.

$$\frac{r}{t} = \frac{.030}{.175} = 0.172, K = 1.74$$

$$f_{\text{max.}} = K f_{\text{nom.}} = \underline{1015 \text{ psi}} \text{ (AREA 1); } \underline{780 \text{ psi}} \text{ (AREA 2)}$$

ALLOWABLE STRESS

$$F_{bu} = \underline{1200 \text{ psi}}$$

MARGIN OF SAFETY

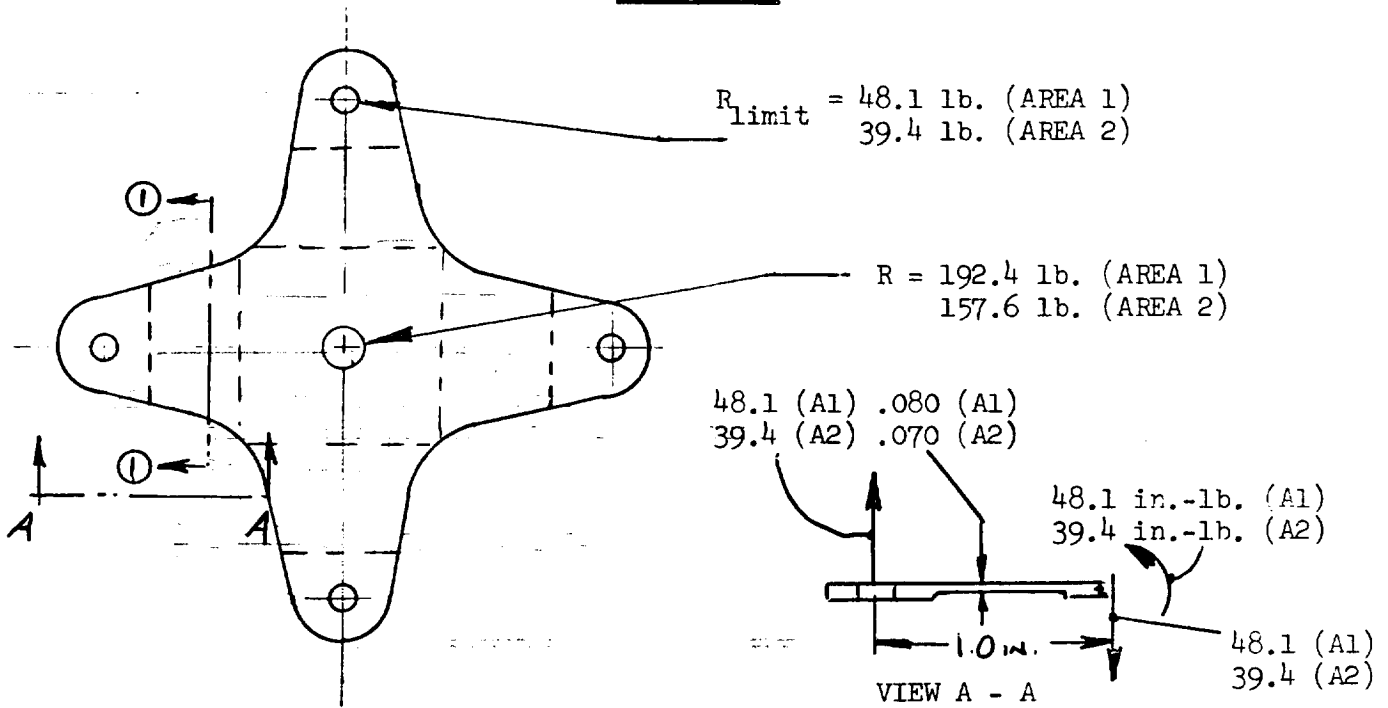
$$M.S. = F_{bu}/f_b - 1 = + \underline{.18} \text{ (AREA 1); } + \underline{.54} \text{ (AREA 2)}$$

(c) HAYNES 188 SUPPORT PLATE

$$q_{\text{crit}} = -3.0 \text{ psi (AREA 1); } -3.0 \text{ psi (AREA 2)}$$

$$F_{ty} = 53000 \text{ psi}$$

APPENDIX F (Continued)



$$M_{\text{section } \textcircled{1} - \textcircled{1}} = 42.2 \text{ in.-lb (AREA 1); } 34.6 \text{ in.-lb. (AREA 2)}$$

MAXIMUM BENDING STRESS

$$f_b = \frac{6M}{bt^2} = \underline{45000 \text{ psi}} \text{ (AREA 1); } \underline{48100 \text{ psi}} \text{ (AREA 2)}$$

ALLOWABLE STRESS

$$F_{ty} = \underline{53000 \text{ psi}}$$

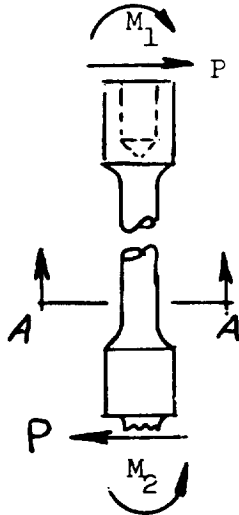
MARGIN OF SAFETY

$$\text{M.S.} = \frac{F_{ty}}{f_b} - 1 = \underline{+.18} \text{ (AREA 1); } \underline{+.10} \text{ (AREA 2)}$$

APPENDIX F (Continued)

(d) HAYNES 188 STANDOFF

n (In-Plane Vibration Loading) = 20 g's (LIMIT)



$$P^* = 12.5 \text{ lb. (AREA 1); } 9.6 \text{ lb. (AREA 2)}$$

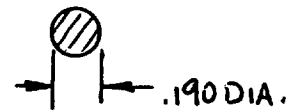
$$M_1 = 2.5 \text{ in.-lb. (AREA 1); } 1.9 \text{ in.-lb. (AREA 2)}$$

$$M_2 = 30.0 \text{ in.-lb. (AREA 1); } 30.7 \text{ in.-lb. (AREA 2)}$$

\* Assume Load Evenly Distributed Among Standoffs

2.2 in. (AREA 1)

3.0 in. (AREA 2)



SECTION A - A

$$M_{\text{section A - A}} = 27.3 \text{ in.-lb. (AREA 1); } 28.6 \text{ in.-lb. (AREA 2)}$$

MAXIMUM BENDING STRESS

$$f_b = \frac{Mc}{I} = \underline{\underline{40600 \text{ psi}}} \text{ (AREA 1); } \underline{\underline{42500 \text{ psi}}} \text{ (AREA 2)}$$

ALLOWABLE STRESS

$$F_{ty} = \underline{\underline{45000 \text{ psi}}}$$

MARGIN OF SAFETY

$$M.S. = \frac{F_{ty}}{f_b} - 1 = \underline{\underline{+.11}} \text{ (AREA 1); } \underline{\underline{+.06}} \text{ (AREA 2)}$$